The Dysfunctional Brain Dynamic of Lewy Body Dementia and its Behavioural and Clinical Correlates: An fMRI and EEG Analysis

Julia Schumacher

Institute of Neuroscience

Newcastle University

October 2018

Thesis submitted for the degree of Doctor of Philosophy

Abstract

Background:

Lewy body dementia (LBD), which comprises dementia with Lewy bodies (DLB) and Parkinson's disease dementia (PDD), is characterised by transient clinical symptoms such as cognitive fluctuations which may be caused by alterations of intrinsic brain dynamics. The aim of this thesis is to investigate how dysfunctional brain connectivity and dynamics relate to the cognitive LBD phenotype, especially to attentional impairment and cognitive fluctuations.

Methods:

In order to investigate behavioural aspects of cognitive fluctuations in LBD, reaction time (RT) data from an attention task were analysed to study how attentional impairment in LBD differs from Alzheimer's disease (AD) and healthy controls. Additionally, brain structural correlates of attentional dysfunction were assessed using voxel-based morphometry. Subsequently, resting-state fMRI data were analysed using static and dynamic functional connectivity and dynamic network analyses. Faster brain dynamics were assessed by EEG microstate analysis.

Results:

AD and LBD patients exhibited slower and more variable RTs than controls, with greater impairment in LBD than AD. Extremely slow responses occurred with comparable frequency in both dementia groups. There were widespread correlations between RT abnormalities and structural changes in AD patients, but not LBD.

Functional connectivity was decreased in DLB patients compared to controls, mainly in motor, temporal, and frontal networks with sparing of the DMN. Differences between AD and DLB were subtle. Considering time-varying connectivity, AD and DLB patients spent more time in sparse connectivity configurations than controls and switched less often into more highly connected states. Compared to controls, variability of global network efficiency was reduced in patients with DLB.

Microstate analysis revealed a marked and generalised increase in microstate duration in LBD patients compared to controls, which was not seen in AD and was related to a loss of dynamic connectivity between basal ganglia/thalamic and large-scale cortical networks. Microstate slowing was correlated with fluctuation severity in the DLB group and with RT slowing and variability across all participants.

Conclusions:

Different aspects of RT performance are differentially affected by AD and LBD, with a

difference in structural neural correlates. The dynamic connectivity and microstate results indicate a loss of brain dynamics in LBD which might lead to a breakdown of the intricate dynamic properties of the brain, thereby causing loss of flexibility that is crucial for healthy brain function. This might lead to a network configuration which gives rise to the cognitive LBD phenotype characterised by attentional impairment and cognitive fluctuations.

Acknowledgements

First and foremost, I would like to thank my supervisors Dr John-Paul Taylor and Dr Luis Peraza for their constant support, guidance, advice, and encouragement throughout my PhD. I also wish to thank my co-supervisors Dr Peter Gallagher, Prof Marcus Kaiser, and Prof Andrew Blamire for their support and advice.

I was fortunate to work with several pre-existing datasets and I am therefore extremely grateful to everyone who was involved in collecting these data and all the research participants who took part in the different studies.

I wish to thank the Alzheimer's Society for funding this project. Thanks are also due to everyone who was involved in the Doctoral Training Centre and, in particular, the Research Network monitors for their enthusiasm and valuable feedback.

I would like to thank all the members of the Lewy body lab, especially Dr Sean Colloby and Dr Michael Firbank for advice on statistics and imaging methods, and my progression advisors Dr Peter Taylor and Dr Fiona LeBeau for their advice at different stages of the project. I am very grateful to Dr Ruth Cromarty for all her help with the behavioural analyses, statistics, and general PhD advice. Additionally, I would like to thank Paul Zhutovsky for all the very helpful discussions about preprocessing and neuroimaging statistics.

I also wish to thank my friends and family and everyone (in Newcastle and elsewhere) who has made the last three years (inside and outside of the lab) so enjoyable. Finally, a very special thank you to my sister for her support throughout my PhD and always!

Declaration

I have not been involved in any data collection for this thesis. Data for the different studies analysed here were collected by Dr Ruth Cromarty, Alison Killen, Dr Michael Firbank, Dr John-Paul Taylor, and the ICICLE team led by Prof David Burn. The analyses of behavioural data described in Chapter 2 were performed in collaboration with Dr Ruth Cromarty. The cleaning of the EEG data presented in Chapter 6 was completed by Dr Luis Peraza. All of the other analyses as well as the interpretation and the writing of this thesis are entirely my own work.

The following publications have been submitted/published based on work contained in this thesis.

Chapter 2:
Cromarty, R.A.*, Schumacher, J.*, Graziadio, S., Gallagher, P., Killen, A., Firbank, M.J., Blamire, A., Kaiser, M., Thomas, A.J., O'Brien, J.T., Peraza, L.R., and Taylor, J.-P., 2018. Structural Brain Correlates of Attention Dysfunction in Lewy Body Dementias and Alzheimer's Disease. *Frontiers in Aging Neuroscience*, 10, 347. *joint first authors

Chapter 3:
Schumacher, J., Cromarty, R.A., Gallagher, P., Firbank, M.J., Thomas, A.J., Kaiser, M., Blamire, A.M., O'Brien, J.T., Peraza, L.R., and Taylor, J.-P., 2018. Structural correlates of attention dysfunction in Lewy body dementia and Alzheimer's disease: An ex-Gaussian analysis. *Under review Journal of Neurology*

Chapter 4:
Schumacher, J., Peraza L.R., Firbank, M., Thomas, A.J., Kaiser, M., Gallagher, P., O'Brien J.T., Blamire, A.M., and Taylor, J.-P., 2018. Functional connectivity in dementia with Lewy bodies: A within- and between-network analysis. *Human Brain Mapping*, 39 (3), 1118-1129

Chapter 5:
Schumacher, J., Peraza, L.R., Firbank, M., Thomas, A.J., Kaiser, M., Gallagher, P., O'Brien, J.T., Blamire, A.M., and Taylor, J.-P., 2018. Dynamic functional connectivity changes in dementia with Lewy bodies and Alzheimer's disease. *Under review NeuroImage: Clinical*

Chapter 6:
Schumacher, J., Peraza, L.R., Firbank, M., Thomas, A.J., Kaiser, M., Gallagher, P., O'Brien J.T., Blamire, A.M., and Taylor, J.-P., 2018. Dysfunctional brain dynamics and their origin in Lewy body dementia. 2018. *Provisionally accepted Brain*

Table of Contents

List of Figures

List of Tables

Abbreviations

ACC – Anterior cingulate cortex

AD – Alzheimer's disease

ANOVA – Analysis of variance

ANT – Attention Network Test

CAF – Clinician Assessment of Fluctuation

CAMCOG – Cambridge Cognitive Examination

CI – Confidence interval

CRT – Choice reaction time

CSF – Cerebrospinal fluid

DLB – Dementia with Lewy bodies

DMN – Default mode network

DTI – Diffusion tensor imaging

EEG – Electroencephalogram

FDR – False discovery rate

FEAT – FMRI Expert Analysis Tool

fMRI – Functional magnetic resonance imaging

FSL – FMRIB's software library

FWE – Family-wise error

GEV – Global explained variance

GFP – Global field potential

GIFT – Group ICA of fMRI toolbox

GLM – General linear model

GM – Grey matter

HC – Healthy control

ICA – Independent component analysis

LBD – Lewy body dementia

LEDD – Levodopa equivalent daily dose

MANOVA – Multivariate analysis of variance

MCFLIRT – Motion Correction FMRIB's Linear Image Registration Tool

MCI – Mild cognitive impairment

MELODIC – Multivariate Exploratory Linear Optimised Decomposition into Independent Components

MMSE – Mini Mental State Examination

MNI – Montreal Neurological Institute coordinates

MPRAGE – Magnetisation prepared rapid gradient echo

MRS – Magnetic resonance spectroscopy

NAA/Cr – N-acetylaspartate/creatine

NBM – Nucleus basalis of Meynert

NPI – Neuropsychiatric Inventory

PD – Parkinson's disease

PDD – Parkinson's disease dementia

PET – Positron emission tomography

RBD – REM sleep behaviour disorder

REM – Rapid eye movement

RSN – Resting-state network

RT – Reaction time

SD – Standard deviation

SPECT – Single photon emission computed tomography

SPM – Statistical Parametric Mapping

TAAHC – Topographic atomize and agglomerate hierarchical clustering

TANOVA – Topographic analysis of variance

TFCE – Threshold-free cluster enhancement

TR – Repetition time

UPDRS – Unified Parkinson's Disease Rating Scale

VBM – Voxel-based morphometry

WM – White matter

Chapter 1. Introduction

1.1 Lewy Body Dementia

Lewy body dementia (LBD) is an umbrella term describing two common forms of neurodegenerative dementia in older age that present with a similar clinical phenotype and which share the same underlying neuropathology: dementia with Lewy bodies (DLB) and Parkinson's disease dementia (PDD) (McKeith et al., 2017, 2005). Accounting for approximately 10-15% of all neuropathologically defined dementia cases, LBD is the second most common form of neurodegenerative dementia after Alzheimer's disease (AD) (McKeith et al., 1996; Vann Jones and O'Brien, 2014).

1.1.1 Clinical features

The central requirement for a diagnosis of DLB or PDD is dementia which is defined as a progressive decline in cognition of sufficient severity to interfere with normal social or occupational functions (McKeith et al., 2017). In addition, there are a number of clinical symptoms associated with LBD including (1) complex and recurrent visual hallucinations, (2) rapid eye movement (REM) sleep behaviour disorder (RBD), (3) spontaneous Parkinsonism, and (4) cognitive fluctuations (McKeith et al., 2017, 2005). These are core diagnostic features of DLB, but frequently occur in PDD as well (Emre et al., 2007).

Visual hallucinations occur in up to 80% of LBD patients and typically present in the form of well-formed and detailed images of people, animals, and objects (Aarsland et al., 2001; Mosimann et al., 2006). RBD is characterised by an absence of normal REM sleep atonia leading to dream enactment behaviour, and can precede the onset of other symptoms by many years (Ferman et al., 2011). Parkinsonism in DLB and PDD is often associated with postural instability, gait, and speech disturbances. Rest tremor is not as common as in Parkinson's disease (PD) patients without dementia (Burn et al., 2003). Apart from motor disturbances, Parkinsonism in LBD is also commonly associated with a slowness of thinking referred to as bradyphrenia (Firbank et al., 2018). Cognitive fluctuations are characterised by pronounced variations in attention and alertness over time. They will be discussed in more detail in Section 1.2.

Other features that are associated with LBD and that can help inform a clinical diagnosis include autonomic dysfunction, syncope, repeated falls, neuroleptic sensitivity, delusions, apathy, anxiety, and depression (McKeith et al., 2017). From a neuropsychological perspective, both DLB and PDD are characterised by marked deficits in executive, visuospatial, visuoperceptual, and attentional function (Emre et al., 2007; Ferman et al., 2006;

Walker et al., 2015).

Currently, there are no disease-modifying treatments for LBD. However, acetylcholinesterase inhibitors have been used in LBD patients with positive effects on overall cognition, visual hallucinations and other neuropsychiatric symptoms, as well as attentional impairment (Aarsland et al., 2004; McKeith et al., 2000b; Stinton et al., 2015; Wang et al., 2015; Wesnes et al., 2002). Similarly, memantine has been shown to improve overall cognition, attention, and episodic memory in DLB and PDD (Aarsland et al., 2009a; Emre et al., 2010; Wesnes et al., 2015). Furthermore, dopaminergic medication is used to treat motor symptoms in LBD (Bonelli et al., 2004; Molloy et al., 2005).

1.1.2 Neuropathology

A definitive diagnosis of LBD is dependent on the presence of Lewy body pathology at autopsy which is characterised by abnormal aggregations of the presynaptic protein alpha-synuclein in the form of Lewy bodies (found in the neuronal cytoplasm) or Lewy neurites (found inside dystrophic neurons) (Dickson, 2002; McKeith et al., 2005). These can be widely distributed throughout the peripheral and central nervous system and are found in the brainstem, basal forebrain, limbic regions, and the neocortex (Beach et al., 2009; Braak et al., 2003). Lewy body pathology is also characteristic of other neurodegenerative disorders including PD and multiple system atrophy which together with LBD are collectively referred to as alpha-synucleinopathies (Jellinger, 2003) (see Figure 1.1). In the context of PD, it has been suggested that accumulation of Lewy bodies follows an ascending pathway, starting in the lower brainstem and progressing to limbic and subsequently to neocortical regions in a caudo-rostral distribution (Braak et al., 2003). This is also thought to reflect the clinical phenotype with brainstem-predominant pathology being associated with PD without dementia and the accumulation of pathology in higher-order regions being related to a clinical presentation with more severe cognitive impairment (Braak et al., 2004; Halliday and McCann, 2010). However, many DLB cases do not necessarily follow this staging system, i.e. Lewy body pathology may be found in neocortical areas with sparing of lower brain regions (Frigerio et al., 2011; Parkkinen et al., 2005; Zaccai et al., 2008) and significant Lewy body pathology may be present without the development of cognitive or motor impairment (Colosimo, 2003; Parkkinen et al., 2008). A further pathological finding that is characteristic of both DLB and PDD is the loss of midbrain dopaminergic neurons and cholinergic neurons in the ventral forebrain nuclei (Kövari et al., 2009), leading to marked dopaminergic and cholinergic deficits (Lippa et al., 1999).

In many LBD cases, especially those with DLB, significant concurrent AD pathology is

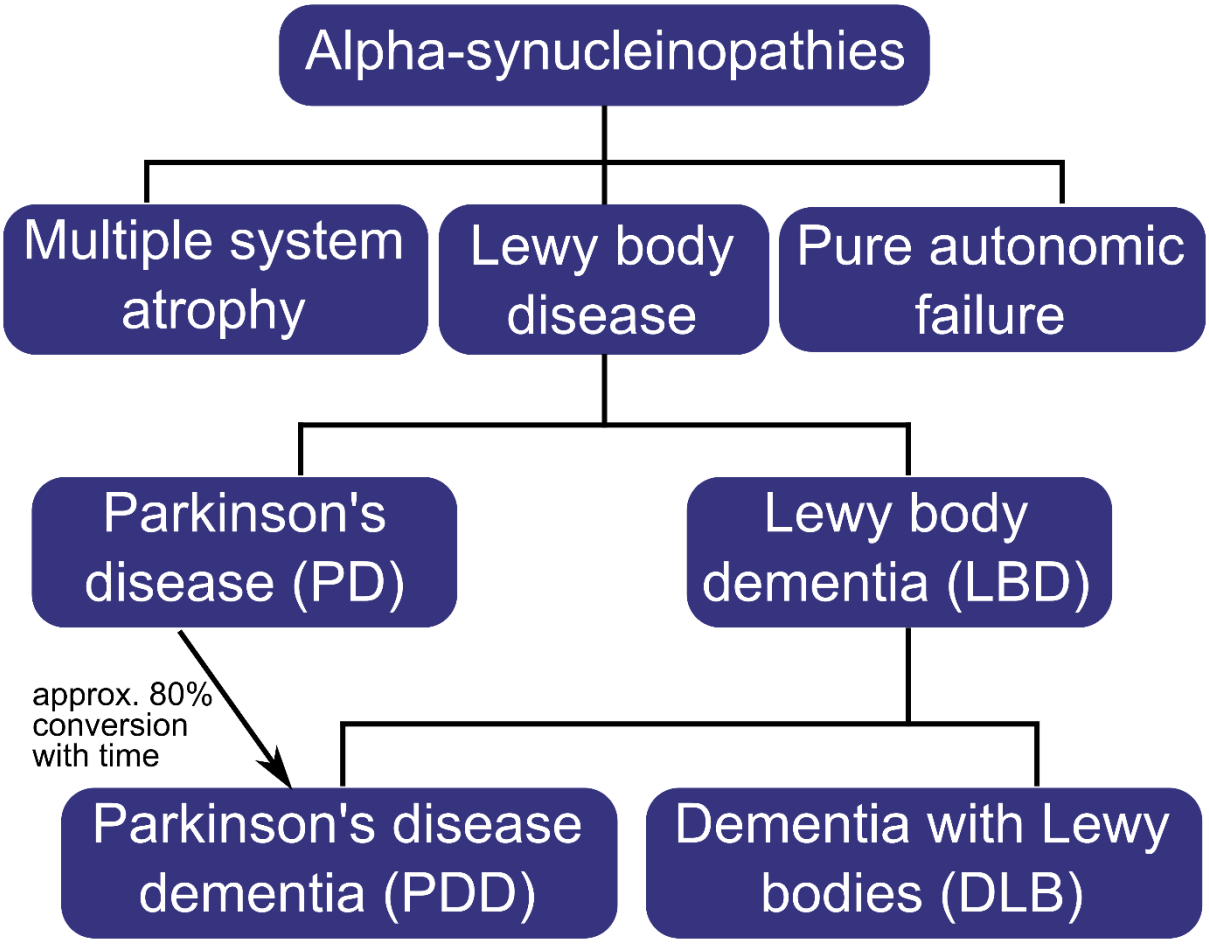

Figure 1.1. Overview of diseases that are characterised by Lewy body pathology.

present in the form of neuritic plaques (extracellular amyloid-beta aggregations) and neurofibrillary tangles (intraneuronal accumulation of hyperphosphorylated tau) (Dugger et al., 2014; Howlett et al., 2015). Conversely, Lewy body pathology can also be present in cases with clinical AD and is typically found in the amygdala (Lippa et al., 2005; Popescu et al., 2004).

While it is still unclear how Lewy body and other pathologies lead to the clinical manifestation of the disease, several studies have identified possible clinicopathological correlations. In PD, the development of dementia has been associated with the presence of cortical and limbic Lewy bodies (Hurtig et al., 2000; Kövari et al., 2003) as well as cholinergic deficits (Klein et al., 2010), and the level of cognitive impairment in DLB has been related to the severity of Lewy body pathology (Beach et al., 2009). Furthermore, Lewy bodies in the hippocampus have been shown to be associated with memory impairment in DLB (Adamowicz et al., 2017). Neuronal loss in the substantia nigra is the strongest correlate of Parkinsonism in LBD (McKeith et al., 2017). The presence of visual hallucinations has been related to Lewy body pathology in limbic regions (Ferman et al., 2013a) and the

temporal lobe (Harding et al., 2002) (with relative sparing of early visual areas (Erskine et al., 2015)) and to disturbances in cholinergic neurotransmission (Ballard et al., 2000). The relation between pathological changes and cognitive fluctuations is less clear (Harding et al., 2002). There is, however, evidence that higher binding of nicotinic receptors in the temporal cortex and thalamus may be associated with fluctuating cognition (Ballard et al., 2002b; Pimlott et al., 2006). Additionally, it has been suggested that cognitive fluctuations are more prevalent in patients with neocortical Lewy bodies as opposed to patients with predominantly striatal or limbic pathology (Schneider et al., 2012). The effect of concomitant AD pathology on the clinical presentation of LBD will be discussed in more detail in Section 1.1.4.

1.1.3 DLB vs PDD

DLB and PDD are differentiated clinically based on the time-course of symptom development: DLB is diagnosed if dementia occurs before or simultaneously with Parkinsonism whereas PDD is diagnosed if dementia develops in the context of well-established PD. For practical purposes the one-year rule is applied where DLB is diagnosed in patients who develop cognitive symptoms before or within one year of the onset of Parkinsonism and where PDD is diagnosed if the onset of motor symptoms precedes the development of cognitive symptoms by more than a year (Aarsland et al., 2009b; McKeith et al., 2017, 2005). Numerous studies have investigated similarities and differences between DLB and PDD in terms of behavioural, clinical, morphological, and neurochemical characteristics. However, it is still debated whether they represent distinct disease entities or merely different points on the same disease spectrum (e.g. Friedman, 2018; Jellinger and Korczyn, 2018) (see Table 1.1 for a comparison of clinical and pathological characteristics between DLB and PDD).

Table 1.1. Comparison of clinical and pathological characteristics between DLB and PDD.

	DLB	PDD
Attention	+++	+++
Executive dysfunction	+++	+++
Cognitive fluctuations	+++	++
Parkinsonism	variable	present
Visual hallucinations	+++	++
Delusions	+++	++
Responsiveness to levodopa	+/-	+
Nigrostriatal loss	+	+++
Cortical/striatal pathology	+++	++
Amyloid deposition	moderate – high	low

DLB, dementia with Lewy bodies; PDD, Parkinson's disease dementia.

From a neuropathological and neurochemical perspective, DLB and PDD are difficult to discriminate, with no hallmark pathological feature that distinguishes the two (Harding and Halliday, 2001; Klein et al., 2010; Tsuboi and Dickson, 2005). Neuronal loss in the substantia nigra might be more severe in PDD relative to DLB (Tsuboi and Dickson, 2005), whereas pathological burden in the striatum has been found to be higher in DLB than in PDD (Jellinger and Attems, 2006). Additionally, more severe Lewy body pathology in the temporal lobe has been reported in DLB than in PDD (Harding et al., 2002). Nevertheless, similar striatal dopaminergic deficits have been observed in both conditions (Klein et al., 2010). Some studies report a higher prevalence of AD pathology in DLB than in PDD (Edison et al., 2008; Gomperts et al., 2008; Harding and Halliday, 2001; van Steenoven et al., 2016) whereas others have failed to find such differences (Tsuboi and Dickson, 2005).
Studies of grey and white matter differences between DLB and PDD have found conflicting results. While one study did not find any differences in white matter hyperintensities (Burton et al., 2006), others have found more severe white matter abnormalities in DLB than in PDD which has been hypothesised to be due to concurrent AD pathology in DLB patients (Joki et al., 2018; Lee et al., 2010). Similarly, for grey matter atrophy some studies described more pronounced loss in DLB compared to PDD (Beyer et al., 2007; Joki et al., 2018; Lee et al., 2010) whereas other studies could not identify differences between the groups (Burton et al., 2004; Hattori et al., 2012; Janzen et al., 2012; Kenny et al., 2008; Tam et al., 2005). DLB and PDD show similar deficits in blood perfusion across the brain with slightly more pronounced hypoperfusion in DLB than in PDD (Hattori et al., 2012; Mito et al., 2005). Additionally, functional connectivity has been shown to be comparable between the two conditions, with only subtle differences in motor- and attention-related networks (Peraza et al., 2015a). Overall, cognitive and neuropsychological profiles have been shown to be similar (Aarsland et al., 2003; Aldridge et al., 2018; Noe et al., 2004), with slight differences in verbal learning and memory which may be more impaired in DLB than in PDD (Brønnick, 2015; Filoteo et al., 2009; Mondon et al., 2007; Park et al., 2011). Sleep and motor abnormalities are comparable in DLB and PDD (Boddy et al., 2007; McKeith et al., 2005) as are visuoperceptual impairment and neuropsychiatric symptoms (Fields, 2017; Mosimann et al., 2004). The phenomenology of visual hallucinations and delusions is similar in the LBD subgroups (Aarsland et al., 2001; Mosimann et al., 2006). However, both delusions and hallucinations have been shown to be more prevalent in DLB than in PDD (Aarsland et al., 2001; Savica et al., 2013). While cognitive fluctuations are clinically indistinguishable between DLB and PDD (Ballard et al., 2002a; Varanese et al., 2010) they occur with a higher prevalence in DLB (Savica et al., 2013). Furthermore, attentional and executive impairment

has been reported to be comparable in both conditions (Ballard et al., 2002a; Firbank et al., 2016; Mondon et al., 2007), with one study reporting slightly worse deficits in DLB than in PDD (Park et al., 2011). In particular, a functional neuroimaging study of attentional dysfunction in LBD did not find any behavioural and only subtle neuroimaging differences between DLB and PDD, indicating that similar processes underlie attentional-executive impairment in both groups (Firbank et al., 2016). From an electrophysiological perspective, there are no differences between DLB patients and PDD patients with cognitive fluctuations (Bonanni et al., 2008). Further support comes from a meta-analysis of attention and executive dysfunction in DLB and PDD in which the authors did not find statistical evidence for a difference between the two groups (Brønnick, 2015).

In summary, while some clinical and neuropsychological studies have found subtle differences between DLB and PDD, the overall presentation of the two patient groups seems to be similar, especially with respect to attentional impairment and cognitive fluctuations. DLB and PDD patients were therefore combined into one Lewy body dementia group for most analyses in this thesis. Nevertheless, since the exact relationship between DLB and PDD is still unclear and previous studies have reported conflicting results, additional analyses were performed to investigate potential differences between the two groups in terms of the clinical, behavioural, and neuroimaging measures presented in this thesis.

1.1.4 LBD vs AD

While the specificity of the clinical diagnostic criteria for LBD is high, i.e. most patients with a clinical diagnosis of LBD will show significant Lewy body pathology at autopsy (McKeith et al., 2000a), their sensitivity can be low which is mainly due to patients being misdiagnosed with AD (Litvan et al., 2003, 1998; Lopez et al., 2002; Rizzo et al., 2017). This prevents misdiagnosed patients from receiving appropriate treatment, can have potentially adverse effects due to neuroleptic sensitivity in LBD (McKeith et al., 1992a), and constitutes a problem when stratifying patients for research studies or clinical trials. While LBD and AD are in theory characterised by different phenotypes, there is often considerable clinical overlap (Thomas et al., 2018). While AD is characterised by more pronounced impairment in episodic memory relative to LBD in the early stages (Calderon, 2001; Economou et al., 2016; Kraybill et al., 2005; Noe et al., 2004), memory impairment usually develops with disease progression in LBD (McKeith et al., 2017). In contrast, LBD patients show more severe attentional and executive impairment than AD patients (Kraybill et al., 2005; Noe et al., 2004), and cognitive fluctuations (Ferman et al., 2004) as well as visual hallucinations (Thomas et al., 2018) seem to be the most distinguishing features.

Many LBD cases, especially those with DLB, exhibit significant concurrent AD pathology (Dugger et al., 2014; Howlett et al., 2015) which can be assessed at autopsy or in vivo using positron emission tomography (PET) imaging or analysis of cerebrospinal fluid (CSF) markers (Donaghy et al., 2015). This additional pathological burden has been related to higher global atrophy rates in LBD (Nedelska et al., 2015; Sarro et al., 2016; Shimada et al., 2013) and to medial temporal lobe atrophy which is typically seen in clinical AD (Elder et al., 2017; van der Zande et al., 2018). Amyloid-beta deposition has also been associated with lower medial temporal lobe perfusion in DLB (Donaghy et al., 2018). From a clinical point of view, the severity of AD pathology is inversely related to the LBD clinical phenotype (Ballard et al., 2004; Fujishiro et al., 2008; McKeith et al., 2005), and LBD patients with mixed pathology show more severe memory impairment than pure Lewy body cases (Kraybill et al., 2005). Furthermore, coexisting AD pathology in LBD is associated with a more severe manifestation of the disease (van Steenoven et al., 2016), a higher risk of institutionalisation and mortality (Graff-Radford et al., 2016; Lemstra et al., 2017), lower cognitive performance (Foster et al., 2010), and a more rapid cognitive decline (Blanc et al., 2017; Howlett et al., 2015; Kraybill et al., 2005; Sarro et al., 2016).

Based on these considerations, the reasons for including an AD group in the analyses of this thesis are two-fold. Firstly, AD patients were included so as to get a better understanding of commonalities and differences between these two common forms of dementia which may be important in the context of a differential diagnosis. Secondly, AD patients were included as a disease-comparator group to disentangle which of the differences that were observed in the comparison between patients with LBD and healthy controls might be a general dementia phenomenon and which might be specific LBD-related changes.

1.2 Cognitive Fluctuations

Even though the recognition of DLB as a distinct diagnostic entity is relatively recent (McKeith et al., 1992b), cognitive fluctuations have long been recognised as a salient feature of the phenotype, as described in early clinicopathological series (Forno et al., 1978; Gibb et al., 1987; Woodard, 1962). This culminated in the identification of cognitive fluctuations as a key feature of the disease in the first consensus criteria (McKeith et al., 1996). They are now regarded as one of the most characteristic features of the condition and form an important element in differential diagnosis (McKeith, 2002; McKeith et al., 1992b). However, accurate identification of cognitive fluctuations can pose a clinical challenge (Cummings, 2004; Litvan et al., 1998; Mega et al., 1996).

Data pertaining to the prevalence of cognitive fluctuations in DLB are heterogeneous, with

rates of 45-90% reported (Bradshaw et al., 2004; Byrne et al., 1989; Lee et al., 2012; Varanese et al., 2010; Verghese et al., 1999). They are also common in PDD, albeit being slightly less prevalent than in DLB (Ballard et al., 2002a; Savica et al., 2013).
While some data suggest that cognitive fluctuations are a late manifestation of the disease, occurring on average 4.5 years after onset of cognitive symptoms (Molano et al., 2010), others have identified cognitive fluctuations in the prodromal phase in 30% (Jicha et al., 2010) to 60% (Cagnin et al., 2015) of patients. Furthermore, the presence of cognitive fluctuations in non-amnestic mild cognitive impairment (MCI) cohorts has been shown to be predictive of conversion to DLB (Ferman et al., 2013b; Sadiq et al., 2017), and it has been described as one of the most characteristic features of prodromal DLB (Donaghy et al., 2017). Cognitive fluctuations are associated with impaired quality of life and inability to perform activities of daily living (Brønnick et al., 2006; Sun et al., 2018). They contribute to greater disability and caregiver burden (Ballard et al., 2001b; Lee et al., 2013), and can present the clinician with significant challenges in the assessment of decision-making capacity (Shulman et al., 2015; Trachsel et al., 2015). Cognitive fluctuations therefore constitute an important therapeutic target. However, their aetiology is still poorly understood.

1.2.1 Clinical and behavioural manifestation of cognitive fluctuations

Qualitatively, the clinical manifestation of cognitive fluctuations in LBD is primarily that of an altered level of alertness and attention with a marked amplitude between best and worst performances ranging from episodes of switching off or going blank, to spontaneous remission to normal or near-normal performance (Ballard et al., 2002a; McKeith, 2002; McKeith et al., 1996) (see Figure 1.2). This is described as having a spontaneous, periodic, and transient quality, as opposed to the fluctuations in cognitive performance seen in AD in response to inter-current environmental demands; informants in the latter circumstance more frequently cite episodes of memory failure rather than significant alterations in alertness (Bradshaw et al., 2004). As such, cognitive fluctuations in LBD are largely an internally-mediated process, whilst fluctuations in AD are more frequently a consequence of an altered external environment. While fluctuations in LBD are classically transient, clinical experience has long suggested that there may be a spectrum of severity, from periods of altered attention or drowsiness – lasting seconds or minutes – to days of obtundation (McKeith et al., 1996, 1992b). However, there does not seem to be a clear diurnal pattern, and mild diurnal/nocturnal variations that occur in other dementia subtypes should not be considered to support a clinical diagnosis of cognitive fluctuations (McKeith et al., 1996).

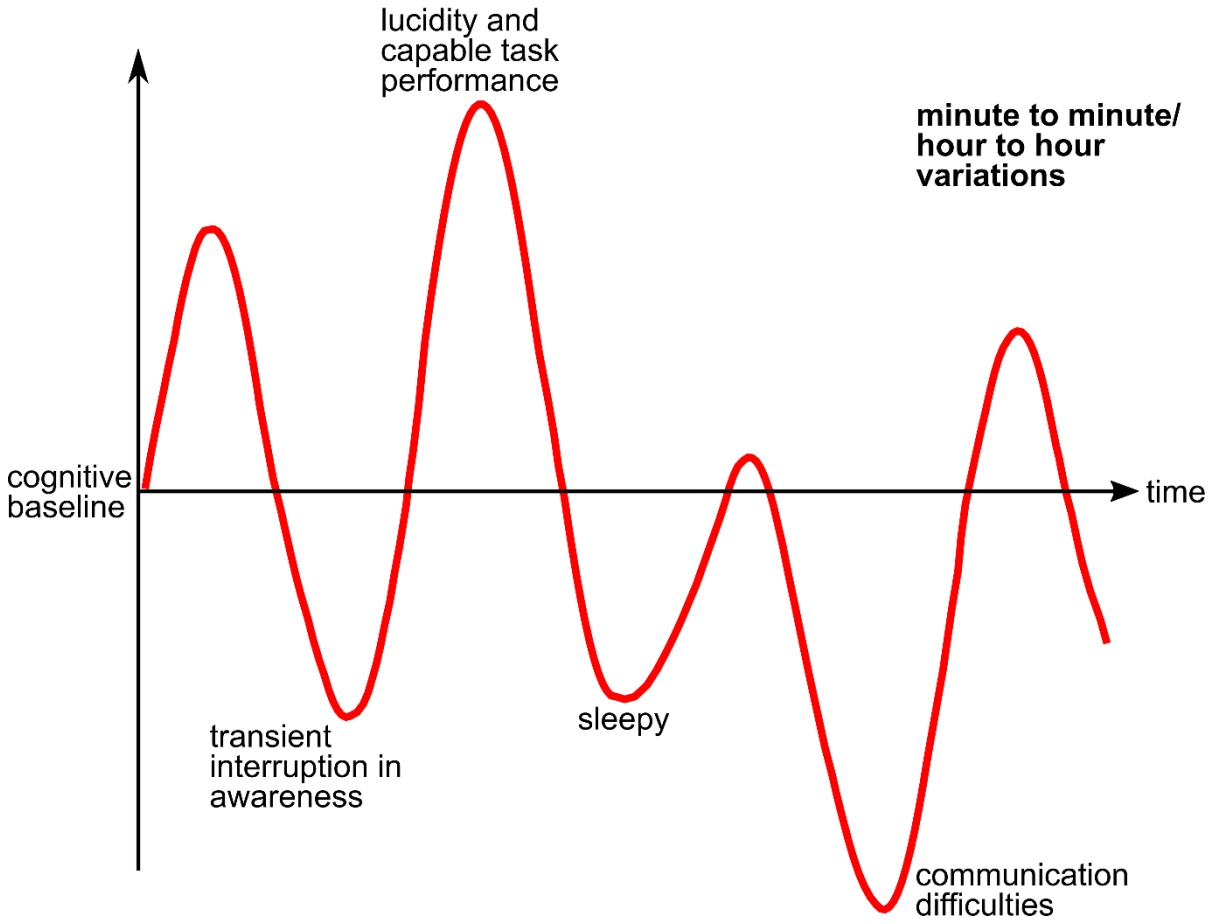

Figure 1.2. Cognitive fluctuations in LBD.

Behaviourally, cognitive fluctuations have been associated with impairments in reaction time (RT) performance on tests of sustained attention. LBD patients with a higher severity of cognitive fluctuations show slower RTs, impaired vigilance, and higher variability in RT performance than those with less severe fluctuations (Ballard et al., 2002a, 2001b; Onofrj et al., 2003; Walker et al., 2000a). Furthermore, the severity of cognitive fluctuations as assessed by clinical fluctuation scores has been shown to correlate with variability in attentional performance across 90 seconds (Walker et al., 2000a, 2000b, 2000c). These results highlight the relationship between cognitive fluctuations and fluctuations in attention and alertness, and indicate that cognitive fluctuations might be associated with perturbations in attentional circuitry. Furthermore, it has been suggested that measures of attentional variability might represent an objective and accurate tool to characterise and quantify cognitive fluctuations in LBD (Walker et al., 2000a).

In addition to attentional impairment, there seems to be a sleep/arousal dimension contributing to cognitive fluctuations. Patients with advanced LBD have extremely poor sleep efficiency and may demonstrate profound distortions in sleep-wake architecture (Pao et al., 2013). Hypersomnolence has been incorporated as a supportive feature in the most recent

DLB diagnostic criteria (McKeith et al., 2017), and one of the clinical tools to investigate cognitive fluctuations specifically enquires as to the presence of excessive daytime somnolence (Ferman et al., 2004). The presence of RBD appears to correlate with cognitive fluctuations in DLB (Escandon et al., 2010), and some studies suggest that sleep disturbances and cognitive fluctuations may reciprocally potentiate each other (Cagnin et al., 2016). However, this may also represent concomitant pathological involvement of anatomically related structures in brainstem-thalamo-cortical networks (Antelmi et al., 2016; Terzaghi et al., 2013). Additionally, other studies do not find any correlations between polysomnography parameters as well as multiple sleep latency tests and cognitive fluctuations in DLB (Bliwise et al., 2014; Ferman et al., 2014). Nevertheless, certain findings suggest that there may be two distinct dimensions to fluctuations, one related to attention and one related to arousal/alertness.

1.2.2 Clinical assessment tools

A number of clinical assessment tools have been devised in an effort to better identify cognitive fluctuations and distinguish fluctuations in LBD from those seen in other dementia subtypes (Ferman et al., 2004; Lee et al., 2014; Walker et al., 2000b).

The Clinician Assessment of Fluctuation (CAF), a series of questions administered to an informant by an experienced clinician, assesses the severity and duration of fluctuations in cognition and levels of confusion during the month prior to the assessment (Walker et al., 2000b). Cognitive fluctuations are considered to be present, if the informant is able to provide a clear example. If present, severity and duration of the cognitive fluctuations are rated on a scale from 0-4; both scores are then multiplied to obtain a total score ranging from 0-12 with a score of 0 representing no fluctuations and a score of 12 representing severe fluctuations (a score of 16 would indicate a continuously confused state and hence no fluctuations). This scale showed fair inter-rater reliability with excellent reliability in scoring severe fluctuations (Van Dyk et al., 2016) as well as good sensitivity and specificity at distinguishing DLB from AD and vascular dementia (Walker et al., 2000b); however, it needs to be administered by an experienced clinician which makes its application in clinical trials challenging.

Similarly, the Mayo fluctuations scale is a 19-item questionnaire delivered to the patient's caregiver to evaluate fluctuating cognition during the month prior to the assessment (Ferman et al., 2004). A total score is calculated; additionally, a cognitive and an arousal subscore can be derived by focussing on questions related to cognitive and arousal aspects of fluctuations, respectively (Bliwise et al., 2014). It can reliably differentiate DLB from AD (Ferman et al., 2004), however, its utility in distinguishing DLB from other dementia subtypes remains

unclear (Lee et al., 2012).

The One Day Fluctuation Assessment Scale is a brief clinician-rated scale to evaluate cognitive fluctuations over a period of 24 hours prior to the assessment (Walker et al., 2000b). While Walker et al. (2000b) have reported good sensitivity at differentiating DLB from AD and healthy controls, Bradshaw et al. (2004) have only found low sensitivity for detecting cognitive fluctuations in DLB patients.

Building on these fluctuation scales, the Dementia Cognitive Fluctuation Scale is a more recently developed scale aiming to address some of the difficulties associated with previous fluctuation measures (Lee et al., 2014). It demonstrates good test-retest and inter-rater reliability and accurately distinguishes between LBD, AD, and vascular dementia, especially in patients with mild to moderate dementia (Lee et al., 2014). While the full version can be applied in research studies, a shorter four-item clinician version is envisaged to facilitate its use in clinical practice (Lee et al., 2014).

However, many challenges regarding the accurate clinical assessment of fluctuations still remain, and several studies have underscored the importance of developing more objective measures of cognitive fluctuations (Bonanni et al., 2015; Lee et al., 2012; Walker et al., 2000a).

1.2.3 Symptomatic treatment of cognitive fluctuations

The prevalence of cognitive fluctuations in LBD patients and their negative impact on patient and carer quality of life highlights the need for targeted therapies; however, in the therapeutic armoury for LBD, they are something of a neglected symptom.

Acetylcholinesterase inhibitors have shown some efficacy in treating cognitive fluctuations. There is evidence for a role of donepezil (Onofrj et al., 2003) and galantamine (Edwards et al., 2007) in ameliorating clinical features of cognitive fluctuations and associated electroencephalogram (EEG) abnormalities, while the benefit of rivastigmine and memantine in this regard is less certain (Stinton et al., 2015). Similarly, the finding that deep brain stimulation of the nucleus basalis of Meynert (NBM) stabilises alertness and other cognitive features in a PDD patient with cognitive fluctuations (Freund et al., 2009) suggests that this may be a potential therapeutic option. However, a more recent randomised clinical trial of NBM stimulation in patients with PDD did not find the same effects on cognition (Gratwicke et al., 2018). Following the conjecture that fluctuating cognition might be related to a disorder of sleep or arousal, there is encouraging preliminary evidence for the efficacy of modafinil and armodafinil even though numbers are limited (Varanese et al., 2013).

1.2.4 Neural correlates of cognitive fluctuations in LBD

Cognitive fluctuations in LBD are likely to be attributable to a separate pathophysiological process from that driving the progressive cognitive decline, as these fluctuations, by nature, are transient and reversible. This hypothesis has been investigated using structural and functional neuroimaging, as well as electrophysiological techniques. Tables 1.2 - 1.5 show an overview of studies that examined possible neural correlates of cognitive fluctuations in LBD using different neuroimaging methods.

Structural neuroimaging (Table 1.2)

DLB and PDD are generally characterised by less severe structural abnormalities than AD with a relative preservation of the medial temporal lobe (Barber et al., 2000; Beyer et al., 2007; Burton et al., 2009, 2004, 2002; Mak et al., 2014; Takahashi et al., 2010; Tam et al., 2005; Watson et al., 2012). Nevertheless, a recent meta-analysis of voxel-based morphometry (VBM) studies identified consistent grey matter atrophy in the basal ganglia (putamen and globus pallidus), insular cortex, and lateral temporal areas in patients with DLB compared to controls (Zhong et al., 2014). There does not, however, appear to be a clear-cut structural correlate for cognitive fluctuations. No association was found between hippocampal (Elder et al., 2017; Kantarci et al., 2012), cerebellar (Colloby et al., 2014), anterior cingulate or insular (Blanc et al., 2016) grey matter volume and the severity of cognitive fluctuations. A possible contribution of thalamic structural abnormalities has been suggested based on the finding that thalamic atrophy is associated with the severity of attentional deficits in DLB (Watson et al., 2017). Suggesting an involvement of cholinergic structures in cognitive fluctuations, several studies have identified structural abnormalities within the substantia innominata of patients with DLB, which are more pronounced than in patients with AD (Colloby et al., 2017; Hanyu et al., 2007, 2005; Whitwell et al., 2007) and which are related to the severity of cognitive fluctuations (Colloby et al., 2017).

Subcortical and cortical white matter lesions are common in DLB patients (Bozzali et al., 2005; Kantarci et al., 2010; Sarro et al., 2017); however, there appears to be no correlation between the burden of white matter lesions and cognitive fluctuations (Kantarci et al., 2010; Sarro et al., 2017). White matter degeneration in the anterior thalamic radiation which has been observed in DLB is not correlated with fluctuation severity (Delli Pizzi et al., 2015a). Similarly, disturbances in the projections from thalamus to prefrontal and parieto-occipital cortices present in DLB do not correlate with cognitive fluctuation severity (Delli Pizzi et al., 2015b).

Table 1.2. Structural MRI studies of cognitive fluctuations.

	Methods	Participants	Fluctuation measure	Results
Kantarci et al. (2010)	DTI	30 DLB, 30 AD, 60 HC	Mayo	Elevated MD in amygdala and decreased FA in inferior longitudinal fasciculus in DLB compared to HC, but no difference between fluctuating and non-fluctuating DLB patients for these measures
Kantarci et al. (2012)	VBM	21 DLB, 21 AD, 42 HC	Mayo	No difference in hippocampal volume between DLB patients with and without cognitive fluctuations
Colloby et al. (2014)	VBM	41 DLB, 48 AD, 39 HC	CAF	Cerebellar grey matter loss in DLB compared to HC, but no significant correlations with CAF
Delli Pizzi et al. (2015a)	DTI	14 DLB, 14 AD, 15 HC	CAF	Degeneration of anterior thalamic radiation in DLB compared to HC, but no correlation with CAF
Delli Pizzi et al. (2015b)	DTI	16 DLB, 16 AD, 13 HC	CAF	Increased MD in thalamic regions projecting to prefrontal and parieto-occipital cortices in DLB compared to HC, but not correlated with CAF in DLB
Blanc et al. (2016)	VBM	28 pDLB, 27 pAD, 33 HC	CAF	Grey matter atrophy in insulae and anterior cingulate cortex in prodromal DLB compared to HC, but not correlated with CAF in DLB
Colloby et al. (2017)	VBM	41 DLB, 47 AD, 39 HC	CAF	Bilateral grey matter atrophy in substantia innominata (SI) in DLB and AD compared to HC; negative correlation between right SI volume and CAF in DLB
Elder et al. (2017)	cortical thickness	65 DLB, 76 AD, 63 HC	CAF	Hippocampal atrophy less severe in DLB than in AD and not correlated with CAF in DLB
Sarro et al., (2017)	cerebrovascular lesions	81 DLB, 240 AD	Mayo	No difference in white matter hyperintensities between DLB patients with and without cognitive fluctuations
Watson et al. (2017)	thalamic atrophy	35 DLB, 35 HC	attention task	Atrophy of left pulvinar and ventral lateral nucleus of the thalamus associated with impaired attentional function in DLB

AD, Alzheimer's disease; CAF, Clinician Assessment of Fluctuation; DLB, dementia with Lewy bodies; DTI, diffusion tensor imaging; FA, fractional anisotropy; HC, healthy controls; Mayo, Mayo Fluctuation scale; MD, mean diffusivity; MRI, magnetic resonance imaging; pAD, prodromal AD; pDLB, prodromal DLB; SI, substantia innominata; VBM, voxel-based morphometry.

The lack of a clear structural correlate of cognitive fluctuations is not surprising given their transient and reversible nature, and the fact that Lewy body pathology has been shown to have little direct involvement in cerebral atrophy (Burton et al., 2009; Mak et al., 2015a, 2015b). It has therefore been suggested that cognitive fluctuations might arise from large-scale functional network perturbations within the brain. These can be assessed by functional neuroimaging and electrophysiological methods as discussed in the following paragraphs.

Functional neuroimaging (Table 1.3)

A potential involvement of attentional networks in cognitive fluctuations has been investigated through functional connectivity analyses at rest and during task performance using functional magnetic resonance imaging (fMRI). In patients with DLB, Peraza et al. (2014) have identified a desynchronisation of several cortical and subcortical areas related to the left fronto-parietal attention network which was associated with the severity and frequency of cognitive fluctuations. Similarly, Franciotti et al. (2013) have found that functional connectivity between right middle frontal gyrus and right lateral parietal cortex was negatively correlated with fluctuation severity in DLB. Furthermore, attention network connectivity has been found to be decreased in LBD compared to control participants during the execution of an attention task; however, this was not related to the severity of cognitive fluctuations in the patient groups (Kobeleva et al., 2017). A possible relation between cognitive fluctuations and aberrant connectivity in basal ganglia and limbic networks has also been reported (Lowther et al., 2014).

Another neural network potentially involved in cognitive fluctuations is the default mode network (DMN) which is active in resting conditions, but deactivated during task performance (Binder et al., 1999; Buckner, 2005; Gusnard and Raichle, 2001). However, data to support this concept are conflicting. One resting-state fMRI study reported reductions in DMN functional connectivity in patients with DLB compared to AD patients and controls (Lowther et al., 2014) whereas others showed increased DMN connectivity (Kenny et al., 2012) or did not find any evidence for connectivity alterations within the DMN (Galvin et al., 2011; Peraza et al., 2014). In particular, Franciotti et al. (2013) have found no evidence for a correlation between DMN abnormalities and cognitive fluctuations in DLB; even in patients with severe fluctuations, the DMN appeared to be intact, indicating that changes within the DMN alone cannot account for cognitive fluctuations in DLB.

A more intricate explanation may lie in the interplay between attentional and default mode networks which is important for attentional performance (Sonuga-Barke and Castellanos, 2007; Weissman et al., 2006). In support of this, several studies have found

Table 1.3. Functional MRI and MRS studies of cognitive fluctuations.

	Methods	Participants	Fluctuation measure	Results
Sauer et al. (2006)	Attention task-fMRI	9 DLB, 10 AD, 13 HC	attention task	Reduced attention task-related deactivation of the DMN in both AD and DLB
Franciotti et al. (2013)	Rest-fMRI, seed analysis	18 DLB, 18 AD, 15 HC	CAF	No evidence of resting-state DMN disruption in presence of cognitive fluctuations
Lowther et al. (2014)	Rest-fMRI, dual regression	15 DLB, 13 AD, 40 HC	CAF	Positive correlation between basal ganglia and limbic network connectivity and CAF in DLB
Peraza et al. (2014)	Rest-fMRI, dual regression	16 DLB, 17 HC	CAF	Positive correlation of connectivity within left fronto-parietal network clusters in pallidum, lingual gyrus, and putamen with CAF in DLB
Peraza et al. (2015b)	Rest-fMRI, graph theory	18 DLB, 19 AD, 17 HC	CAF	Positive correlation between normative path length and CAF in DLB
Peraza et al. (2016)	Rest fMRI, ReHo	19 DLB, 18 AD, 16 HC	CAF	No significant correlations between ReHo abnormalities and CAF in DLB
Kobeleva et al. (2017)	Attention task-fMRI	30 LBD, 20 AD, 21 HC	CAF, Mayo	Attention network connectivity reduced in LBD compared to HC, but no significant correlations with CAF or Mayo scores in LBD
Chabran et al. (2018)	Visuoperceptual task-fMRI	26 DLB, 29 AD, 22 HC	CAF	Positive correlation between DMN synchronisation with task paradigm and CAF in DLB
Graff-Radford et al. (2014)	MRS	34 DLB, 35 AD, 148 HC	Mayo	No difference in metabolites in frontal, posterior cingulate, and occipital regions between DLB with and without fluctuations
Delli Pizzi et al. (2015b)	MRS	16 DLB, 16 AD, 13 HC	CAF	Increase in tCho/tCr in right thalamus in DLB compared to AD, this increase positively correlates with CAF
Su et al. (2016)	MRS	35 DLB, 36 AD, 35 HC	CAF	Negative correlation between hippocampal NAA/Cr levels and CAF in DLB

AD, Alzheimer's disease; CAF, Clinician Assessment of Fluctuation; CRT, choice reaction time; DLB, dementia with Lewy bodies; DMN, default mode network; fMRI, functional magnetic resonance imaging; HC, healthy controls; LBD, Lewy body dementia; Mayo, Mayo Fluctuation scale; MRS, magnetic resonance spectroscopy; NAA/Cr, N-acetyl-aspartate/total creatine ratio; ODFAS, One Day Fluctuation Assessment Scale; ReHo, regional homogeneity; rest-fMRI, resting-state fMRI; RT, reaction time; tCho/tCr, total choline/total creatine ratio.

abnormalities in the dynamic synchronisation between default mode and attention networks during the execution of an attention task in patients with LBD (Chabran et al., 2018; Firbank et al., 2018, 2016; Kobeleva et al., 2017; Sauer et al., 2006). In particular, Chabran et al. (2018) have shown that disturbances in the task-related modulation of DMN activity are associated with the severity of cognitive fluctuations, suggesting that a disturbance of the dynamic switching between task-positive and default mode networks might be related to cognitive fluctuations in DLB.

Global network measures, analysing the brain's functional connectivity by means of graph theory, have identified a correlation between the severity of cognitive fluctuations and an increase in path length (i.e. less efficient network topography) in DLB (Peraza et al., 2015b). However, this might be a more general marker of disease severity given the relationship between these graph measures and more general markers of cognitive impairment (Peraza et al., 2015b). A study of regional homogeneity measuring local functional connectivity identified DLB-related changes in sensory-motor and temporal regions (Peraza et al., 2016); however, no correlation was found between these regional abnormalities and cognitive fluctuation severity, supporting, indirectly, the hypothesis that cognitive fluctuations might be related to perturbations in large-scale functional networks rather than local changes in connectivity.

Magnetic resonance spectroscopy (Table 1.3)

Magnetic resonance spectroscopy (MRS) can be used to characterise biochemical changes in the brain quantitatively assessing in-vivo levels of several metabolites such as N-acetylaspartate/creatine (NAA/Cr) which is considered to be a marker of neuronal integrity and is commonly reduced in AD patients (Kantarci and Graff-Radford, 2013). While NAA/Cr levels have been found to be reduced in occipital regions in patients with DLB, there does not appear to be a difference in NAA/Cr levels between DLB patients with fluctuations compared to DLB patients without fluctuations in frontal, posterior cingulate, and occipital regions (Graff-Radford et al., 2014a). However, using a whole-brain approach instead of restricting their analysis to *a priori* defined regions, Su et al. (2016) identified a negative correlation between hippocampal NAA/Cr levels and cognitive fluctuation severity in DLB, indicating that neuronal changes within the hippocampus might play a role in cognitive fluctuations in DLB. Furthermore, higher choline/creatine levels as measured by MRS have been observed in the thalamus of DLB patients compared to controls. This increase correlated with fluctuation frequency and severity, suggesting that neurochemical imbalances within the thalamus might be involved in the aetiology of cognitive fluctuations in DLB (Delli Pizzi et al., 2015b).

Radionuclide imaging (Table 1.4)

Occipital hypoperfusion/hypometabolism has been consistently shown in patients with DLB compared to patients with AD and healthy controls (Colloby et al., 2002; Imamura et al., 1999; Ishii et al., 1998; Kantarci et al., 2012; Lobotesis et al., 2001; Minoshima et al., 2001; Perneczky et al., 2008; Sato et al., 2007; Shimizu et al., 2005; Yoshida et al., 2015). This deficit in blood perfusion and energy metabolism affects primary visual as well as visual association areas and the precuneus (Kemp et al., 2005; Mito et al., 2005), and can already be identified at the prodromal stage of DLB (Fujishiro et al., 2013). Several studies suggest that metabolic and perfusion changes might be related to the severity of cognitive fluctuations in LBD: Osaki et al. (2005) have found hypoperfusion in bilateral parietal association areas, medial parietal, and dorsal occipital lobes in PDD patients with cognitive fluctuations compared with non-fluctuators. Similarly, a reduction in occipital metabolism was reported for fluctuating compared to non-fluctuating DLB patients (Kantarci et al., 2012). In a longitudinal study, O'Brien et al. (2005) have found a decrease in occipital perfusion and an increase in thalamic perfusion to be associated with an increase in fluctuation severity over the course of one year.

Metabolism within the posterior cingulate cortex which is markedly affected in AD is normally preserved in DLB (the so-called cingulate island sign) (Graff-Radford et al., 2014b; Iizuka and Kameyama, 2016; Lim et al., 2009; O'Brien et al., 2014), suggesting that this does not affect cognitive fluctuations (Iizuka and Kameyama, 2016). In addition to the fMRI studies discussed above, more evidence for an involvement of complex functional network perturbations in cognitive fluctuations is provided by a perfusion single photon emission computed tomography (SPECT) study observing aberrant perfusion in an interconnected series of structures mainly in parietal and motor areas (including basal ganglia) which was found to be correlated with the severity of cognitive fluctuations (Taylor et al., 2013).

Even though PET and SPECT studies have consistently identified a relative loss of dopaminergic neurons within the substantia nigra in LBD (Colloby et al., 2004; Marquie et al., 2014; McKeith et al., 2007; O'Brien et al., 2004; Walker et al., 2002), results regarding an association between dopamine abnormalities and fluctuation severity in LBD are conflicting. While two studies did not see a difference in striatal dopamine transporter density between DLB patients with cognitive fluctuations compared to those without fluctuations (Shimizu et al., 2017; Ziebell et al., 2013), a third study identified a significant negative correlation between striatal dopamine transporter density and cognitive fluctuation severity in DLB (Iizuka and Kameyama, 2016). However, cognitive fluctuations are generally considered to be

Table 1.4. PET and SPECT studies of cognitive fluctuations.

	Methods	Participants	Fluctuation measure	Results
O'Brien et al. (2005)	Perfusion SPECT	14 DLB, 15 PDD	CAF	Increase in CAF over one year associated with increased thalamic and decreased inferior occipital perfusion
Osaki et al. (2005)	Perfusion SPECT	10 PDD, 20 PD	absent/ present	Hypoperfusion in bilateral parietal association areas, medial parietal, and dorsal occipital lobes in fluctuators compared to non-fluctuators
Foster et al. (2010)	Amyloid PET	6 DLB, 15 PDD, 9 PD-MCI, 9 HC	Mayo	No difference in Mayo fluctuation score between amyloid-positive compared to amyloid-negative LBD patients
Kantarci et al. (2012)	Amyloid PET, FDG-PET	21 DLB, 21 AD, 42 HC	Mayo	No difference in amyloid burden between fluctuating and non-fluctuating DLB patients; occipital FDG uptake lower in fluctuating than in non-fluctuating DLB patients
Taylor et al. (2013)	Perfusion SPECT	19 DLB, 23 AD	CAF, CRT task	Positive correlation between DLB-cognitive motor pattern (characterised by increased perfusion in cerebellum, basal ganglia, and supplementary motor area and decreased perfusion in parietal regions) and CAF and CRT task variability
Ziebell et al. (2013)	DAT-SPECT	51 DLB, 28 HC	absent/ present	No difference between fluctuating and non-fluctuating DLB patients in DAT density in striatum, caudate, and putamen
Iizuka and Kameyama (2016)	FDG-PET, DAT-SPECT	24 DLB, 24 AD	CAF	Negative correlation between striatal DAT density and CAF in DLB; no correlation between cingulate island sign ratio and CAF in DLB
Shimizu et al. (2017)	DAT-SPECT	133 DLB, 95 AD	absent/ present	No difference in striatal DAT binding between fluctuating and non-fluctuating DLB patients
Donaghy et al. (2018)	Amyloid PET	37 DLB, 20 AD, 20 HC	CAF	No difference in CAF between amyloid-positive and amyloid-negative DLB patients and no correlation between amyloid burden and CAF in DLB

AD, Alzheimer's disease; CAF, Clinician Assessment of Fluctuation; CRT, choice reaction time; DAT, dopamine transporter; DLB, dementia with Lewy bodies; FDG-PET; fluorodeoxyglucose PET; HC, healthy controls; LBD, Lewy body dementia; Mayo, Mayo Fluctuation scale; MCI, mild cognitive impairment; PDD, Parkinson's disease dementia; PET, positron emission tomography; SPECT, single photon emission computed tomography.

a non-dopaminergic phenomenon as levodopa does not seem to exert a significantly beneficial effect on cognitive performance in patients or animal models (Kulisevsky et al., 1996; Molloy et al., 2006; Schneider et al., 2013). Finally, there does not seem to be an association between amyloid burden and cognitive fluctuations in LBD (Donaghy et al., 2018; Foster et al., 2010; Kantarci et al., 2012).

Electrophysiology (Table 1.5)

In addition to fMRI and nuclear imaging techniques, electrophysiological methods have provided insights into the functional perturbations underlying cognitive fluctuations. Evoked potential paradigms suggest that delayed P300 latency and reduced amplitude, which are associated with impaired stimulus detection and attention, are related to cognitive fluctuation severity in DLB (Bonanni et al., 2010; Onofrj et al., 2003).

Early resting-state EEG studies in DLB patients have found a correlation between the variability of mean and delta-band EEG frequency and cognitive fluctuation severity as measured by clinical scales as well as trial-to-trial variability on a choice RT test (Walker et al., 2000a, 2000b). These correlations were observed across different timescales, ranging from 90 s to 1 hour to 1 week (Walker et al., 2000b). These early EEG findings suggest that instabilities of oscillatory EEG activity might be related to cognitive fluctuations.

Furthermore, the presence of prominent posterior slow wave activity has strong discriminatory value over AD and correlates with the presence of cognitive fluctuations in LBD (Bonanni et al., 2008, 2016; Stylianou et al., 2018). In addition, temporal slow wave activity has been associated with a history of loss of consciousness in DLB (Briel et al., 1999). The dominant EEG rhythm which is normally within the alpha range, is thought to be slowed down towards pre-alpha/fast theta in LBD patients and the variability of dominant frequency over time has been shown to be increased (Babiloni et al., 2017; Bonanni et al., 2016; Cromarty et al., 2015; Onofrj et al., 2003; Peraza et al., 2018; Stylianou et al., 2018). These EEG abnormalities correlate with the severity of cognitive fluctuations in DLB and can already be identified at the MCI stage, indicating that they might even precede the clinical manifestation of cognitive fluctuations (Bonanni et al., 2015). A slowing of the EEG rhythm has been suggested to be related to cholinergic neurodegeneration (Jeong, 2004; Stoffers et al., 2007), which further highlights the possible involvement of the cholinergic system in the aetiology of cognitive fluctuations.

An analysis of EEG network structure has found a decrease in brain efficiency and impaired neural synchronisation in patients with DLB and PDD compared to patients with AD and controls; however, these abnormalities did not correlate with cognitive fluctuation severity in

Table 1.5. EEG studies of cognitive fluctuations.

	Methods	Participants	Fluctuation measure	Results
Briel et al. (1999)	Rest-EEG	14 DLB, 11 AD	loss of consciousness	Relation between temporal lobe slow wave activity and clinical history of loss of consciousness
Walker et al. (2000a)	Rest-EEG	37 DLB, 61 AD, 22 VaD, 35 HC	CAF, CRT task	Positive correlation between variability of mean EEG frequency across 90 s and CAF and CRT variability
Walker et al. (2000b)	Rest-EEG	15 DLB, 15 AD, 10 HC	CAF, ODFAS	CAF, ODFAS, and CRT variability positively correlated with variability in delta-band EEG frequency
Walker et al. (2000c)	Rest-EEG	15 DLB, 15 AD, 10 HC	CAF, CRT task	CAF positively associated with greater RT variability across different timescales (90 s, 1 hour, 1 week) and greater variability of slow-wave delta EEG across 1 hour
Onofrj et al. (2003)	Rest-EEG, ERP	11 dementia with CF, 12 dementia without CF, 20 HC	CAF, ODFAS	Fluctuating dementia patients show higher P300 trial-to-trial variability, more slow-wave activity, and greater dominant frequency variability than non-fluctuating dementia patients; donepezil has a larger effect in fluctuating compared to non-fluctuating patients
Bonanni et al. (2008)	Rest-EEG	50 DLB, 40 PDD, 50 AD	CAF, ODFAS	Correlation between CAF and dominant frequency, dominant frequency variability, and degree of residual alpha in DLB and PDD
Bonanni et al. (2010)	ERP	36 DLB, 40 AD, 50 HC	CAF, ODFAS	CAF correlated with delayed P300 latency and reduced P300 amplitude in DLB
Bonanni et al. (2015)	Rest-EEG	20 MCI-DLB, 14 MCI-AD, 8 HC	CAF	Correlation between CAF and reduced dominant frequency and increased dominant frequency variability in MCI-DLB
Peraza et al. (2018)	Rest-EEG, graph theory	25 DLB, 21 PDD, 26 AD, 17 HC	CAF	No correlations between EEG network measures and CAF in DLB and PDD
Stylianou et al. (2018)	Rest-EEG	17 DLB, 17 PDD, 18 AD, 21 HC	CAF	Positive correlation between CAF and dominant frequency variability in the theta range and slow-theta frequency prevalence

AD, Alzheimer's disease; CAF, Clinician Assessment of Fluctuation; CF, cognitive fluctuations; CRT, choice reaction time; DLB, dementia with Lewy bodies; EEG, electroencephalography; ERP, event-related potential; HC, healthy controls; Mayo, Mayo Fluctuation scale; MCI, mild cognitive impairment; ODFAS, One Day Fluctuation Assessment Scale; PDD, Parkinson's disease dementia; rest-EEG, resting-state EEG; RT, reaction time.

the LBD groups (Peraza et al., 2018). Overall, EEG findings in LBD suggest that cognitive fluctuations might be related to instabilities in brain oscillations and a slowing of the EEG background rhythm, indicating that temporal aspects of brain functioning might also be related to the emergence of cognitive fluctuations in LBD.

Further evidence

A role of the cholinergic system in the aetiology of cognitive fluctuations mentioned above is further supported by studies showing that anticholinergic medication can induce a symptom similar to cognitive fluctuations (Perry et al., 1999) as well as by studies showing that acetylcholinesterase inhibitors ameliorate the clinical features of cognitive fluctuations (Edwards et al., 2007; McKeith et al., 2000b; Onofrj et al., 2003; Wesnes et al., 2002). Lesional work in primates identified a deleterious impact on attention upon targeting basal forebrain cholinergic nuclei such as the NBM (Voytko et al., 1994). The NBM is important for relaying "bottom-up" signals of attention and is particularly vulnerable to alpha-synuclein pathology (Liu et al., 2015). Pathological series in DLB have demonstrated a correlation between neuronal loss in the NBM and reduced cortical choline acetyltransferase levels (Lippa et al., 1999). Evidence for a hypocholinergic aetiology is further provided by a highly selective animal lesioning model (Cyr et al., 2015). Cyr and colleagues demonstrated a behavioural correlate of cognitive fluctuations – variable response latencies on an attention task – in rats subjected to cholinergic denervation of the pedunculopontine tegmental nucleus. Furthermore, as mentioned above, alterations in nicotinic receptor binding in temporal cortex (Ballard et al., 2002b) and thalamus (Pimlott et al., 2006) have been described in relation to cognitive fluctuations in DLB.

The thalamus is another subcortical structure which has been shown to be involved in the aetiopathogenesis of cognitive fluctuations. Pathological data implicates a predilection for alpha-synuclein pathology in thalamic centres, which are integral to the reticulo-thalamo-cortical activating system and therefore the mediation of consciousness (Braak et al., 2003; Henderson et al., 2000; Rüb et al., 2002). Subcortical thalamic cholinergic denervation has been established in DLB (Kotagal et al., 2012) and imbalances within this system could thus contribute to cognitive fluctuations (Ballard et al., 2002b; Pimlott et al., 2006).

Given the importance of noradrenaline for the integrity of the attentional system (Buschman and Miller, 2007; Gratwicke et al., 2015), a noradrenergic deficit may also be an important player in the aetiopathogenesis of cognitive fluctuations in LBD. This is supported by reports of cell loss within the locus coeruleus in Lewy body diseases (Del Tredici and Braak, 2013), and by evidence that noradrenaline re-uptake inhibitors increase sustained attention in PD

(Kehagia et al., 2014; Rae et al., 2016). However, there remains little research into the role of a direct relationship between deficiency of the noradrenergic system and cognitive fluctuations.

1.2.5 Summary

Collating evidence from different modalities, several theories have emerged regarding the possible aetiology of cognitive fluctuations in LBD.

Firstly, there is evidence that cognitive fluctuations might be related to network perturbations in attentional circuitry. Evidence for this theory comes from studies relating cognitive fluctuations to RT performance on tests of sustained attention (Ballard et al., 2002a, 2001b; Onofrj et al., 2003; Walker et al., 2000a) and from fMRI and EEG studies showing an association between abnormalities in structures and networks related to attentional processing and fluctuation severity (Bonanni et al., 2010; Chabran et al., 2018; Kobeleva et al., 2017; Peraza et al., 2014; Sauer et al., 2006).

Secondly, there is evidence for a relation between corticopetal deafferentiation and cognitive fluctuations, in particular with respect to disturbances within the cholinergic system and the thalamus. Support for the hypocholinergic theory comes from the beneficial effect of acetylcholinesterase inhibitors on the clinical manifestation of cognitive fluctuations (Edwards et al., 2007; McKeith et al., 2000b; Onofrj et al., 2003; Wesnes et al., 2002), from the observation of grey matter loss in subcortical cholinergic structures (Colloby et al., 2017), from animal studies (Cyr et al., 2015; Voytko et al., 1994), and from findings of biochemical changes within the cholinergic system (Ballard et al., 2002b; Pimlott et al., 2006). In regard to the thalamus, this has been implicated in cognitive fluctuations on structural (Watson et al., 2017) as well as biochemical studies (Ballard et al., 2002b; Delli Pizzi et al., 2015b; Pimlott et al., 2006).

Thirdly, there might be an association between disturbances in the sleep-wake cycle and cognitive fluctuations (Cagnin et al., 2016); however, the exact relationship between the two still remains to be elucidated.

1.3 Resting-State Brain Dynamics

This thesis will focus on the analysis of resting-state neuroimaging and electrophysiology data, i.e. participants were not asked to perform any task during data acquisition. In recent years, there has been an increasing interest in this kind of data. The following section will provide an overview of previous work in this field and present an argument for the importance of studying the brain at rest, especially with respect to cognitive fluctuations in LBD.

1.3.1 The resting state of the brain

Traditionally, functional neuroimaging studies have focussed on analysing task-evoked brain activity, i.e. changes in brain signal that are associated with a specific task or stimulus (Raichle, 2009). This approach reflects a view of the brain that has dominated the field of cognitive neuroscience for a long time where the brain is seen as being a primarily reflexive organ which is mainly driven by momentary demands of the environment (Raichle, 2010). There is also a pragmatic benefit of task/stimulus data as this allows the use of time-locked averaging across repeated trials to ameliorate the inherently noisy nature of the fMRI and EEG signals by removing non-neuronal noise sources from the data in order to be able to visualise task-related changes in brain activity (Raichle, 2015).

However, the focus on task-related brain activity largely ignores the fact that much of the brain's energy is devoted to intrinsic brain activity and that task-evoked activity usually only adds a small increment to this continuously ongoing energy demand (Raichle and Mintun, 2006). In this regard, it is therefore important to distinguish between the behavioural resting state – as defined by the absence of a specific task – and the resting state of the brain which is by no means a *resting* state; in fact, the brain is never physiologically at rest and there is constant intrinsic activity at various levels of organisation (Faisal et al., 2008; Yuste et al., 2005).

The field of resting-state neuroimaging was greatly advanced by a chance discovery from early PET and fMRI studies, which found that there are brain regions that show a decrease in activity during many attention-demanding and goal-directed tasks (Binder et al., 1999; Shulman et al., 1997). This set of brain regions was later labelled the default mode network (DMN) and provided first neuroimaging evidence for a functional significance of brain activity during the resting state (Gusnard and Raichle, 2001; Raichle et al., 2001). Furthermore, it was shown that the different areas of the DMN do not only show consistent task-related decreases, but they also show coherent activity during rest, suggesting a systematic network organisation of the brain at rest (Greicius et al., 2003). This network organisation is not unique to the DMN and many other brain regions exhibit correlated activity during rest (Biswal et al., 1995; Fox and Raichle, 2007; Lowe et al., 1998). These so-called resting-state networks (RSNs) have been linked to different cognitive functions based on the involvement of brain regions that are known to be related to certain functions including visual, motor, executive, salience, and attention networks (Beckmann et al., 2005; Damoiseaux et al., 2006; Smith et al., 2009). While there is some degree of overlap between structural connectivity, as assessed by diffusion tensor imaging, and functional connectivity

within RSNs (Greicius et al., 2009), these functional networks are not necessarily constrained by anatomical connections (Honey et al., 2009). Furthermore, there is not only an intricate functional organisation within each network, but interrelations exist between different networks (Fox et al., 2009, 2005). This is particularly important with regards to the intricate anti-correlated interplay between the DMN and task-positive attentional networks (Fox et al., 2005) which has been related to the efficiency of stimulus processing on attention tasks thus showing its behavioural relevance (Weissman et al., 2006).

The study of resting-state data comes with certain challenges. This is due to the fact that one is interested in neuronal "noise" (i.e. task- or stimulus-independent changes in brain activity) which can be hidden by non-neuronal noise (e.g. due to movement or physiological artefacts). Furthermore, resting-state data show large heterogeneity across participants due to the unconstrained nature of the respective experiment. While the analysis of brain activity in response to external stimuli can be rigorously controlled, the analysis of spontaneous brain activity is more elusive (Raichle, 2010).

However, resting-state scans are easy and relatively fast to acquire, they do not depend on a person's cognitive abilities, and the signal is not directly confounded by individual differences in behavioural performance. This makes resting-state studies especially suitable for older patient populations and patients who might not be able to perform a cognitive task while lying in the scanner (Raichle, 2010; Zhang and Raichle, 2010).

1.3.2 The importance of resting-state brain dynamics

Most resting-state studies have focussed on average connectivity over the duration of a scan of several minutes, thereby implicitly assuming that the functional architecture of the brain remains stationary over time. However, it has recently been shown that functional connectivity can vary substantially in both strength and directionality on a timescale of seconds to minutes (Chang and Glover, 2010; Hutchison et al., 2013b). Studying these dynamics can provide important complementary information to the analysis of stationary functional connectivity (Calhoun et al., 2014; Hutchison et al., 2013a). Several studies have furthermore provided support for a cognitive role of dynamic connectivity by showing that changes in connectivity are related to changes in behavioural or vigilance states (Jia et al., 2014; Kucyi et al., 2017; Thompson et al., 2013).

However, moment-to-moment signal variability cannot only be observed on the level of large-scale RSNs; it is rather a universal feature of the brain that is present at different levels of the nervous system (Faisal et al., 2008; McDonnell and Ward, 2011). More generally, the brain can be considered a nonlinear dynamical system in which the intrinsic activity and

connectivity structure varies over time and which operates at a point of criticality (Garrett et al., 2013b; Hesse and Gross, 2014). In such a system, fluctuations are important because they allow an exploration of the state space (Ghosh et al., 2008) and provide greater dynamical range, i.e. a larger range of possible responses to incoming stimuli (Deco and Jirsa, 2012). Brain variability has also been related to more optimal and efficient network structure (Garrett et al., 2018; Mišić et al., 2011), and higher signal variability indicates a system that operates closer to a critical state (He, 2011). Additionally, it has been shown that disturbances to these intricate dynamics can cause the system to lose its optimal network properties (Van De Ville et al., 2010).

In addition, various studies have provided evidence for a behavioural relevance of intrinsic brain dynamics by relating more dynamic brain activity to faster, more accurate, and more consistent performance on a wide range of cognitive tasks (Garrett et al., 2011; McIntosh et al., 2008; Mišić et al., 2010). Ageing has been shown to be associated with a reduction in brain variability (Garrett et al., 2013a, 2011) and a loss of complexity within the brain network (Takahashi et al., 2009), and different diseases have also been related to a loss of brain variability and complexity (Garrett et al., 2013b).

Brain dynamics can be assessed with different methodologies and on different timescales: while dynamic connectivity analysis from fMRI data allows the characterisation of slower brain dynamics with high spatial resolution (see Chapter 5), dynamic changes on a sub-second timescale can be studied using EEG. One method that is particularly suitable to study the dynamic properties of the EEG signal is microstate analysis (Michel and Koenig, 2017) where the EEG signal is segmented into short, non-overlapping states whose temporal characteristics can provide insight into the brain's dynamic properties (see Chapter 6).

1.3.3 Resting-state brain dynamics in LBD

An important characteristic of cognitive fluctuations in LBD is that they occur spontaneously and in the absence of a specific situational demand or external explanation, i.e. they can occur while the patient is at rest. This stands in contrast to AD where cognitive fluctuations seem to be related to difficulties when responding to a specific task or certain situational demands (Bradshaw et al., 2004). Furthermore, fluctuations in LBD by their nature are transient and reversible and remission to near-normal levels of cognitive functioning can occur (McKeith, 2002; McKeith et al., 1996) making it unlikely that they are primarily driven by progressively worsening structural changes. Instead, it has been suggested that they might be related to transient functional changes in the brain, i.e. dynamic changes in the brain's activity and its functional network organisation (Sourty et al., 2016; Taylor et al., 2013). Therefore, a better

characterisation of resting-state brain dynamics in patients with LBD compared to patients with AD and healthy controls might provide important insight into the aetiology of cognitive fluctuations and might, more generally, provide a better understanding of the LBD cognitive phenotype. Furthermore, it might help reveal details of differences and similarities between AD and LBD and the changes in brain dynamics that might underlie the clinically observed differences.

1.4 Description of Study Cohort

1.4.1 Study data

Data from several previous dementia research studies conducted at Newcastle University were used in the different analyses comprising this thesis. RT, EEG, and fMRI data from AD, DLB, and PDD patients as well as healthy controls were obtained from the CATFieLD study. Participants in this study were assessed using an RT based attention test while undergoing high-density EEG and fMRI recordings on two separate occasions. Additionally, resting-state EEG and fMRI data were acquired. This thesis will focus on the analysis of the RT and resting-state EEG and fMRI data while the task-based EEG and fMRI data have been analysed previously (Cromarty, 2016; Firbank et al., 2016; Kobeleva et al., 2017). Additional resting-state fMRI data from AD and DLB patients and healthy controls were obtained from the ARThippo study. This study did not collect RT or EEG data and did not involve PDD patients. For the creation of the fMRI resting-state network templates (Chapter 4), healthy control data from an independent cohort was required which was taken from two additional independent studies, the ICICLE and VEEG-Stim studies. All studies were approved by the local ethics committee and written informed consent was obtained from each participant prior to study participation. Patients were recruited from the local community-dwelling population who had been referred to old-age psychiatry and neurology services. Dementia diagnoses were performed independently by two experienced clinicians in alignment with consensus criteria for probable DLB (McKeith et al., 2017, 2005), PDD (Emre et al., 2007), and AD (McKhann et al., 1984, 2011). Age-matched healthy controls were recruited from friends/acquaintances of the patients with no history of psychiatric or neurological illness. Participants from all included studies underwent detailed clinical and cognitive assessments. Clinical scores that were of interest for this thesis were scores of global cognition as well as measures of the core LBD symptoms of Parkinsonism, visual hallucinations, and cognitive fluctuations (see Section 1.4.2 for a more detailed description of the included scores). Furthermore, detailed information about medication usage was available for all participants; for this thesis information on the use of acetylcholinesterase inhibitors and dopaminergic

medication in the dementia patients was extracted given the potential impact of these on the dynamic measures of interest in this thesis.
A more detailed description of each study group and reasons for inclusion/exclusion of participants are provided in the methods sections of the respective chapters.

1.4.2 Clinical measures

Global cognition

Global cognitive functioning was assessed using the Mini Mental State Examination (MMSE) and Cambridge Cognitive Examination (CAMCOG) in patients and healthy control participants in all studies. The MMSE is designed to measure different aspects of cognitive functioning including short-term memory, immediate recall, calculation, language, construction, and orientation, with a total score of 30 points (Folstein et al., 1975). It is widely used to assess cognitive impairment in dementia cohorts and a total score of <24 points in addition to impairments in activities of daily living is usually considered to support a diagnosis of dementia. Similarly, the CAMCOG is designed to assess different cognitive domains such as orientation, language, memory, attention, calculation, perception, and executive function with a total score of 105 points (Roth et al., 1986). A cut-off of <80 points is usually considered to indicate dementia.

Parkinsonism

The motor subsection of the Unified Parkinson's Disease Rating Scale (UPDRS III) was administered to all healthy control and dementia participants (Fahn and Elton, 1987). The UPDRS III is used to assess five aspects of motor functioning: rigidity, tremor at rest, bradykinesia, action tremor, and facial expression. Scores from the five subsections are summed to obtain a total score with a score of ≥8 indicating the presence of Parkinsonism.

Visual hallucinations

The carer-administered Neuropsychiatric Inventory (NPI) was used to assess psychiatric symptoms in all dementia patients (Cummings et al., 1994). It is designed to measure presence, frequency, and severity of symptoms in ten behavioural domains over the month prior to the assessment, including delusions, hallucinations, agitation/aggression, dysphoria, anxiety, euphoria, apathy, disinhibition, irritability, and aberrant motor behaviour. The hallucination subscale was of particular interest for the analyses described in this thesis as, when this domain was assessed there was a specific focus on visual hallucination occurrence in the dementia patients.

Cognitive fluctuations

The severity and duration of cognitive fluctuations was assessed by the CAF scale in all dementia patients (Walker et al., 2000b). Additionally, for all dementia patients included in the CATFieLD study the Mayo fluctuations scale was used (Ferman et al., 2004) (see Section 1.2.2 for a more detailed description and discussion of clinical fluctuation scales).

1.5 Aims and Hypotheses

1.5.1 Aims

The objective of this thesis is to integrate behavioural and neuroimaging data from patients diagnosed with dementia in order to study their brain dynamics as well as behavioural and clinical correlates, especially with respect to attentional impairment and cognitive fluctuations.
More specifically, the aims of the thesis are:

- to analyse how different aspects of RT performance are differentially affected by AD and LBD and how these map onto clinical measures in LBD, particularly to clinical measures of cognitive fluctuations (Chapter 2 and 3),
- to analyse disruptions in functional connectivity of RSNs in LBD patients compared to AD and healthy controls, and relate these to the clinically observed cognitive fluctuations (Chapter 4), and
- to compare the dynamics of fMRI functional connectivity as well as EEG dynamics in LBD, AD, and healthy controls to study associations between the dynamic properties of the brain network and the clinical LBD phenotype, especially with respect to cognitive fluctuations (Chapter 5 and 6).

1.5.2 Hypotheses: RT data

- Response times in an attention task will be slower and show higher intraindividual variability in both dementia groups compared to healthy controls and this will be more pronounced in LBD than in AD.
- Compared to AD and healthy controls, LBD will be characterised by an increase in attentional lapses and this will correlate with the severity of cognitive fluctuations.

- There will be a relation between structural brain changes and different aspects of attention in the AD group which will be less pronounced in the LBD group given less atrophic changes in this condition compared to AD.

1.5.3 Hypotheses: fMRI data

- Compared to controls, there will be a reduction in functional connectivity in the motor, basal ganglia, attentional, and possibly visual RSNs in patients with LBD.
- The overall dynamics of functional connectivity will be reduced in both dementia groups compared to controls, with greater impairment in LBD compared to AD.
- Disturbances within the dynamic architecture of the functional brain network will be related to cognitive fluctuation severity in LBD.

1.5.4 Hypotheses: EEG data

- There will be a slowing of microstate dynamics in LBD which will be related to the cognitive phenotype, and in particular, cognitive fluctuations.
- Disturbances in microstate dynamics in LBD will be contingent upon a loss of dynamics within cortical-basal ganglia-thalamic connections.

Chapter 2. Analysis of Attention Components and Brain Structural Correlates

2.1 Introduction

Previous investigations using attention tasks have found that LBD patients show slower RTs and higher intra-individual variability than AD patients (Ballard et al., 2001a; Bradshaw et al., 2004), and that this difference is accentuated when the task involves an executive or spatial aspect (Bradshaw et al., 2004). This deficit in RT performance has also been related to the severity of cognitive fluctuations; patients with more severe fluctuations show more impaired RT performance and higher trial-to-trial variability (Ballard et al., 2002a, 2001b; Onofrj et al., 2003; Walker et al., 2000a).

It has been proposed that attention can be modelled as three anatomically distinct, but functionally inter-related systems: alerting, orienting, and executive control or conflict (Posner and Petersen, 1990). The efficiency of these three attention systems is commonly assessed using the Attention Network Test (ANT) (Fan et al., 2002) combining elements of the Posner cueing paradigm (Posner and Petersen, 1990) and the Eriksen flanker task (Eriksen and Eriksen, 1974) to test all three components in a single session. The significance and size of the alerting, orienting, and executive conflict effects is measured by differences in RT performance between different cue and target conditions. First, the alerting effect is assessed as the benefit of a simple warning cue (compared to no cue) on subsequent RT performance. The size of this effect is therefore an indicator for the ability to achieve and maintain a vigilant or alert state (Posner and Petersen, 1990). Second, the orienting effect is measured by the difference in RT when presenting stimuli in a previously cued location in space compared to an uncued location. Its size therefore indicates how efficient a participant can select information from sensory input (Fan et al., 2005). Finally, the size of the executive conflict effect is tested using a flanker task, i.e. by measuring the effect of distracting targets on RT performance (Eriksen and Eriksen, 1974). An increase in the executive conflict effect thus indicates an impairment in resolving conflict amongst responses.

To date, very little research has been conducted to investigate how the efficiency of the different attentional systems is affected by dementia, and the findings of previous studies are inconsistent (Fernandez-Duque and Black, 2006; Fuentes et al., 2010). The aim of this chapter is to determine the extent to which the efficiency of the attentional systems is differentially affected in LBD patients relative to AD patients and age-matched healthy participants. The alerting component is purported to be modulated by noradrenergic projections from the locus coeruleus (Coull et al., 2001; Raz, 2004). Given that LBD patients have been found to have a

paucity of noradrenergic neurons in the locus coeruleus (Szot, 2006), my first hypothesis was that there will be an impairment in alerting efficiency in LBD patients. Secondly, as the orienting component has been suggested to be modulated by the basal forebrain cholinergic system (Fan et al., 2005) which is more markedly affected in LBD patients than in AD patients (Ballard et al., 2013), I hypothesised that LBD patients will exhibit differentially reduced orienting efficiency compared to AD patients and controls. Thirdly, based on previous studies I also hypothesised that AD patients will exhibit reduced executive conflict efficiency relative to healthy controls (Fernandez-Duque and Black, 2006). Given that deficits in executive functioning are also a common feature of LBD, I expected that the LBD group will also exhibit reduced executive conflict processing efficiency. Furthermore, executive control has been shown to be modulated by the dopaminergic and cholinergic systems (Noudoost and Moore, 2011) which are more affected in LBD compared to AD (Ballard et al., 2013; O'Brien et al., 2004; Walker et al., 2002). Thus, I hypothesised that the impairment in executive conflict efficiency will be greater in LBD compared to AD.

Previous studies have also investigated how inter-individual differences in the efficiency of the attentional systems, as measured by the ANT, are related to differences in brain structure in healthy participants (Hao et al., 2015; Westlye et al., 2011) and amnestic MCI (Borsa et al., 2016). However, to date, no studies have examined the relationship between the efficiency of these attentional systems and structural alterations in more severe neurodegenerative disease. A further aim of this chapter is therefore to study macrostructural neural correlates of attentional dysfunction in AD and LBD using a VBM analysis. Previously, Borsa et al. (2016) found an association between impairment in the executive conflict component in MCI patients and decreased grey matter volume in the anterior cingulate cortex (ACC). Given that MCI is associated with a high conversion rate to AD (Petersen, 2004), I hypothesised that there might be a similar or possibly even stronger relationship between conflict monitoring and brain volume in the ACC in the AD group. However, given the general paucity of previous research in this area, the analysis of brain structural correlates of the attentional systems was conducted in a more exploratory manner, using a whole-brain approach rather than restricting the analysis to *a priori* defined regions.

Finally, as cognitive fluctuations have been correlated with other RT measures in DLB (Bradshaw et al., 2006; Walker et al., 2000a), it is of interest to know how the efficiency of the different ANT systems may relate to the clinical symptoms of LBD. The association between the ANT components and cognitive fluctuation severity will be explored.

2.2 Methods

2.2.1 Participants

This analysis involved 104 participants from the CATFieLD study, including 49 patients diagnosed with probable LBD (26 DLB and 23 PDD), 33 with probable AD, and 22 age-matched healthy controls (HC).

DLB and PDD patients were combined into one LBD group *a priori* for this analysis as previous studies have shown similar attentional and executive impairment in DLB and PDD (Ballard et al., 2002a; Firbank et al., 2016) and similar patterns of brain structural alterations (Burton et al., 2004).

2.2.2 Modified Attention Network Test

The CATFieLD study used a modified version of the ANT (Cromarty, 2016; Firbank et al., 2016) based on the version described by Fan et al. (2007). The main rationale for adapting the ANT was to make it suitable for older adults and dementia patients. This was achieved by increasing the size of the stimuli to account for participants with poor visual acuity and by adjusting the timings to account for slower cognitive processing speed in older adults. Furthermore, an additional level of executive conflict complexity was added to create a more graded task difficulty (see below).

The computerised task was programmed by Dr Michael Firbank using the Cogent toolbox in Matlab (http://www.vislab.ucl.ac.uk/cogent_2000.php). Participants completed between 3 and 14 runs of the task (median=8), each run consisting of 36 trials. Throughout the task a central fixation cross and three boxes were presented on a screen (Figure 2.1). At the beginning of each trial, one of three possible cues (no, neutral, or spatial cue) was presented for 200 ms. In the no cue condition, the boxes remained unchanged. During the neutral cue condition, the central box flashed and during the presentation of a spatial cue, one of the boxes either above or below the central box flashed (to indicate the box in which a subsequent target would appear). The disappearance of the cue was followed by a target comprising four arrowheads in a row, either in the box above or below the central fixation. The time between the disappearance of the cue and the appearance of the target was one of the following exponentially distributed times: 700, 770, 850, 960, 1080, 1240, 1430, 1660, 1940, 2300, 2700, 3200 ms. The target stimuli could be congruent or incongruent; congruent targets were arrowheads which were all pointing in the same direction (left or right), whereas for incongruent targets one arrowhead was pointing in the opposite direction. In the incongruent condition, the incongruent arrowhead appeared either on the end of the row (easy

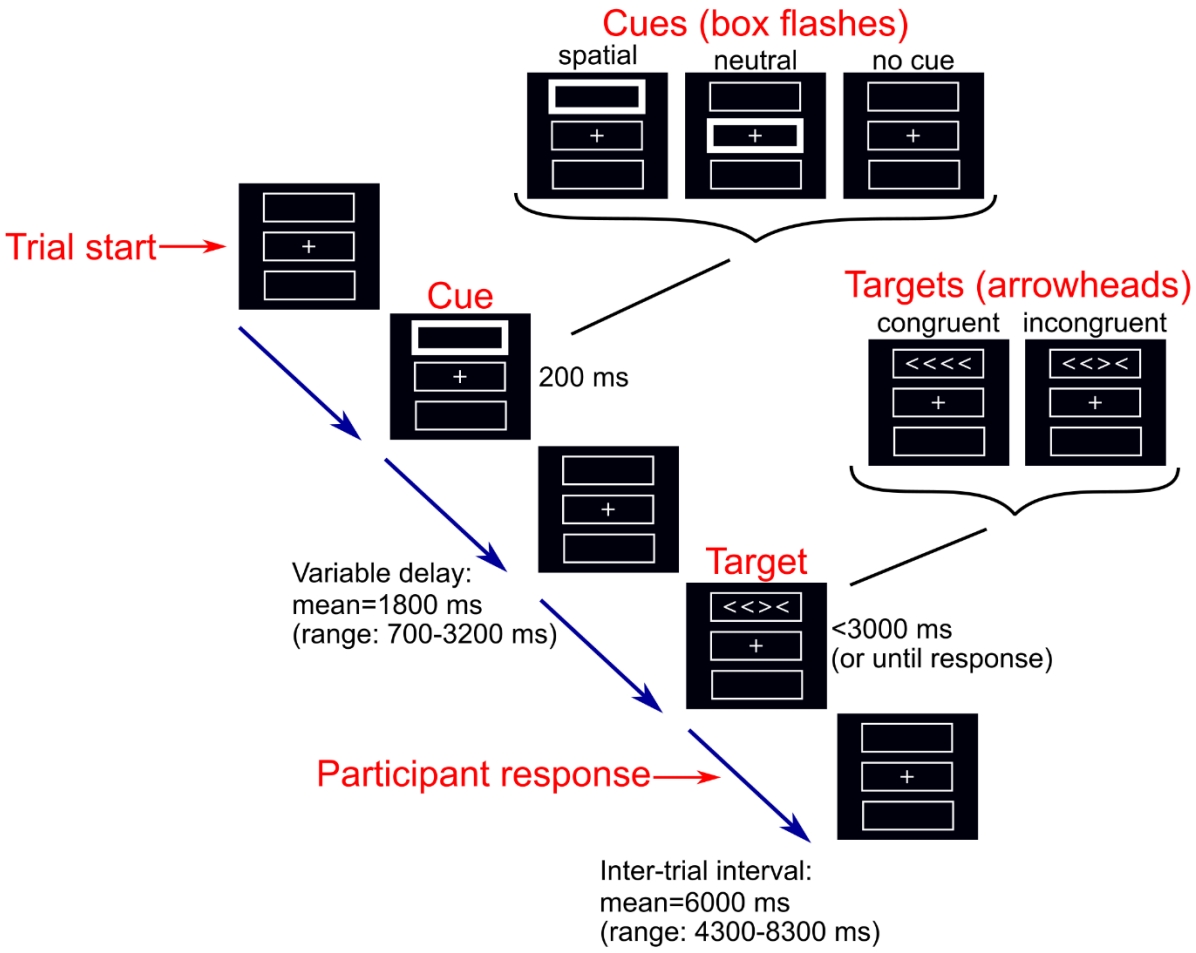

Figure 2.1. Depiction of a single trial of the modified Attention Network Test.

incongruent) or as one of the two arrowheads in the middle (hard incongruent). The target was presented on screen until the participant made a response by squeezing a right or left hand air pressure bulb to indicate the direction in which the majority of arrowheads were facing, or until 3000 ms had elapsed. The intertrial interval was one of the following: 4300, 4500, 4750, 5000, 5350, 5700, 6100, 6400, 6800, 7200, 7700, 8300 ms, with each time occurring three times during each run in random order.

During each run, the six trial types were presented in a predetermined counterbalanced order; each cue appeared 12 times and there were 18 congruent and 18 incongruent target trials (9 easy incongruent and 9 hard incongruent). All trials from runs with less than 2/3 correct responses were excluded from further analysis as performance below this was not different from chance (Firbank et al., 2016).

2.2.3 Analysis of ANT effects

Mean RTs for each cue and target condition were calculated in Matlab (R2015b), using only the trials in which the participants gave correct responses in alignment with previous studies. The ANT effects were calculated as defined by Fan et al. (2002):

Alerting effect = no cue - neutral cue
Orienting effect = neutral cue - spatial cue
Executive conflict effect = incongruent target - congruent target

The alerting effect is therefore a measure of the extent to which response speed is facilitated by the presence of a warning, indicating that a response is imminently required. The orienting effect is the extent to which responses are further facilitated when the actual spatial location of the oncoming target is cued, rather than a simple warning that a response is imminent. Finally, the executive conflict effect pools all types of cued conditions and examines the impairing/interfering effect of having conflicting information regarding the target stimuli (in terms of the direction in which each of the arrowheads are pointing), compared to the facilitative effect of having target stimuli which are all pointing in the same direction.
To calculate the alerting and orienting effects, mean RTs from congruent and incongruent trials were averaged. Similarly, the executive conflict effect was calculated by averaging mean RTs across the cue conditions. For the purpose of this thesis, easy and hard incongruent conditions were not analysed separately. Error rates were also determined for each task condition by dividing the number of incorrect and missed response trials by the number of recorded trials for each participant.

2.2.4 MR imaging and analysis

Structural MR images were acquired with a 3 T Philips Intera Achieva scanner with a magnetisation prepared rapid gradient echo (MPRAGE) sequence, sagittal acquisition, echo time 4.6 ms, repetition time (TR) 8.3 ms, inversion time 1250 ms, flip angle = 8°, SENSE factor = 2, and in-plane field of view 240 x 240 mm^2 with slice thickness 1.0 mm, yielding a voxel size of 1.0 x 1.0 x 1.0 mm^3.
A VBM analysis was performed in SPM12 (Statistical Parametric Mapping, www.fil.ion.ucl.ac.uk/spm/) to assess voxel-wise correlations between the ANT results and mean RT and grey matter and white matter volume. Images were first segmented into grey matter, white matter, and CSF. The segmented grey and white matter images were then co-registered and normalised to MNI space using SPM's DARTEL algorithm (Ashburner, 2007) and modulated. Finally, images were smoothed with an 8 mm full width at half maximum Gaussian kernel.

2.2.5 Statistics

Statistical analyses were carried out in IBM SPSS Statistics version 22 and R version 3.5.1 (http://www.R-project.org/). For the mean RT data for each cue and target condition, a

repeated measures (cue x target) analysis of variance (ANOVA) was conducted with a between-subject factor of group (HC, AD, LBD). Subsequently, separate repeated measures (cue x target) ANOVAs were conducted for each group; post- hoc pairwise comparisons were used to calculate RT differences between the cue and target conditions, thus determining the significance of the ANT effects. The magnitude of the ANT effects was compared between groups using univariate ANOVAs; the dependent variable being the ANT effect with group as a fixed factor. For each ANOVA analysis Mauchly's sphericity test was used and F-values were adjusted accordingly. Post-hoc pairwise comparisons were corrected for multiple comparisons using Bonferroni correction. The same analysis was repeated for the error rates. Additionally, to control for the effect of overall processing speed and to test whether between-group differences in overall processing speed influenced the analyses of the ANT effects, I repeated all analyses using normalised RTs; for each participant, the mean RT for each condition was divided by the participant's overall mean RT in alignment with previous studies (Faust and Balota, 1997; Fernandez-Duque and Black, 2006).

Spearman's correlations were calculated to investigate associations between the behavioural data (overall mean RT and the ANT effects) and clinical variables in the dementia groups. In the LBD group, correlations were calculated for cognitive fluctuation scores (Mayo and CAF total and subscores); supplementary analyses were performed for measures of overall cognition (MMSE, CAMCOG), the UPDRS motor subscale, and the NPI hallucination scale. In the AD group, correlations were calculated for MMSE and CAMCOG. P-values were false discovery rate (FDR)-corrected for multiple comparisons.

Correlations between the ANT behavioural data and grey and white matter volume were assessed using a general linear model (GLM) in SPM12. The GLM combined all three ANT effects (alerting, orienting, and executive) as variables of interest in one design matrix and a separate model was used for mean RT. Covariates of no interest for age, sex, total intracranial volume, and UPDRS motor scores (in LBD) were included. An explicit mask was estimated to restrict the statistical analysis to voxels which represented grey and white matter, respectively (Ridgway et al., 2009). Significant results are reported at a voxel-level p-value<0.001. Additionally, the minimum cluster size for a multiple comparison corrected threshold of $p<0.05$ was determined by Monte Carlo simulations using the REST software (www.restfmri.net).

To study the possible influence of dopaminergic medication on the ANT effects in the LBD group, the repeated-measures (cue x target) ANOVA was repeated including a covariate for levodopa equivalent daily dose (LEDD) (Tomlinson et al., 2010). This was tested for both raw and normalised RT.

2.3 Results

2.3.1 Demographics

Two AD, one DLB, and three PDD patients were excluded from the analysis because they did not meet the minimum performance criteria (Section 2.2.2). Thus, 31 AD, 45 LBD (25 DLB and 20 PDD), and 22 HC participants were further analysed (Table 2.1). All groups were matched for age and sex. LBD patients were slightly less impaired in terms of overall cognition (MMSE and CAMCOG) and had had a shorter duration of cognitive symptoms compared to AD patients. The proportion of patients taking acetylcholinesterase inhibitors did not differ between the dementia groups. As expected, many LBD patients were taking dopaminergic medication (none of the AD patients took dopaminergic medication). Furthermore, compared to the AD group, LBD patients were more impaired in terms of the core LBD symptoms of Parkinsonism, cognitive fluctuations, and visual hallucinations.
To ensure that differences between the dementia groups in terms of behavioural data were not due to differences in MMSE, all analyses reported below were repeated with matched dementia groups. To create these matched dementia groups, four AD patients with MMSE<16 and ten LBD patients (six DLB and four PDD) with MMSE>26 were excluded from the analysis. Subsequently, the two groups did not differ with respect to duration of dementia (Mann-Whitney U test, U=358, p=0.10), MMSE (Student's t-test, t_{60}=0.38, p=0.71) or CAMCOG (Student's t-test, t_{60}=0.39, p=0.70).
There were no significant differences between DLB and PDD subgroups in terms of age, overall cognition, and dementia duration whereas PDD patients had more severe Parkinsonism, psychiatric symptoms, and cognitive fluctuations than DLB patients (Table 2.1). To ensure that combining DLB and PDD patients into one LBD group was appropriate, mean RT, error rates, and the ANT effects were compared between the two groups, revealing no significant differences (Table 2.2).

2.3.2 Reaction time analysis

The number of recorded trials per participant did not differ significantly between the groups (mean (SD) HC: 301.1 (17.7), AD: 290.3 (41.5), LBD: 304.8 (37.3); univariate ANOVA, F(2,95)=1.56, p=0.22). Overall, the error rate was lower in the control group than in AD and LBD but did not significantly differ between the dementia groups (Table 2.4 and 2.7). In AD and LBD, there was a significant negative correlation between overall error rate and MMSE and CAMCOG scores (Table 2.8 and Figure 2.3B).

Table 2.1. Demographics and clinical information; mean (standard deviation).

	HC (N=22)	AD (N=31)	LBD (N=45)	Group differences	DLB (N=25)	PDD (N=20)	Group differences
Male: female	15:7	24:7	38:7	χ^2=2.36, p=0.31[a]	19:6	19:1	χ^2=3.05, p=0.08[h]
Age	75.9 (5.4)	77.1 (7.9)	74.5 (6.3)	$F_{2,95}$=1.41, p=0.25[b]	76.1 (6.2)	72.6 (5.9)	t_{43}=1.95, p=0.06[j]
AChEI	-	28	39	χ^2=0.24, p =0.63[c]	23	16	χ^2 =1.39, p =0.24[h]
PD meds	-	0	33	χ^2=40.2, p<0.001[c]	13	20	χ^2 =13.09, p<0.001[h]
Duration	-	3.9 (2.1)	3.1 (2.1)	U=509, p=0.043[d]	3.6 (2.4)	2.6 (1.5)	U =1.14, p=0.29[k]
MMSE	29.2 (0.9)	21.1 (3.7)	23.3 (3.8)	t_{74}=2.5, p =0.01[e]	23.0 (4.2)	23.7 (3.2)	t_{43} =0.54, p =0.60[j]
CAMCOG	96.7 (3.7)	68.8 (13.3)	75.9 (12.6)	t_{74}=2.4, p =0.02[e]	74.5 (14.7)	77.7 (9.3)	t_{43} =0.85, p =0.40[j]
UPDRS	1.1 (1.4)	2.4 (2.2)	20.5 (9.3)	t_{74}=10.6, p<0.001[e]	15.6 (7.2)	26.6 (7.9)	t_{43} =4.86, p<0.001[j]
CAF total	-	0.8 (1.7)[f]	5.1 (4.5)[g]	t_{71}=4.9, p<0.001[e]	4.00 (4.4)	6.6 (4.3)[l]	t_{41} =1.89, p=0.07[j]
Mayo total	-	9.1 (4.1)[f]	13.5 (5.8)[g]	t_{71}=3.6, p=0.001[e]	12.3 (6.2)	15.2 (5.0)[l]	t_{41}=1.67, p=0.10[j]
Mayo cogn	-	1.8 (1.8)[f]	2.8 (1.9)[g]	t_{71}=2.4, p=0.02[e]	2.2 (1.8)	3.7 (1.8)[l]	t_{41}=2.59, p=0.01[j]
NPI total	-	6.9 (6.2)[f]	13.4 (9.7)	t_{73} =3.3, p=0.002[e]	9.1 (4.9)	18.8 (11.6)	t_{43}=3.78, p<0.001[j]
NPI hall	-	0.03 (0.2)[f]	1.8 (2.0)	t_{73} =4.8, p<0.001[e]	1.4 (1.7)	2.2 (2.2)	t_{43}=1.37, p=0.18[j]

AChEI, number of patients taking acetylcholinesterase inhibitors; AD, Alzheimer's disease; CAF total, Clinician Assessment of Fluctuations total score; CAMCOG, Cambridge Cognitive Examination; DLB, Dementia with Lewy bodies; Duration, duration of cognitive symptoms in years; HC, healthy controls; LBD, Lewy body dementia; Mayo Fluctuations, Mayo Fluctuations cognitive subscale; MMSE, Mini Mental State Examination; PDD, Parkinson's disease dementia; PD meds, number of patients taking dopaminergic medication; UPDRS, Unified Parkinson's Disease Rating Scale III; NPI, Neuropsychiatric Inventory; NPI hall, NPI hallucination subscore.

[a] Chi-square test HC, AD, LBD; [b] One-way ANOVA HC, AD, LBD; [c] Chi-square test AD, LBD; [d] Mann Whitney U test AD, LBD; [e] Student's t-test AD, LBD; [f]N=30, [g]N=43

[h] Chi-square test DLB, PDD; [j] Student's t-test DLB, PDD; [k] Mann Whitney U test DLB, PDD; [l] N=18.

Table 2.2. Mean RT, error rates, and ANT effects for DLB and PDD subgroups (standard deviations are presented in brackets). Comparison between groups were conducted using Student's t-tests.

	DLB	PDD	Between-group differences
Mean RT	1483.6 (382.3)	1651.7 (391.0)	t_{43}=1.45, p=0.15
Mean error rate (%)	14.2 (8.4)	12.2 (10.0)	t_{43}=0.74, p=0.47
Alerting			
Raw RT	10.9 (87.7)	-11.2 (101.7)	t_{43}=0.78, p=0.44
Normalised RT	0.01 (0.06)	-0.0006 (0.05)	t_{43}=0.65, p=0.52
Orienting			
Raw RT	85.0 (98.8)	82.5 (131.1)	t_{43}=0.07, p=0.94
Normalised RT	0.06 (0.06)	0.05 (0.07)	t_{43}=0.19, p=0.85
Executive			
Raw RT	548.9 (281.6)	596.7 (219.4)	t_{43}=0.62, p=0.54
Normalised RT	0.35 (0.12)	0.36 (0.10)	t_{43}=0.32, p=0.75

DLB, dementia with Lewy bodies; PDD, Parkinson's disease dementia; RT, reaction time

Table 2.3. Mean RTs from correct trials (ms) for each task condition (cue x target), for the controls, AD and LBD patients. Standard deviations are presented in brackets.

		HC	AD	LBD
Mean RT (ms)				
All trials		964.6 (147.5)	1319.8 (322.6)	1558.3 (391.0)
	Overall	1025.1 (162.6)	1363.2 (325.3)	1587.0 (377.4)
No Cue	Congruent	806.7 (110.2)	1059.8 (270.2)	1280.4 (288.4)
	Incongruent	1243.4 (241.4)	1666.6 (402.4)	1893.6 (491.9)
	Overall	978.9 (147.3)	1334.1 (309.5)	1585.9 (413.0)
Neutral	Congruent	795.7 (98.8)	1072.0 (267.7)	1293.7 (302.6)
	Incongruent	1162.0 (222.4)	1596.1 (383.6)	1878.2 (553.6)
	Overall	900.00 (136.4)	1262.0 (342.9)	1502.0 (395.8)
Spatial	Congruent	710.5 (89.5)	989.1 (314.1)	1245.7 (355.7)
	Incongruent	1069.5 (203.5)	1534.9 (411.0)	1758.4 (478.9)
Congruent	Overall	771.0 (97.6)	1040.3 (278.0)	1273.3 (302.8)
Incongruent	Overall	1158.3 (220.8)	1599.2 (393.0)	1843.4 (496.4)
ANT effects (ms)				
Alerting		46.2 (37.0)*	29.14 (80.84)	1.1 (93.7)
Orienting		88.9 (35.0)*	72.07 (74.62)*	83.9 (112.9)*
Executive conflict		387.4 (171.9)*	558.88 (217.13)*	570.1 (254.2)*

AD, Alzheimer's disease; HC, healthy controls; LBD, Lewy body dementia; RT, reaction time.
*Significant ANT effect, p-value<0.05 for normalised RTs.

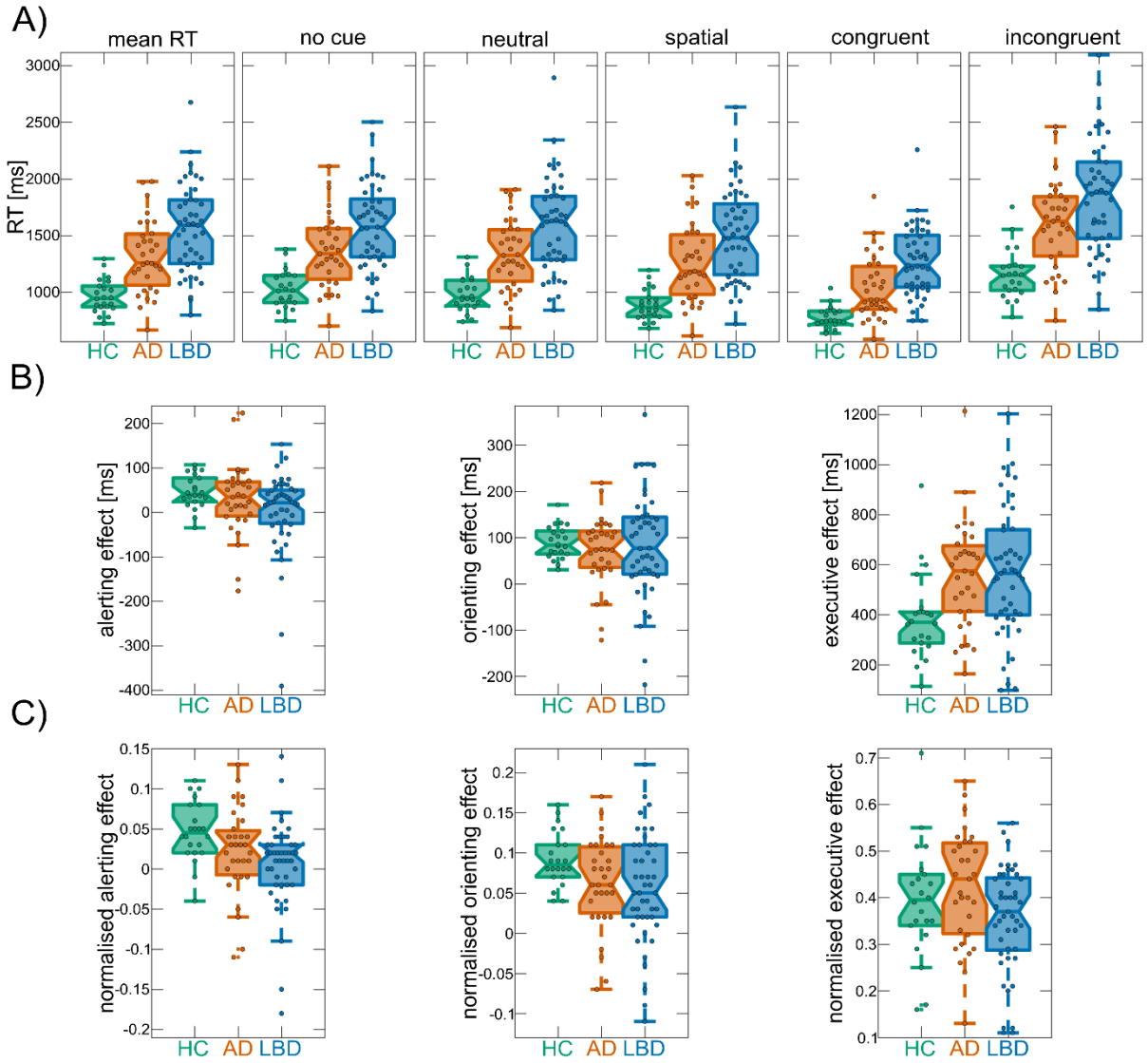

Figure 2.2. Group comparison of reaction times for the different ANT effects. A) Overall mean RT and mean RT for the different cue and target conditions of the ANT within each group. B) ANT effects from raw RTs. C) ANT effects from normalised RTs. In each boxplot the central line corresponds to the sample median, the upper and lower border of the box represent the 25th and 75th percentile, respectively, and the length of the whiskers is 1.5 times the interquartile range. Corresponding results from statistical comparisons between the three groups are presented in Table 2.5.
AD, Alzheimer's disease; HC, healthy controls; LBD, Lewy body dementia; RT, reaction time.

Overall mean RT

There was a main effect of group across all cue and target conditions; control participants had faster overall mean RT relative to AD and LBD patients, and the LBD mean RT was slower than the AD mean RT (Tables 2.3 and 2.5 and Figure 2.2A). Mean RT was significantly negatively correlated with overall cognition (MMSE and CAMCOG) in AD (Table 2.8 and Figure 2.3A). In LBD patients, mean RT was positively correlated with the UPDRS motor

score and the Mayo cognitive subscale (Table 2.8); however, these correlations in the LBD group did not survive correction for multiple comparisons.

Alerting and orienting effects

There was a main effect of cue; across all groups, mean RT for neutral cue trials was faster than no cue trials for both raw and normalised RT, i.e. there was an overall significant alerting effect. Furthermore, there was an overall significant orienting effect (difference between spatial and neutral cue trials) for raw and normalised RT (Table 2.5).

When considering raw RT, the group x cue interaction was not significant, however it was significant for normalised RT. Subsequent post-hoc tests of normalised RT at the individual group level revealed that controls had significant alerting and orienting effects. In AD and LBD participants, the alerting effect was not significant, however, both dementia groups demonstrated a significant orienting effect (Table 2.5 and Figure 2.2B and 2.2C). Restricting the analysis to matched dementia subgroups did not change the results significantly (Table 2.6). The analysis of error rates did not show any difference between the different cue conditions with no significant cue x group interaction (Table 2.7).

Comparing the magnitude of the alerting effect between groups did not reveal a significant difference for raw RT, whereas there was a significantly smaller alerting effect in LBD patients compared to controls when considering normalised RT (Table 2.5). The orienting effect was not different in magnitude between groups for raw and normalised RT. Additionally, there were no group differences in the magnitude of the alerting and orienting effects on error rates (Table 2.7).

Finally, there were no significant correlations between the alerting and orienting effects and any clinical variables after correcting for multiple comparisons (Table 2.8).

Executive conflict effect

There was a main effect of target; across all groups, mean RT for congruent trials was faster than for incongruent trials (Table 2.5). Additionally, there was a significant target x group interaction (albeit only marginally significant for normalised RT) and post-hoc tests revealed that the executive conflict effect was significant in all three groups (Figure 2.2B and 2.2C). Comparing the magnitude of the effect between groups, gave a larger conflict effect in both dementia groups than in healthy controls with no difference between AD and LBD patients for raw RT. In contrast, for normalised RT there was no significant difference in the executive conflict effect between controls and either dementia group, although there was a trend for a larger effect in AD patients than in LBD patients. Again, analysing matched dementia

subgroups did not change the results significantly (Table 2.6). Considering error rates, the executive conflict effect was significant in all groups, and compared to controls, it was significantly larger in both AD and LBD patients (Table 2.7). There were no significant correlations between the executive conflict effect RT and clinical variables even for uncorrected $p<0.05$. While there was a significant interaction between cue and target for both raw and normalised RT (Table 2.5), this interaction did not differ between groups and was not analysed further.

Table 2.4. Mean error rates (%) for each task condition (cue x target), for the controls, AD and LBD patients. Standard deviations are presented in brackets.

		HC	AD	LBD
Mean error rates (%)				
All trials		1.8 (1.7)	9.7 (8.6)	13.3 (9.1)
	Overall	1.9 (2.4)	9.8 (7.5)	14.1 (10.3)
No Cue	Congruent	1.1 (2.1)	4.3 (6.0)	5.8 (6.0)
	Incongruent	2.8 (3.8)	15.3 (11.6)	22.4 (17.5)
	Overall	2.1 (1.8)	9.5 (9.1)	12.8 (9.1)
Neutral	Congruent	1.1 (1.5)	5.4 (5.8)	7.6 (8.1)
	Incongruent	3.1 (2.6)	13.7 (13.4)	18.0 (14.2)
	Overall	1.5 (1.8)	9.8 (9.9)	13.0 (9.5)
Spatial	Congruent	0.7 (1.7)	5.2 (7.6)	6.4 (7.5)
	Incongruent	2.3 (2.5)	14.5 (15.0)	19.6 (14.2)
Congruent	Overall	0.9 (1.5)	4.9 (6.0)	6.6 (6.2)
Incongruent	Overall	2.7 (2.4)	14.5 (12.8)	20.0 (14.3)
ANT effects (%)				
Alerting		-0.2 (2.2)	0.2 (3.5)	1.3 (3.5)
Orienting		0.6 (1.3)	-0.3 (3.7)	-0.3 (3.7)
Executive		1.78 (2.1)*	9.7 (10.2)*	9.6 (10.2)*

AD, Alzheimer's disease; HC, healthy controls; LBD, Lewy body dementia;
*Significant ANT effect, p-value<0.05 for error rates.

Table 2.5. Results from statistical tests for raw and normalised RT. Repeated measures (cue x target) ANOVA effects with group (HC, AD, LBD) as between-subject factor (F value, degrees of freedom (df), error df, and p-value), and post-hoc tests ([95% confidence interval of the mean difference], Bonferroni-corrected p-values).

		Effect significance, raw RT	Effect significance, normalised RT
Main effects			
Group		F(2,95)=24.19, p<0.001	
Post-hoc	HC-AD	[-578.9, -131.4], p=0.001	
	HC-LBD	[-802.5, -384.9], p<0.001	
	AD-LBD	[-425.9, -51.2], p=0.008	
Cue		F(2,190)=73.97, p<0.001	F(2,190)=131.81, p<0.001
Post-hoc	Alerting	[4.9, 46.1], p=0.01	[0.011, 0.038], p<0.001
	Orienting	[58.7, 104.5], p<0.001	[0.055, 0.085], p<0.001
Target		F(1,95)=448.04, p<0.001	F(1,95)=981.64, p<0.001
Interactions			
Cue x group		F(4,190)=1.64, p=0.17	F(4,190)=6.97, p<0.001
HC	Cue		F(2,42)=167.0, p<0.001
	Alerting		[0.026, 0.068], p<0.001
	Orienting		[0.073, 0.111], p<0.001
AD	Cue		F(2,60)=33.33, p<0.001
	Alerting		[-0.003, 0.047], p=0.10
	Orienting		[0.037, 0.089], p<0.001
LBD	Cue		F(2,88)=24.89, p<0.001
	Alerting		[-0.015, 0.026], p=1.0
	Orienting		[0.03, 0.080], p<0.001
Target x group		F(2,95)=5.30, p=0.007	F(2,95)=3.01, p=0.054
HC	Executive	F(1,21)=111.68, p<0.001	F(1,21)=227.05, p<0.001
AD	Executive	F(1,30)=205.38, p<0.001	F(1,30)=370.25, p<0.001
LBD	Executive	F(1,44)=226.33, p<0.001	F(1,44)=443.46, p<0.001
Cue x target		F(1.7,157.1)=6.51, p=0.002	F(1.9,177.8)=14.53, p<0.001
Cue x target x group		F(3.3,157.1)=0.9, p=0.46	F(3.7,177.8)=1.44, p=0.22
Magnitude group differences			
Alerting	ANOVA	F(2,95)=2.63, p=0.08	F(2,95)=4.85, p=0.01
Post-hoc	HC-AD		[-0.010, 0.060], p=0.25
	HC-LBD		[0.009, 0.074], p=0.008
	AD-LBD		[-0.013, 0.046], p=0.52
Orienting	ANOVA	F(2,95)=0.27, p=0.77	F(2,95)=3.06, p=0.052
Executive	ANOVA	F(2,95)=5.30, p=0.007	F(2,95)=3.01, p=0.054
Post-hoc	HC-AD	[-325.5, -17.55], p=0.02	[-0.111, 0.049], p=1.0
	HC-LBD	[-326.4, -39.1], p=0.008	[-0.039, 0.111], p=0.73
	AD-LBD	[-140.2, 117.7], p=1.0	[-0.0001, 0.134], p=0.05

AD, Alzheimer's disease; HC, healthy controls; LBD, Lewy body dementia; RT, reaction time.

Table 2.6. Results from statistical tests for raw and normalised RT analysing matched dementia subgroups (see Section 2.3.1). Repeated measures (cue x target) ANOVA effects with group (HC, AD, LBD) as between-subject factor (F value, degrees of freedom (df), error df, and p-value), and post-hoc tests ([95% confidence interval of the mean difference], Bonferroni-corrected p-values).

		Effect significance, raw RT	Effect significance, normalised RT
Main effects			
Group		F(2,81)=29.6, p<0.001	
Post-hoc	HC-AD	[-557.0, -118.7], p=0.001	
	HC-LBD	[-857.5, -442.3], p<0.001	
	AD-LBD	[-507.4, -116.6], p=0.001	
Cue		F(2,162)=63.3, p<0.001	F(2,162)=115.9, p<0.001
Post-hoc	Alerting	[-4.2, 37.6], p=0.16	[0.006, 0.032], p=0.002
	Orienting	[59.9, 109.1], p<0.001	[0.073, 0.106], p<0.001
Target		F(1,81)=440.1, p<0.001	F(1,81)=978.0, p<0.001
Interactions			
Cue x group		F(4,162)=2.00, p=0.10	F(4,162)=8.4, p<0.001
HC	Cue		F(2,42)=167.0, p<0.001
	Alerting		[0.026, 0.068], p<0.001
	Orienting		[0.073, 0.111], p<0.001
AD	Cue		F(2,52)=27.3, p<0.001
	Alerting		[-0.012, 0.037], p=0.62
	Orienting		[0.044, 0.113], p<0.001
LBD	Cue		F(2,68)=16.4, p<0.001
	Alerting		[-0.025, 0.020], p=1.0
	Orienting		[0.024, 0.078], p<0.001
Target x group		F(2,81)=6.4, p=0.003	F(2,81)=3.10, p=0.051
HC	Executive	F(1,21)=111.68, p<0.001	F(1,21)=227.05, p<0.001
AD	Executive	F(1,26)=187.8, p<0.001	F(1,26)=428.5, p<0.001
LBD	Executive	F(1,34)=194.6, p<0.001	F(1,34)=361.2, p<0.001
Cue x target		F(1.6,132.9)=4.7, p=0.01	F(1.9,150.5)=10.7, p<0.001
Cue x target x group		F(3.3,132.9)=1.1, p=0.37	F(3.7,150.4)=1.39, p=0.24
Magnitude group differences			
Alerting	ANOVA	F(2,81)=3.58, p=0.03	F(2,81)=7.0, p=0.002
Post-hoc	HC-AD	[-21.5,86.5], p=0.44	[0.000, 0.068], p=0.047
	HC-LBD	[4.8,107.1], p=0.03	[0.017, 0.081], p=0.001
	AD-LBD	[-24.7,71.7], p=0.71	[-0.016, 0.045], p=0.72
Orienting	ANOVA	F(2,81)=0.15, p=0.87	F(2,81)=3.0, p=0.055
Executive	ANOVA	F(2,81)=6.4, p=0.003	F(2,81)=3.1, p=0.051
Post-hoc	HC-AD	[-341.6, -29.7], p=0.01	[-0.120, 0.039], p=0.65
	HC-LBD	[-353.3, -57.7], p=0.003	[-0.044, 0.107], p=0.93
	AD-LBD	[-159.0, 119.3], p=1.0	[0.001, 0.143], p=0.05

AD, Alzheimer's disease; HC, healthy controls; LBD, Lewy body dementia; RT, reaction time.

Table 2.7. Results from statistical tests for error rates. Repeated measures (cue x target) ANOVA effects with group (HC, AD, LBD) as between-subject factor (F value, degrees of freedom (df), error df, and p-value), and post-hoc tests ([95% confidence interval], Bonferroni-corrected p-values).

		Effect significance, error rates
Main effects		
Group		F(2,95)=15.59, p<0.001
	HC-AD	[-13.3, -2.5], p=0.002
Post-hoc	HC-LBD	[-16.5, -6.5], p<0.001
	AD-LBD	[-8.1, 0.9], p=0.17
Cue		F(1.8,172.4)=0.67, p=0.51
Target		F(1,95)=57.70, p<0.001
Cue x group		F(3.6,172.4)=0.65, p=0.63
Interactions		
Target x group		F(2,95)=9.38, p<0.001
HC	Executive	F(1,21)=15.98, p=0.001
AD	Executive	F(1,30)=27.10, p<0.001
LBD	Executive	F(1,44)=51.82, p<0.001
Cue x target		F(1.9,176.2)=3.87, p=0.02
Cue x target x group		F(3.7,176.2)=1.76, p=0.14
Magnitude group differences		
Alerting	ANOVA	F(2,95)=0.79, p=0.46
Orienting	ANOVA	F(2,95)=0.44, p=0.65
Executive	ANOVA	F(2,95)=9.38, p<0.001
	HC-AD	[-14.8, -0.8], p=0.02
Post-hoc	HC-LBD	[-18.1, -5.1], p<0.001
	AD-LBD	[-9.6, 2.0], p=0.35

AD, Alzheimer's disease; HC, healthy controls; LBD, Lewy body dementia.

Table 2.8. Spearman's correlations between clinical scores and ANT effects using raw and normalised RT in the dementia groups. All correlations are shown that have uncorrected p-values<0.05. Correlations surviving FDR-correction are marked with an asterisk.

		Raw RT	Normalised RT
AD			
Mean RT	MMSE	ρ=-0.52 (p=0.002, p_{FDR}=0.02)*	/
	CAMCOG	ρ=-0.47 (p=0.007, p_{FDR}=0.02)*	/
Error rate	MMSE	ρ=-0.47 (p=0.007, p_{FDR}=0.02)*	/
	CAMCOG	ρ=-0.45 (p=0.01, p_{FDR}=0.02)*	/
LBD			
Mean RT	UPDRS	ρ=0.32 (p=0.03, p_{FDR}=0.20)	/
	Mayo cogn[a]	ρ=0.30 (p=0.05, p_{FDR}=0.50)	/
Error rate	MMSE	ρ=-0.60 (p<0.001, p_{FDR}<0.001)*	/
	CAMCOG	ρ=-0.68 (p<0.001, p_{FDR}<0.001)*	/
Orienting	CAF freq	ρ=0.32 (p=0.03, p_{FDR}=0.50)	ρ=0.30 (p=0.05, p_{FDR}=0.62)

AD, Alzheimer's disease; CAF freq, Clinician Assessment of Fluctuation frequency subscale; CAMCOG, Cambridge Cognitive Examination; LBD, Lewy body dementia; Mayo cogn, Mayo Fluctuations cognitive subscale; MMSE, Mini Mental State Examination; RT, reaction time; UPDRS, Unified Parkinson's Disease Rating Scale

[a]N=43.

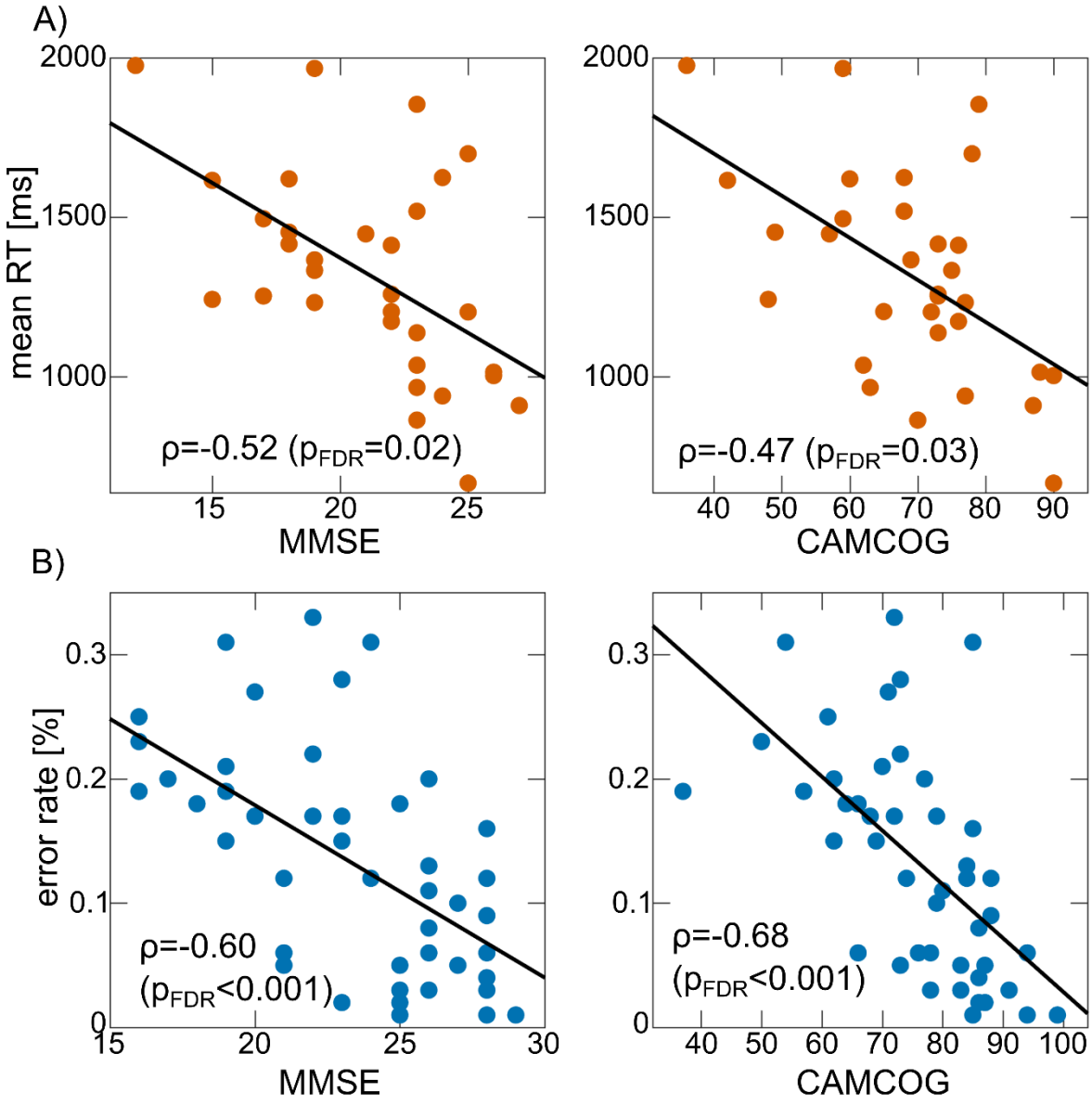

Figure 2.3. A) Spearman's correlations between global cognition and mean RT in the AD group. B) Spearman's correlation between global cognition and error rates in in the LBD group. All p-values are FDR-corrected for multiple comparisons.
MMSE, Mini Mental State Examination; CAMCOG, Cambridge Cognitive Examination; RT, reaction time.

2.3.3 Effect of dopaminergic medication in the LBD group

For raw RT, there was no interaction between LEDD and cue ($F(2,84)=0.15$, $p=0.86$) or target ($F(1,42)=0.003$, $p=0.96$). There was a main effect of cue ($F(2,84)=9.34$, $p<0.001$) with post-hoc tests revealing no alerting effect (no cue compared to neutral cue, 95% confidence interval (CI)=[-34.4, 37.5], $p=1.0$), but a significant orienting effect (neutral cue compared to spatial cue, 95% CI=[39.7, 126.4], $p<0.001$). Furthermore, there was a main effect of target with slower RTs in incongruent compared to congruent trials ($F(1,42)=104.1$, $p<0.001$).
For normalised RT, there was no interaction between LEDD and cue ($F(2,84)=0.08$, $p=0.92$) and no target by LEDD interaction ($F(1,42)=0.85$, $p=0.36$). There was a main effect of cue ($F(2,84)=12.20$, $p<0.001$) with no alerting effect (95% CI=[-0.02, 0.03], $p=1.0$), but a significant orienting effect (95% CI=[0.03, 0.08], $p<0.001$). There was also a significant main effect of target ($F(1,42)=224.01$, $p<0.001$).
These results indicate that dopaminergic medication dose does not significantly influence the ANT effects in LBD.

2.3.4 VBM analysis

Four DLB and two AD patients did not have structural scans and were therefore excluded from the VBM analysis.
In AD patients, a significant negative correlation was found between mean RT and grey matter volume in a large cluster at the lingual gyrus (Figure 2.4A). All other results in the AD group did not survive correction for multiple comparisons and are therefore reported as an exploratory analysis at a voxel-level threshold of $p<0.001$ in Tables 2.9 and 2.10. The alerting effect negatively correlated with grey matter volume in parietal regions and positively correlated with white matter volume in occipital regions. For the orienting effect there were positive correlations with grey matter volume in occipital and white matter volume in temporal regions. Additionally, grey matter volume in different parts of the cerebellum in the AD group correlated with the executive conflict effect.
In LBD patients, a significant negative correlation was found between the white matter volume in a large cluster at the lateral occipital cortex and the orienting effect (Figure 2.4B). Other results did not survive correction for multiple comparisons and are therefore reported at $p<0.001$ in Tables 2.11 and 2.12. There were positive correlations between grey matter volume in temporal and parietal regions and the alerting effect in patients with LBD. The orienting effect was positively correlated with grey matter volume in the parietal lobe and the executive conflict effect was negatively correlated with small grey matter clusters in temporal regions.

Table 2.9. Correlations between mean RT and ANT effects and grey matter volume in AD. All clusters are larger than five voxels and significant at p<0.001, uncorrected. Correction for multiple comparisons was performed with AlphaSim at p<0.05 resulting in minimum cluster sizes of 223 voxels for mean RT and 256 voxels for the ANT effects. Clusters surviving correction are highlighted with an asterisk. Locations were estimated from the Harvard-Oxford atlas in FSL.

Cluster location	size	MNI (X,Y,Z)
Mean RT, negative correlation		
L lingual gyrus	805*	-21,-58,-9
L angular gyrus	74	-45,-50,22
L paracingulate gyrus	56	-12,52,-6
R cerebellum Crus I	43	20,-86,-22
L middle frontal gyrus	31	-34,14,36
L post. supramarginal gyrus	30	-58,-46,30
L superior lateral occipital cortex	14	18,-62,50
L cerebellum Crus I	13	-24,-87,-28
R occipital pole	9	36,-93,9
L superior lateral occipital cortex	7	-18,-69,40
Alerting, negative correlation		
L anterior supramarginal gyrus	129	-51,-27,36
L posterior cingulate cortex	26	-9,-22,44
R postcentral gyrus	20	66,-10,14
L anterior supramarginal gyrus	14	-60,-34,45
L frontal orbital cortex	11	-22,32,-26
R occipital pole	9	26,-87,32
Orienting, negative correlation		
R frontal pole	7	52,39,15
Orienting, positive correlation		
R occipital pole	74	33,-92,20
R lateral occipital cortex	47	34,-76,39
L sup. lateral occipital cortex	23	-27,-80,32
R frontal pole	19	34,57,22
R superior lateral occipital cortex	16	34,-72,20
R superior lateral occipital cortex	15	26,-68,50
Executive, negative correlation		
R paracingulate gyrus	22	6,40,34
R cerebellum Crus I	20	48,-74,-30
R cerebellum Crus I	11	34,-82,-21
Executive, positive correlation		
R cerebellum V	24	8,-57,-27
R cerebellum Crus II	19	32,-63,-42

MNI, Montreal Neurological Institute coordinates; RT, reaction time.

Table 2.10. Correlations between mean RT and ANT effects and white matter volume in AD. All clusters are larger than five voxels and significant at p<0.001, uncorrected. Correction for multiple comparisons was performed with AlphaSim at p<0.05 resulting in minimum cluster sizes of 233 voxels for mean RT and 228 voxels for the ANT effects. There were no clusters which survived correction. Locations were estimated from the Harvard-Oxford atlas in FSL and white matter regions were identified from the nearest grey matter structure.

Cluster location	size	MNI (X,Y,Z)
Mean RT, negative correlation		
R inferior frontal gyrus	193	51,33,8
L postcentral gyrus	92	-54,-14,22
L middle temporal gyrus	85	-56,-36,-14
L lateral occipital cortex	49	-33,-69,0
L occipital fusiform gyrus	41	-22,-66,-8
R lateral occipital cortex	38	27,-82,21
L lingual gyrus	8	-12,-72,-8
L precentral gyrus	8	-46,-9,28
R inferior temporal gyrus	3	57,-36,-21
R frontal pole	2	45,40,-8
Alerting, positive correlation		
L lateral occipital cortex	36	-38,-64,33
Orienting, positive correlation		
R inferior temporal gyrus	7	56,-39,-18

MNI, Montreal Neurological Institute coordinates; RT, reaction time.

Table 2.11. Correlations between mean RT and ANT effects and grey matter volume in LBD. All clusters are larger than five voxels and significant at p<0.001, uncorrected. Correction for multiple comparisons was performed with AlphaSim at p<0.05 resulting in minimum cluster sizes of 230 voxels for mean RT and 242 voxels for the ANT effects. There were no clusters which survived correction. Locations were estimated from the Harvard-Oxford atlas in FSL.

Cluster location	size	MNI (X,Y,Z)
Mean RT, positive correlation		
L frontal pole	79	-24,58,27
L superior parietal lobule	23	-44,-40,54
L cerebellum X	7	-24,-40,-44
Alerting, positive correlation		
R parahippocampal gyrus	120	18,3,-42
L frontal pole	21	-8,44,51
R posterior temporal fusiform gyrus	11	39,-15,-27
Orienting, positive correlation		
L parahippocampal gyrus	81	-12,-38,-6
R frontal pole	11	30,48,34
R angular gyrus	11	46,-50,27
Executive, negative correlation		
R temporal pole	38	39,15,-46
Executive, positive correlation		
R frontal pole	7	42,54,18

MNI, Montreal Neurological Institute coordinates; RT, reaction time.

Table 2.12. Correlations between mean RT and ANT effects and white matter volume in LBD. All clusters are larger than five voxels and significant at $p<0.001$, uncorrected. Correction for multiple comparisons was performed with AlphaSim at $p<0.05$ resulting in minimum cluster sizes of 257 voxels for mean RT and 262 voxels for the ANT effects. Clusters surviving correction are highlighted with an asterisk. Locations were estimated from the Harvard-Oxford atlas in FSL and white matter regions were identified from the nearest grey matter structure.

Cluster location	size	MNI (X,Y,Z)
Mean RT, positive correlation		
R cerebellum I-IV	6	9,-48,-21
R temporal fusiform	2	39,-16,-22
R temporal fusiform	1	39,-21,-22
Orienting, negative correlation		
R lateral occipital	484*	24,-58,45
R paracingulate gyrus	159	9,22,45
R suppl. motor area	80	8,-10,54
L suppl. motor area	80	-8,-12,54
L frontal pole	79	-33,39,18
L precuneus	74	-8,-64,46
R angular gyrus	21	50,-46,18
R inferior temporal	17	45,-28,-22
R paracingulate gyrus	9	9,34,38
Orienting, positive correlation		
R occipital pole	12	24,-93,15

MNI, Montreal Neurological Institute coordinates; RT, reaction time.

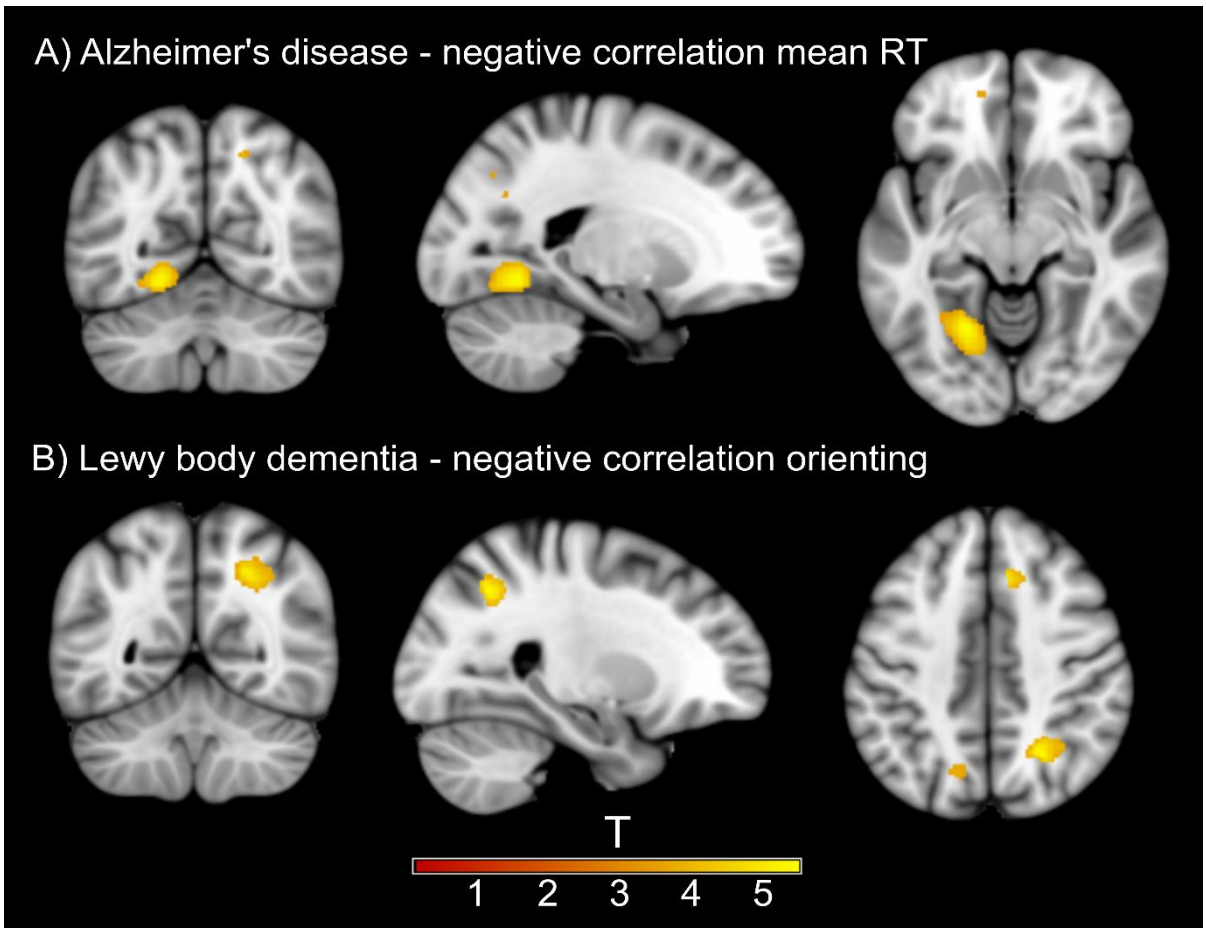

Figure 2.4. Significant clusters from VBM analysis. A) Negative correlation between mean reaction time (RT) and grey matter volume at the left lingual gyrus in the AD group. B) Negative correlation between the size of the orienting effect and white matter volume at the right lateral occipital cortex in the LBD group. Information on all uncorrected results can be found in Tables 2.9 - 2.12.

2.4 Discussion

In this chapter, the efficiency of different attentional systems in patients with AD and LBD was compared to healthy controls, in addition to examining the relationship between attentional deficits and structural abnormalities in the dementia groups.

2.4.1 Mean RT

Both dementia groups showed slower overall mean RTs than controls, and the LBD group showed slower RTs than the AD group. This is comparable to previous ANT studies in dementia cohorts (Fernandez-Duque and Black, 2006; Fuentes et al., 2010) and more general RT studies comparing AD and LBD (Ballard et al., 2001a; Bradshaw et al., 2004). In AD, the observed RT slowing was related to diminished overall cognitive functioning, i.e. patients with poorer cognitive function demonstrated more impaired RT performance. This finding in AD patients is in agreement with a previous study showing that increased RT during a choice

RT task is associated with reduced global cognitive functioning in AD and DLB patients (Ballard et al., 2001a). In contrast, this relationship was not observed in the present LBD group. However, DLB patients in Ballard et al. (2001a) were cognitively more impaired than our LBD patients which may explain the lack of association in the present analysis. A significant correlation was found between mean RT and grey matter volume at the lingual gyrus in AD patients, suggesting that lower brain volume in this area is related to general RT slowing. The ANT involves visual processing and therefore RT slowing in AD might be related to occipital/visual structural abnormalities. This agrees with previous studies showing associations between occipital cortex and visual impairments in AD and LBD (Firbank et al., 2003; Ossenkoppele et al., 2015; Taylor et al., 2012).

Compared to controls, the accuracy with which participants performed the task was lower in both dementia groups; however, error rates seen in the LBD group did not exceed those in the AD patients, indicating that LBD-related deficits seem to be specific to response speed, with limited impact on accuracy. In both dementia groups, there was a significant negative correlation between mean error rate and measures of overall cognition, indicating that both in AD and in LBD the overall severity of cognitive impairment has an influence on the patients' ability to accurately perform the task.

2.4.2 Alerting effect

With respect to the alerting effect, group differences only became apparent when studying normalised RT. This indicates that differences in alerting might have been obscured by overall differences in RT speed. The absence of a significant alerting effect in both dementia groups, i.e. the inability of patients to benefit from the cueing effect, is indicative of reduced efficiency of the alerting system which seems to be a general dementia phenomenon and not specific to LBD or AD. In LBD, this result is expected given the association between alerting efficiency and noradrenergic projections from the locus coeruleus which are affected by LBD (Coull et al., 2001; Raz, 2004). In AD, however, this result stands in contrast to a previous study which has found a significant alerting effect in this group (Fernandez-Duque and Black, 2006). AD patients in the present study were cognitively more impaired compared to the AD patients in the afore-mentioned study, indicating that there might be a loss of alerting efficiency with dementia progression. The absence of a significant correlation between the size of the alerting effect and the severity of cognitive impairment in the AD group, however, indicates that this is not a linear relationship. Another explanation for the lack of a significant alerting effect in the present study might be the modified ANT version that was used here. While Fernandez-Duque and Black (2006) used a display consisting of only two boxes that

both lit up in case of a neutral cue, in the present version the neutral cue was conveyed by flashing the central box while the target was presented in one of the boxes either below or above the central box. Thus, participants were required to re-orient their attention following a neutral cue which seemed to have a detrimental effect on some participants' RT performance, as suggested by negative alerting effects in some dementia patients (see Figure 2.2).
There were no significant associations between the alerting effect and grey and white matter volume in either dementia group. Using participants from the CATFieLD study, an fMRI study of the efficiency of the different attentional components found LBD, AD, and healthy control groups to have comparable fronto-parietal-occipital activations associated with the alerting effect (Firbank et al., 2016). Together with the results presented here, this suggests that the lack of a behavioural alerting effect in the dementia groups is unlikely to be due to region-specific functional or structural deficits.

2.4.3 Orienting effect

The orienting effect did not show group differences. This is comparable to previous literature showing preservation of the orienting system in AD patients (Fernandez-Duque and Black, 2006). However, given that the orienting system is postulated to be modulated by the basal forebrain cholinergic system (Fan et al., 2005), which is markedly affected in DLB (Clerici et al., 2007; Grothe et al., 2014), I expected the LBD group to exhibit reduced orienting efficiency. Given the marginally significant overall ANOVA for normalised RT and the prior hypothesis of reduced orienting efficiency in LBD, I conducted an exploratory post-hoc analysis which demonstrated a marginally significant lower orienting effect in LBD compared to controls ($p=0.049$), thus tentatively supporting the *a priori* hypothesis that this component of attention would be reduced in LBD, particularly when overall processing speed is considered. Orienting efficiency was related to white matter abnormalities in the occipital cortex in patients with LBD, indicating a relationship between less efficient use of the orienting cue and reduced white matter volume in the lateral occipital cortex. Previous fMRI studies have found brain activations for the orienting effect in occipital and parietal cortices (Fan et al., 2005; Firbank et al., 2016). The present results further suggest that structural alterations in these regions might also contribute to orienting inefficiency in LBD.
Associations with occipital cortical volume were also found for alerting and orienting effects in patients with AD. Even though these clusters did not survive correction for multiple comparison, they nevertheless suggest a trend for involvement of occipital regions in the efficiency of the ANT effects in both dementia groups.

2.4.4 Executive conflict effect

In agreement with previous studies (Fernandez-Duque and Black, 2006), the magnitude of the executive conflict effect was substantially greater in both dementia groups relative to controls, suggesting that dementia patients have a reduced ability to resolve conflict amongst responses. Executive dysfunction is characteristic of LBD patients (Noe et al., 2004). The reduced executive conflict efficiency in LBD patients fits with the notion of dopaminergic mediated frontal-striatal dysfunction being a contributory factor to the executive dysfunction in LBD (Fan et al., 2005; Kehagia et al., 2012). However, the group differences were greatly diminished when considering normalised RTs, indicating that this effect was partly due to differences in overall processing speed. No strong association between the efficiency of the executive conflict component and cortical volume was observed in either dementia group. In particular, contrary to a previous study in individuals with MCI (Borsa et al., 2016), there was no association between grey matter volume at the ACC and the executive conflict effect in patients with AD (even when considering uncorrected results). This might be due to higher inter-subject variability in ACC volume in MCI compared to AD. Furthermore, Borsa et al. (2016) restricted their analysis to relations between the ACC and the executive conflict effect which makes their approach more sensitive compared to the whole-brain approach across all attentional components applied here. Overall, the present results for the executive conflict effect suggest that the dementia-related inefficiency of this component might be related to functional or microstructural rather than macrostructural changes.

2.4.5 Clinical correlations

Contrary to the hypothesis, there were no significant correlations between cognitive fluctuation severity and attentional measures in patients with LBD. At an uncorrected threshold of $p<0.05$, there was a correlation between the size of the orienting effect and the CAF frequency score which indicates that in LBD, there might be a relationship between loss of orienting efficiency and more frequent cognitive fluctuations. This would be in line with previous reports in DLB showing associations between greater RT slowing and cognitive fluctuations (Bradshaw et al., 2006; Walker et al., 2000a). However, these results did not survive correction for multiple comparison and should therefore be interpreted with caution.

2.4.6 Limitations

Seeing as the orienting and executive conflict components are believed to be modulated by cholinergic and dopaminergic systems (Fan et al., 2005), a potential confound was the fact that most patients were taking cholinergic and/or dopaminergic medication. Regarding

dopaminergic medication, I showed that covarying for levodopa equivalent daily dose did not change the results (see Section 2.3.3). The small number of patients not taking acetylcholinesterase inhibitors did not allow for a more in-depth analysis of the effect of cholinergic medication on orienting and executive conflict effects; this remains a limitation of this work. A further limitation might be the fact that the two dementia groups were not completely matched in terms of overall cognitive impairment. Repeating the analysis using data from two subgroups of AD and LBD patients that were matched in terms of overall cognition, as measured by the MMSE, showed that results remained largely the same.

2.4.7 Conclusion

In contrast to previous studies in less impaired patients, this investigation did not find a significant alerting effect for either of the dementia groups. This might indicate that a loss of the facilitating cue effect occurs with dementia progression. In contrast, orienting was largely preserved with a slight impairment in patients with LBD that was not observed in the AD patients, and this might be related to structural abnormalities in occipital regions. Finally, the resolution of executive conflict was clearly impaired in both dementia groups but did not appear to be related to macrostructural changes in brain volume in either group.

Chapter 3. Ex-Gaussian Analysis of Reaction Time Data and Brain Structural Correlates

3.1 Introduction

In studies utilising cognitive tests with outcomes based on RT, it is common to focus on analysing mean RT. However, RT is usually not normally distributed, but positively skewed (Balota and Yap, 2011). Describing this distribution by more than central tendency measures therefore provides a more detailed and accurate analysis method (Balota and Yap, 2011). One distribution that has been used successfully to model empirical RT distributions is the exponentially modified Gaussian (ex-Gaussian) distribution. This is a convolution of a Gaussian and an exponential distribution characterised by three parameters – mu, sigma, and tau – that represent different aspects of the ex-Gaussian distribution. Mu and sigma describe the mean and standard deviation of the Gaussian part, respectively, while tau quantifies the right tail of the distribution which describes the subset of extremely slow responses (Ratcliff, 1979). The ex-Gaussian analysis therefore allows investigation of the effect of ageing and dementia on different aspects of RT distributions. An overall shift of the distribution to higher or lower values will be primarily reflected by a change in mu, whereas changes in skewness will be indicated by a change in tau. While ageing has been shown to affect all three parameters, AD has been shown to only affect the tau component compared to age-matched controls without dementia (Jackson et al., 2012; Tse et al., 2010). An increase in tau can also be observed when comparing individuals without dementia who later developed AD to those who did not, suggesting that these changes can be observed early in the course of the disease (Balota et al., 2010).

Even though attentional dysfunction is a core feature of LBD, no previous investigation has analysed RT data in LBD with an ex-Gaussian analysis. The aim of this chapter is therefore to investigate how different aspects of RT distributions – as modelled by the ex-Gaussian distribution – are differentially affected in LBD compared to AD and healthy ageing. Based on previous studies, I hypothesised that there will be an increase in tau in the AD group compared to healthy controls, with little change in mu and sigma (Jackson et al., 2012; Tse et al., 2010). Given that attentional impairment is more pronounced in LBD than in AD, I hypothesised to see an increase in all three ex-Gaussian parameters in patients with LBD compared to healthy controls and patients with AD. In addition, I expected this difference to be especially pronounced for tau, given that tau represents extremely slow responses which can be seen as lapses in attention (Schmiedek et al., 2007). Furthermore, I also explored the relationship between the different ex-Gaussian parameters and clinical scores in the LBD

group to investigate associations between clinical symptoms and different aspects of RT performance. Here, I hypothesised a correlation between cognitive fluctuation severity and the ex-Gaussian parameters in LBD, especially with respect to tau.
Previous studies have suggested that there might be an association between RT deficits and structural brain abnormalities in AD (Jackson et al., 2012). I therefore also investigated possible macrostructural neural correlates of RT deficits by analysing voxel-wise relations between the three ex-Gaussian parameters and grey and white matter volume in both dementia groups. I hypothesised to find correlations between grey and white matter volume loss and the ex-Gaussian parameters in AD, and that this relation would be less pronounced in LBD.

3.2 Methods

3.2.1 Participants

Data for this analysis were the same as in Chapter 2 (Section 2.2.2) involving the same participants from the CATFieLD study; 49 were diagnosed with probable LBD (26 DLB and 23 PDD patients), 33 with probable AD, and 22 were age-matched healthy controls. Again, all trials from runs with less than 2/3 correct responses were excluded from the analysis as performance below this was not different from chance (Firbank et al., 2016). Additionally, participants with fewer than 70 remaining correct trials were excluded to allow a robust fit of the ex-Gaussian distribution.

3.2.2 Ex-Gaussian analysis

Response times from the ANT were analysed by fitting an ex-Gaussian distribution to the RTs from all correct trials for each participant individually (combining all cue and target conditions). The ex-Gaussian distribution is a convolution of a Gaussian and an exponential distribution and can be described by three parameters: mu and sigma represent the mean and standard deviation of the Gaussian component, respectively, while tau is the decay parameter of the exponential component and characterises the slow tail of the distribution (Figure 3.1). Ex-Gaussian parameters for each participant were estimated using the DISTRIB toolbox in Matlab (R2015b) which applies a maximum likelihood approach with a bounded search (Lacouture and Cousineau, 2008).

3.2.3 VBM analysis

A VBM analysis was performed for all LBD and AD patients in SPM12 to assess voxel-wise correlations between the ex-Gaussian parameters and cortical volume, separately in each dementia group. Using the preprocessed images from Chapter 2 (Section 2.2.4),

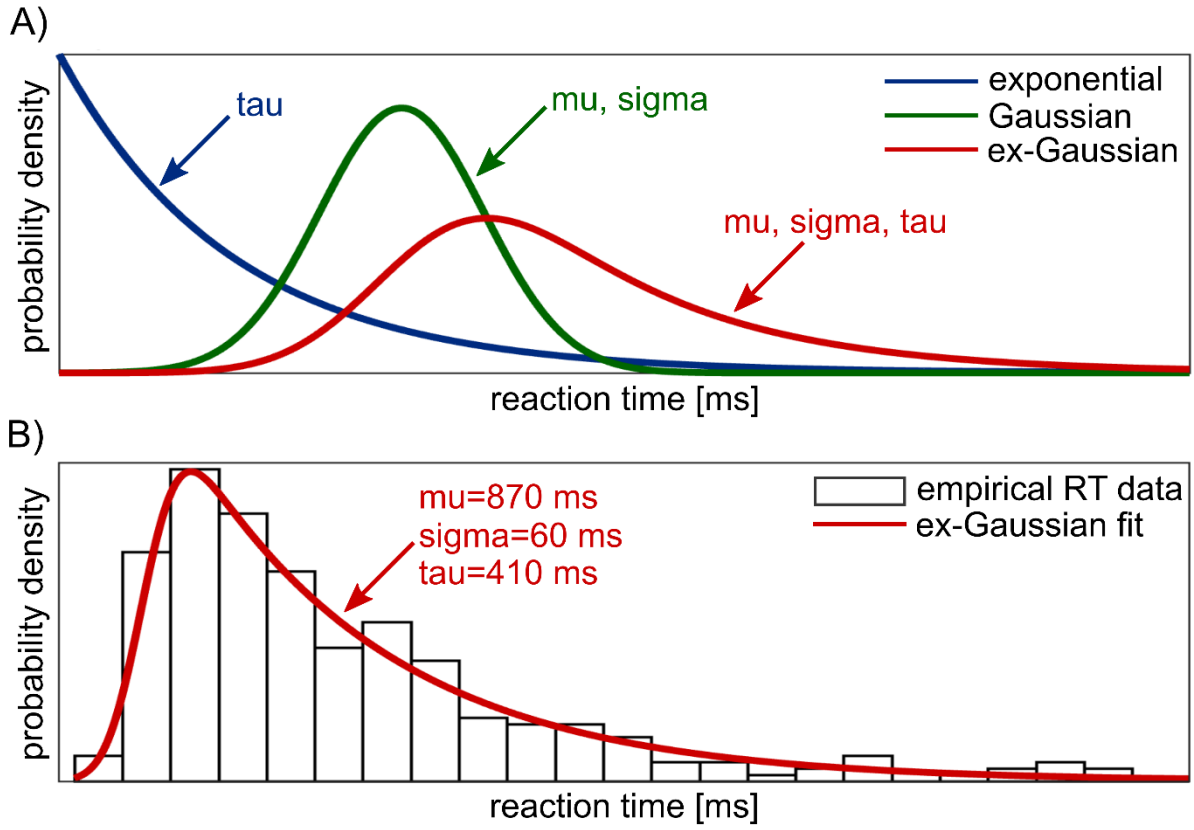

Figure 3.1. A) Ex-Gaussian function as a convolution of a Gaussian function with mean mu and standard deviation sigma and an exponential function with decay parameter tau. B) Example fit of the ex-Gaussian function to an empirical reaction time (RT) distribution.

correlations between grey and white matter volume and the ex-Gaussian parameters were assessed using a GLM in SPM for each parameter separately. Covariates of no interest for age, sex, total intracranial volume, and UPDRS motor scores (in LBD) were included in the design matrix. An explicit mask was estimated using the SPM Masking Toolbox (Ridgway et al., 2009) to restrict the statistical analysis to voxels that represent grey and white matter, respectively. An uncorrected voxel-level threshold of $p<0.001$ was chosen and the minimum cluster size for a corrected threshold of $p<0.05$ was determined by AlphaSim via Monte Carlo simulation using the REST software.

3.2.4 Statistics

Statistical analyses were carried out in IBM SPSS Statistics version 23 and R version 3.5.1. The three ex-Gaussian parameters were compared between the groups by a Kruskal-Wallis test and post-hoc Dunn's tests with Bonferroni correction. Correlations between the ex-Gaussian parameters and different clinical scores were assessed by Spearman's rank correlations. In the LBD group, correlations were calculated for cognitive fluctuation scores (Mayo and CAF total and subscores); supplementary analyses were performed for measures

of overall cognition (MMSE, CAMCOG), the UPDRS motor subscale, and the NPI hallucination scale. In the AD group, correlations were calculated for MMSE and CAMCOG. P-values were FDR-corrected for multiple comparisons.

To study possible effects of dopaminergic medication on the ex-Gaussian distribution in the LBD group, correlations between the three ex-Gaussian parameters and LEDD (Tomlinson et al., 2010) were investigated using Spearman's correlations.

3.3 Results

3.3.1 Demographics

Five AD, three DLB, and eight PDD patients were excluded because they did not meet the minimum RT performance criteria (Section 3.2.1). Therefore, 28 AD patients, 39 LBD patients (23 DLB and 16 PDD), and 22 healthy controls were included for further analysis. The lower number of included participants compared to Chapter 2 is due to the additional exclusion criterion (<70 correct trials) that was needed for a successful fit of the ex-Gaussian distribution (see Section 3.2.1).

Demographic and clinical information for all included participants is presented in Table 3.1. All three groups were matched for age and sex. As expected, the LBD group had more frequent occurrence of the core LBD symptoms (cognitive fluctuations, visual hallucinations, and Parkinsonism) than the AD group. However, they were slightly less impaired in terms of overall cognition (MMSE and CAMCOG) and the time since onset of cognitive symptoms was shorter in the LBD group compared with the AD group. To ensure that group differences in overall cognition did not influence the results, all analyses were repeated on AD and LBD subgroups matched for overall cognition. These matched dementia groups were created by excluding one AD patient with MMSE<16 and seven LBD patients (five DLB and two PDD) with MMSE>27. Subsequently, the two groups did not differ with respect to either dementia duration (Mann-Whitney U test, U=329, p=0.11), MMSE (Student's t-test, t_{57}=0.49, p=0.63) or CAMCOG (Student's t-test, t_{57}=0.31, p=0.76).

Similar to the standard RT analysis in Chapter 2, it was decided *a priori* to combine the DLB and PDD patients into one LBD group as previous studies have shown similar attentional and executive impairment in DLB and PDD (Ballard et al., 2002a; Firbank et al., 2016) as well as similar brain structural abnormalities (Burton et al., 2004). Both groups were matched in terms of age, overall cognition, and dementia duration. PDD patients were more impaired in terms of Parkinsonism, psychiatric symptoms, and cognitive fluctuations, and were more often on dopaminergic medication (Table 3.1).

Table 3.1. Demographics and clinical information, mean (standard deviation).

	HC (N=22)	AD (N=28)	LBD (N=39)	Group differences	DLB (N=23)	PDD (N=16)	Group differences
Male: female	15:7	22:6	34:5	χ^2=3.18, p=0.20[a]	18:5	16:0	χ^2=3.99, p=0.046[g]
Age	75.9 (5.4)	76.6 (8.1)	75.5 (5.5)	$F_{2,86}$=0.22, p=0.80[b]	76.4 (5.9)	74.2 (4.7)	t_{37}=1.27, p=0.21[h]
AChEI	na	26	35	χ^2=0.19, p=0.66[c]	21	14	χ^2 =0.15, p =0.70[g]
PD meds	na	0	28	χ^2=34.54, p<0.001[c]	12	16	χ^2 =10.66, p=0.001[g]
Duration	na	3.9 (2.1)	3.0 (1.9)	U=395, p=0.05[d]	3.4 (2.1)	2.6 (1.5)	U =142.50, p=0.22[j]
MMSE	29.2 (0.9)	21.8 (3.1)	23.5 (3.7)	t_{65}=1.94, p=0.06[e]	23.5 (4.0)	23.4 (3.4)	t_{37} =0.12, p =0.91[h]
CAMCOG	96.7 (3.7)	71.0 (11.5)	76.2 (12.5)	t_{65}=1.73, p=0.09[e]	76.0 (14.4)	76.5 (9.6)	t_{37} =0.13, p =0.90[h]
UPDRS	1.1 (1.4)	2.1 (2.0)	19.2 (8.4)	t_{65}=10.47, p<0.001[e]	14.3 (5.3)	26.2 (7.0)	t_{37} =6.08, p<0.001[h]
CAF total	na	0.7 (1.7)[f]	5.0 (4.7)	t_{64}=4.46, p<0.001[e]	3.8 (4.5)	6.6 (4.6)	t_{37} =1.93, p=0.06[h]
Mayo total	na	8.8 (4.0)[f]	13.2 (5.9)	t_{64}=3.39, p=0.001[e]	11.9 (6.1)	15.0 (5.3)	t_{37}=1.65, p=0.11[h]
Mayo cogn	na	1.8 (1.8)[f]	2.7 (1.9)	t_{64}=1.96, p=0.05[e]	2.1 (1.8)	3.5 (1.8)	t_{37}=2.35, p=0.02[h]
NPI total	na	6.9 (6.4)[f]	13.3 (10.4)	t_{64}=2.89, p=0.005[e]	8.7 (4.8)	20.1 (12.5)	t_{37}=3.99, p<0.001[h]
NPI hall	na	0.04 (0.2)[f]	1.7 (2.1)	t_{64}=4.14, p<0.001[e]	1.4 (1.7)	2.1 (2.5)	t_{37}=1.09, p=0.28[h]

AChEI, number of patients taking acetylcholinesterase inhibitors; AD, Alzheimer's disease; CAF total, Clinical Assessment of Fluctuations total score; CAMCOG, Cambridge Cognitive Examination; DLB, Dementia with Lewy bodies; Duration, duration of cognitive symptoms in years; HC, healthy controls; LBD, Lewy body dementia; Mayo cogn, Mayo Fluctuations cognitive subscale; Mayo total, Mayo Fluctuations Scale; Mayo arousal, Mayo Fluctuations arousal subscale; MMSE, Mini Mental State Examination; na, not applicable; PDD, Parkinson's disease dementia; PD meds, number of patients taking dopaminergic medication; UPDRS, Unified Parkinson's Disease Rating Scale III; NPI, Neuropsychiatric Inventory; NPI hall, NPI hallucination subscore

[a] Chi-square test HC, AD, DLB; [b] One-way ANOVA HC, AD, DLB; [c] Chi-square test AD, DLB; [d] Mann Whitney U test AD, DLB; [e] Student's t-test AD, DLB.

[f] N=27

[g] Chi-square test DLB, PDD; [h] Student's t-test DLB, PDD; [j] Mann Whitney U test DLB, PDD.

The number of recorded trials did not differ between the three groups (mean HC: 301.1, mean AD: 295.7, mean LBD: 302.8; Kruskal-Wallis test, F_2=1.07, p=0.59). The percentage of correct trials was higher in the control group than in the AD and LBD groups, but did not significantly differ between the two dementia groups (mean HC: 98%, mean AD: 90%, mean LBD: 85%; Kruskal-Wallis test, F_2=33.04, p<0.001; post-hoc Dunn's test, p(HC,AD)<0.001, p(HC,LBD)<0.001, p(AD,LBD)=0.27).

3.3.2 Comparison of ex-Gaussian parameters

Mu was significantly increased in the LBD group compared to both healthy controls and patients with AD. The difference between healthy controls and AD patients was not significant. The same effect was observed for sigma. Compared to controls, tau was significantly increased in both dementia groups, but there was no significant difference in tau between the two dementia groups (Figure 3.2 and Table 3.2). These results persisted when analysing matched dementia subgroups (Table 3.3).

Table 3.4 shows a comparison of ex-Gaussian parameters when DLB and PDD were treated as separate groups. Overall, the PDD group seemed to be more impaired than the DLB group (higher mu, sigma, and tau); however, none of the differences between DLB and PDD were significant after correcting for multiple comparisons.

Table 3.2. Ex-Gaussian parameters, mean (standard deviation). Between-group differences were assessed by Kruskal-Wallis tests with Dunn's post-hoc tests, Bonferroni-corrected for multiple comparisons.

	HC	AD	LBD	Kruskal-Wallis	post-hoc tests		
					HC vs AD	HC vs LBD	AD vs LBD
Mu	649.43 (73.88)	748.90 (139.38)	930.73 (166.22)	F_2=40.49, p<0.001	p=0.06	p<0.001	p<0.001
Sigma	59.85 (22.87)	78.57 (46.98)	125.03 (62.75)	F_2=23.25, p<0.001	p=0.86	p<0.001	p=0.001
Tau	313.48 (119.50)	523.28 (202.89)	572.99 (213.21)	F_2=24.16, p<0.001	p<0.001	p<0.001	p=1.00

AD, Alzheimer's disease; HC, healthy controls: LBD, Lewy body dementia.

Table 3.3. Ex-Gaussian parameters, mean (standard deviation) for matched dementia subgroups. Between-group differences were assessed by Kruskal-Wallis tests with Dunn's post-hoc tests, Bonferroni-corrected for multiple comparisons.

	HC	AD	LBD	Kruskal-Wallis	post-hoc tests		
					HC vs AD	HC vs LBD	AD vs LBD
Mu	649.43 (73.88)	738.21 (129.81)	958.61 (162.50)	F_2=42.57, p<0.001	p=0.10	p<0.001	p<0.001
Sigma	59.85 (22.87)	76.34 (46.34)	127.80 (65.09)	F_2=22.55, p<0.001	p=1.0	p<0.001	p=0.001
Tau	313.48 (119.50)	522.70 (206.74)	616.30 (204.76)	F_2=27.62, p<0.001	p=0.001	p<0.001	p=0.36

AD, Alzheimer's disease; HC, healthy controls: LBD, Lewy body dementia.

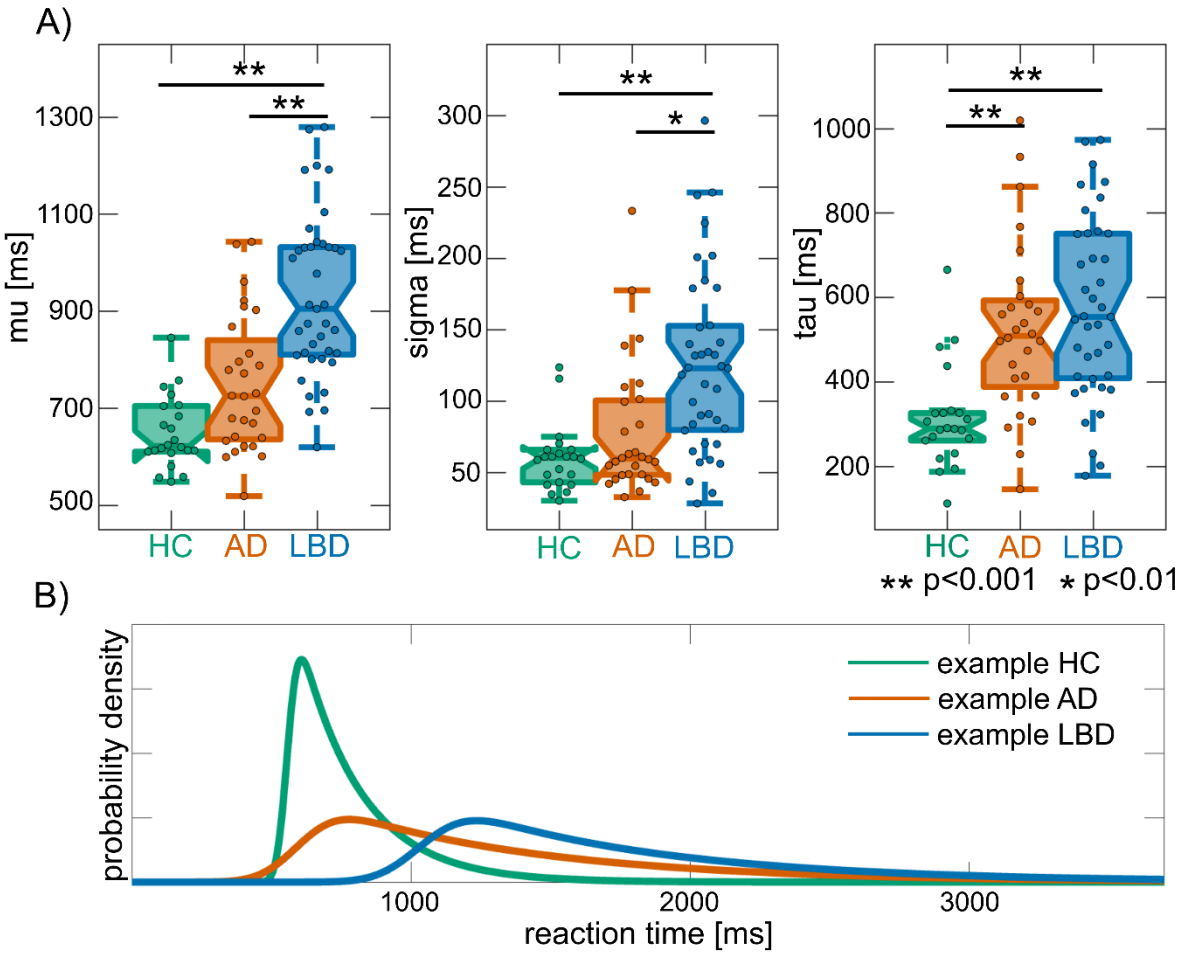

Figure 3.2. A) Comparison of ex-Gaussian parameters between HC, AD, and LBD (see Table 3.2 for more detailed statistics). B) Fitted ex-Gaussian distributions for three exemplary participants illustrating the effect of increased tau in AD compared to an increase in all three parameters in LBD.
AD, Alzheimer's disease; HC, healthy controls; LBD, Lewy body dementia.

Table 3.4. Mean (standard deviation), Kruskal-Wallis test for between-group differences with post-hoc Dunn's test (Bonferroni corrected for multiple comparisons), treating DLB and PDD as separate groups.

	HC	AD	DLB	PDD	Kruskal-Wallis	post-hoc tests					
						HC vs AD	HC vs DLB	HC vs PDD	AD vs DLB	AD vs PDD	DLB vs PDD
Mu	649.43 (73.88)	748.90 (139.38)	879.89 (143.68)	1003.81 (173.36)	F_3=42.77, p<0.001	p=0.11	p<0.001	p<0.001	p=0.039	p=0.001	p=0.79
Sigma	59.85 (22.87)	78.57 (46.98)	104.92 (46.69)	153.94 (72.57)	F_3=26.08, p<0.001	p=1.0	p=0.009	p<0.001	p=0.128	p=0.001	p=0.554
Tau	313.48 (119.50)	523.28 (202.89)	545.86 (226.29)	611.99 (193.15)	F_3=25.29, p<0.001	p=0.001	p=0.001	p<0.001	p=1.0	p=1.0	p=1.0

AD, Alzheimer's disease; DLB, dementia with Lewy bodies; HC, healthy controls; PDD, Parkinson's disease dementia.

3.3.3 Clinical correlations

In the LBD group, there was a trend for a positive correlation between the UPDRS and mu and sigma, however, this correlation did not survive correction for multiple comparisons. There were no significant correlations between any of the ex-Gaussian parameters and any clinical fluctuation score (Table 3.5).

In the AD group, all three ex-Gaussian parameters were negatively correlated with both MMSE and CAMCOG, except for tau which only showed a significant correlation with MMSE (Table 3.5 and Figure 3.3).

Table 3.5. Spearman's correlations of ex-Gaussian parameters with clinical scores in the LBD and AD groups separately, correlation coefficient (p-value, FDR-corrected for multiple comparisons).

	Mu	Sigma	Tau
LBD			
CAF total	ρ=0.09 (p=0.60, p_{FDR}=0.86)	ρ=0.12 (p=0.48, p_{FDR}=0.86)	ρ=0.04 (p=0.83, p_{FDR}=0.86)
CAF duration	ρ=0.03 (p=0.86, p_{FDR}=0.86)	ρ=0.08 (p=0.63, p_{FDR}=0.86)	ρ=0.05 (p=0.74, p_{FDR}=0.86)
CAF freq	ρ=0.12 (p=0.45, p_{FDR}=0.86)	ρ=0.17 (p=0.29, p_{FDR}=0.76)	ρ=0.03 (p=0.85, p_{FDR}=0.86)
Mayo total	ρ=0.23 (p=0.15, p_{FDR}=0.55)	ρ=0.20 (p=0.22, p_{FDR}=0.65)	ρ=0.26 (p=0.11, p_{FDR}=0.51)
Mayo cogn	ρ=0.31 (p=0.06, p_{FDR}=0.42)	ρ=0.29 (p=0.07, p_{FDR}=0.42)	ρ=0.32 (p=0.04, p_{FDR}=0.42)
Mayo arousal	ρ=0.07 (p=0.67, p_{FDR}=0.86)	ρ=0.03 (p=0.86, p_{FDR}=0.86)	ρ=0.07 (p=0.66, p_{FDR}=0.86)
UPDRS	ρ=0.34 (p=0.03, p_{FDR}=0.19)	ρ=0.38 (p=0.02, p_{FDR}=0.19)	ρ=0.23 (p=0.15, p_{FDR}=0.46)
AD			
MMSE	ρ=-0.59 (p=0.001, p_{FDR}=0.003)*	ρ=-0.52 (p=0.005, p_{FDR}=0.009)*	ρ=-0.42 (p=0.03, p_{FDR}=0.03)*
CAMCOG	ρ=-0.60 (p=0.001, p_{FDR}=0.003)*	ρ=-0.47 (p=0.01, p_{FDR}=0.02)*	ρ=-0.23 (p=0.23, p_{FDR}=0.23)

AD, Alzheimer's disease; CAF, Clinician Assessment of Fluctuation; CAF duration, Clinician Assessment of Fluctuation duration subscale; CAF freq, Clinician Assessment of Fluctuation frequency subscale; CAMCOG, Cambridge Cognitive Assessment; FDR, false discovery rate; LBD, Lewy body dementia; Mayo arousal, Mayo Fluctuations arousal subscale; Mayo total, Mayo Fluctuations scale; Mayo cogn, Mayo Fluctuations cognitive subscale; MMSE, Mini Mental State Examination; UPDRS, Unified Parkinson's Disease Rating Scale III.

3.3.4 Effect of dopaminergic medication in the LBD group

There was no significant correlation between LEDD and mu (ρ=0.19, p=0.25) or tau (ρ=0.04, p=0.79) in the LBD group. However, there was a significant correlation between sigma and LEDD (ρ=0.38, p=0.02).

3.3.5 VBM analysis

Three DLB and two AD patients did not have structural MRI scans available and were therefore not included in the VBM analysis.

In AD, mu was negatively correlated with numerous clusters in widespread parts of the brain, including bilateral occipital, frontal, and temporal cortices (Figure 3.4 and Table 3.6). Two larger clusters in right frontal and left temporal regions survived correction for multiple comparisons. There was one very small cluster of positive correlation between mu and grey matter volume in the AD group. Sigma was negatively correlated with grey matter volume in right and left frontal pole and left supramarginal gyrus (after correction for multiple comparisons), and smaller clusters in left temporal and frontal regions, and the precuneus. There was a positive correlation between sigma and grey matter volume in bilateral temporal gyri and the cerebellum. Tau was negatively correlated with clusters in the right cerebellum while it was positively correlated with very small clusters in right temporal and frontal regions.

Two larger clusters of negative correlation between sigma and white matter volume in the left temporal gyrus survived multiple comparison correction (Figure 3.4 and Table 3.7). Mu was negatively correlated with white matter volume in the middle temporal regions, and tau was negatively correlated with white matter volume in left lingual regions. However, none of these clusters remained significant after correcting for multiple comparisons.

In the LBD group, when considering clusters with $p<0.001$ (uncorrected) mu was negatively correlated with grey matter volume in a cluster at the right lingual gyrus and frontal pole and smaller clusters at the right paracingulate and thalamus (Table 3.8). Mu and sigma were both negatively correlated with grey matter volume in the right supplementary motor area. Sigma was also negatively correlated with bilateral frontal and subcortical regions (left and right thalamus, bilateral basal ganglia, and right amygdala), right temporal pole, and precuneus. There was one smaller cluster of positive correlation with sigma in the right frontal pole. Tau was positively correlated with grey matter volume in the bilateral cerebellum and left frontal pole.

Mu and sigma were both negatively correlated with white matter volume in frontal regions and around the primary motor cortices and supplementary motor areas (Table 3.9). There was no significant correlation between white matter volume and tau. None of the grey matter and white matter clusters found in the LBD group survived correction for multiple comparisons.

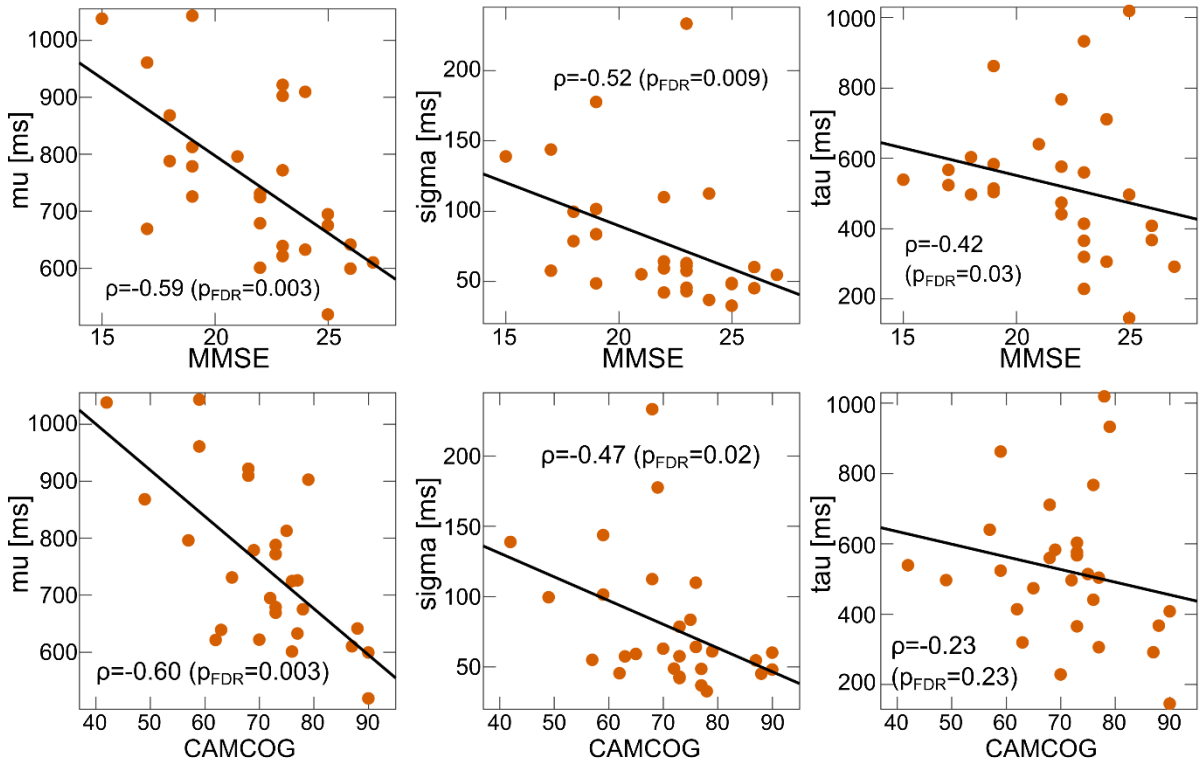

Figure 3.3. Spearman's correlations between global cognition and the three ex-Gaussian parameters in the AD group. All p-values are FDR-corrected for multiple comparisons. FDR, false discovery rate; MMSE, Mini Mental State Examination; CAMCOG, Cambridge Cognitive Examination.

Table 3.6. Correlations between ex-Gaussian parameters and grey matter volume in AD. All clusters are larger than five voxels and significant at p<0.001, uncorrected. Correction for multiple comparisons was performed using AlphaSim at p<0.05 which resulted in a minimum cluster size of 232 voxels for mu, 241 voxels for sigma, and 236 voxels for tau. Clusters surviving multiple comparison correction are highlighted with an asterisk. Anatomical labels were determined from the Harvard-Oxford Structural Atlas in FSL.

Cluster location	size	MNI (X,Y,Z)
Mu, negative correlation		
R frontal pole	422*	42, 36, 14
L planum polare	316*	-48, -4, -4
L middle temporal gyrus	156	-54, -45, -6
L lingual gyrus	127	-18, -62, -6
R inferior lateral occipital cortex	90	48, -66, 12
L postcentral gyrus	71	-56, -15,32
L posterior temporal fusiform cortex	61	-40,-40,-30
L paracingulate cortex	52	-14, 50,-3
R inferior lateral occipital cortex	52	33, -81, 10
L angular gyrus	37	-46, -50,22
R inferior lateral occipital cortex	34	40, -66,-4
R occipital pole	33	34, -94, 6
L posterior cingulate gyrus	32	-2, -38, 42
R frontal pole	29	27, 52, -20
R posterior middle temporal gyrus	21	54, -34, 0
R white matter	19	52, -34, 12
L posterior supramarginal gyrus	17	-58, -45,27
R middle temporal gyrus	14	46, -57, -2
L angular gyrus	10	-54, -57,36
L precentral gyrus	7	-62, -3, 6
R white matter	6	14, -78, 22
R cerebellum IX	6	9, -46, -38
L frontal pole	5	-18, 57, 28
Sigma, negative correlation		
R frontal pole	689*	42, 48, 12
L posterior supramarginal	428*	-60, -50, 12
L frontal pole	245*	-18, 52, 12
L frontal operculum cortex	178	-39, 28, 6
L middle temporal gyrus	97	-54, -44, -8
L precuneus	75	-15,-70, 24
L frontal pole	65	-15, 70, -3
L postcentral gyrus	40	-58,-18, 28
L planum polare	30	-48, -2, -9
L precentral gyrus	17	-46, 9, 30
L posterior middle temporal gyrus	17	-60, -15, -9
L frontal pole	10	-16, 62, 24
L posterior middle temporal gyrus	10	-52, -32, -14
L middle frontal gyrus	7	-34, 33, 44
Sigma, positive correlation		
R middle temporal gyrus	28	64, 0, -24
L anterior middle temporal gyrus	21	-66, -6,-16
L cerebellum Crus II	6	-33,-86,-45

Table 3.6 (continued). Correlations between ex-Gaussian parameters and grey matter volume in AD.

Cluster location	size	MNI (X,Y,Z)
Tau, negative correlation		
R cerebellum Crus I	143	18, -84,-24
L temporal occipital fusiform cortex	34	-28, -62,-9
Tau, positive correlation		
R post. superior temporal gyrus	9	69, -18, 0
R frontal pole	6	33, 34, -21

MNI, Montreal Neurological Institute coordinates.

Table 3.7. Correlations between ex-Gaussian parameters and white matter volume in AD. All clusters are larger than five voxels and significant at $p<0.001$, uncorrected. Correction for multiple comparisons was performed using AlphaSim at $p<0.05$ which resulted in a minimum cluster size of 204 voxels for mu, 224 voxels for sigma, and 231 voxels for tau. Clusters surviving multiple comparison correction are highlighted with an asterisk. Anatomical labels were determined from the Harvard-Oxford Structural Atlas in FSL and white matter regions were identified from the nearest grey matter structure.

Cluster location	size	MNI (X,Y,Z)
Mu, negative correlation		
L middle temporal gyrus	91	-54,-38,-10
R middle temporal gyrus	80	42, -48, 9
L occipital fusiform gyrus	30	-32, -69, 0
Sigma, negative correlation		
L superior temporal	588*	-54,-38, 12
L inferior temporal gyrus	584*	-45, -48,-8
L postcentral gyrus	144	-56,-18, 28
L cuneal cortex	125	-4, -87, 26
R intracalcarine cortex	99	9, -80, 15
R supramarginal gyrus	77	45, -44, 15
R superior temporal	62	56, -6, -9
L middle frontal gyrus	40	-28, 6, 42
L central opercular	31	-34, 2, 15
L middle frontal gyrus	25	-27, 28, 34
R postcentral gyrus	19	42, -21, 51
R lateral occipital cortex	15	28, -88, 6
L lingual gyrus	13	-12, -78, -8
L frontal pole	11	-24, 51, 10
L frontal pole	10	-32, 52,-10
R precentral gyrus	6	38, -2, 44
L frontal pole	5	-36, 46, 6
R intracalcarine cortex	5	21, -75, 10
Tau, negative correlation		
L lingual gyrus	30	-10, -72, -6

MNI, Montreal Neurological Institute coordinates.

Table 3.8. Correlations between ex-Gaussian parameters and grey matter volume in LBD. All clusters are larger than five voxels and significant at $p<0.001$, uncorrected. Correction for multiple comparisons was performed using AlphaSim at $p<0.05$ which resulted in a minimum cluster size of 228 voxels for mu, 220 voxels for sigma, and 229 voxels for tau. No clusters survived multiple comparison correction. Anatomical labels were determined from the Harvard-Oxford Structural Atlas in FSL.

Cluster location	size	MNI (X,Y,Z)
Mu, negative correlation		
R lingual gyrus	63	6, -92, -14
R white matter	37	12, 30, 45
R frontal pole	34	12, 54, 34
R thalamus	20	3, -16, 10
R paracingulate gyrus	16	3, 42, 34
R supplementary motor area	14	12, 0, 54
R thalamus	6	18, -34, 8
L thalamus	5	-20, -34, 6
Sigma, negative correlation		
R frontal pole	169	33, 40, 26
L middle frontal gyrus	152	-39, 14, 45
R superior frontal gyrus	116	14, 9, 56
L inferior frontal gyrus	111	-50, 15, 24
L frontal pole	91	-27, 39,-10
R amygdala	32	22, -8, -9
R supplementary motor area	31	3, -4, 62
R temporal pole	29	26, 6, -21
R precuneus	25	14, -48, 52
R middle frontal gyrus	24	34, 12, 33
R superior frontal gyrus	18	4, 33, 46
R thalamus	16	12, -36, 4
L middle frontal gyrus	14	-33, 14, 57
L thalamus	12	-10, -36, 3
R caudate	10	8, 18, 0
L pallidum	9	-20, -8, -9
L white matter	9	-40, 18, 14
Sigma, positive correlation		
R frontal pole	12	36, 42, 39
Tau, positive correlation		
L cerebellum Crus I	141	-39,-70,-34
R cerebellum IX	89	12,-58,-39
L frontal pole	64	-24,57,27
R cerebellum IX	62	6,-46,-54

MNI, Montreal Neurological Institute coordinates.

Table 3.9. Correlations between ex-Gaussian parameters and white matter volume in LBD. All clusters are larger than five voxels and significant at $p<0.001$, uncorrected. Correction for multiple comparisons was performed with AlphaSim at $p<0.05$ which resulted in a minimum cluster size of 253 voxels for mu, 244 voxels for sigma. No clusters survived multiple comparison correction. Anatomical labels were determined from the Harvard-Oxford Structural Atlas in FSL and white matter regions were identified from the nearest grey matter structure.

Cluster location	size	MNI (X,Y,Z)
Mu, negative correlation		
L precentral gyrus	186	-16,-27,57
R superior frontal gyrus	26	14,4,63
R superior frontal gyrus	26	22, 24, 40
R superior frontal gyrus	10	9, 34, 44
R frontal pole	9	15, 48, 34
R supplementary motor area	7	10, -3, 48
L cerebellum VIIb	6	-24,-69,-45
Sigma, negative correlation		
L frontal pole	146	-22, 51,-14
L frontal pole	71	-34, 46, -9
R frontal pole	32	44, 42, -8
L frontal pole	24	-38, 45, 4
R supplementary motor area	19	8, -4, 58
L middle frontal gyrus	14	-34, 12, 28
L frontal pole	8	-42,40,-10
L middle frontal gyrus	7	-36, 8, 42
R superior frontal gyrus	6	9, 46, 33
L precentral gyrus	5	-38, -16,63

MNI, Montreal Neurological Institute coordinates.

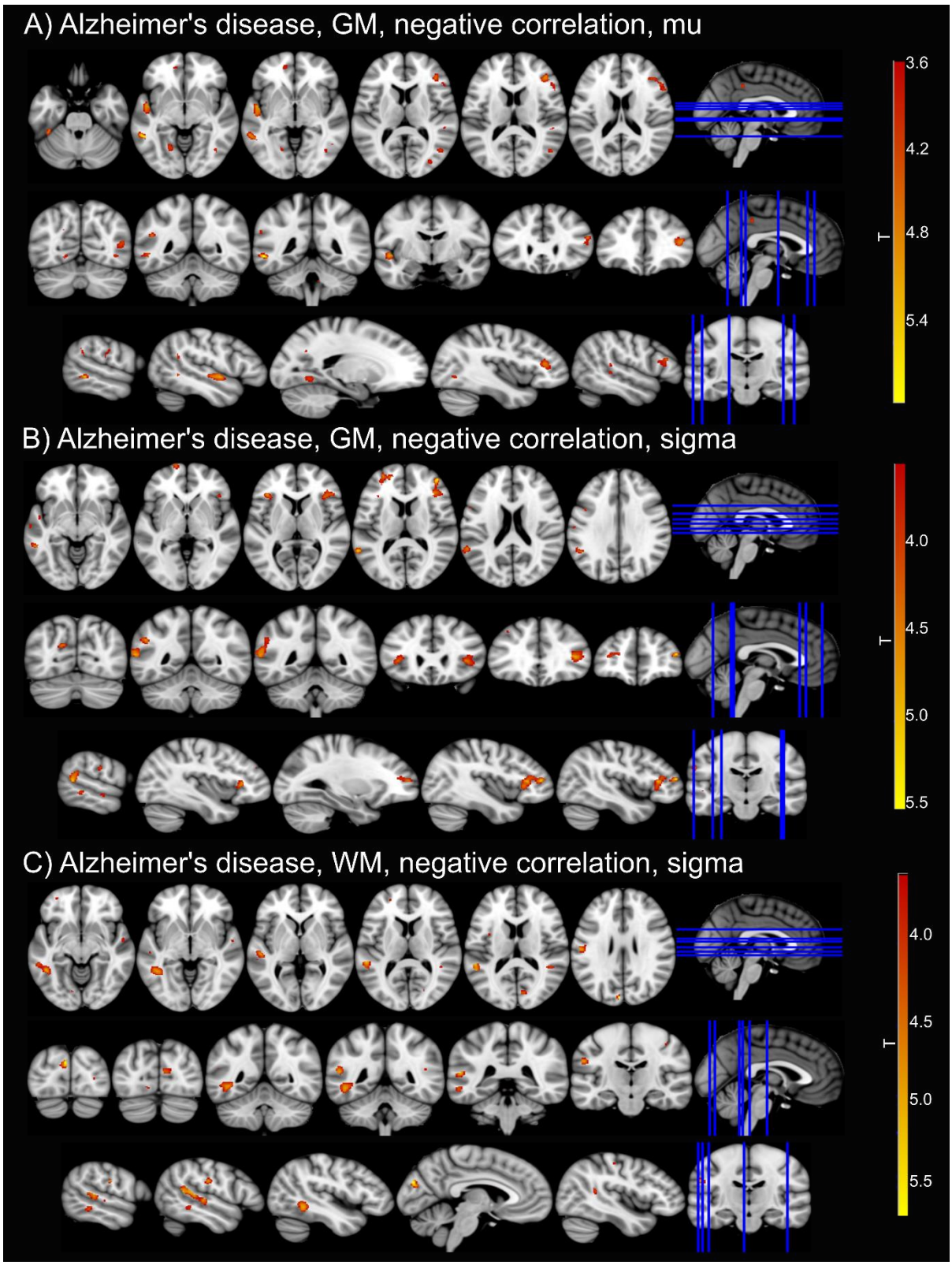

Figure 3.4. Correlations between ex-Gaussian parameters and grey matter (GM) and white matter (WM) volume in AD. See Tables 3.6 and 3.7 for all uncorrected clusters.

3.4 Discussion

In this chapter, using an ex-Gaussian modelling analysis, differences in RT distributions from an attentional task were investigated in LBD and AD patients compared to healthy controls. Differential effects were found for the different ex-Gaussian parameters, indicating that different aspects of RT distributions are differentially affected by the two forms of dementia. The two dementia groups could be distinguished by a relative lack of overall RT slowing in the AD group. While dementia in general led to more fluctuations in RT performance as indicated by an increased tau parameter, this did not appear to be associated with the clinical fluctuations observed in the LBD group. In AD patients, there were correlations between the Gaussian parameters and grey as well as white matter volume. In contrast, in LBD patients there was a relative lack of significant results with respect to correlations between RT performance and cortical volume.

3.4.1 More extremely slow responses in AD compared to controls

Results from the standard RT analysis described in Chapter 2 suggested a slowing of RT performance in both dementia groups as indicated by an increased mean RT (with more pronounced deficits in LBD compared to AD). The ex-Gaussian distributional analysis presented here allowed for a more detailed and specific characterisation of RT performance changes in dementia compared to standard RT analyses. The lack of a significant increase in the mean of the Gaussian component in AD compared to controls indicated that no major overall slowing of RTs occurred in the AD group. This was contrary to what had been suggested by the results of the standard RT analysis using arithmetic mean RTs. The increased tau parameter showed that the overall increase in mean RT in AD patients was being driven by an increase in extremely slow responses. These extremely slow responses could be seen as temporary attentional lapses in some but not all trials. They are thought to be more directly linked to attentional difficulties than an overall slowing of RTs (Hervey et al., 2006). It has also been argued that the tau parameter reflects more dynamic processes of attention such as attentional control and working memory; in AD, an increase in tau might thus reflect a breakdown of attentional control systems and poorer working memory capacities (Schmiedek et al., 2007; Tse et al., 2010). The present result is in line with previous studies that have consistently associated mild AD with an increase in tau and no change in mu or sigma across different tasks (Jackson et al., 2012; Tse et al., 2010). The same has been reported in individuals without dementia who later developed AD. This suggests that an increase in tau might be a very early indicator of the disease (Balota et al., 2010). Hence, the present results show that the overall pattern observed in pre-clinical and early-stage AD,

seems to persist in patients at a mild to moderate stage of dementia. However, in addition to an increase in tau, I also found a trend for a larger mu in AD compared to controls, indicating that a more general slowing of RTs might develop in AD patients as the disease progresses. This hypothesis is supported by a negative correlation between mu and dementia severity as measured by MMSE and CAMCOG, suggesting that more severe dementia is related to slower overall RTs in the AD group.

3.4.2 Overall RT slowing in LBD compared to AD and controls

In addition to the increase in excessively slow responses that was observed in both dementia groups, LBD patients also showed an overall slowing (increased mu) and higher variability (increased sigma) of RTs compared to controls. In addition, this slowing of RTs in patients with LBD was significantly larger than in the AD group and might be linked to greater attentional impairment in LBD relative to AD (Ballard et al., 2001a; Bradshaw et al., 2006). However, there was no difference between the two dementia groups with respect to the slow tail of the distribution, i.e. there was no further increase in attentional lapses in LBD patients compared to patients with AD. This is in contrast to my hypothesis given that tau is thought to capture attentional fluctuations (Schmiedek et al., 2007) which are a core symptom of LBD and less common in AD (Bradshaw et al., 2004). However, correlation analysis with the clinical fluctuation scales did not reveal any significant correlation between the severity of cognitive fluctuations and any of the ex-Gaussian parameters, suggesting that tau, contrary to my hypothesis, might not be a suitable measure of cognitive fluctuations in LBD. It also suggests that the fluctuations that are commonly observed in LBD patients and that are measured by clinical scales might not correspond well to trial-to-trial fluctuations observed upon the execution of the ANT task. This is in contrast to early studies in DLB that found a positive relation between the severity of cognitive fluctuations and trial-to-trial fluctuations on choice RT tasks (Ballard et al., 2002a, 2001b; Walker et al., 2000a). However, LBD patients in earlier studies were more impaired than the present LBD group and in contrast to most of our patients, they were not taking acetylcholinesterase inhibitors (Ballard et al., 2002a, 2001b; Walker et al., 2000a). Cholinesterase inhibitors have been shown to reduce RT variability in patients with cognitive fluctuations (Onofrj et al., 2003); the discrepancy between the present results and previous studies could therefore indicate that the association between clinical fluctuation severity and trial-to-trial RT variability is specific to unmedicated LBD patients. There was a correlation trend between the Gaussian parameters, mu and sigma, and the severity of Parkinsonism, suggesting that motor problems in LBD might have an influence on the general slowing of RT performance (Ballard et al., 2002a). This was supported by the fact

that the PDD group which generally showed more severe motor impairment also seemed to be more impaired in terms of the ex-Gaussian parameters than the DLB patients. However, these differences did not remain significant after correcting for multiple comparisons.

3.4.3 Structural correlates of RT deficits in LBD and AD

This is the first investigation assessing the association between ex-Gaussian parameters and cortical volume in LBD. There were more significant correlations between grey and white matter loss and RT deficits in AD patients than in LBD patients, indicating that attentional deficits in AD might be more strongly linked to regional brain volume than in LBD. The AD group showed negative correlations between grey matter volume in widespread cortical regions, such as temporal, lingual, and left frontal cortex, and the Gaussian part of the RT distribution (mu and sigma). Furthermore, white matter loss in temporal regions was related to increased sigma which corroborates the grey matter results. Both mu and sigma also correlated with MMSE and CAMCOG in AD, suggesting that correlations between cortical volume and these ex-Gaussian parameters may be related to global cognition in AD. This is supported by the negative correlations between mu and sigma and grey matter volume in several brain regions related to the DMN such as the occipital cortex, temporal gyrus, paracingulate cortex, frontal pole, and the precuneus (Mevel et al., 2011). The DMN has been associated with memory recall and is highly affected by AD pathology (Agosta et al., 2012). When considering results at an uncorrected threshold, the LBD group showed negative correlations in the frontal cortex, more specifically, a negative correlation between grey matter volume of the right frontal pole and RT variability. This agrees with Sanchez-Castaneda et al. (2009) who reported a relation between a reduction in cortical volume within frontal regions and worse performance on a test of maintained attention and response inhibition in patients with LBD. On the contrary, tau showed a positive correlation with grey matter volume of the left cerebellar Crus I. This region has been associated with the dorsal attention network (Peraza et al., 2014) and has been found to be structurally altered in patients with DLB (Colloby et al., 2014). The observed association of a higher number of extremely slow responses with an increase in grey matter volume might seem counter-intuitive, but may represent an imbalance within the attention system, where a structurally intact cerebellum may drive an “over-thinking” in the decision-making during the ANT task, causing higher values of tau. Although non-significant after multiple comparison correction, these regions showed some correspondence with the AD results and may deserve further investigation regarding their similarities and differences between both conditions. However, the overall lack of significant VBM correlations in the LBD group suggests that attentional dysfunction

in LBD might be more related to microstructural changes and functional changes that are not observable by volume estimators such as VBM (Kramer and Schulz-Schaeffer, 2007).

3.4.4 Limitations

Similar to Chapter 2 (Section 2.4.6), a possible limitation is the use of cholinergic and/or dopaminergic medication in many of the dementia patients. There was a positive correlation between LEDD and sigma in the LBD group, indicating that dopaminergic medication might have an influence on the variability of RT performance in LBD. Again, analysing the effect of cholinergic medication was not possible due to the small number of patients who were not taking acetylcholinesterase inhibitors.

Furthermore, the two dementia groups were not completely matched in terms of overall cognitive impairment; however, restricting the analysis to subgroups of AD and LBD patients that were matched in terms of overall cognition did not change the results.

As described in Chapter 2, the ANT was designed to probe three different aspects of attention – alerting, orienting, and executive conflict – by comparing RT performance between the different cue and target conditions (Fan et al., 2002). In the ex-Gaussian analysis, I combined trials from all conditions and could only consider overall effects on the three ex-Gaussian parameters. While the ex-Gaussian analysis provides a useful tool to separate different parts of the RT distribution, a problematic aspect is its need for a relatively high number of trials to obtain a good model fit. The low number of trials that was available for each cue and target condition did not allow for a successful fit of the ex-Gaussian distribution to trials from each condition individually. Therefore, it was not feasible to perform the ex-Gaussian analysis for the different components of the ANT. Future studies with a larger number of trials will be needed to study the effect of the different ANT conditions on the three ex-Gaussian parameters.

3.4.5 Conclusion

The ex-Gaussian analysis showed that different aspects of RT distributions are differentially affected by AD and LBD. Furthermore, the neural correlates of impaired attentional performance were shown to differ between the two forms of dementia. While impaired RT performance is linked to grey and white matter atrophy in AD, the more pronounced behavioural deficits that were observed in the LBD group did not exhibit strong correlations with brain structure, similar to what was shown in Chapter 2.

The following chapters will therefore focus on the analysis of functional neuroimaging and

electrophysiological data to investigate possible brain functional correlates of attentional impairment and cognitive fluctuations in LBD.

Chapter 4. Within- and between-network analysis of fMRI functional connectivity

4.1 Introduction

Resting-state fMRI can be used to study brain functional connectivity and enables characterisation of resting-state networks (RSNs) which are sets of brain regions that are spatially distinct, but show coordinated activity in the absence of a specific task (Biswal et al., 1995; Lowe et al., 1998). Several RSNs have been consistently found in healthy participant studies and involve brain regions that are related to different functions such as visual, motor and sensory processing, attention, salience, and memory (Damoiseaux et al., 2006). One RSN that has been of particular interest is the DMN which is typically active during rest and deactivated upon the execution of a task (Raichle et al., 2001).

Most studies investigating resting-state functional connectivity in DLB have used seed-based approaches (Galvin et al., 2011; Kenny et al., 2013, 2012) or only considered a small set of RSNs based on *a priori* hypotheses (Franciotti et al., 2013; Lowther et al., 2014; Peraza et al., 2014) and overall findings are somewhat inconsistent. While some studies have found that connectivity was generally decreased in DLB compared to age-matched healthy controls (Lowther et al., 2014; Peraza et al., 2014), other studies only report increased connectivity in DLB compared to controls (Kenny et al., 2013, 2012). Furthermore, the networks that have been found to be altered in DLB differ between studies. Decreased connectivity in DLB was reported for salience, executive (Lowther et al., 2014), frontoparietal, sensorimotor, and temporal networks (Peraza et al., 2014) whereas increased connectivity has been found for basal ganglia (Kenny et al., 2013; Lowther et al., 2014) and thalamic networks (Kenny et al., 2013). While functional connectivity within the DMN has been consistently found to be reduced in AD patients compared to healthy controls (Binnewijzend et al., 2012; Greicius et al., 2004), the role of the DMN in DLB has been debated with different studies showing increased (Galvin et al., 2011; Kenny et al., 2012), decreased (Lowther et al., 2014) or unchanged connectivity within this network compared to controls (Franciotti et al., 2013; Peraza et al., 2014). In addition to reporting inconsistent findings, previous analyses have been limited to studying within-network connectivity without considering connectivity changes between different RSNs. Therefore, the first aim of this chapter is to investigate functional connectivity changes in DLB patients compared to healthy controls and patients with AD within and between a wide range of RSNs without *a priori* selection. I hypothesised that DLB patients will show functional connectivity alterations in the following networks: motor and basal ganglia networks because of previous evidence for their implication in

Parkinsonism (Szewczyk-Krolikowski et al., 2014), attentional networks based on previous results in DLB (Peraza et al., 2014) and the presence of a wide range of attentional deficits in DLB (Ballard et al., 2001a), and visual networks given DLB-related impairments in visual processing (Mosimann et al., 2004).

Previous studies have found an association between resting-state functional connectivity measures and cognitive fluctuation severity, suggesting an involvement of connectivity alterations in attention-related networks (Franciotti et al., 2013; Peraza et al., 2014). The second aim of this chapter is therefore to investigate whether the observed connectivity changes in DLB are related to the clinical scores of cognitive fluctuations and test if this analysis could help in furthering our understanding of the etiological mechanisms underlying DLB core symptoms.

4.2 Methods

4.2.1 Participants

Data from the CATFieLD and ARThippo studies were combined for this analysis. This analysis involved 102 participants: 33 were diagnosed with probable DLB, 36 with probable AD, and 33 participants were healthy controls. Because the ARThippo study did not include PDD patients, this analysis was restricted to the DLB group without PDD patients.

4.2.2 Data acquisition

MR imaging for the CATFieLD and ARThippo studies was performed on the same 3T Philips Intera Achieva scanner. The imaging acquisition protocol was the same in both studies except for a different resolution of the structural scans. To account for this, in the group analysis a dichotomous covariate of no interest for study membership was included. Structural images were acquired with a MPRAGE sequence, sagittal acquisition, echo time 4.6 ms, TR 8.3 ms, inversion time 1250 ms, flip angle = 8°, SENSE factor = 2, and in-plane field of view 256 x 256 mm^2 with slice thickness 1.2 mm, yielding a voxel size of 0.93 x 0.93 x 1.2 mm^3 (ARThippo study) and in-plane field of view 240 x 240 mm^2 with slice thickness 1.0 mm, yielding a voxel size of 1.0 x 1.0 x 1.0 mm^3 (CATFieLD study). Resting-state scans for both studies were obtained with a gradient echo echo-planar imaging sequence with 25 contiguous axial slices, 128 volumes, anterior-posterior acquisition, in plane resolution = 2.0 x 2.0 mm, slice thickness = 6 mm, TR = 3000 ms, echo time = 40 ms, and field of view = 260 x 260 mm^2. DLB patients who were taking dopaminergic medication were scanned in the motor ON state.

4.2.3 Preprocessing

A first preprocessing step was carried out using FEAT (FMRI Expert Analysis Tool) version 6.0 which is part of the FMRIB's software library (FSL, www.fmrib.ox.ac.uk/fsl) including motion correction using FMRIB's Linear Image Registration Tool (MCFLIRT), slice-timing correction, and spatial smoothing with a 6.0 mm full width at half maximum Gaussian kernel. Participants were excluded if the MCFLIRT-estimated motion parameters exceeded 2 mm translation and/or 2° rotation. To assess differences in movement between the three groups due to patients with Parkinsonian symptoms the following formula was used (Liao et al., 2010):

$$\text{head motion/rotation} = (M-1)^{-1} \sum_{i=2}^{M} \sqrt{|x_i - x_{i-1}|^2 + |y_i - y_{i-1}|^2 + |z_i - z_{i-1}|^2},$$

where M is the total number of volumes (M=128), index i denotes the time points, and x_i, y_i, and z_i are the translations/rotations at the ith time point in x, y, and z direction. This analysis was done for translations and rotations separately.

Denoising was performed with ICA-AROMA in FSL which performs single-subject independent component analysis (ICA) to remove motion components from each participant's functional data (Pruim et al., 2015b, 2015a). Additionally, eroded CSF and white matter masks were estimated using FAST in FSL and the mean signal inside the mask was regressed out of each participant's cleaned functional data. Functional and structural images were then coregistered using boundary based registration in FSL, and normalised to the standard MNI template using Advanced Normalization Tools (Avants et al., 2011; Klein et al., 2009). Finally, functional data were temporally high-pass filtered with a cutoff of 150 s and resampled to a resolution of 4 x 4 x 4 mm^3. Grey matter probability maps were obtained from the FAST-segmented T1 images and included as voxel-wise spatial covariates in the group comparison analyses.

4.2.4 Analysis of resting-state data

To estimate independent healthy RSNs, 44 healthy control participants from the ICICLE and VEEG-Stim studies were selected. All participants were scanned on the same scanner as the participants from the main analysis. Eighteen of the additional HC participants were scanned with a slightly different scanner protocol with a change in the TR to 2072 ms and a change in the voxel size of the resting-state scans to 3 x 3 x 4 mm^3. The resting-state data were preprocessed in the same way as described in Section 4.2.3. Two subjects were excluded because they exceeded the motion exclusion criteria resulting in 42 independent HC

participants that were included in the generation of the RSN templates.

The temporally concatenated data from all independent HC participants were subjected to a group-ICA using FSL's Multivariate Exploratory Linear Optimised Decomposition into Independent Components (MELODIC). To obtain more reliable components, a meta ICA approach was adopted (Biswal et al., 2010; Poppe et al., 2013). To this end, MELODIC was repeated 25 times on randomised subsets of 30 out of the 42 HC participants. Subsequently, a meta ICA run was performed on the concatenated components from all individual ICA runs. A model order of 70 independent components was chosen for the individual as well as the meta ICA as this has been shown to be optimal for assessing disease-related group differences (Abou Elseoud et al., 2011; Dipasquale et al., 2015). To identify reliable components, the spatial correlation of each meta component across the individual ICA runs was calculated and components with a correlation <0.6 across runs were excluded (Cerliani et al., 2015). Furthermore, the meta ICA procedure was repeated using all HC participants from the main analysis and compared to the components from the independent group to ensure that the selected RSNs were present in both cohorts. All meta ICA components from the independent cohort that survived these reliability checks were visually inspected with respect to their spatial maps (Kelly et al., 2010) and 27 were identified as being of biological interest according to the previous literature (Agosta et al., 2012; Beckmann et al., 2005; Damoiseaux et al., 2008) (Figure 4.1 and Table 4.1).

Subsequently, within-network connectivity was assessed by running FSL-dual regression with all 27 identified RSNs concatenated in a single 4D image. First, for each participant, the RSN spatial maps were regressed (as spatial regressors in a multiple regression) into the participant's 4D dataset, resulting in a subject-specific timeseries, one for each RSN. Second, these timeseries were regressed (as temporal regressors, again in a multiple regression) into the same 4D dataset, resulting in a set of subject-specific spatial maps, one for each RSN. These spatial maps represent the participant's functional connectivity map for the respective RSN. Group differences in these functional connectivity maps between AD and HC, between DLB and HC, and between DLB and AD were assessed using FSL's randomise function with 10,000 permutations and family-wise error (FWE) correction for multiple comparisons using threshold-free cluster enhancement (TFCE). Covariates of no interest were included to control for age, sex, and study membership. Additionally, in order to reduce the impact of cortical atrophy differences between the participant groups, grey matter probability maps were also included as voxel-wise regressors in the linear model (Damoiseaux et al., 2012). To investigate between-network connectivity, the FSLNets package was applied to the subject-specific time series from dual regression (http://fsl.fmrib.ox.ac.uk/fsl/fslwiki/FSLNets). Full

and partial correlations were calculated between all pairs of RSNs and the resulting correlation coefficients were converted to z-scores for further analysis. Partial correlations are computed as correlations between two RSNs while controlling for the effect of all other RSNs and are thought to reflect more direct connections (Smith et al., 2011). FSL-randomise with 10,000 permutations was then applied to assess group differences in between-network connectivity including covariates for age, sex, and study membership. Results were FWE-corrected for multiple comparisons.

Table 4.1. List of all resting-state networks (RSNs) included in the analysis. Anatomical labels refer to bilateral areas if not stated otherwise. Locations of RSNs were estimated from the Harvard-Oxford Cortical and Subcortical Structural Atlases and the Cerebellar Atlas in FSL.

RSN name		Brain regions
Lateral sensorimotor network	LSMN	Pre- and postcentral gyrus
Medial sensorimotor network	MSMN	Pre- and postcentral gyrus, supplementary motor area
Supplementary motor area network	SMAN	Supplementary motor area, precentral gyrus
Left motor network	LMN	Left post- and precentral gyrus
Right motor network	RMN	Right post- and precentral gyrus
Basal ganglia network	BGN	Putamen, caudate
Thalamic network	THN	Thalamus
Cerebellar network 1	CBN1	Cerebellum crus I, crus II
Cerebellar network 2	CBN2	Cerebellum V, VI
Medial visual network	MVN	Intracalcarine cortex, supracalcarine cortex, lingual gyrus
Lateral visual network	LVN	Superior lateral occipital cortex, precuneus
Occipital pole network	OPN	Occipital pole
Lingual gyrus network	LGN	Lingual gyrus, intracalcarine cortex
Superior visual network	SVN	Superior lateral occipital cortex, occipital pole
Temporal network	TN	Planum temporale, Heschl's gyrus
Temporal pole network	TPN	Temporal pole
Insular network 1	ISN1	Insular cortex, frontal operculum cortex
Insular network 2	ISN2	Insular cortex, planum polare
Anterior cingulate network	ACN	Anterior cingulate cortex
Default mode network 1	DMN1	Precuneus, posterior cingulate cortex
Default mode network 2	DMN2	Precuneus
Default mode network 3	DMN3	Precuneus, superior lateral occipital cortex
Supramarginal gyrus network	SPGN	Supramarginal gyrus
Right fronto-parietal network	RFPN	Right superior lateral occipital cortex, right angular gyrus, right middle frontal gyrus, left superior lateral occipital cortex
Left fronto-parietal network	LFPN	Left superior lateral occipital cortex, right angular gyrus, left middle frontal gyrus, right superior lateral occipital cortex
Dorsal attention network	DAN	Superior parietal lobule, supramarginal gyrus, superior lateral occipital cortex
Ventral attention network	VAN	Middle frontal gyrus, inferior frontal gyrus

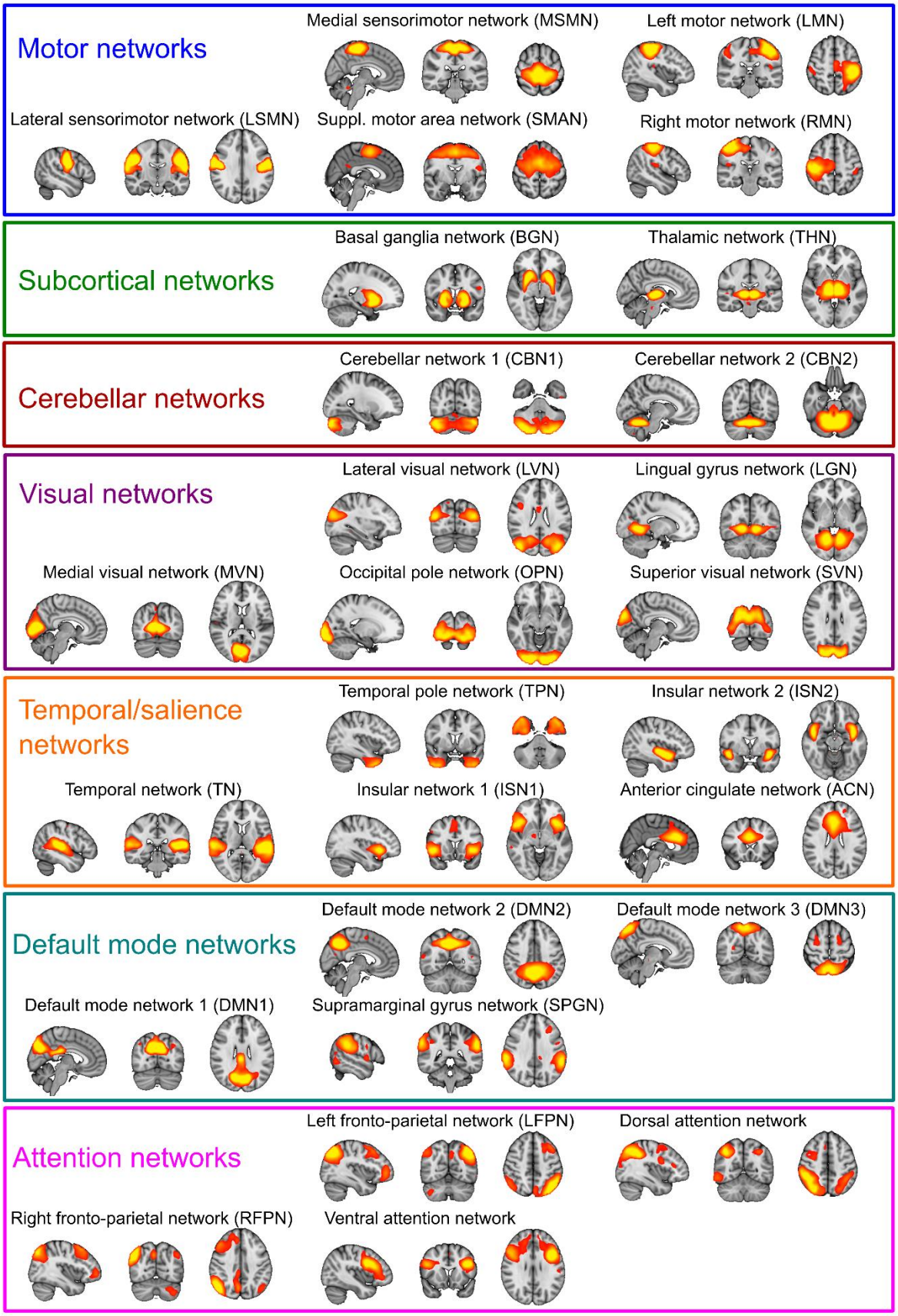

Figure 4.1. Spatial maps of the 27 resting-state networks (RSNs) obtained from the independent healthy control group. RSN maps are thresholded at 3<z<12. Images are shown in radiological convention, i.e. the left side of the image corresponds to the right hemisphere.

4.2.5 Statistical analysis

Statistical analyses were carried out in IBM SPSS version 23 and R version 3.5.1. In the DLB group, Spearman's correlations were calculated to assess relations between functional connectivity and clinical fluctuation scores (CAF total and subscores). The Mayo fluctuation scale was not assessed in the ARThippo study and was therefore not included in this analysis. Additional correlation analyses were performed for measures of overall cognition (MMSE and CAMCOG), the UPDRS motor subscore for Parkinsonism, and the NPI hallucination subscale for visual hallucination severity. Correlations were computed between these clinical scores and the mean connectivity within clusters with significant differences between DLB and controls (from dual regression) and for between-network connectivity scores for connections with significant between-group differences (from FSLNets). In the AD group, correlations were computed between overall cognitive scores (MMSE and CAMCOG) and mean connectivity of dual regression clusters that showed significant differences between AD patients and controls as well as between-network connectivity scores for connections with significant between-group differences from the FSLNets analysis.

In the DLB group, in addition to investigating correlations with mean connectivity within a cluster, voxel-wise correlations with cognitive fluctuation scores were also tested. To this end, the dual regression z-scores for all DLB participants were concatenated in one 4D image and correlations with clinical scores were tested using a GLM in FSL with the respective clinical score as covariate in the design matrix. Statistical significance was assessed using FSL randomise with 5,000 permutations including a mask for the significant clusters from the HC-DLB group comparisons. This analysis was also repeated for the other clinical scores (MMSE, CAMCOG, UPDRS, and NPI hallucination score).

To assess the effect of dopaminergic medication in the DLB group, a group comparison of the dual regression results was performed between patients who were taking dopaminergic medication (N=18) and those who were not on these medications (N=13) using FSL-randomise with 10,000 permutations and TFCE-correction.

4.3 Results

One AD patient was excluded due to coregistration errors. Additionally, two HC, six AD, and two DLB participants were excluded because of excessive motion. Therefore, 31 DLB patients, 29 AD patients, and 31 healthy controls were included in the analysis. The overall motion for all included participants was not significantly different between the three groups (Kruskal-Wallis test; rotation, H_2=1.93, p=0.38; translation, H_2=1.13, p=0.57).

4.3.1 Demographics

All three groups were matched for age and sex and the two dementia groups were matched in terms of overall cognition (MMSE and CAMCOG) and duration of dementia (Table 4.2). As expected, many DLB patients were taking dopaminergic medication whereas none of the AD patients were on these medications. The number of patients taking acetylcholinesterase inhibitors was not significantly different between the dementia groups. DLB patients were significantly more impaired in terms of Parkinsonism, visual hallucinations, and cognitive fluctuations than the AD patients.

The 42 independent HC participants whose fMRI data were used to estimate the RSNs, were significantly younger than the HC participants in the main analysis, but matched in terms of overall cognition (Table 4.3).

Table 4.2. Demographic and clinical variables, mean (standard deviation).

	HC (N=31)	AD (N=29)	DLB (N=31)	Between-group differences
Male: female	22:9	20:9	19:12	χ^2=0.73, p=0.70[a]
Study 1: study 2	15:16	13:16	12:19	χ^2=0.60, p=0.74[a]
Age	76.4 (7.2)	75.2 (8.6)	78.13 (6.7)	$F_{2,88}$=1.16, p=0.32[b]
AChEI	-	26	28	χ^2=0.007, p=0.93[c]
PD meds	-	0	18	χ^2=24.06, p<0.001[c]
Duration	-	3.7 (1.7)[f]	3.4 (2.3)	U=339, p=0.14[d]
MMSE	28.9 (1.1)	21.8 (3.8)	22.03 (4.3)	t_{58}=0.20, p=0.85[e]
CAMCOG	96.7 (3.2)	70.3 (13.5)	73.29 (13.6)	t_{58}=0.86, p=0.39[e]
UPDRS III	1.94 (2.8)	3.5 (4.0)	18.1 (10.2)	t_{58}=7.32, p<0.001[e]
CAF total	-	1.00 (2.51)[f]	4.8 (4.9)[g]	t_{56}=3.66, p=0.001[e]
NPI total	-	5.9 (5.5)[h]	14.55 (11.03)[i]	t_{54}=3.68, p=0.001[e]
NPI hall	-	0[j]	1.6 (1.8)[i]	t_{53}=4.53, p<0.001[e]

AChEI, number of patients taking acetylcholinesterase inhibitors; AD, Alzheimer's disease; CAF total, Clinical Assessment of Fluctuations total score; CAMCOG, Cambridge Cognitive Examination; DLB, Dementia with Lewy bodies; Duration, duration of cognitive symptoms in years; HC, healthy controls; Mayo total, Mayo Fluctuations Scale; Mayo cognitive, Mayo Fluctuation cognitive subscale; Mayo arousal, Mayo Fluctuations arousal subscale; MMSE, Mini Mental State Examination; PD meds, number of patients taking dopaminergic medication for the management of Parkinson's disease symptoms; UPDRS III, Unified Parkinson's Disease Rating Scale III (motor subsection); NPI, Neuropsychiatric Inventory; NPI hall, NPI hallucination subscore

[a] Chi-square test HC, AD, DLB; [b] One-way ANOVA HC, AD, DLB; [c] Chi-square test AD, DLB; [d] Mann Whitney U test AD, DLB; [e] Student's t-test AD, DLB.

[f] N=28; [g] N=30; [h] N=27; [i] N=29; [j] N=26.

Table 4.3. Demographics of the independent healthy control group that was used for the estimation of RSNs compared to the control group from the main analysis.

	HC main analysis (N=31)	HC for RSN template estimation (N=42)	Between-group comparison
Male: female	22:9	25:17	χ^2=1.02, p=0.31[a]
Age	76.4 (7.2)	69.0 (8.7)	t_{70}=3.85, p<0.001[b]
MMSE	28.9 (1.1)	29.2 (1.4)	t_{70}=1.08, p=0.29[b]

HC, healthy controls; MMSE, Mini Mental State Examination; RSN, resting state network.
[a] Chi-square test; [b] Student's t-test.

4.3.2 Within-network connectivity

Between-group comparisons of the dual regression results were performed across the whole brain space, i.e. they were not spatially bounded by the thresholded RSN spatial maps shown in Figure 4.1. This was done in order to be able to investigate connectivity between each RSN and the rest of the brain instead of only considering connectivity changes within the main spatial maps of the RSNs.

Decreased connectivity in AD patients compared to controls was found for the default mode network 1, for the lingual gyrus network, and in very small clusters for the right motor network. Connectivity was increased in patients with AD compared to controls in a small cluster within the dorsal attention network (Figure 4.2 and Table 4.4).

Decreased connectivity in DLB compared to controls was observed for ten RSNs including the lateral sensorimotor network, the medial sensorimotor network, the superior visual network, the temporal network, the basal ganglia network, the right motor network, the thalamic network, the insular network 1, the anterior cingulate network, and the temporal pole network (Figure 4.3 and Table 4.5). Increased connectivity in DLB compared to controls was found in very small clusters for the left motor network, the ventral attention network, and the insular network 2 (Figure 4.3 and Table 4.5).

In the comparison between the two dementia groups, very small clusters of increased connectivity were found in patients with DLB compared to patients with AD for the default mode network 1 (Table 4.6). There were no clusters of decreased connectivity in DLB patients compared to patients with AD.

Although decreased connectivity in the DLB group is reported for all clusters in panels A-F of Figure 4.3, it was evident that some of these results were due to correlations shifting from positive in the control group to negative in the DLB group (e.g. TN-1, Figure 4.4). Similarly, increased connectivity in the DLB group could also be due to correlations being negative in healthy controls, and shifting to positive correlations in DLB (e.g. ISN2-1).

Table 4.4. Dual regression results comparing AD and HC. All clusters are reported with p<0.05, TFCE-corrected. The table shows the number of significant voxels per cluster, the minimal p-value inside the cluster, the MNI coordinates of the voxel with minimal p-value, and the location of the cluster (estimated from the Harvard-Oxford Cortical and Subcortical Structural Atlases and the Cerebellar Atlas in FSL).

	N	p-value	MNI (X, Y, Z)	Location
HC > AD				
Default mode network 1				
DMN1-1	61	<0.001	20, 22, 24	L posterior cingulate, R posterior cingulate
DMN1-2	1	0.044	26, 13, 25	L precuneus
Lingual gyrus network				
LGN-1	20	0.001	20, 37, 27	R paracingulate gyrus
Right motor network				
RMN-1	1	0.03	10, 37, 15	R frontal orbital cortex
RMN-2	1	0.048	12, 33, 24	R precentral gyrus, R inferior frontal gyrus
AD > HC				
Dorsal attention network				
DAN-1	5	0.024	34, 17, 24	L angular gyrus

AD, Alzheimer's disease; HC, healthy controls; MNI, Montreal Neurological Institute coordinates.

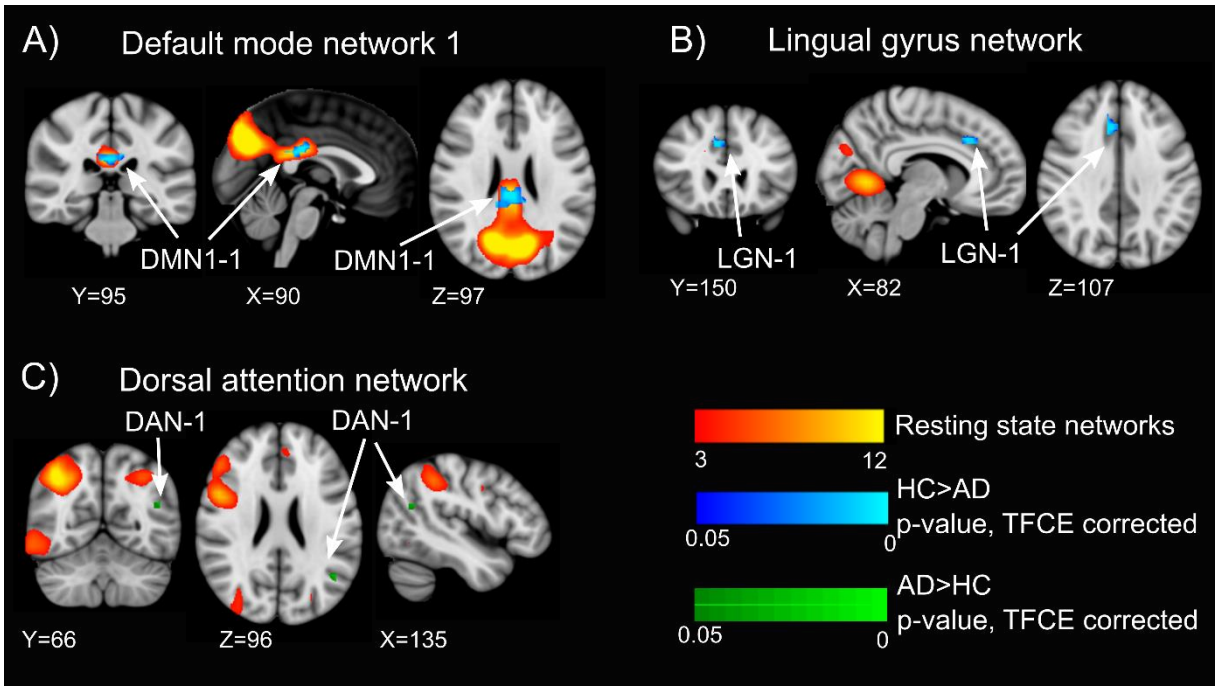

Figure 4.2. Dual regression results comparing AD and HC. RSN maps are shown in red-yellow. A, B) Clusters with decreased connectivity in AD; HC>AD, p<0.05, TFCE-corrected, shown in blue. C) Cluster with increased connectivity in AD; AD>HC, p<0.05, TFCE-corrected, shown in green. See Table 4.4 for more information on cluster locations and sizes. All images are shown in radiological convention.
AD, Alzheimer's disease; DAN, dorsal attention network; DMN 1, default mode network 1; HC, healthy controls; LGN, lingual gyrus network; TFCE, threshold-free cluster enhancement.

Table 4.5. Dual regression results comparing DLB and HC. All clusters are reported with p<0.05, TFCE-corrected. The table shows the number of significant voxels per cluster, the minimal p-value inside the cluster, the MNI coordinates of the voxel with minimal p-value, and the location of the cluster (from the Harvard-Oxford Cortical and Subcortical Structural Atlases and the Cerebellar Atlas in FSL).

	N	p-value	MNI (X, Y, Z)	Location
HC > DLB				
Lateral sensorimotor network				
LSMN-1	1	0.046	24, 28, 30	L supplementary motor cortex
Medial sensorimotor network				
MSMN-1	1	0.048	26, 21, 19	L hippocampus, white matter
Superior visual network				
SVN-1	1	0.036	19, 11, 12	R cerebellum Crus I
Temporal network				
TN-1	34	0.002	17, 12, 16	R lingual gyrus, R occipital fusiform gyrus
TN-2	20	0.014	21, 21, 26	R posterior cingulate gyrus, R precuneus
TN-3	10	0.02	26, 15, 15	L lingual gyrus
TN-4	9	0.017	30, 8, 16	L inferior lateral occipital cortex
TN-5	6	0.007	34, 18, 14	L inferior temporal gyrus
TN-6	5	0.033	33, 11, 13	L inferior lateral occipital cortex
TN-7	2	0.043	34, 14, 23	L superior lateral occipital cortex
TN-8	1	0.04	37, 17, 13	L inferior temporal gyrus
Basal ganglia network				
BGN-1	5	0.039	15, 29, 21	R putamen
BGN-2	2	0.035	17, 32, 22	R caudate
BGN-3	1	0.037	19, 31, 21	R caudate
Right motor network				
RMN-1	142	0.001	15, 26, 30	R precentral gyrus
RMN-2	54	0.003	14, 34, 24	R middle frontal gyrus, R inferior frontal gyrus
RMN-3	22	0.007	25, 15, 23	L precuneus
Thalamic network				
THN-1	5	0.039	30, 9, 24	L superior lateral occipital cortex
Insular network 1				
ISN1-1	1	0.032	13, 34, 24	R inferior frontal gyrus
Anterior cingulate network				
ACN-1	11	0.028	29, 37, 24	L superior and middle frontal gyrus
ACN-2	4	0.044	20, 37, 25	R anterior cingulate cortex
ACN-3	1	0.027	34, 18, 15	L inferior temporal gyrus
Temporal pole network				
TPN-1	190	0.005	24, 40, 19	R/L anterior cingulate, R/L paracingulate
TPN-2	100	0.003	31, 44, 16	L frontal pole, L inferior/orbital frontal gyrus
TPN-3	3	0.041	21, 22, 30	R precuneus, R precentral gyrus
DLB > HC				
Left motor network				
LMN-1	4	0.012	16, 26, 31	R precentral gyrus, white matter
Ventral attention network				
VAN-1	1	0.036	27, 16, 22	L precuneus
Insular network 2				
ISN2-1	6	0.021	29, 42, 24	L frontal pole

DLB, dementia with Lewy bodies; HC, healthy controls; MNI, Montreal Neurological Institute coordinates.

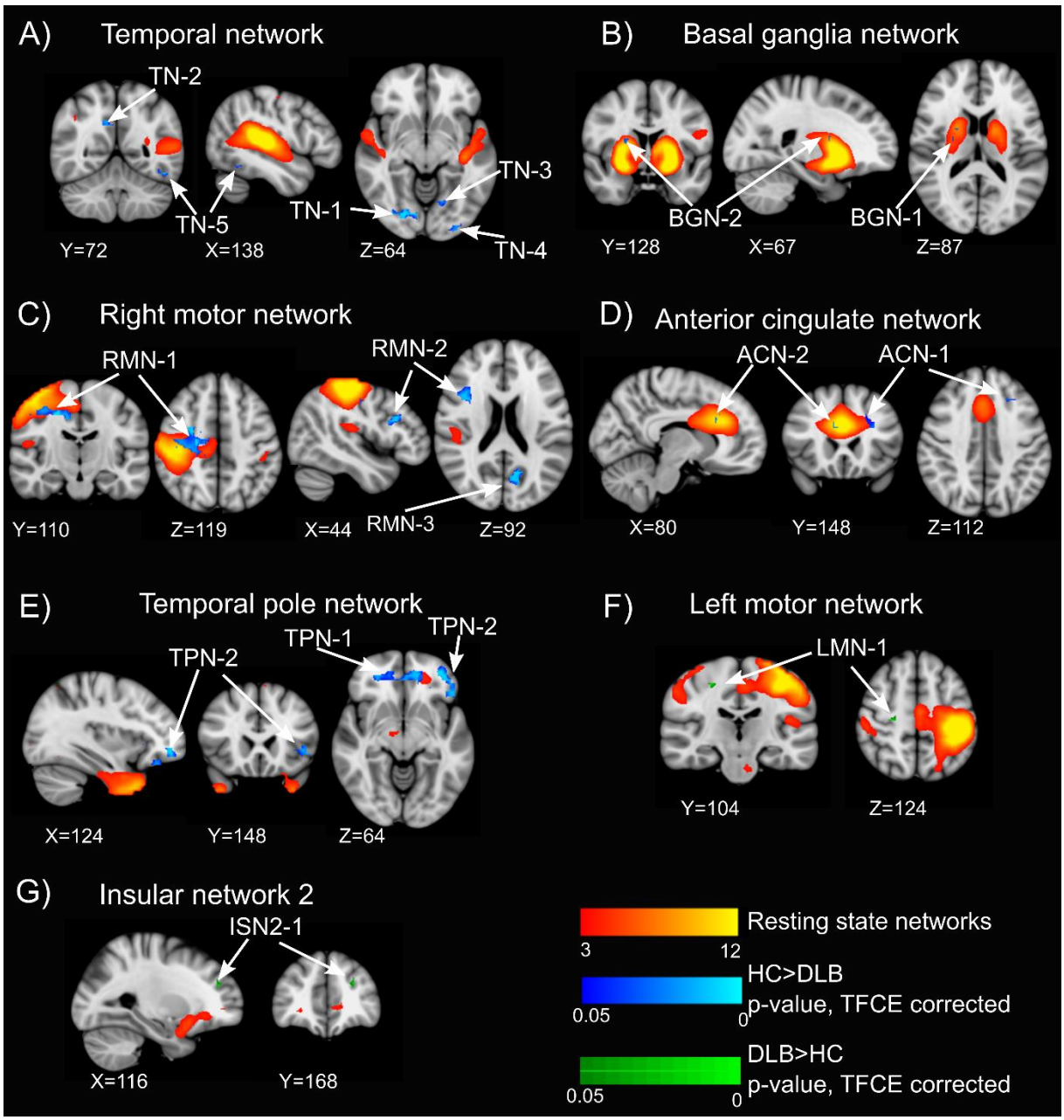

Figure 4.3. Dual regression results comparing DLB and HC. RSN maps are shown in red-yellow. A-F) Clusters with decreased connectivity in DLB; HC>DLB, p<0.05, TFCE-corrected, shown in blue. G) Clusters with increased connectivity in DLB; DLB>HC, p<0.05, TFCE-corrected, shown in green. See Table 4.5 for more information on cluster locations and sizes. All images are shown in radiological convention.
ACN, anterior cingulate network; AD, Alzheimer's disease; BGN, basal ganglia network; DLB, dementia with Lewy bodies; HC, healthy controls; ISN 2, insular network 2; LMN, left motor network; RMN, right motor network; TFCE, threshold-free cluster enhancement; TN, temporal network; TPN, temporal pole network.

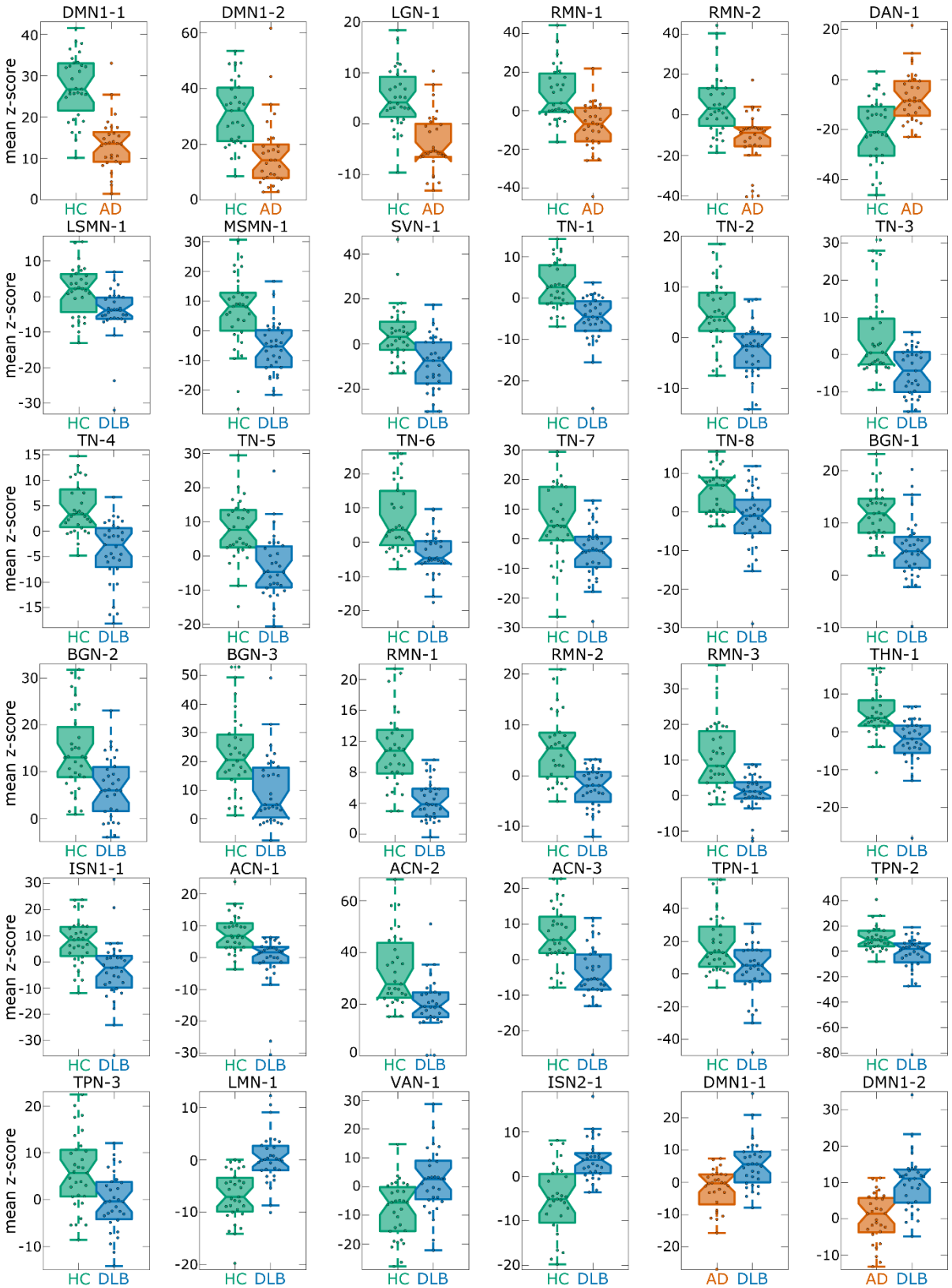

Figure 4.4. Mean z-scores for all dual regression clusters that showed significant group differences (see Tables 4.4 - 4.6). In each boxplot the central line corresponds to the sample median, the upper and lower border of the box represent the 25th and 75th percentile, respectively, and the length of the whiskers is 1.5 times the interquartile range.
AD, Alzheimer's disease; DLB, dementia with Lewy bodies; HC; healthy controls.

Table 4.6. Dual regression results comparing AD and DLB. All clusters are reported with p<0.05, TFCE-corrected. The table shows the number of significant voxels per cluster, the minimal p-value inside the cluster, the MNI coordinates of the voxel with minimal p-value, and the location of the cluster (estimated from the Harvard-Oxford Cortical and Subcortical Structural Atlases and the Cerebellar Atlas in FSL).

	N	p-value	MNI (X, Y, Z)	Location
AD > DLB				
No significant clusters				
DLB > AD				
Default mode network 1				
DMN1-1	1	0.044	13, 12, 24	R superior lateral occipital cortex
DMN1-2	1	0.025	13, 12, 27	R superior lateral occipital cortex

AD, Alzheimer's disease; DLB, dementia with Lewy bodies; Montreal Neurological Institute coordinates.

4.3.3 Between-network connectivity

When considering full correlations, there was a decrease in connectivity between the thalamic network and the default mode network 2 in AD patients compared to controls (Figure 4.5). Comparing DLB patients and controls, there was a change in connectivity between the temporal pole and the anterior cingulate networks. While this connection showed a negative correlation in controls, the mean correlation was around zero in the DLB group. There were no connections with decreased connectivity in AD or DLB patients compared to controls. When comparing the AD and DLB groups, a significant difference was found for the connection between the left fronto-parietal and the occipital pole networks which were positively correlated in the AD group, but showed a negative correlation in patients with DLB (Figure 4.5). There were no significant group differences for any comparison when considering partial correlations.

4.3.4 Clinical correlations

There was a negative correlation between the CAF total and its subscores and a cluster belonging to the temporal network in the left inferior temporal cortex (TN-8). A positive correlation was observed between MMSE and a cluster in the left supplementary motor cortex belonging to the lateral sensorimotor network (LSMN-1) in the DLB group (Table 4.7). However, both clusters only comprised one voxel and the correlations did not survive multiple comparison correction. Similarly, in the AD group there was a negative correlation between CAMCOG and mean connectivity within a very small cluster belonging to the right motor network which did not survive correction for multiple comparisons (Table 4.7).
As an additional exploratory analysis, I also investigated voxel-wise correlations between clinical scores and connectivity within the clusters resulting from the group comparison.

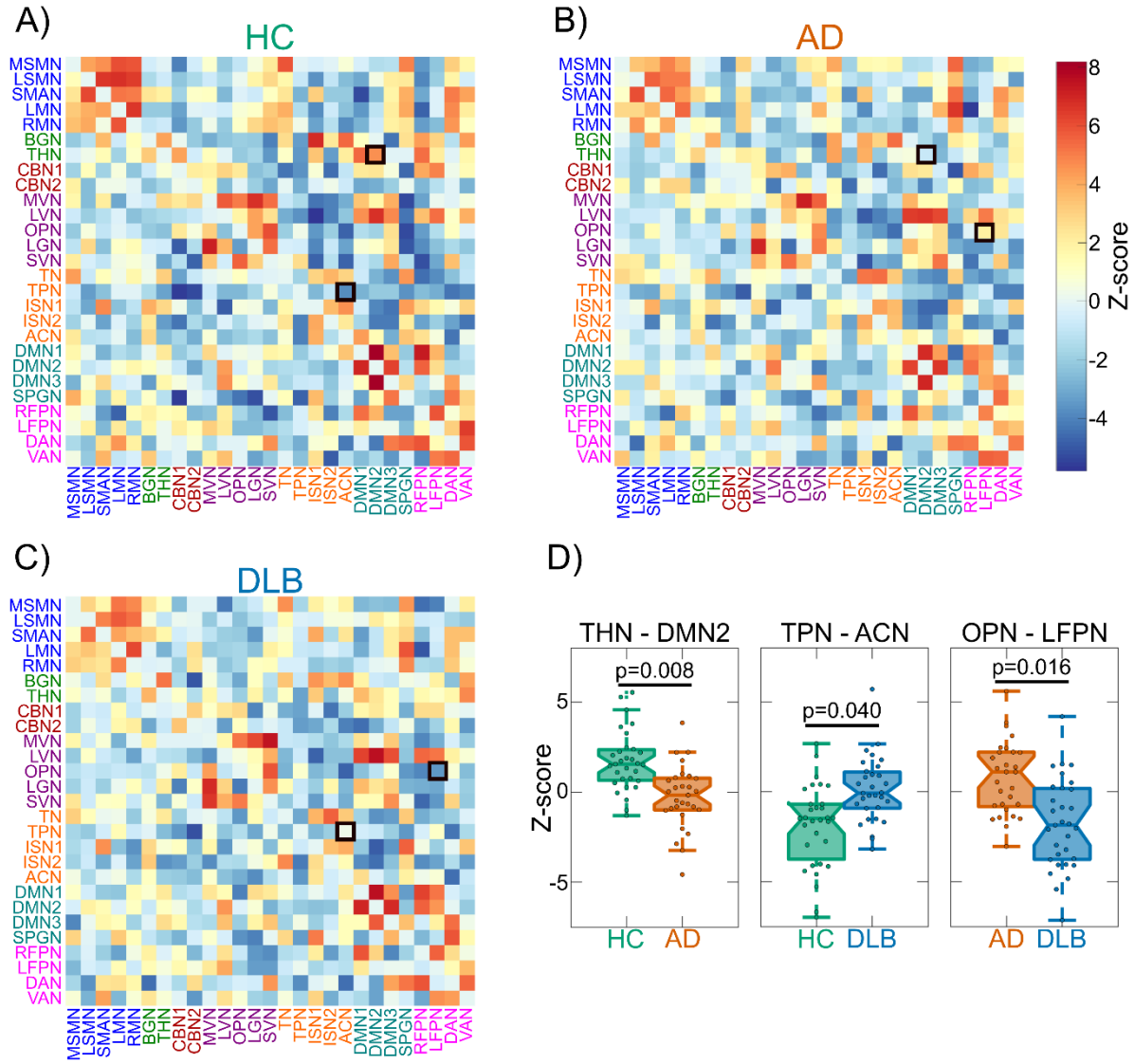

Figure 4.5. Correlation matrices from FSLNets analysis for A) HC, B) AD, and C) DLB. Upper triangular matrices show full correlations while partial correlations are plotted in the lower triangular matrices. D) Boxplots of z-scores for edges with significant group differences for full correlations (black squares in panel A-C, $p<0.05$, FWE-corrected for multiple comparisons). In each boxplot the central line corresponds to the sample median, the upper and lower border of the box represent the 25th and 75th percentile, respectively, and the length of the whiskers is 1.5 times the interquartile range.
ACN, anterior cingulate network; DMN2, default mode network 2; LFPN, left fronto-parietal network; OPN, occipital pole network; THN, thalamic network; TPN, temporal pole network.

There was one cluster of 4 voxels in the right occipital fusiform gyrus belonging to the temporal network that showed a negative correlation with the CAF total score (Table 4.8). Additionally, there was a very small cluster in the right motor network where connectivity was positively correlated with the CAF total and subscores. Furthermore, a one-voxel cluster in the lateral sensorimotor network showed negative correlations with CAF and UPDRS and a cluster in the anterior cingulate network exhibited a negative correlation with the MMSE.

Table 4.7. Spearman's correlations between mean functional connectivity within significant clusters from dual regression and clinical scores in the DLB and AD groups. All correlations are shown that have an uncorrected p-value<0.05.

LBD	
TN-8 – CAF total[a]	ρ = -0.49 (p=0.006, p_{FDR}=0.26)
TN-8 – CAF duration[a]	ρ = -0.49 (p=0.006, p_{FDR}=0.26)
TN-8 – CAF frequency[a]	ρ = -0.46 (p=0.01, p_{FDR}=0.30)
LSMN-1 – MMSE	ρ = 0.37 (p=0.04, p_{FDR}=0.94)
AD	
RMN-1 – CAMCOG	ρ = -0.38 (p=0.04, p_{FDR}=0.31)

AD, Alzheimer's disease; CAF, Clinician Assessment of Fluctuation; CAF duration, Clinician Assessment of Fluctuation duration subscale; CAF frequency, Clinician Assessment of Fluctuation frequency subscale; CAMCOG, Cambridge Cognitive Assessment; DLB, dementia with Lewy bodies; FDR, false discovery rate; LSMN, lateral sensorimotor network; MMSE, Mini Mental State Examination; RMN, right motor network; TN, temporal network

[a] N=30.

Table 4.8. Results from voxel-wise correlations between z-scores (from dual regression) and clinical scores in the DLB group. All correlations are shown that have an uncorrected p-value<0.05.

cluster name	N voxels	MNI (X,Y,Z)	clinical correlations
LSMN-1	1	24, 28, 30	negative correlation with CAF total (p=0.035), CAF duration (p=0.042), and UPDRS (p=0.018)
TN-1	4	16, 11, 16	negative correlation with CAF total (p=0.022)
RMN-1	1	13, 27, 30	positive correlation with CAF total (p=0.01), CAF duration (p=0.037), and CAF frequency (p=0.01)
ACN-3	1	34, 18, 15	negative correlation with MMSE (p=0.045)

ACN, anterior cingulate network; AD, Alzheimer's disease; CAF, Clinician Assessment of Fluctuation; CAF duration, Clinician Assessment of Fluctuation duration subscale; CAF frequency, Clinician Assessment of Fluctuation frequency subscale; CAMCOG, Cambridge Cognitive Assessment; DLB, dementia with Lewy bodies; LSMN, lateral sensorimotor network; MMSE, Mini Mental State Examination; RMN, right motor network; TN, temporal network.

4.3.5 Effect of dopaminergic medication in the DLB group

There were no significant differences in connectivity between the DLB patients who were taking dopaminergic medication compared to those not taking these medications except for two very small clusters of increased connectivity in the medicated patients comprising one

voxel for the supplementary motor area network in left frontal orbital cortex and right superior frontal gyrus.

4.4 Discussion

In this chapter, I investigated within- and between-network connectivity in a wide range of RSNs in DLB compared to healthy controls as well as AD patients. With respect to within-network connectivity more decreases than increases in connectivity were identified in the DLB group compared to controls, mainly in motor, temporal, and frontal networks. The analysis of between-network connectivity suggests that long-range functional connections are largely intact in DLB as there was only one connection between a frontal and a temporal network that showed altered between-network connectivity compared to controls. When directly comparing both dementia groups there were only very small differences, indicating that AD and DLB might not be that different with respect to their resting-state functional connectivity. Furthermore, there was no consistent relation between altered connectivity in DLB and any clinical variables, in particular with respect to cognitive fluctuations, suggesting that this analysis method might not be the most suitable to identify neural correlates of clinical DLB symptoms.

4.4.1 Decreased connectivity in motor networks in DLB

Connectivity was decreased in DLB compared to controls in several motor networks, including both sensorimotor, the basal ganglia, and the right motor networks. Overall, the observed changes in these networks correspond well to the clinical manifestation of DLB which is – among other core symptoms – characterised by Parkinsonian motor features (McKeith et al., 2005). Moreover, the results show substantial overlap with previous findings in PD and emphasise the significance of alterations in motor networks in DLB even though this condition is primarily characterised by cognitive decline and, frequently, significant AD co-pathology (Irwin et al., 2017). Decreased connectivity in the basal ganglia network has been found in patients with PD compared to healthy controls and patients with AD and has been suggested as a potential biomarker for early PD (Rolinski et al., 2015; Szewczyk-Krolikowski et al., 2014). While I found similar results in the DLB group, the clusters of decreased connectivity were much smaller than in previous PD studies. This might be due to the use of dopaminergic medication in many DLB patients which has been shown to restore basal ganglia connectivity to near-normal levels (Szewczyk-Krolikowski et al., 2014). The finding of less impaired basal ganglia connectivity in the present DLB group compared to previous PD studies might also be related to the fact that Parkinsonism in DLB is often milder

and has been present for a shorter period than the motor symptoms in PD. The present results stand in contrast to previous studies in DLB that found increased basal ganglia connectivity compared to controls (Kenny et al., 2013; Lowther et al., 2014). The discrepancy between previous results in DLB and the present results and more recent PD studies is likely to be due to the use of different preprocessing methods, especially with respect to the removal of motion artefacts. It has recently been argued that motion correction approaches such as those used in previous DLB studies might have led to spurious findings and that prior results might have to be re-evaluated using more appropriate motion correction techniques such as those applied here (Ciric et al., 2017; Parkes et al., 2018; Power et al., 2015). This is especially crucial when studying elderly patients and comparing groups with different degrees of motor symptoms (van Dijk et al., 2012).

In addition to decreased basal ganglia connectivity there was reduced connectivity within cortical motor networks. The right motor network showed large clusters of decreased connectivity in DLB within primary motor areas. Sensorimotor networks have been commonly shown to be altered in Lewy body diseases (Tessitore et al., 2014; Wu et al., 2011; Yu et al., 2013) and lower connectivity within the motor cortex has been reported previously in DLB (Peraza et al., 2016, 2014; Taylor et al., 2013). In addition to reduced connectivity within the motor network, itself, cognitive control areas, such as frontal and default mode areas, were also less strongly connected to this network in DLB, which might be related to impairments of voluntary movement control in this disease group. However, there were no significant correlations between the reduction in motor network connectivity and the severity of Parkinsonism. It might be that motor connectivity changes are related to the presence of Parkinsonian symptoms, but not their severity in DLB.

4.4.2 DLB-related changes in non-motor networks

With respect to non-motor networks, decreased connectivity in DLB compared to controls was observed mainly in temporal and frontal networks. The temporal network showed a general disconnection from different occipital regions which agrees with previous findings in DLB (Peraza et al., 2014; Taylor et al., 2012). The connections between occipital and temporal cortices represent the ventral visual stream which is involved in object recognition (Ungerleider and Haxby, 1994). A breakdown of this important visual pathway might thus be related to visuo-perceptual difficulties in DLB (Mosimann et al., 2004). However, similar to previous studies, there were no significant correlations with frequency or severity of visual hallucinations (Peraza et al., 2014). It may be that the observed connectivity changes foster a cortical state that is permissive for the occurrence of visual hallucinations, but that is not

directly related to their severity or frequency of occurrence. The temporal pole network demonstrated lower synchronisations in DLB compared to controls, mainly in frontal areas such as ACC and frontal pole. Similarly, the frontal anterior cingulate network showed a disconnection from inferior temporal regions. The observed reduced involvement of the ACC within the temporal pole network in DLB seemed to be compensated by an increase in between-network connectivity between the temporal pole and the anterior cingulate networks. The ACC is an important region involved in cognitive control and emotional processing (Bush et al., 2000) and abnormalities in this region have been associated with different aspects of Lewy body diseases. While reduced metabolism in the ACC has been found in both DLB and PDD (Yong et al., 2007), synaptic and pathological changes in this region have been implicated in visual hallucinations in DLB (Teaktong et al., 2005) and cognitive deficits in PD (Kövari et al., 2003). The present results provide further evidence for the importance of ACC abnormalities in Lewy body diseases and suggest that the previously described changes at the synaptic level might lead to more wide-range disruptions of the functional connectivity profile of this region.

While the common finding of decreased DMN connectivity in the posterior cingulate cortex in AD could be replicated in the present analysis (Binnewijzend et al., 2012; Greicius et al., 2004), there were no changes in DMN connectivity in DLB compared to controls. Additionally, DMN connectivity was increased in patients with DLB compared to AD patients, albeit only for very small clusters. These results confirm that the finding of DMN hypoactivity is rather specific to AD and does not seem to be present in DLB patients (Franciotti et al., 2013; Peraza et al., 2014).

The results of this analysis suggest that long-range connections are largely intact in DLB which is somewhat contradictory to results from a previous graph-based analysis that found a relative loss of medium and long range connections in DLB (Peraza et al., 2015a). However, while the present analysis focuses on spatially distinct networks, the previous graph-theoretic approach is a more global analysis. It might thus be that connections between independent RSNs are relatively intact while this might not be true for long-distance connections in general.

4.4.3 Comparison between the dementia groups

In contrast to previous studies, I did not find large differences between the two dementia groups with respect to their within-network functional connectivity (Galvin et al., 2011; Lowther et al., 2014). An important difference to previous studies was the use of a more stringent motion correction technique and the inclusion of a covariate to control for voxel-

wise grey matter differences. Previous studies on AD-DLB differences did not include a grey matter covariate even though grey matter loss is generally more severe in AD than in DLB (Watson et al., 2012) and might thus lead to spurious results in a group comparison (Damoiseaux et al., 2012). Furthermore, it has been shown that subtle differences in motion between groups can be mistaken for neuronal effects (van Dijk et al., 2012). In the present investigation, however, there was a between-network connectivity difference between patients with AD and patients with DLB for the left frontoparietal and occipital pole networks, which showed opposed synchronisations; positive in AD and negative in DLB. In the healthy control group, the correlation between these two networks was on average negative, which suggests that the positive correlation seen in the AD group is likely to represent an abnormal shift of connectivity from negative to positive correlation. Functional alterations in occipital and attentional systems have been previously reported in AD (Li et al., 2012; Sorg et al., 2007) although not between these two systems. Further research will be needed to corroborate their altered functional inter-relations.

4.4.4 Limitations

Similar to the previous chapters, the use of cholinergic and/or dopaminergic medication might have had an influence on the functional connectivity measures presented here. However, dopaminergic medication has been shown to normalise connectivity towards more healthy levels (Szewczyk-Krolikowski et al., 2014; Tahmasian et al., 2015), suggesting that the observed group differences were not due to medication. Furthermore, there were only very small differences in terms of functional connectivity measures between DLB patients who were taking dopaminergic medication compared to those not on these medications. However, as mentioned before, a comparison between patients on and off acetylcholinesterase inhibitors was not possible due to small numbers in the latter group.

4.4.5 Conclusion

Functional connectivity differences between AD and DLB were subtle and suggest that these two dementias may have more similarities than differences with respect to overall functional connectivity in patients with mild disease. Additionally, this analysis revealed a general decrease in functional connectivity in DLB compared to healthy ageing in motor, frontal, and temporal networks with a relative sparing of the DMN. The observed functional connectivity alterations may be related to the presence of motor and cognitive impairment in DLB as the networks that are commonly associated with these functions showed lower connectivity.

Chapter 5. Dynamic fMRI functional connectivity analysis

5.1 Introduction

To date, most functional connectivity studies have focussed on mean connectivity over the duration of a scan of several minutes (see Chapter 4), thereby implicitly assuming that functional connectivity remains stationary during that time. However, it has recently been shown that functional connectivity can vary substantially in both strength and directionality on a timescale of seconds to minutes (Chang and Glover, 2010; Hutchison et al., 2013b) and that studying these dynamics provides important complementary information to the traditional analysis of stationary functional connectivity (Calhoun et al., 2014; Hutchison et al., 2013a). Several methods have been developed to analyse dynamic functional connectivity in resting-state fMRI, including sliding window approaches (Allen et al., 2014), time-frequency analysis (Chang and Glover, 2010), and change point detection (Cribben et al., 2013). The interpretation, functional significance, and origin of dynamic functional connectivity have been the subject of an extensive debate (Hindriks et al., 2016; Laumann et al., 2016; Lehmann et al., 2017). However, recent studies using concurrent fMRI and EEG measurements point towards a neuronal origin of dynamic functional connectivity (Chang et al., 2013; Tagliazucchi et al., 2012b). Additionally, several studies have provided support for a cognitive role of dynamic connectivity by showing that changes in connectivity are related to changes in behavioural or vigilance states (Jia et al., 2014; Kucyi et al., 2017; Thompson et al., 2013). Finally, the study of dynamic functional connectivity in clinical populations has led to the identification of specific dynamic connectivity alterations associated with specific disorders which provides further evidence of the neurocognitive significance of time-varying functional connectivity (Damaraju et al., 2014; Jones et al., 2012; Kaiser et al., 2015; Rashid et al., 2016, 2014; Sourty et al., 2016).

As discussed in Chapter 1, LBD is characterised by transient clinical symptoms, in particular cognitive fluctuations that occur spontaneously in the absence of clear environmental triggers (Ballard et al., 2001a; Bradshaw et al., 2004). This suggests that cognitive fluctuations in LBD are internally driven and that dynamic changes in brain activity and connectivity might play a role in their aetiology (Sourty et al., 2016). Cognitive fluctuations can occur over days and hours, but variations on shorter timescales occur, with a strong association between sub-second RT variability and cognitive fluctuations over longer time periods (Walker et al., 2000a). Often coupled with fluctuations in LBD is marked slowing of information processing, and mental slowness, also known as bradyphrenia, a phenomenon distinct from motor slowness (Vlagsma et al., 2016).

It is not clear whether there is a pathologic increase or decrease in brain dynamical function associated with cognitive fluctuations. In regard to the former, early studies in LBD posited that a second by second temporal instability in the spectral power of the EEG of DLB patients was associated with the severity of cognitive fluctuations (Bonanni et al., 2008; Walker et al., 2000c). In contrast, a recent study has provided support for the counter-argument of a decrease in brain dynamical function. Firbank et al. (2017) demonstrated that LBD patients who have marked cognitive slowing or bradyphrenia had prolonged cognitive processing on fMRI. These findings suggest that a less dynamic brain may be apposite for the cognitive phenotype of fluctuations that occurs in LBD. This is in alignment with the broader literature which indicates that a dynamic brain, as evidenced by temporal variability and flexibility of brain activity, is important for cognitive functioning (Deco et al., 2011; Garrett et al., 2013b; Zalesky et al., 2014) whereas less dynamic brain activity is associated with worse performance on cognitive tasks (Jia et al., 2014; McIntosh et al., 2008) and ageing (Grady and Garrett, 2018; Guitart-Masip et al., 2016).

The aims of this chapter are therefore to (1) identify the differential dynamic connectivity profile of DLB patients compared to healthy controls, (2) investigate how functional connectivity dynamics in patients with DLB differ from AD patients, and (3) test a possible relation between abnormal connectivity dynamics and the severity of clinical symptoms in the DLB group, especially with respect to cognitive fluctuations. Based on previous evidence for the importance of brain dynamics for healthy cognitive functioning, I hypothesised to find a decrease in the dynamics of functional connectivity in patients with DLB compared to controls. Furthermore, I hypothesised this reduction in variability to be related to the severity of clinical symptoms in DLB, especially with respect to cognitive fluctuations.

5.2 Methods

5.2.1 Participants

This analysis involved the same 102 participants as in Chapter 4, again combining data from CATFieLD and ARThippo studies: 33 were diagnosed with probable DLB, 36 with probable AD, and 33 were healthy controls.

5.2.2 Data acquisition and preprocessing

The analyses in this chapter were conducted with the same resting-state fMRI data that is presented in Chapter 4 (see Sections 4.2.2 and 4.2.3 for details on data acquisition and preprocessing).

5.2.3 Postprocessing

As dynamic functional connectivity measures are especially vulnerable to different non-neuronal artefacts (Hutchison et al., 2013a), several postprocessing steps were applied to the data to remove remaining noise sources. To this end, the subject-specific time courses resulting from dual regression (see Section 4.2.4) were further processed in Matlab (R2016b) using functions from the Group ICA of fMRI toolbox (GIFT, http://mialab.mrn.org/software/gift/index.html). Postprocessing included (1) detrending to remove linear, quadratic, and cubic trends, (2) outlier detection based on AFNI's 3dDespike function (http://afni.nimh.nih.gov/afni) and interpolation of outliers using a third-order spline fit to the clean parts of the time courses, and (3) low-pass filtering using a fifth-order Butterworth filter with a cutoff frequency of 0.15 Hz.

5.2.4 Sliding window analysis

The postprocessed dual regression time series were analysed with a sliding window method to assess changes in between-network connectivity over time (Figure 5.1C). The sliding window approach was chosen because of its relative simplicity and computational efficiency compared to other dynamic connectivity methods which ensures that the results are interpretable and thus makes this approach especially suitable for the investigation of clinical questions. This analysis was performed in Matlab (R2016b) based on functions from GIFT (Allen et al., 2014). A tapered window was created by convolving a rectangle of 22 TR (66 s) with a Gaussian with sigma of 3 TR and moved in steps of 1 TR. Since there were 128 volumes available, this resulted in a total of 107 overlapping time windows for each participant. To assess the robustness of the results with respect to different window sizes, all analyses were repeated for window sizes ranging from 18 to 28 TR.

A covariance matrix between all RSN-to-RSN pairs was estimated for each window separately. Following Allen et al. (2014), regularised inverse covariance matrices were estimated using the graphical LASSO approach because it has been shown that estimation of covariance based on relatively short time series can otherwise be noisy. To achieve regularisation and promote sparsity, an L1-norm constraint was imposed on the inverse covariance matrix. The L1 regularisation parameter λ was optimised for each participant individually by evaluating the log-likelihood of unseen time windows from the same participant using 20-fold cross-validation. All covariances were subsequently converted to correlation values and transformed into z-scores using Fisher r-to-z transformation. To control for the effect of possible covariates, the z-scores were then residualised with respect to age, sex, and study membership using multiple linear regression (Damaraju et al., 2014).

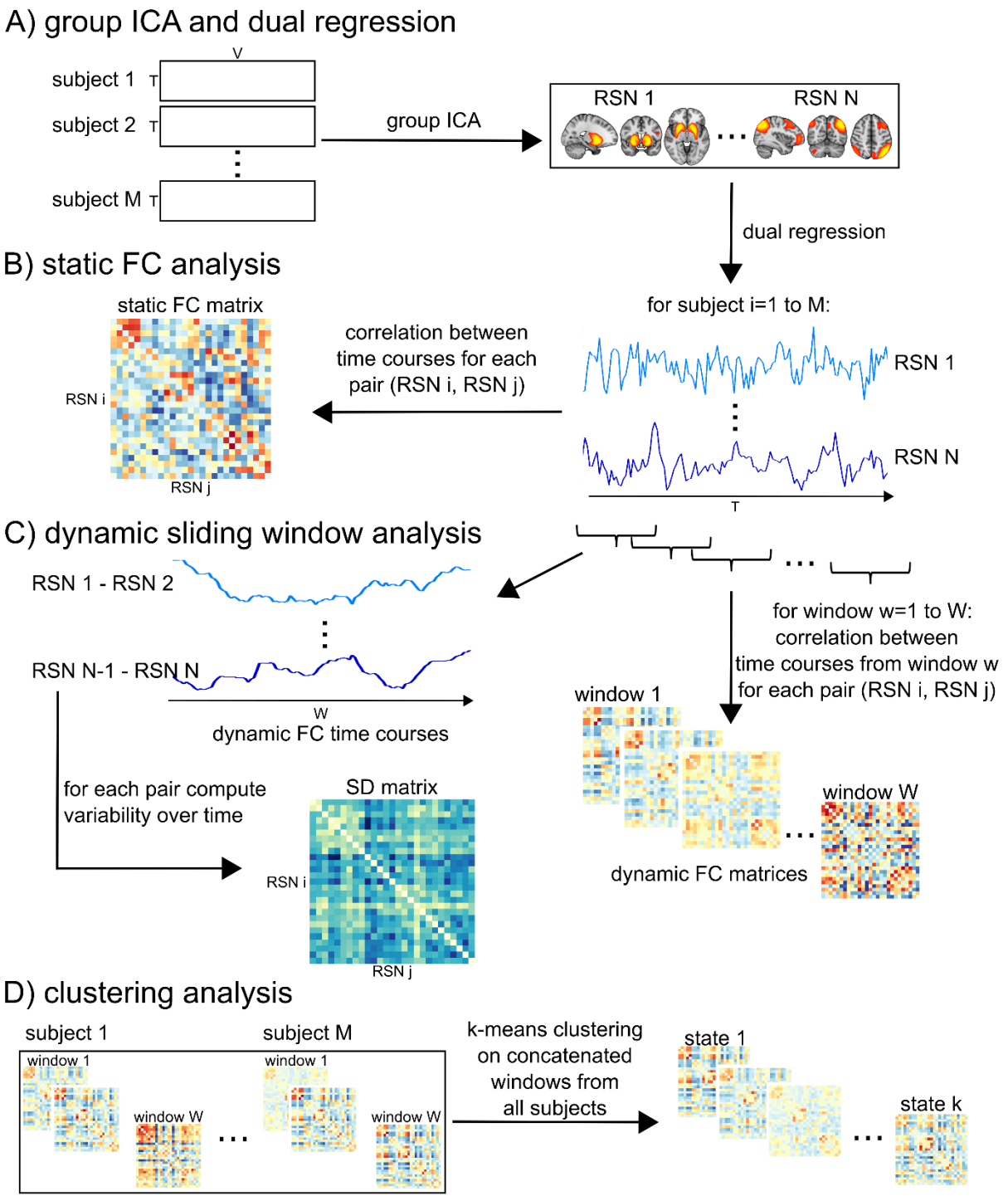

Figure 5.1. Explanation of sliding window and k-means analysis. A) Data from all healthy control subjects from the independent cohort is concatenated in time and subjected to group ICA to identify RSN spatial maps. Subject-specific time courses of each RSN are estimated using dual regression (see Chapter 4). B) Static functional connectivity analysis by calculating correlation between each pair of RSNs using the whole time course (see Chapter 4). C) Sliding window approach and estimation of standard deviation of connectivity over time. D) K-means clustering.
FC, functional connectivity; ICA, independent component analysis; RSN, resting state network; SD, standard deviation.

The variability of the connection strengths between RSNs (dynamic functional connectivity) was assessed by calculating the standard deviation of the RSN-to-RSN correlations across time windows. To assess whole-brain dynamics the mean standard deviation across all connections between RSN pairs was computed. Additionally, the mean standard deviation for each network across all other networks was considered and each RSN-to-RSN connection was also tested separately.

5.2.5 K-means clustering

To assess patterns of functional connectivity that reoccur over time across different participants, k-means clustering was applied to the windowed covariance matrices from all windows and all participants using the Manhattan (L1) distance function (Figure 5.1D). The optimal number of clusters k was chosen based on the elbow criterion of the cluster validity index, computed as the ratio of within-cluster to between-cluster distance, calculated for k between 2 and 14 (Allen et al., 2014). The clustering algorithm was repeated 500 times in Matlab with random initialisations of cluster centroid positions to get a stable solution. In addition to using the optimal value for k, the analyses were repeated for k ranging from 2 to 8 to assess the robustness of the results regarding different values of k.
Group differences were assessed with respect to (1) frequency: proportion of windows assigned to a state, (2) mean dwell time: average number of consecutive windows assigned to a state, (3) intertransition interval: average number of consecutive windows before a state transition occurs, and (4) number of transitions: overall number of transitions between different states (Hutchison and Morton, 2015; Marusak et al., 2016).

5.2.6 Dynamic network analysis

To examine the temporal variability of the brain network's topological organisation, I also considered a graph-theoretic approach studying the dynamics of global and local efficiency using the Brain Connectivity Toolbox (Rubinov and Sporns, 2010). For each time window, a graph was constructed using the 27 RSNs as nodes and the correlation between the RSNs within the respective time window as edge strength. Binarised, unweighted, and undirected graphs were created by thresholding the absolute value of the individual time window correlation matrices to achieve different edge densities. The edge density of a graph is defined as the number of existing edges divided by the maximum number of possible edges (351 in this case). Edge density thresholds ranging from 3.7% to 39.3% were used based on previous network studies (Peraza et al., 2015b; van Wijk et al., 2010). Global and local efficiency were computed for each time window separately (Achard and Bullmore, 2007; Latora and

Marchiori, 2001). Variability of efficiency was then assessed by integrating over all edge density thresholds and computing the standard deviation of the respective measure over time (Kim et al., 2017). The same analysis was repeated in a static way by calculating local and global efficiency from the whole time course.

5.2.7 Statistical analysis

Statistical analyses were performed in IBM SPSS version 23 and in R version 3.5.1. The variability of functional connectivity of each network and each connection was compared between the groups using a non-parametric multivariate ANOVA (MANOVA) (Burchett et al., 2017) with diagnosis as between-subject factor. The different k-means measures were also compared between the groups using non-parametric MANOVAs followed by Kruskal-Wallis ANOVAs and post-hoc Dunn's tests using FDR-correction for multiple comparisons. Spearman's rank correlations were calculated to assess the relation between dynamic functional connectivity measures that showed significant group differences and cognitive fluctuation scores (CAF total and subscores) in the DLB group. Additional correlation analyses were performed for the MMSE and CAMCOG as measures of overall cognition, the UPDRS motor subscale, and the NPI hallucination subscale in DLB. In the AD group, correlations with MMSE and CAMCOG were calculated. P-values from the correlation analyses were FDR-corrected for multiple comparisons.

To assess the effect of dopaminergic medication on dynamic connectivity measures, DLB patients were divided into those patients who were taking dopaminergic medication and those who were not on these medications and all dynamic connectivity measures were compared between the two groups using Mann-Whitney U-tests.

Additionally, to investigate the effect of motion on the dynamic connectivity measures, mean framewise displacement was calculated following the approach of Power et al. (2012) and Spearman's correlations between mean framewise displacement and the dynamic connectivity measures were tested across all participants.

5.3 Results

As described in Section 4.3, one AD patient was excluded due to coregistration errors. Additionally, two controls, six AD, and two DLB participants were excluded because of excessive motion. Thus, 31 DLB, 29 AD, and 31 HC participants were included in the analysis. The overall motion for all included participants did not differ between the groups (see Section 4.3). Furthermore, mean framewise displacement was not different between the groups (HC, mean (SD)=0.24 (0.11); AD, mean (SD)=0.25 (0.15); DLB, mean (SD)=0.24

(0.09); Kruskal-Wallis ANOVA, H_2=1.22, p=0.54). See Section 4.3.1 and Table 4.2 in Chapter 4 for a comparison of group demographics.

5.3.1 Group differences in dynamic connectivity

The subject-specific values for the regularisation parameter λ that resulted from the optimisation procedure did not differ between the three groups (Kruskal-Wallis ANOVA, H_2=0.06,p=0.97).

Figure 5.2 (A-C) shows matrices representing the mean standard deviation of the strength of each RSN-to-RSN connection within each group. The mean variability of RSN connectivity, across all networks, is shown in Figure 5.2D. When considering average variability of each RSN, the overall MANOVA did not show a significant effect of diagnosis (F(10,442)=1.39, p=0.18). Similarly, when considering each individual RSN-to-RSN connection, the MANOVA did not reveal a significant group difference across all variables (F(96,4221)=1.02, p=0.43).

Standard deviation matrices were re-estimated using different window sizes from 18 to 28 TR showing that the overall appearance of the standard deviation matrices was not dependent upon the specific choice of window size (Figure 5.3). Furthermore, repeating the analysis of connectivity variability for different window sizes did not show any significant group differences (all p>0.05).

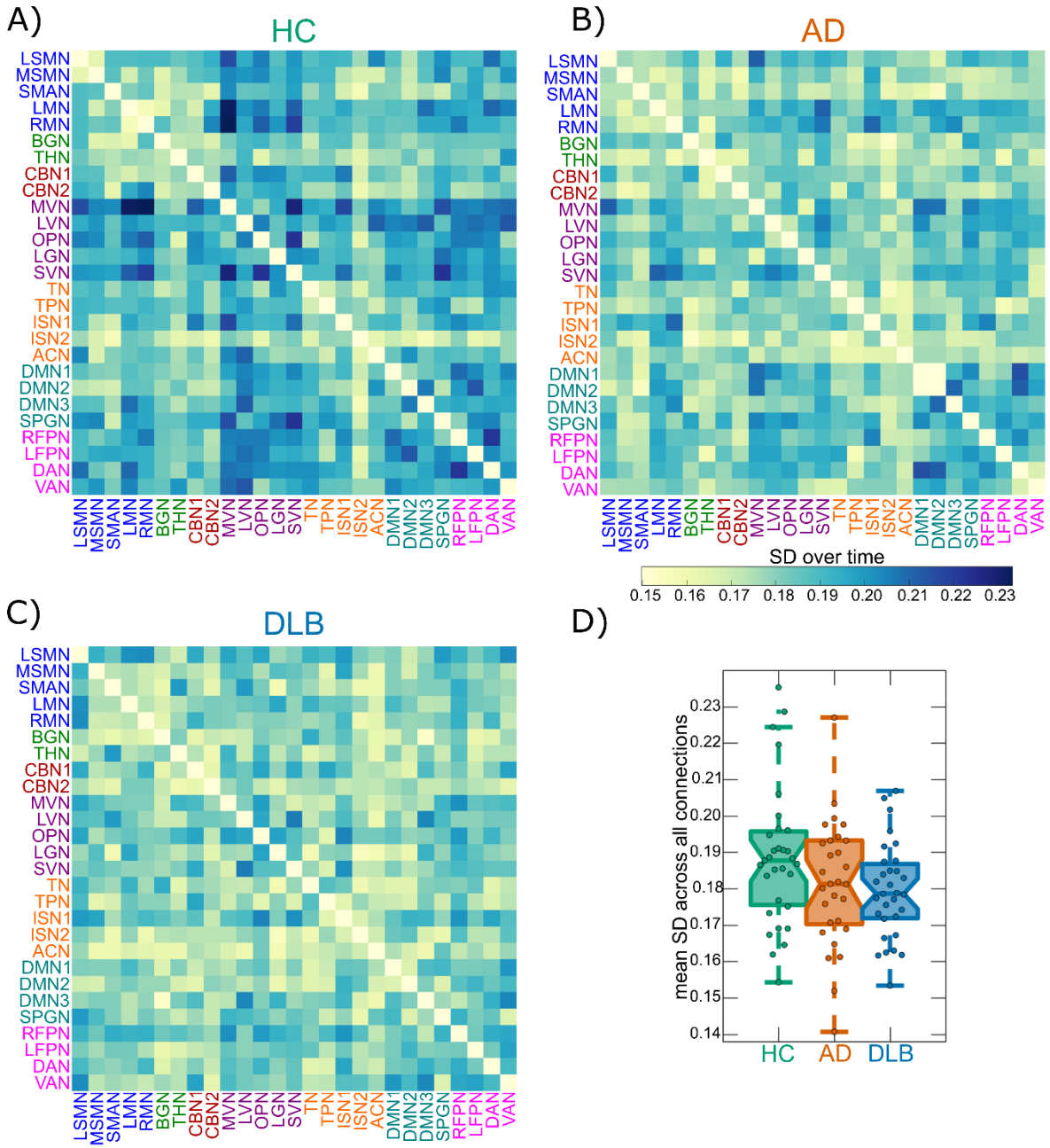

Figure 5.2. Results from dynamic functional connectivity analysis. A-C) Matrices represent mean standard deviation over time for all HC, AD, and DLB participants. D) Boxplot of group comparison of mean standard deviation across all connections. In the boxplot the central line corresponds to the sample median, the upper and lower border of the box represent the 25th and 75th percentile, respectively, and the length of the whiskers is 1.5 times the interquartile range.
AD, Alzheimer's disease; DLB, dementia with Lewy bodies; HC, healthy controls; SD, standard deviation; see Table 4.1 in Chapter 4 for the abbreviations of the RSN names.

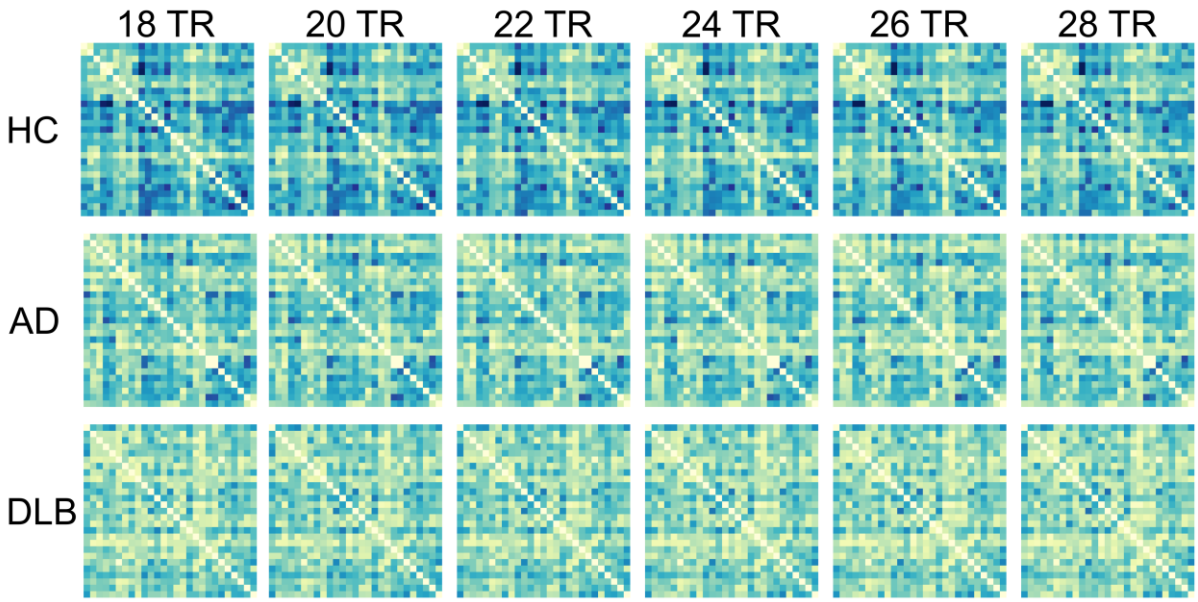

Figure 5.3. Mean standard deviation matrices for healthy controls, AD, and DLB for different window sizes ranging from 18 TR to 28 TR.
AD, Alzheimer's disease; DLB, dementia with Lewy bodies; HC, healthy controls; TR, repetition time.

5.3.2 K-means clustering

An optimal number of k=3 clusters was determined by the elbow criterion (Figure 5.4). State 1 was characterised by relatively strong positive and negative between-network correlations (Figure 5.5). Especially strong positive correlations were present within the visual and the motor networks and between these two groups of networks (Figure 5.6). Additionally, the motor and visual networks showed negative correlations with cognitive control, salience, and temporal networks, and there was a strong connection between two components of the DMN. In contrast, state 2 was characterised by much sparser connections, with weaker connectivity within visual and motor networks and a relative lack of connections between the two groups of networks. There were a few positive connections between visual and default mode networks and additional positive connections between DMN and attention networks. State 2 was the most common state, being present in almost all participants and accounting for 50% of all time windows across all participants. Similar to state 2, state 3 was characterised by weaker connections and a relative absence of strong anti-correlations. In addition to some within-module connections in the visual, motor, and default mode networks, there were weak connections between visual and DMN and attention networks.

Non-parametric MANOVAs revealed that there was a significant effect of diagnosis on frequency and mean dwell time across all three states (Table 5.1). Follow-up univariate Kruskal-Wallis ANOVAs and pairwise post-hoc tests demonstrated that state 1 occurred less

frequently in the AD and DLB groups compared to controls with no difference between the dementia groups (Figure 5.7A and Table 5.1). In contrast, state 2 occurred more often in DLB patients compared to controls. However, there was no difference between controls and patients with AD or between AD and DLB patients for frequency of state 2. The mean dwell time of state 1 and 2 followed the same pattern as the frequency, i.e. DLB patients spent shorter periods of time in state 1 and longer periods of time in state 2 than controls; AD patients spent shorter times in state 1 than controls with no difference for state 2, and there was no difference between the dementia groups (Figure 5.7B). For state 3 there were no group differences in frequency or dwell time (Table 5.1).

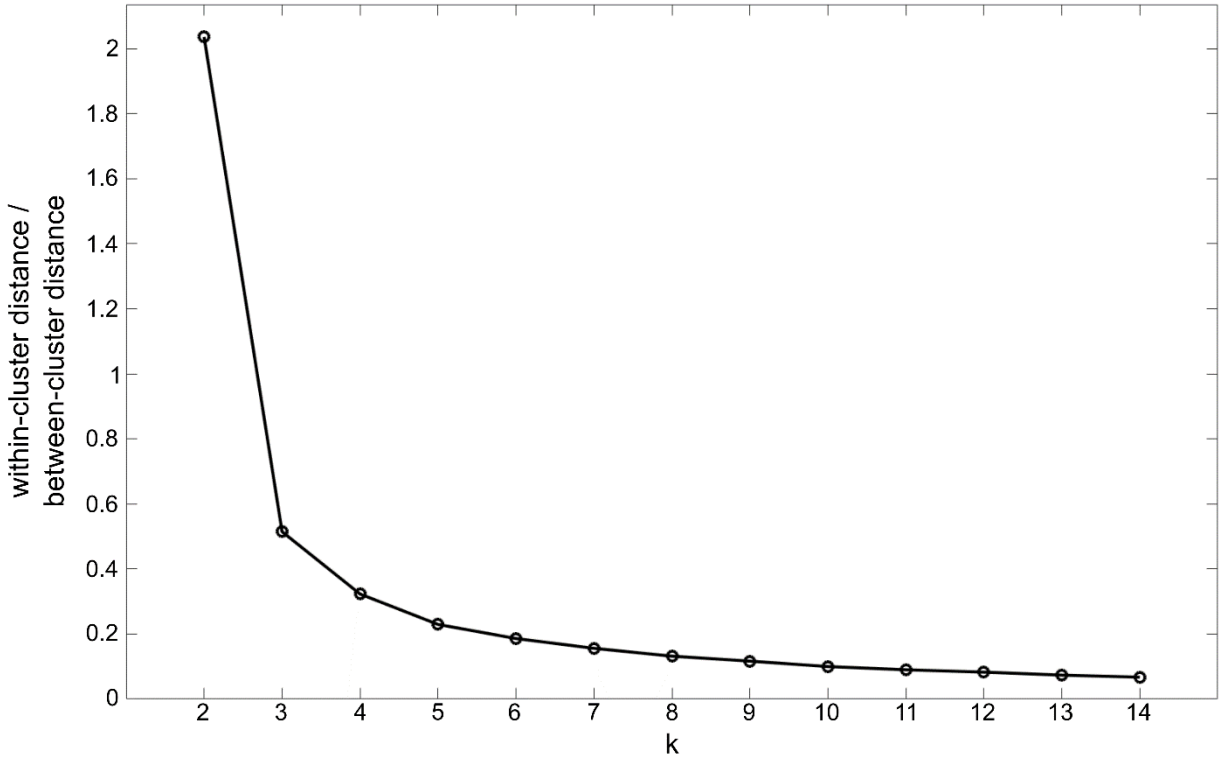

Figure 5.4. Elbow plot of the cluster validity index, i.e. ratio of within-cluster distance to between-cluster distance, for k=2 to 14.

Table 5.1. Results from overall non-parametric multivariate ANOVA (MANOVA) and follow-up Kruskal-Wallis ANOVAs per state for group comparison of k-means characteristics and static and dynamic efficiency measures between HC, AD, and DLB.

		Three-group comparison	Post-hoc tests (p-value) HC-AD	HC-DLB	AD-DLB
Frequency					
MANOVA		F=2.69 (p=0.034)			
	State 1	H=8.61 (p=0.014, p_{FDR}=0.040)	p=0.02 (p_{FDR}=0.04)	p=0.01 (p_{FDR}=0.03)	p=0.69 (p_{FDR}=0.74)
Post-hoc ANOVAs	State 2	H=6.95 (p=0.031, p_{FDR}=0.046)	p=0.1 (p_{FDR}=0.17)	p=0.01 (p_{FDR}=0.03)	p=0.29 (p_{FDR}=0.39)
	State 3	H=0.98 (p=0.61, p_{FDR}=0.61)	-	-	-
Mean dwell time					
MANOVA		F=2.85 (p=0.023)			
	State 1	H=8.49 (p=0.014, p_{FDR}=0.043)	p=0.03 (p_{FDR}=0.04)	p=0.01 (p_{FDR}=0.04)	p=0.75 (p_{FDR}=0.76)
Post-hoc ANOVAs	State 2	H=6.05 (p=0.048, p_{FDR}=0.072)	p=0.1 (p_{FDR}=0.12)	p=0.02 (p_{FDR}=0.04)	p=0.57 (p_{FDR}=0.66)
	State 3	H=2.71 (p=0.26, p_{FDR}=0.26)	-	-	-
Number of transitions		F=3.16 (p=0.21)	-	-	-
Intertransition interval		F=3.21 (p=0.20)	-	-	-
SD of local efficiency		F=0.89 p=(0.64)	-	-	-
SD of global efficiency		F=6.08 p=(0.047)	p=0.28 (p_{FDR}=0.28)	p=0.01 (p_{FDR}=0.041)	p=0.18 (p_{FDR}=0.28)
static local efficiency		F=2.30 (p=0.32)	-	-	-
static global efficiency		F=2.01 (p=0.37)	-	-	-

AD, Alzheimer's disease; ANOVA, analysis of variance; DLB, dementia with Lewy bodies; FDR, false discovery rate; MANOVA, multivariate ANOVA; SD, standard deviation.

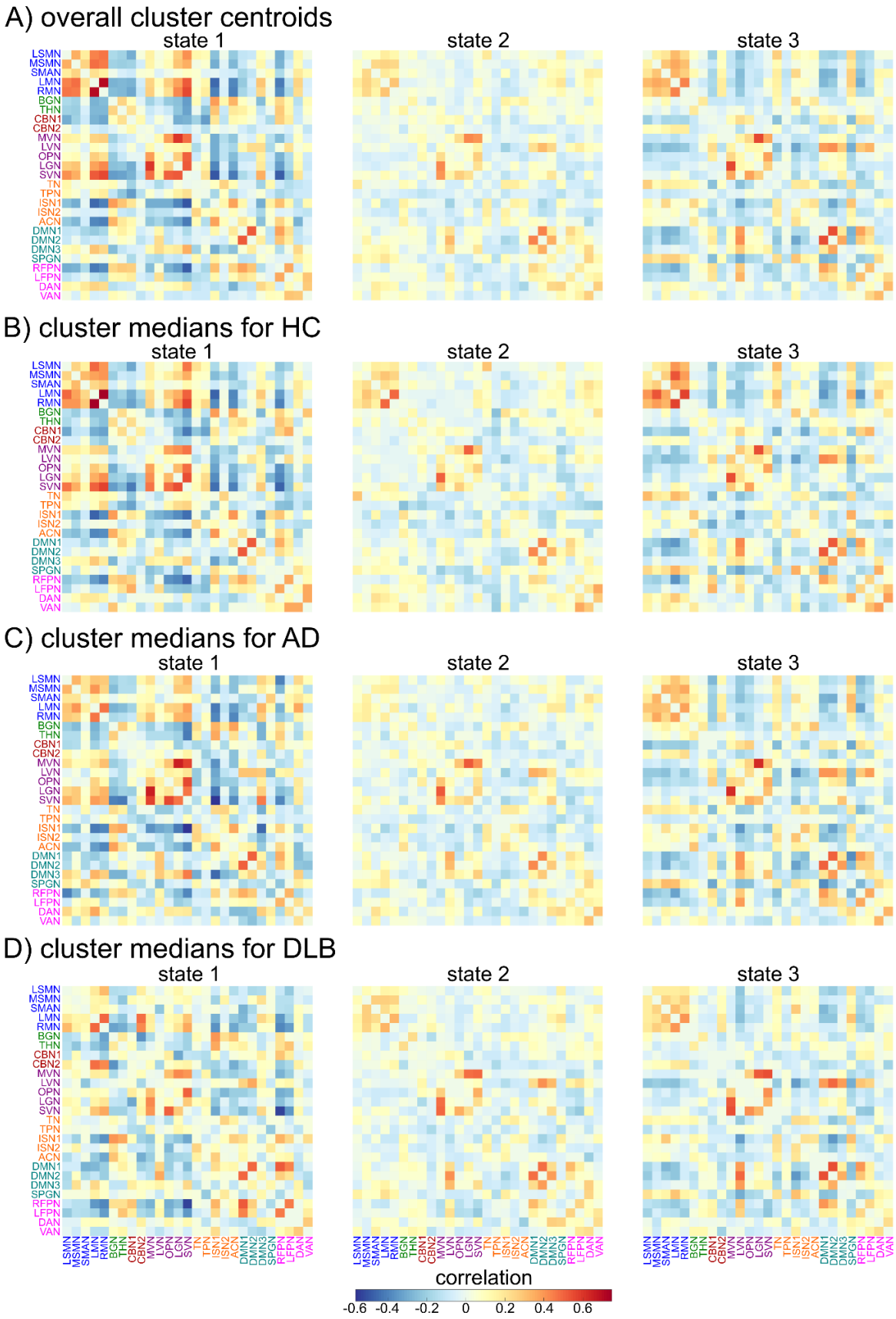

Figure 5.5. Results from the k-means analysis. A) Centroids resulting from clustering on all windows and participants. B) Cluster medians in the healthy control group. C) Cluster medians in the AD group. D) Cluster medians in the DLB group.
AD, Alzheimer's disease; DLB, dementia with Lewy bodies; HC, healthy controls.

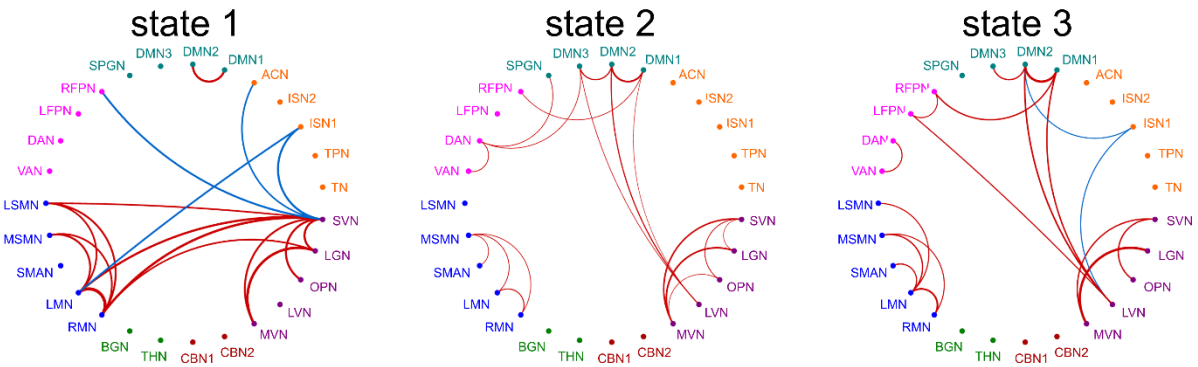

Figure 5.6. Network representation of cluster centroids resulting from k-means analysis. The graphs are showing only the 5% strongest positive (red) and negative (blue) connections. See Table 4.1 in Chapter 4 for the abbreviations of the RSN names.

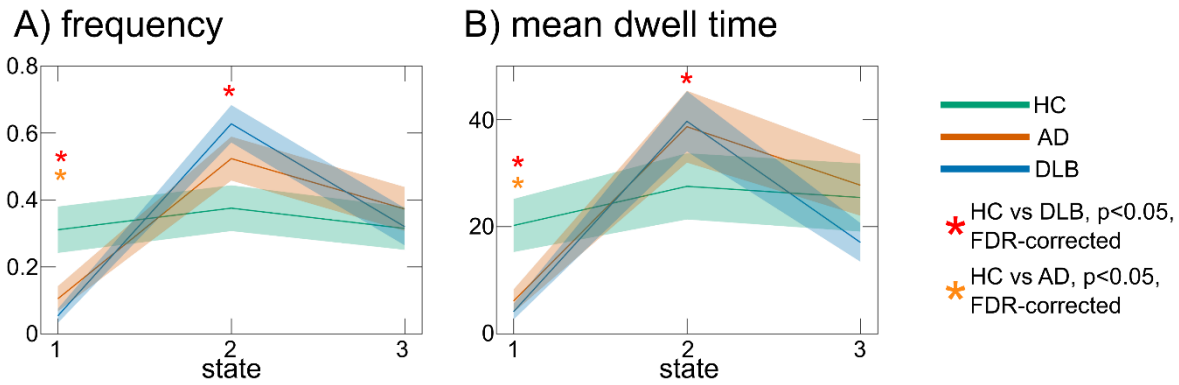

Figure 5.7. A) Comparison of frequency of occurrence between the three groups for each state. B) Comparison of mean dwell time in each state between the three groups. Solid lines represent the means per group, shaded areas represent error bars of the standard error. FDR-corrected p-values<0.05 (from post-hoc tests) are marked with an asterisk (see Table 5.1 for detailed statistics).
AD, Alzheimer's disease; DLB, dementia with Lewy bodies; FDR, false discovery rate; HC, healthy controls.

Table 5.2. Correlations between time and the occurrence of the three states from Spearman's rank correlations across all participants.

Correlation with time	ρ	$p_{uncorrected}$	p_{FDR}
Occurrence of state 1	-0.03	0.78	0.78
Occurrence of state 2	0.05	0.62	0.78
Occurrence of state 3	-0.19	0.045	0.13

FDR, false discovery rate.

Several further analyses were performed to assess the robustness of the k-means analysis. Figure 5.8 shows results for different numbers of clusters demonstrating that the main result of differences in frequency and dwell time of state 1 and 2 persisted when using a higher k. Additionally, repeating the k-means analysis with k=3 for different window sizes confirmed that the specific choice of window length did not influence the state identification (Figure 5.9). I also repeated the k-means analysis on split-half and bootstrap resamples of the data. Bootstrapping was performed by randomly selecting 31 HC, 29 AD, and 31 DLB participants with replacement and was repeated five times. Split-half resampling was performed by splitting the whole group of participants in half, with the constraint that each half contained approximately the same number of participants from each of the three groups. This analysis showed that states 1 and 2 were consistently identified in both split-half and all bootstrap resamples, while state 3 failed to be identified in some of the bootstrap resamples (Figure 5.10).

There were no significant differences between AD, DLB, and healthy control groups in the number of state transitions or the intertransition interval (Table 5.1). The frequency of occurrence of the three states was not correlated with time, i.e. there was no increase or decrease in the occurrence of any state over the duration of the scan (Table 5.2).

5.3.3 Dynamic network measures

Global efficiency variability differed significantly between the groups (Table 5.1). Post-hoc tests revealed that it was less variable in DLB compared to controls with no significant difference between AD patients and controls as well as between the two dementia groups (Figure 5.11A). In contrast, there was no difference between the groups in terms of variability of local efficiency (Figure 5.11B and Table 5.1). Also, the static analysis of global and local efficiency did not reveal any group differences (Table 5.1).

5.3.4 Clinical correlations

There were no significant correlations between the dynamic connectivity measures and cognitive fluctuation scores in DLB, even before correcting for multiple comparisons (all uncorrected $p>0.5$). Frequency of state 2 was positively correlated with the UPDRS in DLB ($\rho=0.39$, $p=0.03$). However, this correlation did not survive correction for multiple comparisons ($p_{FDR}=0.61$). There were no significant clinical correlations in the AD group (all uncorrected $p>0.1$).

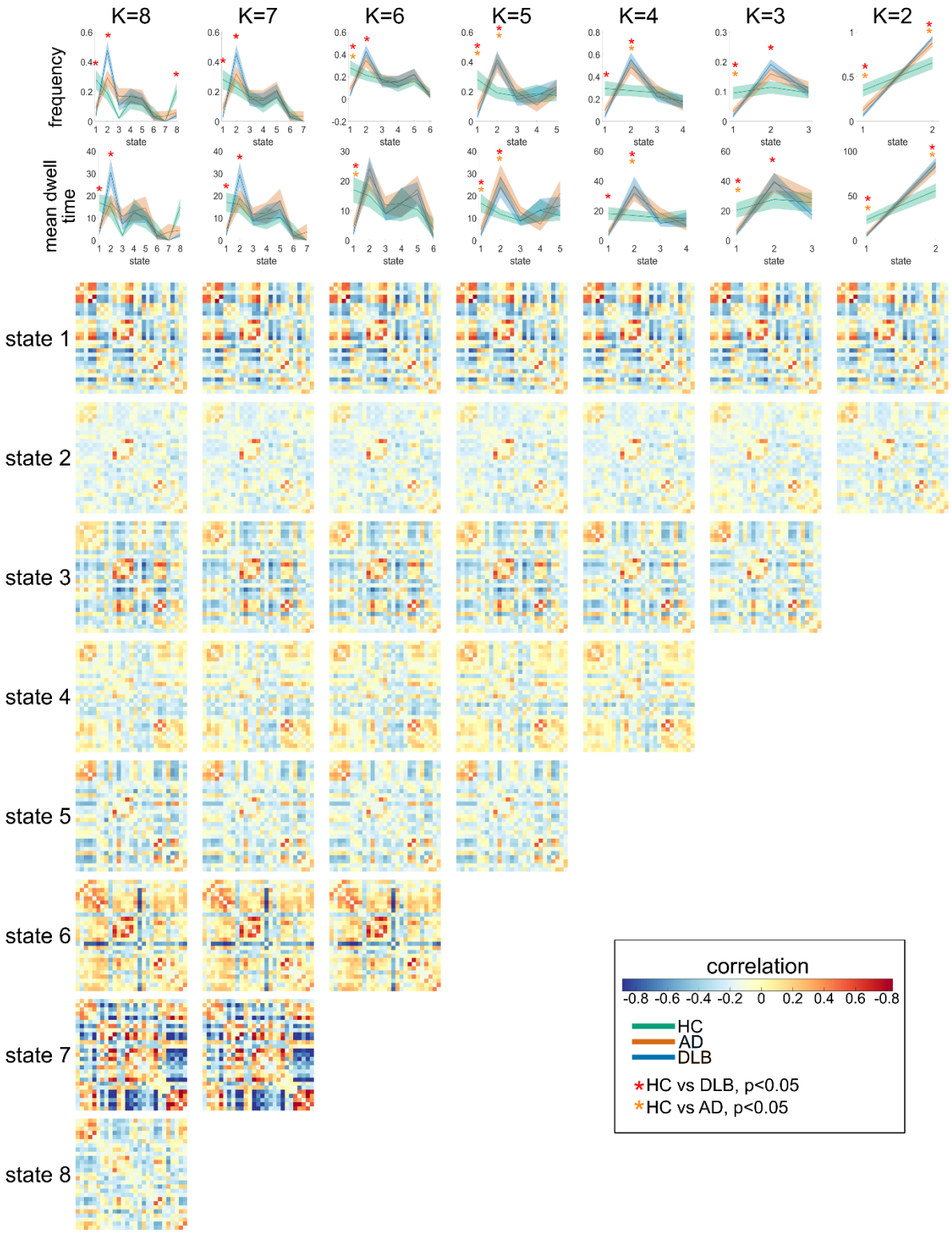

Figure 5.8. Results from k-means analysis (cluster centroids, frequency, and mean dwell time for the different states) for different values of k. FDR-corrected p-values<0.05 (from post-hoc tests) are marked with an asterisk.
AD, Alzheimer's disease; DLB, dementia with Lewy bodies; FDR, false discovery rate; HC, healthy controls.

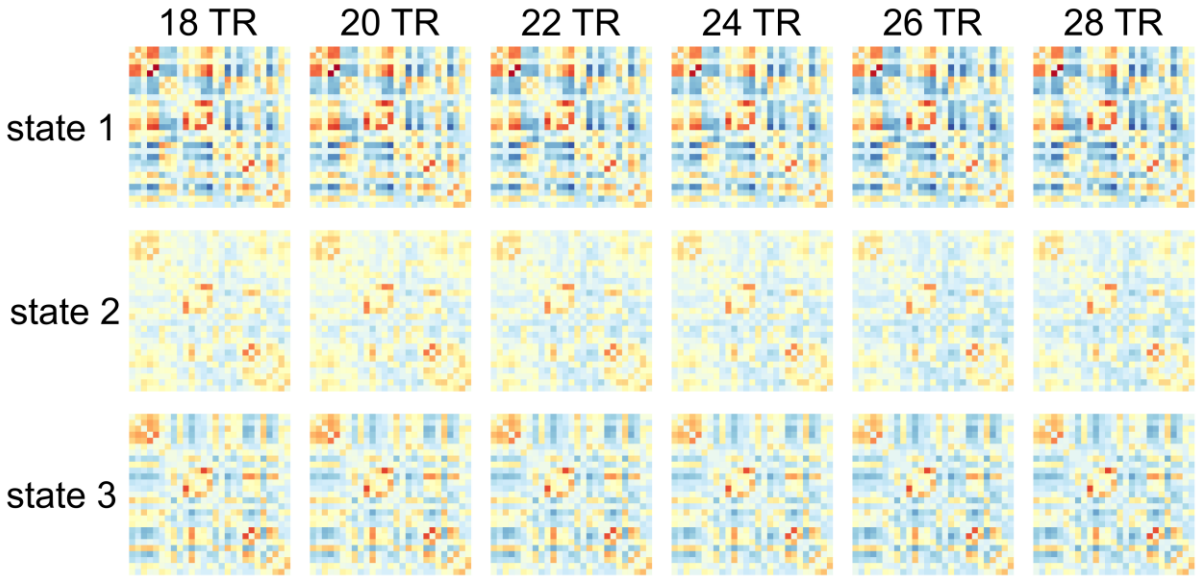

Figure 5.9. States from k-means analysis with k=3 for different window sizes ranging from 18 TR to 28 TR.
TR, repetition time.

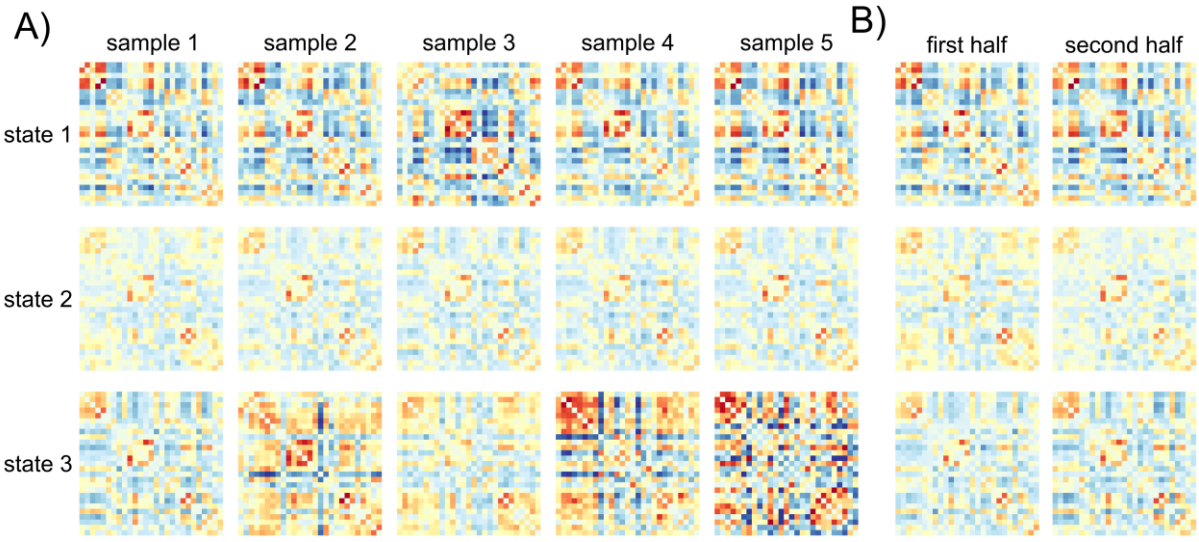

Figure 5.10. K-means analysis with k=3 on A) bootstrap resamples of the data and B) split-half samples. Bootstrapping was performed by randomly selecting 31 HC, 29 AD, and 31 DLB participants with replacement and was repeated five times. Split-half resampling was performed by splitting the whole group of participants in half with the constraint that each half contained approximately the same number of participants from each of the three groups.

5.3.5 Effect of dopaminergic medication in the DLB group

Comparing DLB patients who were on dopaminergic medication to those who were not, did not reveal any significant differences between the two groups with respect to the k-means parameters and the variability of local and global efficiency (Table 5.3).

Table 5.3. Group comparison between DLB patients who were on dopaminergic medication (DLB on PD meds, N=18) and those patients not taking dopaminergic medication (DLB not on PD meds, N=13) using independent samples Mann-Whitney U-tests.

	mean (SD)		group comparison
	DLB on PD meds	DLB not on PD meds	
overall SD	0.18 (0.01)	0.18 (0.01)	U=111.00 (p=0.83)
frequency state 1	0.04 (0.08)	0.07 (0.16)	U=111.00 (p=0.83
frequency state 2	0.65 (0.36)	0.59 (0.23)	U=95.50 (p=0.40)
frequency state 3	0.31 (0.37)	0.33 (0.22)	U=90.00 (p=0.30)
mean dwell time state 1	4.22 (8.30)	3.95 (8.42)	U=115.00 (p=0.95)
mean dwell time state 2	43.38 (36.05)	34.50 (23.68)	U=112.00 (p=0.86)
mean dwell time state 3	17.78 (25.78)	16.03 (7.72)	U=82.50 (p=0.17)
number of transitions	2.67 (1.88)	3.85 (1.52)	U=5.00 (p=0.10)
intertransition interval	41.65 (36.40)	24.77 (11.50)	U=88.50 (p=0.26)
SD of local efficiency	0.04 (0.006)	0.03 (0.01)	U=86.00 (p=0.23)
SD of global efficiency	0.02 (0.009)	0.02 (0.005)	U=110.00 (p=0.80)

DLB, dementia with Lewy bodies; PD meds, dopaminergic medication; SD, standard deviation.

5.3.6 Effect of motion

There were no significant correlations between the dynamic connectivity measures that showed group differences and mean framewise displacement (Table 5.4).

Table 5.4. Spearman's correlations between dynamic connectivity measures and mean framewise displacement across all participants.

	ρ	p-value
frequency state 1	-0.08	0.43
frequency state 2	0.14	0.18
mean dwell time state 1	-0.06	0.56
mean dwell time state 2	0.12	0.27
SD of local efficiency	0.07	0.49
SD of global efficiency	-0.09	0.42

SD, standard deviation.

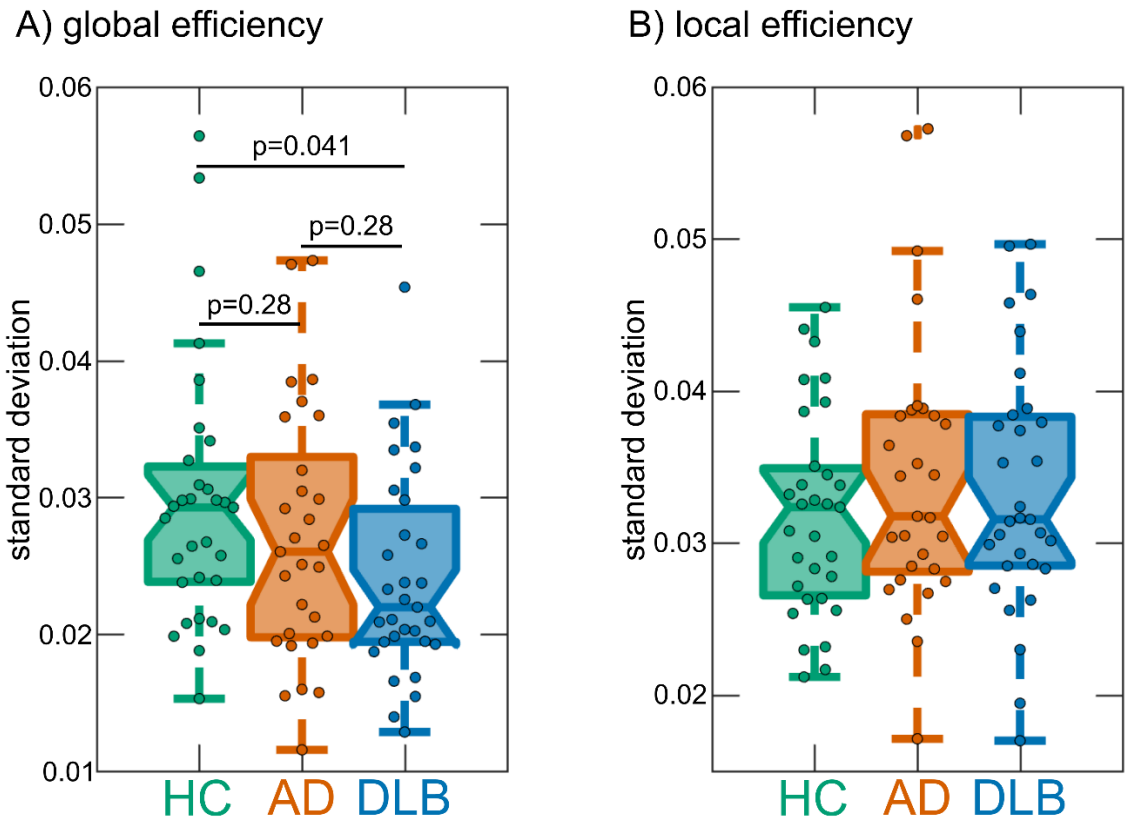

Figure 5.11. Results from dynamic network analysis. Comparison of the variability of A) global efficiency (p-values FDR-corrected) and B) local efficiency between groups (all post-hoc p-values>0.05) (see Table 5.1 for detailed statistics).
AD, Alzheimer's disease; DLB, dementia with Lewy bodies; FDR, false discovery rate; HC, healthy controls.

5.4 Discussion

In this chapter, I investigated differences in functional connectivity dynamics and dynamic brain network topology between patients with DLB, patients with AD, and healthy controls. In terms of dynamic changes in overall network structure, there was a reduction in variability of global efficiency in the DLB group compared to controls which was not observed in the AD group. Using a state-based analysis, it became evident that both dementia groups spent less time in a state of strong inter-network connectivity than controls, indicating transiently reduced functional connectivity in both dementia groups. Additionally, DLB patients spent more time in a more sparsely connected state characterised by the relative loss of strong anti-correlations and an isolation of motor networks relative to other networks. While dynamic connectivity measures of the AD group were often between those of the control and DLB groups, there were no significant differences in the direct comparison between both dementia groups.

5.4.1 State-based analysis

While the number of visited states and the number of state changes were not altered in the dementia groups, there was a significant difference in the type of state changes in the dementia patients compared to controls. The frequency with which the control participants visited each of the three states was relatively balanced, i.e. they spent about a third of their time in each state. In contrast, the distribution of states in the AD and DLB groups was more out of balance compared to controls with a clear decrease in frequency of state 1 in both dementia groups accompanied by an increased frequency of state 2 in DLB. In addition to visiting state 1 less often, the dementia patients also switched out of this state more rapidly and DLB patients stayed in state 2 for longer consecutive periods of time. In accordance with previous reports in healthy participants (Allen et al., 2014), brain development (Marusak et al., 2016), ageing (Viviano et al., 2017), and PD (Kim et al., 2017), the most common state in the present analysis (state 2) was characterised by a sparse connectivity profile with relatively weak inter-network connections and the absence of strong anti-correlations. The frequency of this state has been linked to the amount of self-focused thought (Marusak et al., 2016) and it has been suggested to represent a general connectivity pattern that participants spend most of their time in, with other states reflecting temporary deviations that might be due to cognitive, physiological, or motion-related processes (Viviano et al., 2017). State 1 deviated from this state by stronger positive and negative connections. It seems that AD as well as DLB patients remain in states of low inter-network connectivity and switch less often into more highly and specifically connected network configurations. This may relate to the presence of dementia in general even though there were no specific correlations between the time spent in different states and the severity of cognitive impairment. A specific hallmark of state 1 is strong connectivity within visual and motor networks and between these two groups of networks that is not present in state 2. A reduced ability to switch into this state thus accords with Sourty et al. (2016), who found dynamic connectivity changes in DLB for networks related to visual processing using Hidden Markov Models. Another important characteristic of state 1 that differentiates it from state 2 is the existence of strong anti-correlations in the former. Furthermore, while the DMNs do not show strong correlations with task-positive networks in state 1, the other two states are characterised by positive connections between DMN and visual and attention networks. Anti-correlation between default mode and task-positive networks has been shown to be important for attentional function (Fox et al., 2005) and a loss of anti-correlations has been associated with ageing, MCI, and cognitive impairment in PD (Baggio et al., 2015; Esposito et al., 2017). The present results further suggest that an absence

of this antithetic relationship between default mode and task-positive networks might also be a feature of more established neurodegenerative disease in the case of AD and DLB.

5.4.2 DLB-related changes in dynamic network topology

Regarding dynamic network topology, global efficiency was found to be less variable in DLB compared to controls. Global efficiency is a measure of communication efficiency across the whole brain network (Latora and Marchiori, 2001). In general, more pronounced variability of functional connectivity has been shown to be related to superior performance on a range of behavioural tests including attention and memory tasks (Jia et al., 2014), indicating that the dynamic and flexible engaging and disengaging of different brain regions seems to be crucial for efficient and adaptable communication within the brain (Zalesky et al., 2014). Reduced dynamics in turn can lead to less flexible and ineffective communication as well as a reduced ability of the network to respond to situational demands. The reduced variability of global efficiency in DLB might thus indicate a disease-related and abnormal rigidity of the brain network which might relate to the cognitive slowing (bradyphrenia) that is observed in DLB patients (Firbank et al., 2018). In contrast, in healthy brains efficiency is temporally modulated, which has been shown to represent more economical network dynamics allowing for a more specific response to situational demands (Zalesky et al., 2014). In contrast to the dynamic analysis, there were no significant group differences when considering efficiency across the whole time course. This finding stands in contrast to a previous study which reported increased global efficiency in DLB patients compared to patients with AD (Peraza et al., 2015b). However, while Peraza et al. (2015b) analysed a brain network that was based on individual atlas-defined regions of interest, the network nodes in the present analysis were large-scale RSNs themselves, thereby assessing the interconnections between different networks. There is no complete correspondence between the two approaches (Rosazza et al., 2012) which might explain this difference in findings. Nevertheless, similar to the present results, Peraza et al. (2015b) reported no difference between patients with AD and controls with respect to global efficiency which indicates that static and dynamic changes in efficiency might be a specific feature of DLB that might not be associated with dementia *per se*. In contrast to the present results, Kim et al. (2017) have found increased variability of global efficiency in patients with PD. However, this finding was not replicated in another study in PD patients with mild cognitive impairment (Díez-Cirarda et al., 2017) and thus further research will be needed to identify the specific changes related to these different Lewy body diseases.

5.4.3 Relation to clinical symptoms in DLB

Given the transient nature of clinical DLB symptoms such as visual hallucinations and cognitive fluctuations, I expected symptom severity to be related to some extent to dynamic connectivity measures. However, there were no significant correlations between dynamic connectivity measures and cognitive fluctuations, even before correcting for multiple comparisons. A possible reason for this might be the difference in timescales: while the fMRI data only allowed the characterisation of dynamics during a 6-minute resting-state scan, the timescale of cognitive fluctuations can be on the order of minutes to hours and even days. Performing repeated scans with DLB patients at different times of the day or over several days might thus help to understand more about the relation between functional connectivity dynamics and clinical symptom severity. There was a trend for an association between frequency of state 2 and severity of Parkinsonism in DLB, i.e. an increased time spent in this sparsely connected state might relate to more severe Parkinsonism. Relative to state 1, this state was characterised by a disconnection of motor networks from other networks and the observed correlation might thus indicate that the isolation of motor networks might contribute to the severity of clinical motor symptoms. However, this is only an exploratory result that did not survive multiple comparison correction and further research will be needed to confirm this conjecture.

5.4.4 Reliability of dynamic connectivity results

The interpretation, functional significance, and origin of dynamic functional connectivity have been the subject of an extensive debate (Hindriks et al., 2016; Laumann et al., 2016). However, recent studies using concurrent fMRI and EEG measurements point towards a neuronal origin of dynamic functional connectivity (Chang et al., 2013). Additionally, several studies have provided support for a cognitive role by showing that temporary changes in connectivity are related to changes in behavioural or vigilance states (Jia et al., 2014; Kucyi et al., 2017; Thompson et al., 2013) and cognitive performance in healthy older adults (Cabral et al., 2017). Finally, the study of dynamic functional connectivity in clinical populations has led to the identification of specific dynamic connectivity alterations associated with specific disorders which provides further evidence of the neurocognitive significance of time-varying functional connectivity (Damaraju et al., 2014; Jones et al., 2012; Sourty et al., 2016). Although the sliding window approach has been widely applied to study dynamic functional connectivity (Allen et al., 2014; Damaraju et al., 2014; Hutchison and Morton, 2015; Jones et al., 2012; Marusak et al., 2016), its validity has been debated (Hindriks et al., 2016). Advantages are its interpretability and computational efficiency which make this kind of

analysis especially suitable for the investigation of clinical questions. However, problematic aspects include the need for an *a priori* specification of parameters such as window length and the number of states for the k-means analysis and the possibility of spurious connectivity fluctuations which can arise due to noise sources such as head motion (Hutchison et al., 2013a). In the present analysis, I applied several pre- and postprocessing steps to reduce the effect of these noise sources (see Section 5.2.3). It was also ensured that the groups did not differ with respect to motion which makes it unlikely that the observed group differences were merely motion artefacts. Additionally, there was no significant relation between dynamic connectivity measures and mean framewise displacement, indicating little influence of motion on the dynamic connectivity measures in the present analysis. Regarding the choice of window length, I showed that the results can be reproduced using windows of different lengths. While most previous studies examined a larger number of states (Allen et al., 2014; Damaraju et al., 2014; Hutchison and Morton, 2015; Marusak et al., 2016; Viviano et al., 2017), I focused on a smaller set of three states which was determined as the optimal number of states in the present dataset and is comparable to a previous report in PD (Kim et al., 2017). The states tended to get more unstable as more states were added with states appearing that were specific to certain participants (see Figure 5.8). This might be due to the small number of participants and large heterogeneity in the present sample. Nevertheless, I showed that the observed group differences in terms of frequency and dwell time remained largely unchanged for different values of k, and states were reproducible on split-half and bootstrap resamples of the data which confirms the robustness of this approach. Notably, adding more states did not result in more significant group differences, indicating that these three states represent the most important states in terms of dementia-related changes in connectivity dynamics.

5.4.5 Limitations

Many of the DLB patients were on dopaminergic medication and scanned in the ON state which might have influenced their dynamic functional connectivity measures. However, dopaminergic medication has been shown to normalise connectivity towards more healthy levels (Tahmasian et al., 2015), suggesting that the observed group differences were not due to medication. Furthermore, there were no differences in terms of dynamic connectivity measures between DLB patients who were taking dopaminergic medication compared to those not on these medications.

5.4.6 Conclusion

The loss of variability of global efficiency in DLB indicates an abnormally rigid brain network. This might be associated with less economical dynamics that can lead to disruptions of normal brain functioning and prevent specific and effective responses of the brain network to situational demands. This loss of dynamics was not observed in AD patients and seems to represent a DLB-specific abnormality that might relate to the cognitive phenotype of DLB. In contrast, the inability to transiently switch out of states of low inter-network connectivity into more highly and specifically connected network configurations was observed in both dementia groups and might thus be related to the presence of dementia in general rather than symptoms that are specific to AD or DLB.

Chapter 6. EEG Microstate Analysis

6.1 Introduction

Brain dynamics can be assessed with different methodologies and on different timescales: while fMRI allows the characterisation of slower brain dynamics with high spatial resolution (see Chapter 5), dynamical changes on a sub-second timescale can be studied using EEG microstate analysis (Michel and Koenig, 2017). Previous research has shown that the EEG signal can be segmented into a number of short, non-overlapping, quasi-stable topographies – the microstates – that remain transiently stable for about 80-120 ms before abruptly transitioning into a new state (Khanna et al., 2015; Lehmann et al., 1987; Michel and Koenig, 2017). Even though there is a large number of possible topographies in multi-channel EEG, more than 70% of its variance can be explained by only a few distinct and stereotypical topographies (Koenig et al., 1999). These microstates have been described as the basic building blocks of human information processing or the "atoms of thought" (Lehmann, 1990) and it has been shown that their temporal dynamics, especially in terms of microstate duration, are important for cognitive functioning (Van De Ville et al., 2010). Furthermore, it has been suggested that investigating temporal aspects of microstate sequences can provide insight into the brain's dynamic repertoire across different timescales. Studying microstate dynamics on a sub-second timescale can therefore provide information about brain dynamics in general with implications for fast and slow dynamic processes (Van De Ville et al., 2010). Thus, interrogation of microstate dynamics in LBD may provide a novel perspective in understanding the basis of cognitive fluctuations and more broadly the LBD cognitive phenotype. These investigations form the first part of this chapter.

In the second part, I address the potential mechanisms of microstate transition and their disruption in LBD. While there is evidence for a relation between specific microstates and the well-known RSNs that can be obtained from fMRI (Britz et al., 2010; Custo et al., 2017; Musso et al., 2010), it remains unclear which processes in the brain drive the abrupt global transitions between different microstates, i.e. the neural correlates of microstate dynamics (Michel and Koenig, 2017). However, subcortical-cortical networks represent one putative system which could globally alter brain dynamics given their significant and widespread cortico-petal connectivity. In particular, both the thalamus and the basal ganglia have extensive connections to various parts of the cortex and form part of the cortical-basal ganglia-thalamic loop which is an important contributor to large-scale network communication within the brain (Bell and Shine, 2016). The thalamus has been suggested to play a role in modulating the cortical EEG signal (Lopes da Silva, 1991) and its activity has

been shown to relate to cortical microstate characteristics (Schwab et al., 2015). From a LBD perspective, structural and functional abnormalities of the thalamus are a common feature in Lewy body diseases (Watson et al., 2017). In particular, microstructural changes and cholinergic imbalance in the thalamus have been suggested to play a role in the aetiology of cognitive fluctuations in DLB (Delli Pizzi et al., 2015b; Pimlott et al., 2006). Similarly, dopaminergic dysfunction of the basal ganglia is a hallmark of Lewy body diseases (McKeith et al., 2007) and aberrant functional connectivity of the basal ganglia network has been found in DLB and PD (Rolinski et al., 2015; Szewczyk-Krolikowski et al., 2014, see also Chapter 4). Both the basal ganglia and the thalamic networks are therefore potential candidate networks whose dynamic interaction with cortical networks might influence microstate dynamics in LBD.

I hypothesised that a less dynamic brain, as evidenced by slowing of microstate dynamics is a feature of LBD which is related to the cognitive phenotype, and in particular, cognitive fluctuations, and that disturbances in microstate dynamics in LBD will be contingent upon a loss of dynamics within cortical-basal ganglia-thalamic connections.

6.2 Methods

6.2.1 Participants

This analysis involved 96 participants from the CATFieLD study comprising 46 diagnosed with probable LBD (25 DLB and 21 PDD), 32 with probable AD, and 18 healthy controls. Patients who were taking dopaminergic medication were assessed in the "ON" motor state.

6.2.2 EEG acquisition and preprocessing

Resting-state EEG recordings were acquired from all participants using Waveguard caps (ANT Neuro, The Netherlands) comprising 128 sintered Ag/AgCl electrodes that were placed according to the 10-5 system. Participants were seated during the recording and were instructed to remain awake, but keep their eyes closed. Electrode impedance was kept below 5 kΩ and 150 s of continuous EEG data were recorded at a sampling frequency of 1024 Hz. The ground electrode was attached to the right clavicle and all EEG channels were referenced to Fz during recording.

Preprocessing of EEG data was performed by Dr Luis Peraza, blinded to group membership and methods applied were the same as described in (Peraza et al., 2018). Data were filtered between 0.3 and 54 Hz using a second order Butterworth filter, noisy EEG segments with artefacts affecting all channels were deleted, and ICA was used for artefact removal. Data were then recomputed against the average reference, bandpass filtered between 2 and 20 Hz,

and split into non-overlapping epochs of 2-second length. For each participant the first 30 2-second long artefact-free epochs were selected for the microstate analysis. Participants with less than 30 artefact-free epochs were excluded from further analysis. 30 epochs were chosen because this allowed to include a large number of patients and is comparable to the number of epochs that is typically used in microstate studies.

6.2.3 Microstate analysis

The microstate analysis was conducted using the Cartool software (Brunet et al., 2011) and functions from the EEGLAB plugin for Microstates (http://www.thomaskoenig.ch/index.php/software/microstates-in-eeglab) in Matlab R2017a. As a first step, the global field power (GFP) was calculated which is equivalent to the standard deviation of the average-referenced signal across all electrodes and whose local maxima represent instants of highest field strength (Lehmann and Skrandies, 1980). EEG topographies tend to remain stable during periods of high GFP and change rapidly around the local minima of the GFP (Lehmann et al., 1987). Thus, topographies at GFP peaks are representative of topographies at surrounding time points and restricting the microstate analysis to these GFP peaks provides optimal topographic signal-to-noise ratios (Lehmann et al., 1987). For each subject separately, topographies at GFP peaks were subjected to a topographic atomize and agglomerate hierarchical clustering (TAAHC) algorithm (Murray et al., 2008) (Figure 6.1A). The optimal number of microstate classes k was determined for each participant individually using the meta-criterion described in Custo et al. (2017), testing the entire range from 1 to 12 classes. The individual maps were then averaged across all participants within each group using a permutation algorithm (Koenig et al., 1999) and overall mean maps across all participants were obtained by averaging the group-specific average maps across groups (Figure 6.1B).

The group microstate maps were then fitted back to the original data at GFP peaks assigning each GFP peak to one microstate class based on the maximal spatial correlation between topographies (Figure 6.1C). Microstate labels for data points between GFP peaks were interpolated with microstates starting and ending halfway between two GFP peaks. Potentially truncated microstates at the beginning and end of each epoch were excluded from the analysis. Microstate duration was thus calculated as the time during which all successive maps were assigned to the same microstate. Additionally, the mean number of occurrences of each microstate class per second (microstate occurrence) and the percentage of total analysis time covered by each microstate (microstate coverage), i.e. the sum of the durations of each occurrence of a certain microstate class across the whole time course, were calculated.

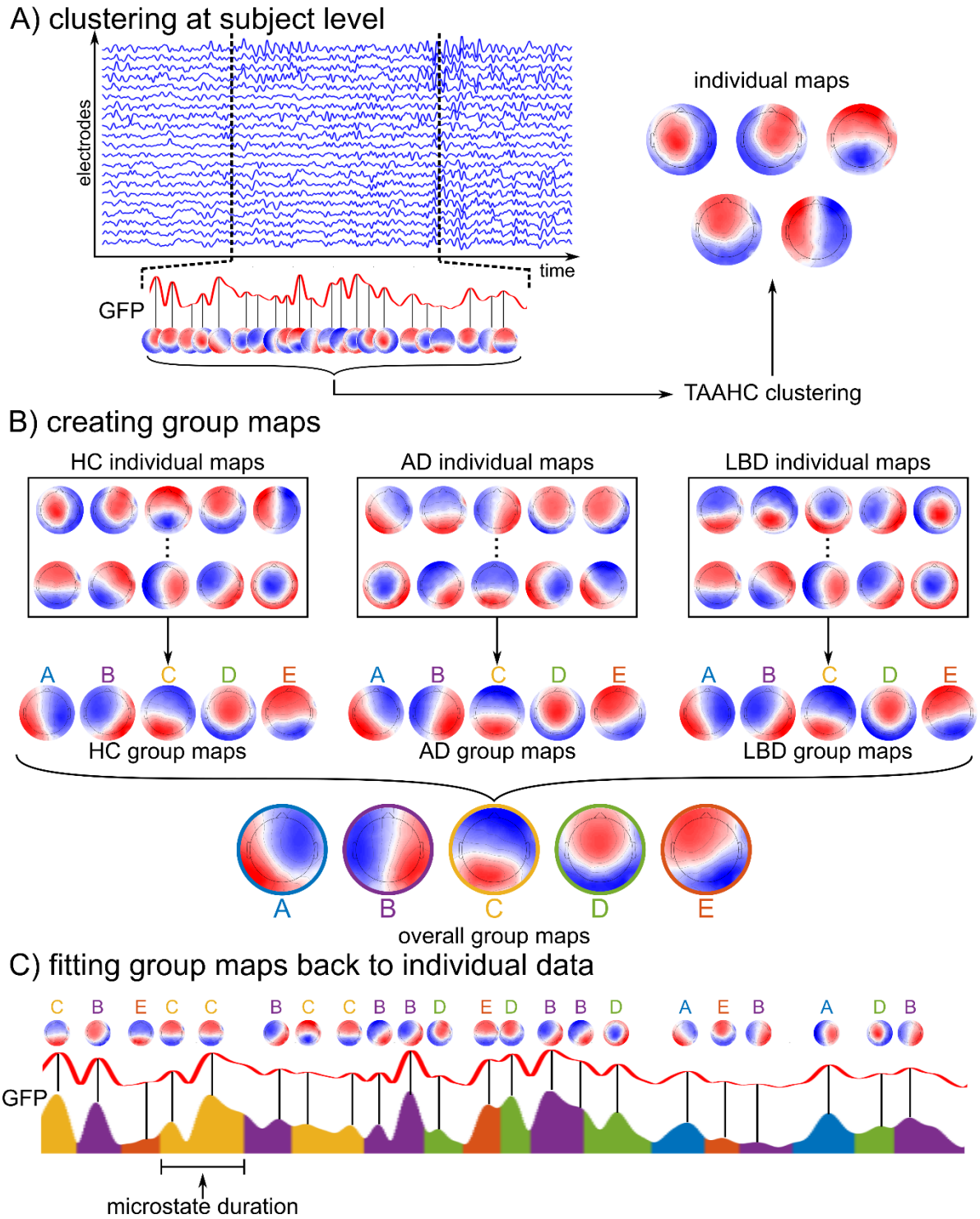

Figure 6.1. Explanation of EEG microstate analysis. A) For each subject, data at global maxima of the GFP are clustered using the TAAHC algorithm to obtain individual microstate maps. B) The individual maps are combined to obtain group maps within each clinical group using a permutation algorithm. C) Group maps are fit back to the data at GFP peaks assigning each GFP peak to the microstate class with the highest topographical correlation. Microstates in-between GFP peaks are interpolated.
AD, Alzheimer's disease; GFP, global field power; HC, healthy controls; LBD, Lewy body dementia; TAAHC, topographic atomize and agglomerate hierarchical clustering.

6.2.4 Microstate statistics

The topographies of the different microstate classes were compared between the groups using topographical analysis of variance (TANOVA) implemented in the Ragu software (Koenig et al., 2011). For this, a non-parametric randomisation test was performed on global map dissimilarity with a within-subject factor of microstate class and a between-subject factor of group.

Microstate duration, occurrence, coverage, and observed transition probabilities were compared between the groups using separate multivariate ANOVAs in IBM SPSS Statistics version 23. In the case of an overall significant test, follow-up univariate ANOVAs were performed to determine which microstate classes showed group differences followed by post-hoc tests with Bonferroni-correction for multiple comparisons.

Transition probabilities between different microstate classes were assessed by counting the number of transitions from each microstate class to any other class and normalising by all between-class transitions for each subject separately. If the transition from one microstate class to the next occurred randomly, i.e. irrespective of the class of the preceding microstate, transition probabilities would be proportional to the relative occurrence of the microstate classes. Under the null hypothesis of random transitions between microstates, the expected transition probability for transitions from microstate class X to class Y is therefore given by (Lehmann et al., 2005):

$$P_{X \to Y}^{exp} = \frac{\text{occurrence}_X \times \text{occurrence}_Y}{1 - \text{occurrence}_X}$$

To assess the randomness of transition probabilities, a non-parametric randomisation test was applied as described in Lehmann et al. (2005). Within each group, the observed and expected transition probabilities were averaged across participants and the overall difference between observed and expected transition probabilities was calculated using the χ^2-distance (Lehmann et al., 2005). Individual observed and expected transition probabilities were then randomly permutated 5,000 times to obtain the distribution of χ^2-distance values under the null hypothesis of random transition probabilities. The p-value was calculated as the fraction of permutations in which the χ^2-distance was larger than the distance using non-permuted transition probabilities.

6.2.5 Clinical and behavioural correlations

Correlation analyses were performed in R version 3.5.1. Spearman's correlations between mean microstate duration and the Mayo fluctuation scale (overall score, cognitive subscore, and arousal subscore) were tested in the combined LBD group as well as in the two subgroups

separately. P-values were FDR-corrected for multiple comparisons. To check whether these correlations were influenced by dopaminergic medication, a linear regression analysis was also performed adding LEDD (Tomlinson et al., 2010) as a covariate in the model. Supplementary correlation analyses were performed for the CAF score, global cognitive scores (MMSE and CAMCOG), the UPDRS motor subscale, and NPI visual hallucinations subscores in the LBD group. In the AD group, correlations were calculated between mean microstate duration and global cognition (MMSE and CAMCOG).
Given that previous studies have reported a relation between a loss of brain dynamics and slower and less consistent RT performance (McIntosh et al., 2008), I was also interested in investigating correlations between mean microstate duration and the ex-Gaussian parameters reported in Chapter 3. To this end, a Spearman's correlation analysis was performed across all groups to test correlations between mu, sigma, and tau and mean microstate duration.

6.2.6 Effect of dopaminergic medication in the LBD group

To assess the effect of dopaminergic medication usage in the LBD group, microstate duration and microstate occurrence per second were compared between LBD patients who were taking dopaminergic medication (N=29) and those LBD patients who were not taking dopaminergic medication (N=13). In addition, Spearman's correlations were calculated between LEDD and mean microstate duration and occurrence in the LBD group.

6.2.7 FMRI dynamic connectivity

Resting-state fMRI was recorded from a subset of the participants included in the EEG analysis (non-concurrent, performed between one and three weeks apart). This subset comprised 12 healthy controls, 14 AD patients, and 29 patients with LBD (17 DLB and 12 PDD). Details on the analysis of dynamic functional connectivity can be found in Section 5.2.4. In the present analysis, given my *a priori* hypothesis, I focussed on dynamic connectivity between two subcortical networks (basal ganglia and thalamic networks) and all other networks (see Table 4.1 in Chapter 4 for a list of all included networks and Figure 4.1 in Chapter 4 for a depiction of the network maps).

6.2.8 Combining EEG microstates and dynamic fMRI connectivity

The mean variability of connectivity (standard deviation over time) between the two subcortical networks of interest – basal ganglia and thalamus – and all other networks was calculated and correlated with mean microstate duration in each group separately using Pearson's correlations. To assess which of the individual network connections contributed

most to the overall correlation, mean microstate duration was correlated with the dynamic connectivity of each connection separately, correcting the resulting p-values for multiple comparisons using FDR-correction.

6.3 Results

6.3.1 Demographics

Data from five AD and four PDD patients were excluded from the microstate analysis because they had fewer than 30 2-second long epochs of cleaned EEG data after preprocessing. Therefore, 18 healthy controls, 27 AD, and 42 LBD (25 DLB and 17 PDD) participants were included in the analysis.

Healthy control, AD, and LBD participants were similar in age and sex (Table 6.1). Additionally, the two dementia groups did not differ significantly in terms of dementia duration. However, the LBD group was significantly less impaired in terms of overall cognition (MMSE and CAMCOG) compared to the AD group. The percentage of patients taking acetylcholinesterase inhibitors did not differ between the dementia groups. As expected the majority of LBD patients were taking dopaminergic medication compared to none of the AD patients. The LBD patients were more impaired than the AD patients with respect to the core LBD symptoms of Parkinsonism, cognitive fluctuations, and visual hallucinations.

To ensure that the difference in overall cognition between the two dementia groups did not influence the results, all analyses described below were rerun with AD and LBD subgroups that were matched for MMSE and CAMCOG. These were created by excluding three AD patients with MMSE<14 and six LBD patients (five DLB and one PDD) with MMSE>27. The two resulting groups did not differ significantly with respect to dementia duration (Mann-Whitney U test, U=322, p=0.19), MMSE (Student's t-test, t_{58}=0.65, p=0.52), and CAMCOG (Student's t-test, t_{58}=0.62, p=0.54).

Demographics for those participants that were included in the combined EEG-fMRI analysis are shown in Table 6.2. All three groups were matched for age and sex, while the two dementia groups were matched in terms of overall cognition.

Table 6.1 shows a comparison of clinical symptoms between DLB and PDD. Both LBD subgroups were matched in terms of age, sex, overall cognition, the percentage of patients taking acetylcholinesterase inhibitors, and cognitive fluctuation and visual hallucination severity. More PDD patients were taking dopaminergic medication and they had worse Parkinsonism than the DLB patients. DLB and PDD patients were combined into one LBD group as preliminary analyses showed that there were no group differences with respect to microstate characteristics (Table 6.3).

Table 6.1. Demographic and clinical variables, mean (standard deviation).

	HC (N=18)	AD (N=27)	LBD (N=42)	Group differences	DLB (N=25)	PDD (N=17)	Group differences
Male: female	11:7	20:7	36:6	χ^2=4.5, p=0.11[a]	20:5	16:1	χ^2=1.65, p=0.20[k]
Age	76.3 (5.5)	74.9 (7.0)	74.8 (6.4)	F(2,84)=0.35, p=0.70[b]	76.2 (6.2)	72.8 (6.2)	t_{40}=1.71, p=0.10[l]
AChEI	-	25	36	χ^2=0.76, p=0.38[c]	23	13	χ^2 =2.00, p=0.16[k]
PD meds	-	0	29	χ^2=32.16, p<0.001[c]	12	17	χ^2 =12.80, p<0.001[k]
Duration	-	3.9 (2.1)[f]	3.2 (2.1)[g]	U=399, p=0.12[d]	3.5 (2.3)	2.8 (1.5)[p]	U =174, p=0.48[m]
MMSE	29.2 (0.9)	20.7 (4.3)	23.1 (3.7)	t_{67}=2.51, p=0.01[e]	22.7 (4.3)	23.8 (2.6)	t_{40} =0.92, p =0.36[l]
CAMCOG	96.7 (3.7)	67.4 (15.7)	75.7 (11.1)	t_{67}=2.57, p=0.01[e]	74.8 (12.8)	77.1 (8.2)	t_{40} =0.63, p =0.53[l]
UPDRS III	1.3 (1.5)	2.4 (3.0)	20.4 (8.5)	t_{67}=10.6, p<0.001[e]	16.2 (7.5)	26.6 (5.5)	t_{40} =4.88, p<0.001[l]
CAF total	-	0.38 (0.98)[g]	5.0 (4.3)[h]	t_{64}=5.31, p<0.001[e]	4.1 (4.1)[o]	6.3 (4.4)[p]	t_{38} =1.55, p=0.13[l]
Mayo total	-	9.4 (4.7)[g]	14.0 (5.7)[h]	t_{64}=3.41, p=0.001[e]	13.3 (5.9)[o]	14.9 (5.4)[p]	t_{38}=0.88, p=0.39[l]
Mayo cogn	-	1.9 (1.8)[g]	2.8 (1.8)[h]	t_{64}=2.06, p=0.043[e]	2.5 (1.8)[o]	3.2 (1.9)[p]	t_{38}=1.10, p=0.28[l]
NPI total	-	6.8 (6.6)[g]	14.3 (10.5)[j]	t_{65}=3.23, p=0.002[e]	10.2 (6.3)[o]	20.1 (12.6)	t_{39}=3.31, p=0.002[l]
NPI hall	-	0.04 (0.20)[g]	1.9 (2.0)[j]	t_{65}=4.90, p<0.001[e]	1.7 (1.9)[o]	2.2 (2.1)	t_{39}=0.85, p=0.40[l]

AChEI, number of patients taking acetylcholinesterase inhibitors; AD, Alzheimer's disease; CAF total, Clinician Assessment of Fluctuation total score; CAMCOG, Cambridge Cognitive Examination; DLB, Dementia with Lewy bodies; Duration, duration of cognitive symptoms in years; HC, healthy controls; LBD, Lewy body dementia; Mayo total, Mayo Fluctuations Scale; Mayo cognitive, Mayo Fluctuation cognitive subscale; MMSE, Mini Mental State Examination; PDD, Parkinson's disease dementia; PD meds, number of patients taking dopaminergic medication for the management of Parkinson's disease symptoms; UPDRS III, Unified Parkinson's Disease Rating Scale III (motor subsection); NPI, Neuropsychiatric Inventory; NPI hall, NPI hallucination subscore

[a] Chi-square test HC, AD, LBD; [b] One-way ANOVA HC, AD, LBD; [c] Chi-square test AD, LBD; [d] Mann Whitney U test AD, LBD; [e] Student's t-test AD, LBD.

[f] N=25, [g] N=26, [h] N=40, [j] N=41

[k] Chi-square test DLB, PDD; [m] Mann Whitney U test DLB, PDD; [l] Student's t-test DLB, PDD.

[o] N=24, [p] N=16.

Table 6.2. Demographic and clinical variables for all participants that were included in the combined EEG-fMRI analysis, mean (standard deviation).

	HC (N=12)	AD (N=14)	LBD (N=29)	Between-group differences
Male: female	9:3	11:3	24:5	χ^2=0.34, p=0.84[a]
Age	76.4 (6.2)	75.0 (8.3)	74.5 (6.6)	F(2,52)=0.33, p=0.72[b]
AChEI	-	13	27	χ^2=0.01, p=0.98[c]
PD meds	-	1	21	χ^2=16.1, p<0.001[c]
Duration	-	3.9 (1.7)	3.4 (2.2)[g]	U=151, p=0.22[d]
MMSE	29.2 (0.8)	21.8 (4.1)	23.1 (3.5)	t_{41}=1.13, p=0.27[e]
CAMCOG	96.3 (2.9)	70.6 (16.4)	75.6 (11.4)	t_{41}=1.15, p=0.26[e]
UPDRS III	1.3 (1.5)	1.1 (1.2)	20.0 (8.3)	t_{41}=8.37, p<0.001[e]
CAF total	-	0.38 (1.12)[f]	5.1 (4.5)[g]	t_{39}=3.66, p=0.001[e]
Mayo total	-	8.9 (4.1)[f]	14.5 (5.4)[g]	t_{39}=3.31, p=0.002[e]
Mayo cogn	-	2.2 (1.9)[f]	2.9 (1.9)[g]	t_{39}=1.05, p=0.30[e]
NPI total	-	5.1 (4.3)[f]	15.2 (10.9)	t_{40}=3.23, p=0.003[e]
NPI hall	-	0 (0)[f]	1.9 (1.7)	t_{40}=3.96, p<0.001[e]

AChEI, number of patients taking acetylcholinesterase inhibitors; AD, Alzheimer's disease; CAF total, Clinical Assessment of Fluctuations total score; CAMCOG, Cambridge Cognitive Examination; Duration, duration of cognitive symptoms in years; HC, healthy controls; LBD, Lewy body dementia; Mayo total, Mayo Fluctuations Scale; Mayo cognitive, Mayo Fluctuation cognitive subscale; MMSE, Mini Mental State Examination; PD meds, number of patients taking dopaminergic medication for the management of Parkinson's disease symptoms; UPDRS III, Unified Parkinson's Disease Rating Scale III (motor subsection); NPI, Neuropsychiatric Inventory; NPI hall, NPI hallucination subscore

[a] Chi-square test HC, AD, LBD; [b] One-way ANOVA HC, AD, LBD; [c] Chi-square test AD, LBD; [d] Mann Whitney U test AD, LBD; [e] Student's t-test AD, LBD.

[f] N=13, [g] N=28, [h] N=13.

Table 6.3. Mean [95% confidence interval] of microstate duration and microstate occurrence per second in the DLB and PDD subgroups and results from group comparison using two-sample t-tests.

	DLB	PDD	t-test
duration			
mean	78.53 [74.9,82.2]	74.86 [69.1,80.6]	t(40)=1.2, p=0.24
A	71.00 [66.9,75.1]	70.93 [65.7,76.2]	t(40)=0.02, p=0.98
B	71.11 [67.2,75.0]	70.77 [64.1,77.5]	t(40)=0.1, p=0.92
C	76.98 [72.2,81.7]	73.89 [68.3,79.4]	t(40)=0.9, p=0.39
D	83.58 [78.0,89.2]	74.92 [67.9,82.0]	t(40)=2.0, p=0.05
E	79.2 [72.3,86.2]	74.26 [67.8,80.7]	t(40)=1.0, p=0.30
occurrence			
mean	13.25 [12.7,13.8]	13.95 [12.8,15.1]	t(40)=1.2, p=0.22
A	2.47 [2.2,2.7]	2.76 [2.4,3.1]	t(40)=1.6, p=0.13
B	2.40 [2.3,2.5]	2.67 [2.4,2.9]	t(40)=2.0, p=0.053
C	2.63 [2.5,2.8]	2.86 [2.6,3.2]	t(40)=1.5, p=0.14
D	3.03 [2.8,3.2]	2.83 [2.5,3.2]	t(40)=1.0, p=0.32
E	2.72 [2.6,2.9]	2.83 [2.6,3.1]	t(40)=0.9, p=0.38

DLB, dementia with Lewy bodies; PDD, Parkinson's disease dementia.

6.3.2 Cluster evaluation

The optimal number of microstate classes for each participant was determined to be between four and eight. The median within each clinical group as well as the overall median was five, with no significant differences between the groups (Kruskal-Wallis ANOVA, $H(2)=0.93$, $p=0.63$). The number of microstate classes was therefore set to five for all subsequent analyses.

Across all participants the mean global explained variance (GEV) of five microstate classes was 70% (SD=6%). The mean and standard deviation in each group was 71% (SD=8%) for healthy controls, 68% (SD=5%) for AD, and 71% (SD=5%) for LBD. A univariate ANOVA showed that there were no significant group differences ($F(2,84)=3.01$, $p=0.06$). Post-hoc tests (Bonferroni-corrected) showed that there were no differences between patients with AD and controls ($p=0.20$) or between LBD patients and controls ($p=1.0$). However, there was a trend for smaller GEV in the AD compared to the LBD group ($p=0.07$).

6.3.3 Microstate topographies

Group microstate maps and the overall maps across all participants are shown in Figure 6.2. Microstate classes A to D corresponded well to the canonical microstate maps that have been reported in the literature (Michel and Koenig, 2017). There was an additional microstate class E that resembles a slightly lateralised version of class D and might be comparable to the deviant microstate topography of class C that has been described in Grieder et al. (2016) in a group of patients with semantic dementia.

The overall TANOVA revealed a significant main effect of microstate class ($p=0.0002$) and a main effect of group ($p=0.0002$), but no interaction between the two factors ($p=0.45$). Follow-up TANOVAs for each microstate class showed that the AD topographies were different from both the healthy controls and LBD topographies for all microstate classes (see Figure 6.2 and Table 6.4). In contrast, there were no significant differences between healthy controls and LBD topographies for any microstate class. These results did not change when analysing matched dementia subgroups (Table 6.5).

Table 6.4. P-values from TANOVA test of microstate topographies for microstate classes A to E between groups. The overall two-way TANOVA with microstate class as within-subject factor and group as between-subject factor resulted in a main effect of group ($p<0.001$), a main effect of microstate class ($p<0.001$), but no interaction between the two factors ($p=0.45$).

	all groups	HC-AD	HC-LBD	AD-LBD
A	<0.001	<0.001	0.15	<0.001
B	<0.001	<0.001	0.36	<0.001
C	0.014	0.021	0.38	0.009
D	0.036	0.049	0.40	0.027
E	0.006	0.048	0.37	<0.001

AD, Alzheimer's disease; HC, healthy controls; LBD, Lewy body dementia.

Table 6.5. P-values from TANOVA test of microstate topographies for microstate classes A to E for matched dementia subgroups. The overall two-way TANOVA with microstate class as within-subject factor and group as between-subject factor resulted in a main effect of group ($p<0.001$), a main effect of microstate class ($p<0.001$), but no interaction between the two factors ($p=0.47$).

	all groups	HC-AD	HC-LBD	AD-LBD
A	<0.001	<0.001	0.11	<0.001
B	<0.001	<0.001	0.22	<0.001
C	0.013	0.017	0.45	0.009
D	0.039	0.034	0.47	0.031
E	0.004	0.027	0.46	<0.001

AD, Alzheimer's disease; HC, healthy controls; LBD, Lewy body dementia

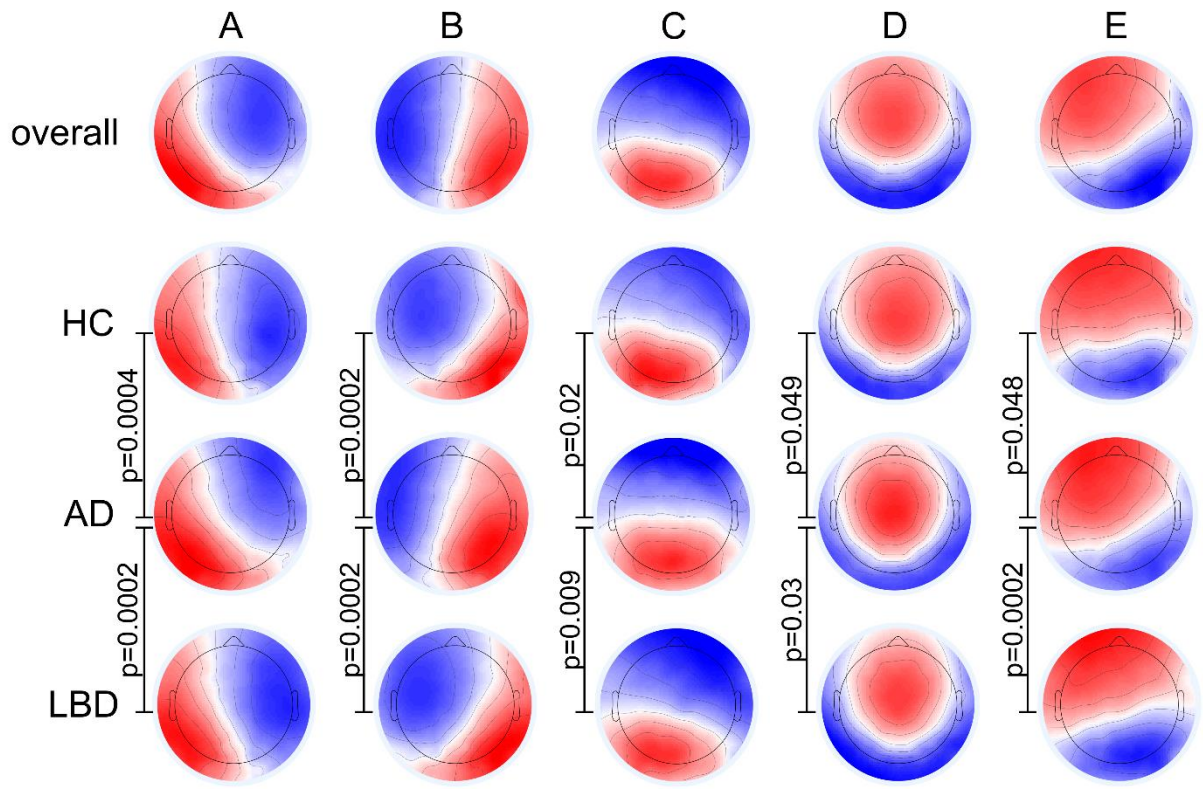

Figure 6.2. Group comparison of microstate topographies. P-values result from comparing microstates topographies between groups using TANOVA. For the comparison between HC and LBD all p-values were above 0.1 (see Tables 6.4 and 6.5).
AD, Alzheimer's disease; HC, healthy controls; LBD, Lewy body dementia.

6.3.4 Microstate temporal characteristics

The mean number of GFP peaks per second was 21.3 in HC, 19.7 in AD, and 17.2 in LBD. There was a significant difference between groups (univariate ANOVA, $F(2,84)=26.6$, $p<0.001$) with Bonferroni-corrected post-hoc tests demonstrating that the number of GFP peaks was lower in patients with AD compared to controls ($p=0.034$), and lower in LBD patients compared to controls ($p<0.001$) and patients with AD ($p<0.001$).
Across all microstate classes mean microstate duration was 65 ms in controls, 67 ms in AD patients, and 77 ms in the LBD group. A univariate ANOVA followed by post-hoc group comparisons showed that mean microstate duration was increased in patients with LBD compared to controls and AD patients with no significant difference between AD patients and controls (see Figure 6.3A and Table 6.6). Correspondingly, the mean number of unique microstate occurrences per second was 16 in controls, 15.5 in AD, and 13.5 in LBD. Univariate ANOVA and post-hoc tests showed that the number of unique microstate occurrences per second was significantly decreased in patients with LBD compared to controls and AD patients with no significant difference between the AD and the control groups (Figure 6.3A and Table 6.7).

Multivariate ANOVAs followed by post-hoc univariate ANOVAs were conducted to test for group differences in mean microstate duration and occurrence for microstate classes A to E (see Figure 6.3B and Tables 6.6 and 6.7). Microstate A duration was increased in both dementia groups compared to controls with a trend for a further increase in patients with LBD compared to AD patients. Occurrence of microstate A was reduced in LBD patients compared to controls and patients with AD with no difference between controls and AD patients. The other microstates (B to E) showed similar patterns in terms of duration with increased duration in LBD patients compared to patients with AD and controls and no difference between AD patients and controls. The occurrence of microstates B and C was decreased in the LBD group compared to the AD and healthy control groups with no difference between controls and AD patients. In contrast, microstate D occurrence was only reduced in patients with LBD compared to controls, but there was no difference between controls and AD patients and between the dementia groups. The occurrence of microstate E was reduced in both dementia groups compared to controls with no difference between the dementia groups.
To test whether group differences in microstate duration and occurrence were merely due to group differences in the number of GFP peaks per second, the microstate analysis was repeated, but this time fitting group microstates to each time point of the individual subject data instead of only fitting to data at GFP peaks. This analysis was performed in Cartool using default smoothing parameters (smoothing half window size of 3 time frames, smoothing strength λ=10, and rejecting small segments below 3 time frames). Subsequently, microstate characteristics were computed in the same way as described above removing possibly truncated microstates from the epoch boundaries. Mean microstate duration and occurrence were compared between the groups using univariate ANOVAs. There was an overall group effect for microstate duration ($F(2,84)=38.66$, $p<0.001$). Post-hoc tests with Bonferroni correction for multiple comparisons revealed that microstate duration was longer in the LBD group compared to both controls ($p<0.001$) and AD patients ($p<0.001$) whereas there was no significant difference between healthy controls and patients with AD ($p=0.40$). There was also an overall group effect for microstate occurrence ($F(2,84)=50.26$, $p<0.001$). Post-hoc tests showed that microstate occurrence per second was lower in the LBD group compared to healthy controls ($p<0.001$) and patients with AD ($p<0.001$) with no significant difference between controls and AD patients ($p=0.07$).
Repeating the group comparison analyses with matched dementia groups did not change the overall results, but enhanced some of the differences between the AD and LBD groups (Table 6.8 and 6.9).
To test whether the marginal group differences in GEV (see Section 6.3.2) had an effect on

the results from the group comparison of microstate characteristics, the analyses were repeated including GEV as covariate. There was a group difference for mean microstate duration ($F(2,83)=17.51$, $p<0.001$) and microstate occurrence ($F(2,83)=17.14$, $p<0.001$). Post-hoc tests revealed that microstate duration was increased in the LBD group compared to controls ($p<0.001$) and patients with AD ($p=0.001$) with no difference between AD patients and controls ($p=0.13$). Microstate occurrence per second was reduced in patients with LBD compared to healthy controls ($p<0.001$) and AD patients ($p=0.003$) with no significant difference between the AD group and healthy controls ($p=0.07$). Thus, including GEV as a covariate did not change the overall significance of the results.

Microstate coverage, i.e. the percentage of time spent within each microstate, was not different between the groups (MANOVA, $F(8,164)=1.79$, $p=0.08$); this was further confirmed with univariate post-hoc analysis which showed that the total time spent in microstate E was slightly reduced in patients with AD compared to controls ($p=0.05$) while there were no other significant differences with respect to microstate coverage (Table 6.10).

Table 6.6. Mean microstate duration [95% confidence intervals] for microstate classes A to E and the three clinical groups, and results from group comparison using univariate ANOVAs and pairwise post-hoc tests. Post-hoc p-values are Bonferroni-corrected for multiple comparisons.

	HC	AD	LBD	ANOVA	post-hoc (p-value)		
					HC-AD	HC-LBD	AD-LBD
mean	64.7 [60.2,69.1]	66.6 [63.0,70.3]	77.0 [74.2,79.9]	F(2,84)=15.5, p<0.001	1.0	<0.001	<0.001
A	56.6 [52.1,61.1]	65.4 [61.7,69.1]	71.0 [68.0,73.9]	F(2,84)=14.2 p<0.001	0.01	<0.001	0.06
B	57.6 [52.9,62.4]	62.3 [58.5,66.2]	71.0 [67.9,74.1]	F(2,84)=12.9 p<0.001	0.38	<0.001	0.003
C	60.8 [56.1,65.4]	66.9 [63.1,70.7]	75.7 [72.7,78.8]	F(2,84)=16.0 p<0.001	0.14	<0.001	0.002
D	64.2 [57.9,70.4]	65.6 [60.5,70.7]	80.1 [76.0,84.2]	F(2,84)=13.9 p<0.001	1.0	<0.001	<0.001
E	67.6 [61.0,74.2]	66.7 [61.3,72.1]	77.2 [72.9,81.5]	F(2,84)=5.7 p=0.005	1.0	0.05	0.01

AD, Alzheimer's disease; ANOVA, analysis of variance; HC, healthy controls; LBD, Lewy body dementia.

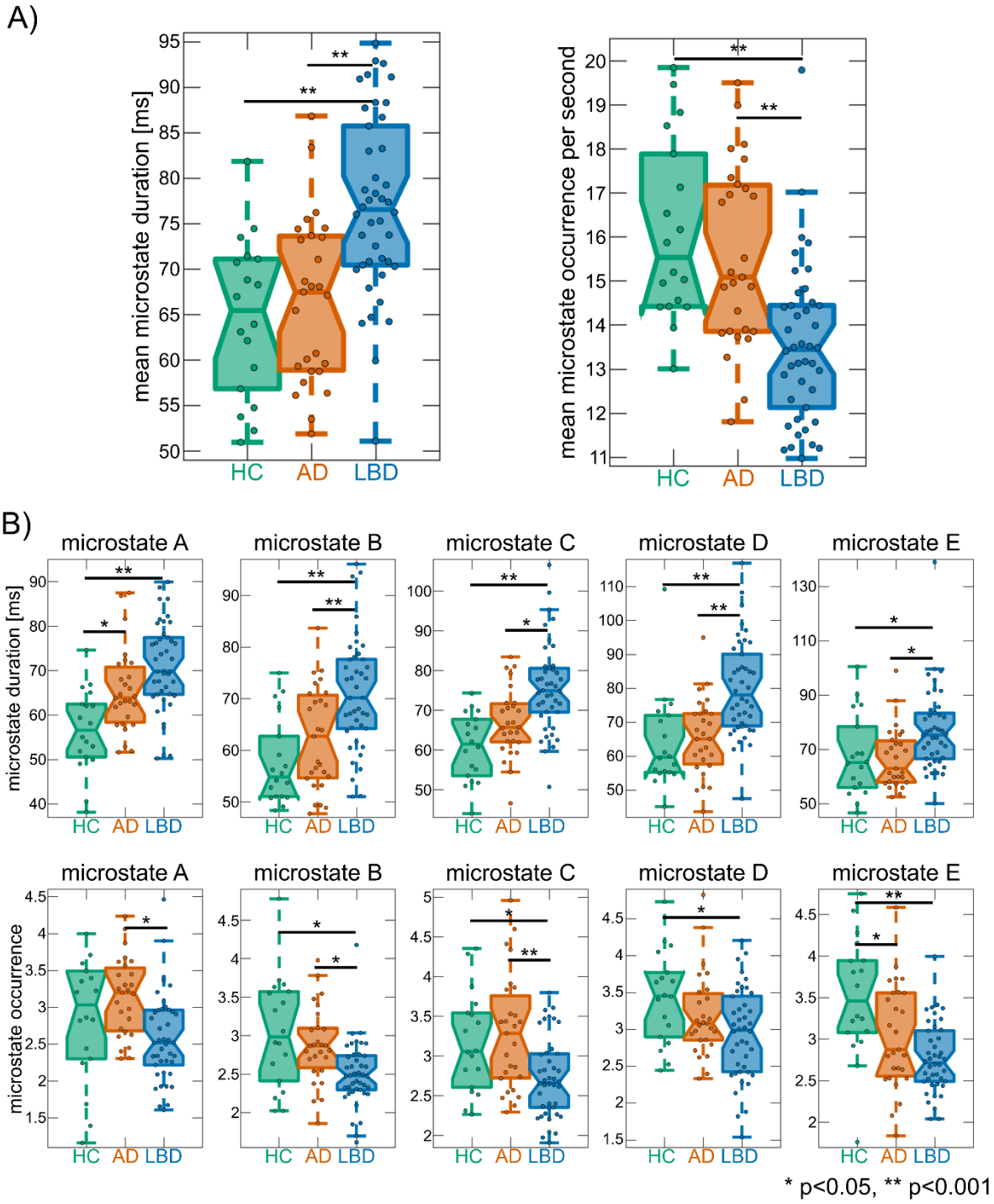

Figure 6.3. Group comparison of microstate duration and occurrence per second A) overall and B) for each microstate class separately. P-values result from pairwise post-hoc tests following univariate ANOVAs and are Bonferroni-corrected. See Tables 6.6 and 6.7 for detailed information on statistics.
AD, Alzheimer's disease; HC, healthy controls; LBD, Lewy body dementia.

Table 6.7. Mean microstate occurrence per second [95% confidence intervals] for microstate classes A to E and the three clinical groups, and results from group comparison using univariate ANOVAs and pairwise post-hoc tests. Post-hoc p-values are Bonferroni-corrected for multiple comparisons.

	HC	AD	LBD	ANOVA	post-hoc (p-value)		
					HC-AD	HC-LBD	AD-LBD
mean	16.1 [15.2,17.0]	15.5 [14.8,16.3]	13.5 [12.9,14.1]	F(2,84)=15.1 p<0.001	0.99	<0.001	<0.001
A	3.0 [2.6,3.3]	3.1 [2.9,3.4]	2.6 [2.4,2.8]	F(2,84)=5.6 p=0.005	1.0	0.17	0.005
B	3.1 [2.8,3.3]	2.9 [2.7,3.1]	2.5 [2.3,2.7]	F(2,84)=8.3 p<0.001	0.87	0.001	0.01
C	3.2 [2.9,3.4]	3.3 [3.1,3.5]	2.7 [2.5,2.9]	F(2,84)=8.2 p<0.001	1.0	0.03	<0.001
D	3.4 [3.1,3.7]	3.2 [3.0,3.4]	3.0 [2.8,3.1]	F(2,84)=4.3 p=0.016	0.58	0.02	0.31
E	3.5 [3.2,3.8]	3.0 [2.8,3.3]	2.8 [2.6,2.9]	F(2,84)=10.8 p<0.001	0.02	<0.001	0.16

AD, Alzheimer's disease; ANOVA, analysis of variance; HC, healthy controls; LBD, Lewy body dementia.

Table 6.8. Mean microstate duration [95% confidence intervals] for microstate classes A to E for matched dementia subgroups (see Section 6.3.1), and results from group comparison using univariate ANOVAs and pairwise post-hoc tests. Post-hoc p-values are Bonferroni-corrected for multiple comparisons.

	HC	AD	LBD	ANOVA	post-hoc (p-value)		
					HC-AD	HC-LBD	AD-LBD
mean	64.7 [60.1,69.2]	65.6 [61.7,69.6]	77.6 [74.4,80.9]	F(2,75)=16.0, p<0.001	1.0	<0.001	<0.001
A	56.6 [52.1,61.1]	64.7 [60.8,68.7]	71.9 [68.7,75.2]	F(2,75)=15.5 p<0.001	0.03	<0.001	0.02
B	57.6 [52.9,62.3]	61.0 [56.9,65.1]	71.6 [68.2,74.9]	F(2,75)=14.4 p<0.001	0.86	<0.001	<0.001
C	60.8 [56.1,65.5]	66.2 [62.1,70.3]	76.4 [73.0,79.7]	F(2,75)=16.6 p<0.001	0.26	<0.001	0.001
D	64.2 [57.7,70.7]	64.7 [59.1,70.3]	79.7 [75.1,84.3]	F(2,75)=11.8 p<0.001	1.0	0.001	<0.001
E	67.6 [60.9,74.3]	65.0 [59.2,70.9]	78.4 [73.6,83.1]	F(2,75)=7.2 p=0.001	1.0	0.03	0.002

AD, Alzheimer's disease; ANOVA, analysis of variance; HC, healthy controls; LBD, Lewy body dementia.

Table 6.9. Mean microstate occurrence per second [95% confidence intervals] for microstate classes A to E for matched dementia subgroups (see Section 6.3.1), and results from group comparison using univariate ANOVAs and pairwise post-hoc tests. Post-hoc p-values are Bonferroni-corrected for multiple comparisons.

	HC	AD	LBD	ANOVA	post-hoc (p-value)		
					HC-AD	HC-LBD	AD-LBD
mean	16.1 [15.2,17.0]	15.8 [15.0,16.6]	13.5 [12.8,14.1]	F(2,75)=15.1 p<0.001	1.0	<0.001	<0.001
A	3.0 [2.6,3.3]	3.2 [2.9,3.5]	2.6 [2.3,2.8]	F(2,75)=4.7 p=0.01	1.0	0.24	0.01
B	3.0 [2.8,3.3]	2.9 [2.7,3.1]	2.5 [2.3,2.7]	F(2,75)=6.9 p=0.002	1.0	0.003	0.03
C	3.1 [2.9,3.5]	3.4 [3.1,3.6]	2.7 [2.5,2.9]	F(2,75)=9.3 p<0.001	0.76	0.04	<0.001
D	3.4 [3.2,3.7]	3.3 [3.0,3.5]	2.9 [2.7,3.1]	F(2,75)=6.1 p=0.004	1.0	0.006	0.05
E	3.5 [3.2,3.8]	3.1 [2.9,3.3]	2.7 [2.6,2.9]	F(2,75)=10.5 p<0.001	0.08	<0.001	0.08

AD, Alzheimer's disease; ANOVA, analysis of variance; HC, healthy controls; LBD, Lewy body dementia.

Table 6.10. Mean microstate coverage [95% confidence intervals] for microstate classes A to E and the three clinical groups, and results from group comparison using univariate ANOVAs and pairwise post-hoc tests. Post-hoc p-values are Bonferroni-corrected for multiple comparisons.

	HC	AD	LBD	ANOVA	post-hoc (p-value)		
					HC-AD	HC-LBD	AD-LBD
A	0.18 [0.15,0.20]	0.20 [0.19,0.22]	0.18 [0.17,0.20]	F(2,84)=2.15 p=0.12	0.20	1.0	0.28
B	0.18 [0.16,0.19]	0.18 [0.16,0.19]	0.18 [0.17,0.19]	F(2,84)=0.04 p=0.96	1.0	1.0	1.0
C	0.19 [0.17,0.21]	0.22 [0.20,0.23]	0.20 [0.19,0.21]	F(2,84)=2.12 p=0.13	0.14	0.99	0.53
D	0.22 [0.20,0.25]	0.21 [0.19,0.23]	0.23 [0.21,0.25]	F(2,84)=1.60 p=0.21	1.0	1.0	0.23
E	0.24 [0.21,0.26]	0.20 [0.18,0.22]	0.21 [0.19,0.23]	F(2,84)=3.09 p=0.051	0.05	0.18	1.0

AD, Alzheimer's disease; ANOVA, analysis of variance; HC, healthy controls; LBD, Lewy body dementia.

6.3.5 Analysis of transition probabilities

The overall randomisation test showed that transition probabilities were non-random in all three groups (controls: p=0.011, AD: p=0.001, LBD: p=0.004). There were, however, no group differences in the transition probabilities between different microstate classes (MANOVA, F(38,134)=1.38, p=0.1) and these were therefore not examined further.

6.3.6 Clinical and behavioural correlations

Figure 6.4 shows results from Spearman's correlations between the Mayo fluctuation scales and mean microstate duration in the DLB patients with FDR-corrected p-values. There was a positive correlation between mean microstate duration and the Mayo total score in the combined LBD group (ρ=0.36, p_{FDR}=0.06) which was mainly driven by the DLB patients (ρ=0.56, p_{FDR}=0.038) and was not present in the PDD group (p>0.1). A similar pattern was observed for the Mayo cognitive subscale whereas correlations were weaker for the Mayo arousal subscale (Figure 6.4 and Table 6.11). There were non-significant trend associations with CAF total score and CAF duration score with mean microstate duration in the DLB group (uncorrected $p \leq 0.10$).

The correlation between mean microstate duration and Mayo total score persisted when including LEDD as a covariate (ρ=0.36, p=0.02).

There were no significant correlations between other clinical scores and mean microstate duration in LBD (all uncorrected p>0.05). In the AD group, there was a significant negative correlation between mean microstate duration and CAMCOG (ρ=0.56, p=0.03); however, this correlation did not survive FDR-correction for multiple comparisons.

Eighteen HC, 23 AD, and 33 LBD (21 DLB and 12 PDD) participants were included in both the microstates and the ex-Gaussian analysis described in Chapter 3. Across these participants, mean microstate duration was positively correlated with mu (ρ=0.43, p=0.0002) and sigma (ρ=0.39, p=0.0006), but not with tau (ρ=0.12, p=0.32), see Figure 6.5. These correlations, however, did not persist when clinical diagnosis (HC, AD, LBD) was added as a covariate (mu: ρ=0.18, p=0.12; sigma: ρ=0.20, p=0.09; tau: ρ=-0.12, p=0.31).

Table 6.11. Spearman's correlation between mean microstate duration and Mayo fluctuation scores in the combined LBD group and in DLB and PDD separately.

	LBD	DLB	PDD
Mayo total	ρ=0.36 (p=0.023, p_{FDR}=0.06)	ρ=0.56 (p=0.004, p_{FDR}=0.04)	ρ=0.07 (p=0.79, p_{FDR}=0.88)
Mayo cognitive	ρ=0.33 (p=0.035, p_{FDR}=0.06)	ρ=0.51 (p=0.012, p_{FDR}=0.05)	ρ=0.17 (p=0.54, p_{FDR}=0.69)
Mayo arousal	ρ=0.27 (p=0.10, p_{FDR}=0.14)	ρ=0.45 (p=0.027, p_{FDR}=0.06)	ρ=0.04 (p=0.88, p_{FDR}=0.88)

DLB, Dementia with Lewy bodies; FDR, false discovery rate; Mayo total, Mayo Fluctuations Scale; Mayo cognitive, Mayo Fluctuation cognitive subscale; Mayo arousal, Mayo Fluctuations arousal subscale; PDD, Parkinson's disease dementia.

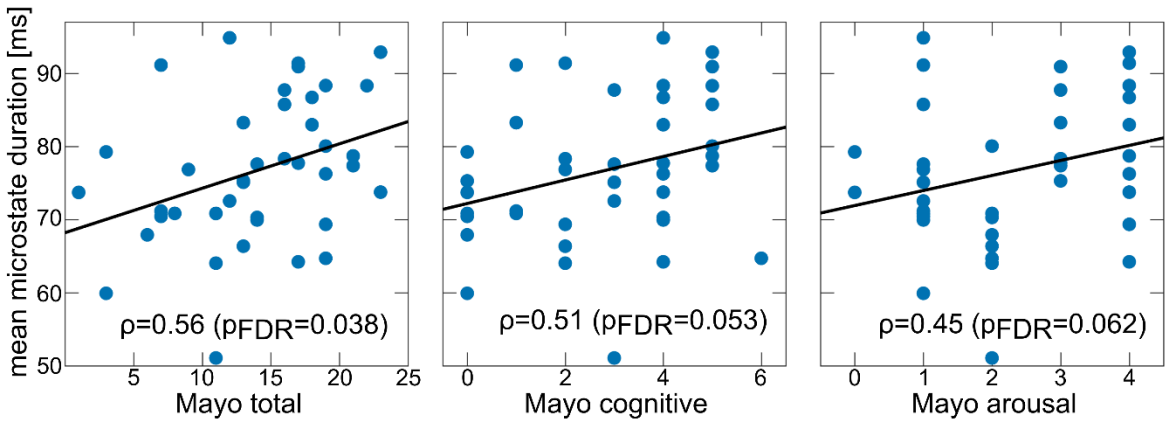

Figure 6.4. Spearman's correlations between mean microstate duration and Mayo fluctuation scores in the DLB group. P-values are FDR-corrected for multiple comparisons (see Table 6.11).
FDR, false discovery rate; Mayo arousal, Mayo Fluctuations arousal subscale; Mayo total, Mayo Fluctuations Scale; Mayo cognitive, Mayo Fluctuation cognitive subscale.

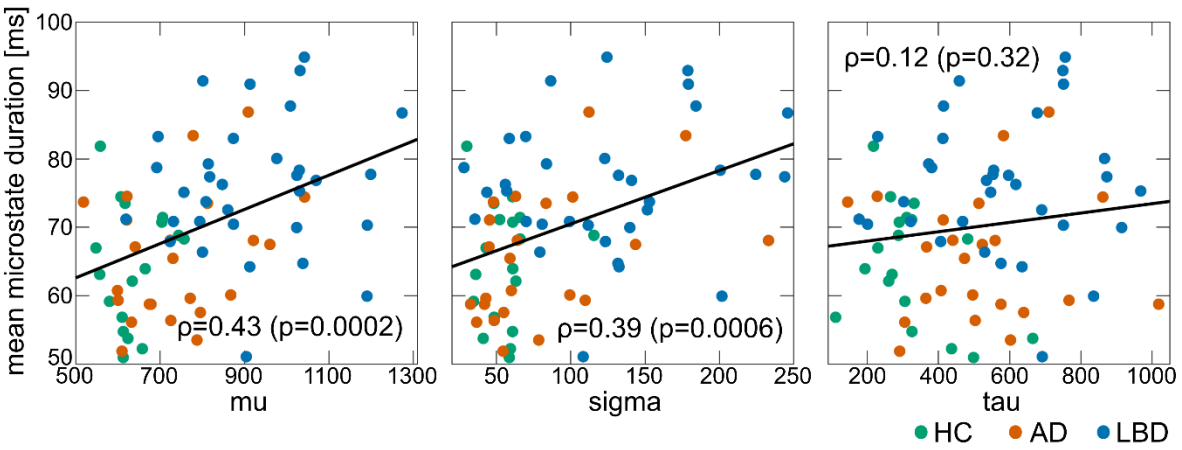

Figure 6.5. Spearman's correlations between mean microstate duration and the three ex-Gaussian parameters (see Chapter 3) across all participants.
AD, Alzheimer' disease; HC, healthy controls; LBD, Lewy body dementia.

6.3.7 Effect of dopaminergic medication in the LBD group

There were no significant differences between LBD patients who were taking dopaminergic medication compared to those who were not on these medications (Table 6.12). Furthermore, there was no significant correlation between LEDD and mean microstate duration (Pearson's r=0.02, p=0.92) as well as mean microstate occurrence per second (Pearson's r=-0.01, p=0.94).

Table 6.12. Mean [95% confidence interval] of microstate duration and microstate occurrence per second comparing LBD patients who were not on dopaminergic medication (no PD meds, N=13) to those LBD patients who were taking dopaminergic medication (PD meds, N=29) and group comparison using two-sample t-tests.

	LBD, no PD meds	LBD, PD meds	t-test
duration			
mean	80.3 [75.1,85.6]	75.6 [71.7,79.5]	t(40)=1.5, p=0.16
A	72.9 [66.9,78.9]	70.1 [66.3,73.9]	t(40)=0.83, p=0.41
B	73.2 [67.3,79.0]	70.0 [65.7,74.3]	t(40)=0.88, p=0.38
C	79.6 [74.1,85.0]	74.0 [69.5,78.5]	t(40)=1.5, p=0.14
D	82.1 [72.7,91.6]	79.1 [74.0,84.3]	t(40)=0.63, p=0.53
E	81.9 [70.2,93.5]	75.1 [70.2,80.1]	t(40)=1.3, p=0.19
occurrence			
mean	12.9 [12.2,13.7]	13.8 [13.0,14.5]	t(40)=1.4, p=0.16
A	2.5 [2.1,2.8]	2.6 [2.4,2.9]	t(40)=0.91, p=0.37
B	2.3 [2.2,2.5]	2.6 [2.4,2.8]	t(40)=1.7, p=0.10
C	2.6 [2.3,2.8]	2.8 [2.6,3.0]	t(40)=1.3, p=0.19
D	2.9 [2.6,3.1]	3.0 [2.7,3.2]	t(40)=0.46, p=0.65
E	2.7 [2.4,3.0]	2.8 [2.6,3.0]	t(40)=0.84, p=0.41

LBD, Lewy body dementia; PD meds, dopaminergic medication.

6.3.8 Relation between dynamic connectivity and microstate duration

In the LBD group, mean variability of connectivity between the basal ganglia network and all other networks was negatively related to mean microstate duration (r=-0.53, p=0.003, Figure 6.6A). When considering each connection separately, there were six networks whose dynamic interaction with the basal ganglia network was negatively correlated with mean microstate duration: two motor networks (right motor network and medial sensorimotor network), three visual networks (medial visual network, superior visual network, and lingual gyrus network) and the default mode network 2 (all $p<0.05$, uncorrected, see Table 6.13). After correcting for multiple comparisons, the dynamic interaction between the basal ganglia network and the medial visual network was still significantly correlated with mean microstate duration.
For the thalamic network, overall dynamic connectivity was also negatively related to mean microstate duration (r=-0.38, p=0.044, Figure 6.6B). When considering each connection separately, there were four networks whose dynamic interaction with the thalamic network was negatively correlated with mean microstate duration: the insular network 2, the lateral sensorimotor network, the occipital pole network, and the cerebellar network 2 (all $p<0.05$, uncorrected, see Table 6.14). After correcting for multiple comparisons, the dynamic interaction between the thalamic network and the lateral sensorimotor network was still significantly correlated with mean microstate duration.

Figure 6.7 shows correlations between overall dynamic connectivity of basal ganglia and thalamic networks in healthy controls and patients with AD, none of which were significant.

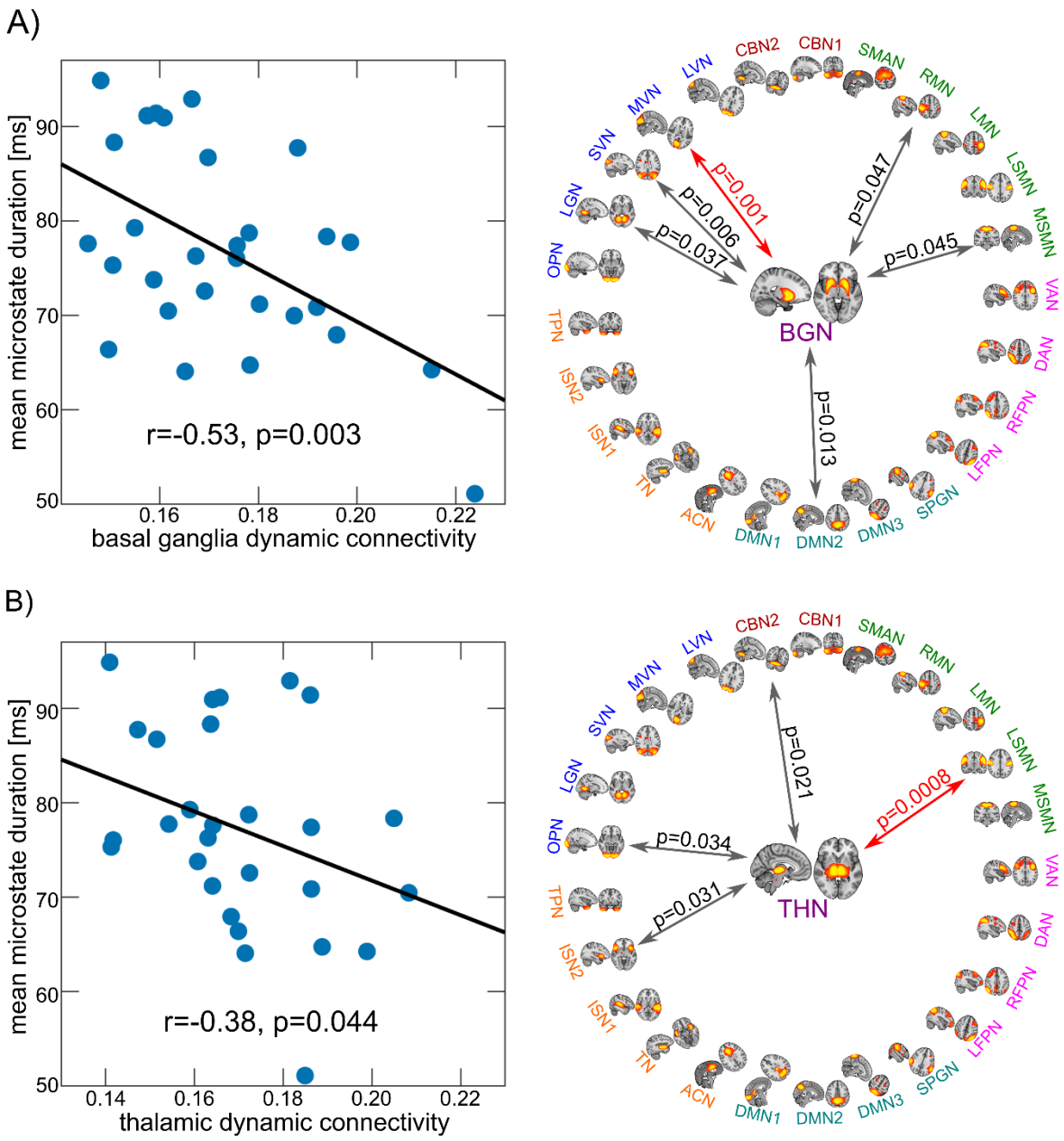

Figure 6.6. Results from Pearson's correlation analysis between mean microstate duration and dynamic functional connectivity of A) the basal ganglia network and B) the thalamic network in the LBD group. The panels on the right show results from correlating mean microstate duration with each individual network connection. Grey arrows indicate significant correlations at an uncorrected threshold of $p<0.05$ and red arrows indicate connections that survive Bonferroni correction for multiple comparisons (all significant correlations were negative). All correlation coefficients and corresponding p-values are shown in Tables 6.13 and 6.14. All network names and locations can be found in Table 4.1 in Chapter 4.

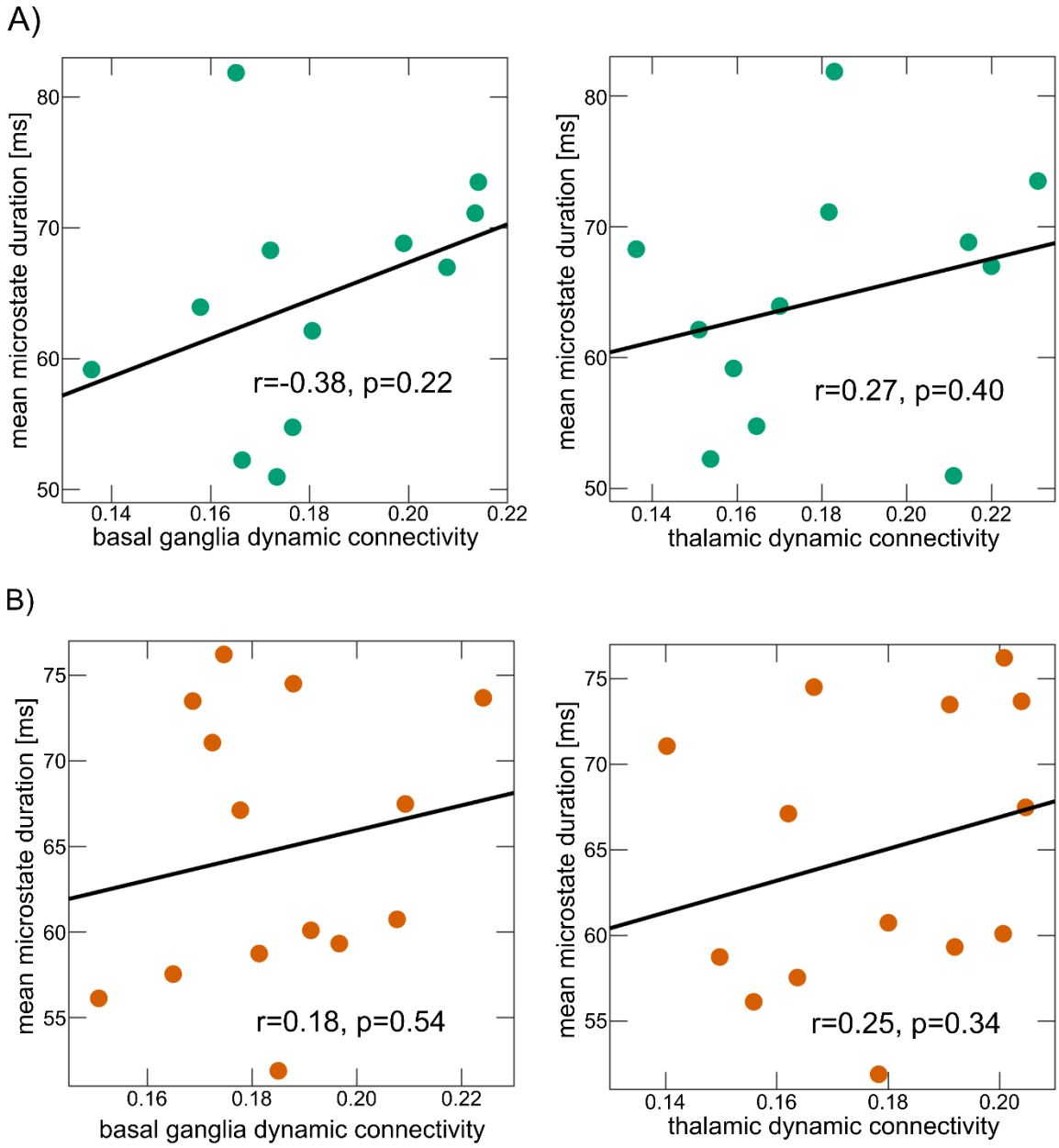

Figure 6.7. Results from Pearson's correlation analysis between mean microstate duration and mean dynamic functional connectivity of basal ganglia and thalamic networks in A) healthy controls and B) AD.

Table 6.13. Pearson's correlation coefficients and p-values from correlation between mean microstate duration and basal ganglia network dynamic connectivity for each network separately in the LBD group.

Network name	r	$p_{uncorrected}$	p_{FDR}
medial visual network	-0.57	0.001	0.029
superior visual network	-0.50	0.006	0.07
default mode network 2	-0.46	0.013	0.11
lingual gyrus network	-0.39	0.037	0.18
medial sensorimotor network	-0.38	0.045	0.18
right motor network	-0.37	0.047	0.18
ventral attention network	-0.36	0.058	0.18
right fronto-parietal network	-0.35	0.059	0.18
dorsal attention network	-0.31	0.10	0.23
cerebellar network 1	-0.31	0.10	0.23
insular network 1	-0.30	0.11	0.23
default mode network 1	-0.30	0.12	0.23
supplementary motor area network	-0.30	0.12	0.23
insular network 2	-0.24	0.20	0.34
left fronto-parietal network	-0.24	0.21	0.34
occipital pole network	-0.24	0.22	0.34
cerebellar network 2	-0.22	0.26	0.39
anterior cingulate network	0.19	0.32	0.45
default mode network 3	0.13	0.49	0.65
temporal pole network	-0.11	0.56	0.70
lateral sensorimotor network	0.05	0.79	0.90
lateral visual network	0.05	0.79	0.90
temporal network	0.04	0.84	0.91
supramarginal gyrus network	-0.02	0.90	0.94
left motor network	0.002	0.99	0.99

FDR, false discovery rate.

Table 6.14. Pearson's correlation coefficients and p-values from correlation between mean microstate duration and thalamic network dynamic connectivity for each network separately in the LBD group.

Network name	r	$p_{uncorrected}$	p_{FDR}
lateral sensorimotor network	-0.59	0.0008	0.019
cerebellar network 2	-0.43	0.021	0.22
insular network 2	-0.40	0.031	0.22
occipital pole network	-0.39	0.034	0.22
ventral attention network	-0.31	0.10	0.51
cerebellar network 1	-0.26	0.17	0.58
supramarginal gyrus network	-0.25	0.20	0.58
lateral visual network	-0.24	0.21	0.58
right motor network	-0.24	0.22	0.58
insular network 1	-0.23	0.23	0.58
supplementary motor area network	-0.19	0.32	0.73
medial sensorimotor network	-0.18	0.35	0.73
left fronto-parietal network	-0.15	0.44	0.85
default mode network 3	-0.12	0.52	0.94
anterior cingulate network	-0.08	0.69	0.98
left motor network	-0.07	0.70	0.98
default mode network 1	0.05	0.78	0.98
default mode network 2	-0.05	0.80	0.98
medial visual network	0.04	0.82	0.98
temporal pole network	-0.04	0.84	0.98
lingual gyrus network	-0.02	0.90	0.98
right fronto-parietal network	-0.02	0.93	0.98
dorsal attention network	-0.01	0.96	0.98
temporal network	0.01	0.96	0.98
superior visual network	0.005	0.98	0.98

FDR, false discovery rate.

6.4 Discussion

In this chapter, I investigated changes in brain dynamics in patients with LBD compared to healthy ageing and AD patients using an EEG microstate analysis to assess temporal characteristics of brain activity on a sub-second timescale and the relation between microstate dynamics and large-scale fMRI network dynamics within the cortical-basal ganglia-thalamic loop.

6.4.1 Microstate dynamics

There was a marked and generalised slowing of microstate dynamics in patients with LBD compared to both healthy controls and AD patients while temporal microstate characteristics in patients with AD were largely comparable to healthy control levels. Patients with LBD stayed in the same microstate class for longer consecutive periods of time and switched less

frequently between different states than healthy controls and AD patients. This was not specific to a certain microstate class as reported for other diseases (Kikuchi et al., 2011; Koenig et al., 1999; Nishida et al., 2013), but rather a general pattern observed for all classes which suggests that general microstate timing mechanisms are affected in LBD.

The observed slowing of microstate dynamics in the LBD group indicates a relative loss of resting-state brain variability compared to healthy ageing and AD patients and is in line with the observation of a loss of brain network flexibility in DLB as evidenced by the dynamic fMRI network analysis in Chapter 5. The importance of variability in the brain has been confirmed in many studies (see Garrett et al. (2013b) for a review) relating less variability to ageing (Grady and Garrett, 2018; Guitart-Masip et al., 2016) and poorer performance on various cognitive tests (Jia et al., 2014; McIntosh et al., 2008). Reduced microstate dynamics in LBD could therefore be an indicator of less flexible, and ineffective, brain functioning.

Apart from being an indicator of brain variability at rest, microstates show elaborate dynamic properties that are important for optimal brain functioning. In the healthy brain, microstate sequences have been shown to exhibit scale-free or fractal dynamics, i.e. the microstate time course is statistically self-similar across multiple timescales (Van De Ville et al., 2010). The observation of scale-free properties in a dynamic system indicates that the system operates near a point of criticality, fluctuating around a phase transition (Hesse and Gross, 2014; Tagliazucchi et al., 2012a). This state makes the system optimally adaptable enabling it to respond to incoming information and unpredictable stimuli by providing a self-organising mechanism and preventing the emergence of excessive periodicity at the same time (Goldberger et al., 2002). The extent of scale-free dynamics can also be used as an indicator of a system's dynamic complexity with a reduction in fractal dimension indicating a loss of system complexity (Zappasodi et al., 2014). In the context of microstate sequences, it was shown that scale-free properties are preserved when the temporal sequence of the microstate labels is randomised, whereas these long-range dependencies are lost when equalising microstate duration (Van De Ville et al., 2010). This shows that the exact sequence of microstate classes is not crucial, but rather their duration seems to be the key parameter for the emergence of scale-free dynamics and thus optimal network properties. The observed abnormalities in microstate timing in LBD could therefore have significant consequences for the functioning of the whole brain network: disturbing its intricate fractal dynamics results in a less complex system that loses its adaptability and lacks flexibility when responding to external environmental stimuli.

6.4.2 Clinical and behavioural relevance of microstate dynamics in LBD

In line with this hypothesis, there was a correlation between the severity of cognitive fluctuations and temporal microstate abnormalities in the DLB group, suggesting that more severe cognitive fluctuations are related to a greater slowing of microstate dynamics; this relationship was stronger for the cognitive/attentional dimensions of cognitive fluctuations as opposed to arousal or alertness (Bliwise et al., 2014). Additionally, microstate dynamics were found to be largely intact in an AD group of comparable dementia severity. This indicates that the alterations in dynamic properties in LBD might drive the brain network away from the point of criticality that is important for healthy cognitive functioning towards a state that allows for the emergence of cognitive symptoms that are specific to LBD such as fluctuating cognition (Ferman et al., 2004). However, the relationship between microstate dynamics and the severity of cognitive fluctuations was specific to the DLB group and was not observed in the PDD patients. This might suggest a different aetiology of cognitive fluctuations in PDD patients even though clinically they present very similarly to DLB (Ballard et al., 2002a; Varanese et al., 2010). Some of this may also relate to difficulties in assessing fluctuating cognition in patients with more advanced PD due to the confounding presence of motor fluctuations or the more significant levodopa load in these patients, although notably, in this investigation there was no association between LEDD and any of the microstate metrics. Furthermore, there was a relation between mean microstate duration and behavioural measures across all participants showing that slower microstate dynamics were associated with slower and less consistent RT performance on the attention task described in Chapter 3. This provides further evidence for the behavioural significance of brain dynamics in LBD and confirms previous studies showing a relationship between fMRI dynamics and RT performance (McIntosh et al., 2008). The present results indicate that this relationship also persists when considering dynamics on a faster timescale as measured by EEG. However, it has to be noted that the correlations were greatly attenuated when considering clinical diagnosis as a covariate, indicating that they were influenced by group differences in microstate duration and behavioural measures.

6.4.3 Microstate dynamics in AD

The observation of largely preserved microstate dynamics in patients with AD agrees with two previous studies that similarly reported no differences between AD patients and age-matched controls in terms of the microstates' temporal characteristics (Grieder et al., 2016; Nishida et al., 2013). In contrast to the present results, Nishida et al. (2013) found that transition probabilities in AD patients showed a pattern that was compatible with random

transitions. AD patients in this previous study showed a comparable level of cognitive impairment to the patients described here. However, patients in the Nishida et al. study were not taking any cholinergic medications whereas the large majority of patients in the present study were on acetylcholinesterase inhibitors which have been shown to alter resting-state EEG characteristics in AD (Babiloni et al., 2013) and might thus be an explanation for the different results.

An alteration in the topographical structure of the microstates was only observed in the AD group while topographies in patients with LBD did not differ significantly from healthy controls. This highlights again that it is primarily microstate dynamics that seem to be affected by LBD. In contrast, the change in microstate topographies in the AD patients might be due to the greater structural abnormalities in this condition compared to LBD (Mak et al., 2015b, 2015a).

6.4.4 Relation to previous EEG findings in LBD

With respect to previous EEG studies in LBD, a general slowing of oscillatory EEG activity as evidenced by a slowing of the dominant frequency is a well-established finding (Bonanni et al., 2016; Cromarty et al., 2015; Peraza et al., 2018; Stylianou et al., 2018) and thus it could be argued that this global change is driving the observed group differences in microstate dynamics. However, when testing the correlation between dominant frequency and mean microstate duration in the LBD group, there was only a weak negative correlation which was not statistically significant (Pearson's $r=-0.25$, $p=0.11$) (see Peraza et al. (2018) for the estimation of dominant frequency). This indicates that while generalised EEG slowing might partially contribute to microstate slowing, it does not fully explain the relative loss of microstate dynamics in LBD. In contrast, the number of GFP peaks per second was positively correlated with dominant frequency in the LBD group ($\rho=0.41$, $p=0.007$), indicating that the group differences in the number of GFP peaks per second were influenced by differences in dominant frequency between the groups (Lehmann et al., 1987; Peraza et al., 2018). However, I showed that the results can be replicated when fitting the microstates on all data instead of the GFP peaks, further indicating that the well-established finding of EEG slowing in LBD is not equivalent to the slowing of microstate dynamics that is described here.

6.4.5 Origins of microstate disturbances in LBD

Even though previous studies have found a link between the rapidly changing EEG microstate sequences and slower changes of the fMRI signal (Britz et al., 2010; Custo et al., 2017; Musso et al., 2010), it remains largely unknown which processes in the brain might be

responsible for the emergence of the precise microstate timing and hence their complex dynamic properties (Michel and Koenig, 2017). In the present analysis, there was an association between less dynamic connectivity between basal ganglia and thalamic networks with large-scale cortical networks and a loss of microstate dynamics in the LBD group. These findings provide, for the first time, evidence to suggest that the dynamic interaction within the cortical-basal ganglia-thalamic loop plays a part in the modulation of global microstate dynamics. This is relevant from a LBD perspective as thalamic and basal ganglia dysfunction is a hallmark of Lewy body diseases (Delli Pizzi et al., 2015a, 2015b; McKeith et al., 2007; Pimlott et al., 2006; Watson et al., 2017). The results therefore support the conjecture that key subcortical abnormalities have broader impacts on the overall functioning of the whole-brain network in LBD. I speculate that structural and functional changes within subcortical structures associated with Lewy body disease contribute to an impairment in the dynamic interaction between these subcortical and large-scale cortical networks. This in turn might lead to the loss of crucial dynamic properties and hence a reduction in brain adaptability and efficiency as described above. Additionally, these results provide a possible explanation for how strategic pathology in subcortical structures in LBD can have more widespread impact on cognitive functions and symptom manifestation, especially with respect to cognitive fluctuations (Delli Pizzi et al., 2015b).

Apart from being relevant to our understanding of brain abnormalities in LBD patients, the present study might also help to further our more general understanding of microstate dynamics by providing a first hint at how dynamic microstate properties might be modulated by subcortical-cortical dynamics. This has wider implications for a better mechanistic understanding of other diseases that are characterised by microstate abnormalities such as schizophrenia and depression (Koenig et al., 1999; Lehmann et al., 2005; Strik et al., 1995).

6.4.6 Limitations

As discussed in previous chapters, most patients were taking medication that might have influenced their fMRI and EEG signals (Babiloni et al., 2013; Szewczyk-Krolikowski et al., 2014). Similar to previous chapters, dopaminergic medication did not seem to have an effect on microstate temporal characteristics whereas an analysis of the effect of acetylcholinesterase inhibitors was prevented by the small number of patients not taking these medications. More broadly this is relevant to the analyses presented in this chapter, given *a priori* evidence demonstrating a relationship between disruption of the cholinergic system and cognitive fluctuations (Ballard et al., 2002b; Colloby et al., 2017; Pimlott et al., 2006) as well as remediation of this symptom with acetylcholinesterase inhibitor treatment in LBD (Onofrj

et al., 2003). The intimate role of cholinergic efferents, for example from the pedunculopontine nucleus, in regulating cortico-thalamic outflow may therefore be apposite in shaping microstate dynamics and contribute to these observations. Further work will be required to unpick this conjecture.

In addition, I used non-concurrent EEG-fMRI recordings in this analysis and thus it is only possible to draw limited conclusions with respect to a causal influence of network dynamics on microstate characteristics. While the present results provide an indication of a link between fMRI and EEG dynamics, studying concurrent EEG-fMRI data in the future will allow us to draw more concrete conclusions, especially with respect to the causal relation between microstate characteristics and large-scale network dynamics.

6.4.7 Conclusion

There was a profound slowing of microstate dynamics in LBD patients which clearly distinguished this form of dementia from AD and healthy ageing and which was related to the severity of cognitive fluctuations in the DLB patients. Disturbances to the precise timing of microstate sequences in LBD may lead to a breakdown of the fractal properties of the brain system therefore causing a loss of complexity and adaptability of the brain network that is crucial for its healthy functioning and which may in turn be related to the emergence of transient clinical symptoms such as cognitive fluctuations and impairment in attentional processing. Additionally, by using LBD as a probe pathology, I found a potential link between large-scale network fluctuations and microstate dynamics, suggesting that dynamic interactions within the cortical-basal ganglia-thalamic loop might play a role in the modulation of EEG dynamics.

Chapter 7. Conclusions and Future Directions

The objective of this thesis was to combine clinical, behavioural, neuroimaging, and electrophysiological data to study how dynamic properties of the brain are differentially affected by AD and LBD and how abnormalities in brain dynamics relate to the cognitive phenotype of LBD, in particular with respect to attentional impairment and cognitive fluctuations.

7.1 Summary of Main Findings

7.1.1 Analysis of behavioural data

Both dementia groups showed slower overall mean RTs than healthy controls, with additional slowing in LBD relative to AD. In AD, this RT slowing was related to a reduction in grey matter volume in occipital regions while the more pronounced behavioural deficits in LBD did not seem to be related to brain structural changes. This implies that either there were more specific structural deficits in LBD or that, in the main, deficits are driven by functional changes, for example in major neurotransmitter systems such as the cholinergic.

There was a significant alerting effect in controls which was absent in the dementia groups. This inability of the dementia patients to benefit from the cueing effect is indicative of reduced efficiency of the alerting system in dementia irrespective of dementia type. In LBD, this finding fits with the idea of an association between alerting efficiency and deficiency of the noradrenergic system (Coull et al., 2001; Raz, 2004). In AD, however, this result contradicts previous findings of maintained alerting efficiency in this group (Fernandez-Duque and Black, 2006). Given that previous studies included less impaired dementia patients, the absent alerting effect in the present analysis may suggest that there is a loss of the facilitating cue effect with dementia progression.

The size of the orienting effect did not differ between AD and controls which agrees with previous studies that indicated a preservation of orienting efficiency in AD (Fernandez-Duque and Black, 2006). In LBD, there was a slight impairment in orienting efficiency which was expected given that the orienting aspect of the attention system is thought to be influenced by the basal forebrain cholinergic system which is markedly affected in LBD (Clerici et al., 2007; Colloby et al., 2017; Grothe et al., 2014). The present study shows that this impairment might also be related to a reduction in white matter volume in occipital regions.

The executive conflict effect was greater in both dementia groups compared to controls, i.e. both dementia groups showed an inability to resolve conflict amongst responses which is indicative of impaired executive function. This replicates previous findings in AD

(Fernandez-Duque and Black, 2006) and is in line with executive dysfunction in LBD (Noe et al., 2004) that might be related to degenerations within the dopaminergic system (Fan et al., 2005; Kehagia et al., 2012). The relative absence of strong correlations between executive dysfunction and brain atrophy in both AD and LBD suggests that executive impairment in the dementia groups might be more related to functional rather than macrostructural pathophysiological changes.

In the ex-Gaussian distributional analysis it became evident that both dementia groups showed an increase in the right tail of the distribution which represents extremely slow responses that can be seen as temporary lapses in attention. While there was no difference between AD and controls with respect to mean and variability of the Gaussian part of the RT distribution, both parameters were significantly increased in LBD patients, indicating a general slowing and higher trial-to-trial variability in LBD than in controls and AD. In AD, these finding are in agreement with previous studies in preclinical (Balota et al., 2010) and early-stage patients (Jackson et al., 2012; Tse et al., 2010), and the present results indicate that the same pattern seems to persist in patients at a mild to moderate stage of the disease. However, contrary to my hypothesis there was no further increase in LBD compared to AD with respect to the number of attentional lapses, and this parameter was not related to cognitive fluctuations in LBD, indicating that it is not suitable to capture cognitive fluctuations in LBD.

There were widespread correlations between mean and variability of the Gaussian part and grey matter loss in AD, but not in LBD. Overall, the ex-Gaussian analysis showed that different aspects of RT performance are differentially affected by AD and LBD, with a difference in structural neural correlates underlying the observed behavioural deficits. While impaired attentional performance is linked to brain atrophy in AD, in LBD it does not seem to be strongly related to macrostructural changes.

7.1.2 Static and dynamic functional connectivity analysis

Within-network functional connectivity was generally decreased in DLB compared to healthy controls, mainly in motor, temporal, and frontal networks. Decreased connectivity in motor structures corresponded well with the clinical manifestation of DLB and agrees with previous studies in DLB and PD (Peraza et al., 2016, 2014; Rolinski et al., 2015; Szewczyk-Krolikowski et al., 2014; Taylor et al., 2013). Reduction in connectivity in non-motor networks was mainly found in temporal and frontal regions which agrees with previous studies in DLB (Peraza et al., 2014; Taylor et al., 2012) and emphasises the role of abnormalities within the ACC in DLB.

With respect to DMN connectivity, the present analysis replicates previous studies in AD showing markedly reduced connectivity in patients with AD compared to controls (Binnewijzend et al., 2012; Greicius et al., 2004). In contrast, the relative sparing of the DMN in patients with DLB indicates that the finding of DMN hypoactivity is specific to AD and is not present in DLB (Franciotti et al., 2013; Peraza et al., 2014).

Long-range connections between different networks were mainly intact in patients with DLB compared to controls; only the connection between a frontal and a temporal network showed increased connectivity in DLB, indicating that temporal/frontal regions are affected in this condition. Overall, differences in functional connectivity between AD and DLB were subtle, suggesting that AD and DLB may show more similarities than differences with respect to static functional connectivity in patients with mild to moderate disease when motion artefacts are adequately controlled. The lack of significant correlations between static connectivity measures and clinical scores indicates that the observed reduced connectivity within these networks might be related to the presence, but not to the severity of motor and cognitive impairment in DLB patients.

When considering changes in functional connectivity over time, it was observed that AD and DLB patients spent more time than controls in sparse connectivity configurations with an absence of strong positive and negative connections and a relative isolation of motor networks from other networks. In contrast, they switched less often into states of high inter-network connectivity. This indicates transiently reduced functional connectivity in both dementia groups and an inability to temporarily switch out of states of low connectivity into more highly and specifically connected network configurations. The fact that this was observed in both AD and DLB indicates that this might be related to the presence of dementia in general rather than any symptom that is more specific to either dementia group. Additionally, the variability of global brain network efficiency was reduced in patients with DLB compared to controls which was not observed in the AD group. The dynamic and flexible engaging and disengaging of different brain regions has been shown to be important for efficient communication within the brain network (Zalesky et al., 2014) and brain variability is important for optimal cognitive performance (Jia et al., 2014). The relative loss of global efficiency variability that was found in the DLB group might thus indicate the presence of an abnormally rigid brain network and the lack of economical dynamics, factors which could contribute to cognitive slowing (Firbank et al., 2018) and an inability to respond appropriately to situational demands.

7.1.3 Dynamic EEG microstate analysis

Microstate duration was increased in LBD for all microstate classes compared to AD and healthy controls with a corresponding reduction in the number of distinct microstates per second, indicating that microstate sequences in LBD are less dynamic over time. In contrast, microstate dynamics in AD were largely comparable to healthy levels, albeit with altered microstate topographies. Given the importance of brain dynamics for healthy cognitive functioning (Jia et al., 2014; McIntosh et al., 2008), the reduced microstate dynamics in LBD could be an indicator of less flexible and ineffective brain functioning. Additionally, it has been shown that microstate sequences exhibit important dynamic properties which can be lost when their intricate temporal structure is destroyed (Van De Ville et al., 2010). The observed abnormalities in microstate timing in LBD could therefore have significant consequences for the functioning of the whole brain network: disturbing its intricate dynamics may result in a less complex system that loses its adaptability and is less responsive to environmental demands, which might give rise to the apparent slowing in thinking and intermittent confusion which typify LBD. This is supported by the finding that a slowing of microstate dynamics was related to more severe cognitive fluctuations in the DLB group as well as to RT slowing and increased inter-trial variability across all participants as measured by the ex-Gaussian analysis, providing evidence for the clinical and behavioural relevance of microstate dynamics in LBD. In the LBD group, mean microstate duration was negatively correlated with fMRI dynamic functional connectivity between the basal ganglia and thalamic networks and large-scale cortical networks, suggesting that dynamic interactions within the cortical-basal ganglia-thalamic loop may play a role in the modulation of EEG dynamics. The results therefore support the conjecture that key subcortical abnormalities may have broader impacts on the overall functioning of the whole-brain network in LBD.

7.2 Strengths

This thesis used clinical, behavioural, imaging, and electrophysiological data from a large group of well-characterised dementia patients and healthy controls by integrating data from several previous studies. Therefore, a particular strength of this work is its multimodal approach: Combining different data modalities allows to make use of specific advantages of each modality. While fMRI has high spatial resolution at the expense of relatively poor temporal resolution, the opposite is true for EEG. This makes the combination of both neuroimaging methods especially suitable for studying spatial as well as temporal aspects of brain function across different timescales. The confirmation of findings across different modalities and analyses strategies strengthens the robustness and reliability of the results and

makes it more likely that these are actual disease-related effects rather than artefacts specific to the type of data or analysis technique that was used.

A strength of the fMRI analyses presented in this thesis is the application of rigorous motion correction techniques prior to the estimation of static and dynamic functional connectivity measures. It has recently been shown that motion can have a great influence on fMRI measures, in particular with respect to (dynamic) connectivity measures (Power et al., 2012) and new methods providing much more stringent control of motion artefacts have been developed (Ciric et al., 2017). While previous studies in DLB have relied on rather weak motion correction techniques, it has been shown that motion artefacts can mimic group differences in fMRI studies (Parkes et al., 2018; Power et al., 2015). Control of these confounds is therefore especially important when analysing differences between clinical groups (van Dijk et al., 2012) and insufficient control of motion artefacts in previous studies might partly explain why functional connectivity findings in DLB are inconsistent. The present study is therefore a first step towards more robust estimation of functional connectivity in LBD. Furthermore, the use of an independent healthy control group in conjunction with meta ICA for RSN estimation allowed to study the effect of DLB and AD on robustly estimated healthy networks instead of studying RSNs estimated from an average of all participants as commonly done in previous studies (Lowther et al., 2014; Peraza et al., 2014). The current approach has also been shown to be more sensitive for finding functional connectivity differences between clinical groups (Griffanti et al., 2016).

The EEG microstate analysis presented here provides a novel approach for studying EEG data that has not been applied to LBD before despite a large body of literature on EEG abnormalities in LBD (Cromarty et al., 2015). Microstates offer a conceptually simple, yet powerful tool to study brain dynamics on a sub-second timescale, they show high test-retest reliability, and can be reliably estimated from a short resting-state EEG recording with as few as eight electrodes (Khanna et al., 2014), which supports their potential use as biomarkers in clinical settings.

Furthermore, combining EEG and fMRI data and using LBD as a probe pathology meant that it was possible to identify a potential link between the dynamic interaction of subcortical and cortical networks and the modulation of the cortical EEG signal. These results do not only provide a better understanding of LBD-related changes in dynamic brain processes, but might have wider implications for other diseases that are characterised by microstate abnormalities such as schizophrenia and depression (Koenig et al., 1999; Lehmann et al., 2005; Strik et al., 1995).

7.3 Limitations

A limitation that this study shares with all ante-mortem dementia studies is that diagnoses were based on clinical assessment rather than pathological confirmation. However, while a definite LBD/AD diagnosis cannot be obtained without post-mortem examination, it has been shown that the standardised clinical criteria used here show high specificity when validated against autopsy findings (McKeith et al., 2000a). In the future, as pathological information becomes available for more participants, it will be important to see how the results hold up and to investigate specific characteristics of mixed AD/DLB cases if possible.

As mentioned in the individual chapters, a further potential limitation is that some of the DLB and PDD patients were on dopaminergic medication and scanned in the ON motor state which might have influenced their functional connectivity and EEG measures (Szewczyk-Krolikowski et al., 2014). However, it has been shown that dopaminergic medication tends to normalise the signals towards more healthy levels (Szewczyk-Krolikowski et al., 2014; Tahmasian et al., 2015), which implies that the group differences that are reported here were not due to medication. Additionally, an analysis of the effect of dopaminergic medication was conducted in each chapter by comparing those patients taking dopaminergic medication to those patients who were not on these medications and by evaluating correlations with LEDD. Overall, these analyses showed that the results presented in this thesis did not seem to be influenced by the use of dopaminergic medication. However, in future studies it would be interesting to compare the same LBD patients on and off medication to better understand the effects of dopaminergic medication on fMRI and EEG dynamics.

The majority of dementia patients were also taking acetylcholinesterase inhibitors which have been shown to influence RT measures (Onofrj et al., 2003), and modulate the EEG (Babiloni et al., 2013; Onofrj et al., 2003) and fMRI signal (Solé-Padullés et al., 2013). In contrast to dopaminergic medication, the influence of acetylcholinesterase inhibitors on the results could not be examined further due to the very small number of patients not on these medications and therefore remains as a potential limitation of this work. This is especially salient given that cognitive fluctuations are thought to be related to alterations within the cholinergic system (Ballard et al., 2002b; Colloby et al., 2017; Pimlott et al., 2006). From a research point of view, further work is therefore required in order to learn more about the influence of cholinergic medication on the results presented in this thesis. However, in clinical practice most dementia patients will be on acetylcholinesterase inhibitors and it is therefore also important to study medicated patients if a potential clinical application should be considered.

Due to the fact that the ARThippo study did not recruit PDD patients, this condition was not

included in the fMRI analyses where data from the CATFieLD and ARThippo studies were combined. While a previous comparison of static fMRI functional connectivity between DLB and PDD patients found only subtle differences (Peraza et al., 2015a), it remains unknown how connectivity dynamics might differ between the two conditions and this will therefore form an important part of future work.

Additionally, there were some limitations with respect to the quality of the fMRI data. In particular, the relatively long TR posed difficulties when trying to assess dynamic connectivity fluctuations. Furthermore, the relatively small number of volumes of the resting-state scans might have resulted in difficulties regarding the robustness of the dynamic connectivity estimates as it has recently been recommended that at least 10 minutes of fMRI resting-state data should be used to obtain reliable dynamic connectivity estimates (Hindriks et al., 2016). The dynamic fMRI results presented in this thesis will therefore need to be replicated in a dataset with longer scan duration and lower TR.

7.4 Conclusions

To summarise, this thesis sought to characterise the brain dynamics of LBD in comparison to AD and healthy ageing and to investigate possible clinical and behavioural correlates. The results suggest that brain dynamics in LBD are dysfunctional and that a disturbance of the intricate temporal coordination of brain activity might give rise to clinical symptoms that are characteristic of LBD such as cognitive fluctuations and attentional impairment. More specifically, I showed that there is a relative loss of brain dynamics in LBD compared to healthy ageing which does not seem to be present in AD patients of comparable disease severity. This result indicates that the complex functional brain network might lose its temporal variability and flexibility when targeted by LBD pathology. The importance of a dynamic brain for healthy cognitive functioning is well-established (Garrett et al., 2011; Jia et al., 2014; McIntosh et al., 2008; Van De Ville et al., 2010; Zalesky et al., 2014); I would therefore argue that dysfunctional brain dynamics in LBD will have a great impact on brain function in these patients with wider consequences in terms of clinical and behavioural symptoms. Evidence for this claim is provided by the observation that a loss of brain dynamics was related to the severity of cognitive fluctuations in DLB and to attentional impairment across the whole study population. Additionally, I showed that dysfunctional whole-brain dynamics in LBD might be driven by abnormalities in subcortical structures that are characteristic of LBD (Delli Pizzi et al., 2015b; McKeith et al., 2007; Pimlott et al., 2006). This emphasises the importance of alterations in subcortical structures in Lewy body diseases

and raises the prospect that therapies targeted at these structures may also have a global effect on overall brain functioning in LBD including cognitive fluctuations.

7.5 Future directions

An important step of future work should be the replication of the results in larger and independent cohorts. This is especially important for the dynamic connectivity measures given potential concerns regarding the quality of the fMRI data as discussed above (see Section 7.3).

Apart from this, several future directions can be taken based on the work presented in this thesis.

This thesis has focussed solely on the analysis of resting-state fMRI and EEG data. An important next step is the extension of these analyses to task-based data which would allow a more direct assessment of the behavioural significance of brain dynamics in LBD. This could, for instance, involve assessing how brain dynamics during task execution are related to task performance and accuracy, or measuring how brain dynamics during pre-stimulus intervals can influence subsequent task performance. Another interesting aspect would be the comparison between brain dynamics during the resting state and upon task execution. In this context, it has been shown that younger and faster performing individuals show a larger increase in brain variability on task compared to rest than older and slower participants, emphasising the importance of an increase in brain variability for optimal task performance (Garrett et al., 2013a). It could thus be hypothesised that in addition to brain variability at rest being diminished in LBD, the increase in dynamics from rest to task may also be smaller in LBD patients compared to healthy individuals, and this might play a role in attentional impairment and cognitive fluctuations.

Regarding dynamic fMRI connectivity measures, there have been rapid developments in new methods over the last few years introducing many emerging techniques that can be more robust and reliable than sliding window approaches (Cabral et al., 2017; Liégeois et al., 2017; Pedersen et al., 2018; Vidaurre et al., 2017). The main advantage of the sliding window approach that was used here is its simplicity and computational efficiency which makes it especially suitable for clinical applications. However, an important aspect of future work will be the application of other dynamic connectivity methods to the present dataset to check whether it is possible to replicate the results using more complex models of dynamic connectivity.

Given the importance of the cholinergic system in the aetiology of cognitive fluctuations in LBD (Ballard et al., 2002b; Colloby et al., 2017; Onofrj et al., 2003; Pimlott et al., 2006), it

would be interesting to study the relationship between cholinergic system degeneration and the loss of brain dynamics described in this thesis. This could be achieved, for instance, by considering the relation between brain dynamics (e.g. microstate duration) and atrophy of cholinergic structures such as the substantia innominata (Colloby et al., 2017), by studying the effect of acetylcholinesterase inhibitors on brain dynamics, or by investigating the relationship between brain dynamics and an EEG-based marker of cholinergic activity (Johannsson et al., 2015).

To better comprehend the relationship between EEG and fMRI dynamics and to further investigate possible drivers of EEG microstate dynamics, it would be interesting to study data from concurrent EEG and fMRI recordings. Importantly, this would allow to draw more direct conclusions about the causal relationship between subcortical functional connectivity alterations and slowing of EEG microstate dynamics in LBD.

There has been a recent initiative in clinical neuroimaging to move away from simple comparisons of means between clinical groups towards more individualised and normative approaches to account for and better understand variability within clinical populations (Marquand et al., 2016). This is especially relevant in the context of dementia, and LBD in particular, where heterogeneity is large and clinical groups might be overlapping. Applying normative approaches to LBD would therefore be an important step towards a better understanding of this clinical heterogeneity and its neural correlates which could eventually pave the way for more personalised interventions and care. It would also help to learn more about the complicated relationship between AD, DLB, and PDD and would be especially helpful in cases of mixed pathologies that might lead to a clinical manifestation where there is no unambiguous assignment to a certain diagnostic group. More generally, while the analyses presented here are useful to provide an idea of overall group differences between LBD, AD, and healthy controls, it will be important to consider approaches that operate on a single-subject level if the eventual goal is to translate these approaches to clinical practice.

Finally, given that cognitive fluctuations have been suggested to be one of the most characteristic features of DLB patients at the preclinical stage (Donaghy et al., 2017), it would be of great interest to repeat the analyses presented here in a cohort of prodromal DLB patients. This would allow us to investigate whether the observed alterations in fMRI and EEG dynamics might already be present at an early stage of the disease and might potentially be used as an early biomarker of LBD and cognitive fluctuations. Additionally, while this thesis focussed on the analysis of cross-sectional data, it will be important to also study longitudinal data to understand how brain dynamics in LBD develop as the disease progresses.

References

Aarsland, D., Andersen, K., Larsen, J.P., Lolk, A., Kragh-Sørensen, P., 2003. Prevalence and characteristics of dementia in Parkinson disease: an 8-year prospective study. Arch. Neurol. 60, 387–392. https://doi.org/10.1001/archneur.60.3.387

Aarsland, D., Ballard, C.G., Larsen, J.P., McKeith, I.G., 2001. A comparative study of psychiatric symptoms in dementia with Lewy bodies and Parkinson's disease with and without dementia. Int. J. Geriatr. Psychiatry 16, 528–536. https://doi.org/10.1002/gps.389

Aarsland, D., Ballard, C.G., Walker, Z., Bostrom, F., Alves, G., Kossakowski, K., Leroi, I., Pozo-Rodriguez, F., Minthon, L., Londos, E., 2009a. Memantine in patients with Parkinson's disease dementia or dementia with Lewy bodies: a double-blind, placebo-controlled, multicentre trial. Lancet Neurol. 8, 613–618. https://doi.org/10.1016/S1474-4422(09)70146-2

Aarsland, D., Londos, E., Ballard, C.G., 2009b. Parkinson's disease dementia and dementia with Lewy bodies: different aspects of one entity. Int. Psychogeriatrics 21, 216. https://doi.org/10.1017/S1041610208008612

Aarsland, D., Mosimann, U.P., McKeith, I.G., 2004. Role of cholinesterase inhibitors in Parkinson's disease and dementia with Lewy bodies. J. Geriatr. Psychiatry Neurol. 17, 164–71. https://doi.org/10.1177/0891988704267463

Abou Elseoud, A., Littow, H., Remes, J.J., Starck, T., Nikkinen, J., Nissilä, J., Timonen, M., Tervonen, O., Kiviniemi, V., 2011. Group-ICA Model Order Highlights Patterns of Functional Brain Connectivity. Front. Syst. Neurosci. 5, 37. https://doi.org/10.3389/fnsys.2011.00037

Achard, S., Bullmore, E., 2007. Efficiency and cost of economical brain functional networks. PLoS Comput. Biol. 3, 0174–0183. https://doi.org/10.1371/journal.pcbi.0030017

Adamowicz, D.H., Roy, S., Salmon, D.P., Galasko, D.R., Hansen, L.A., Masliah, E., Gage, F.H., 2017. Hippocampal α-Synuclein in Dementia with Lewy Bodies Contributes to Memory Impairment and Is Consistent with Spread of Pathology. J. Neurosci. 37, 1675–1684. https://doi.org/10.1523/JNEUROSCI.3047-16.2016

Agosta, F., Pievani, M., Geroldi, C., Copetti, M., Frisoni, G.B., Filippi, M., 2012. Resting state fMRI in Alzheimer's disease: Beyond the default mode network. Neurobiol. Aging

33, 1564–1578. https://doi.org/10.1016/j.neurobiolaging.2011.06.007

Aldridge, G.M., Birnschein, A., Denburg, N.L., Narayanan, N.S., 2018. Parkinson's Disease Dementia and Dementia with Lewy Bodies Have Similar Neuropsychological Profiles. Front. Neurol. 9, 1–8. https://doi.org/10.3389/fneur.2018.00123

Allen, E.A., Damaraju, E., Plis, S.M., Erhardt, E.B., Eichele, T., Calhoun, V.D., 2014. Tracking Whole-Brain Connectivity Dynamics in the Resting State. Cereb. Cortex 24, 663–676. https://doi.org/10.1093/cercor/bhs352

Antelmi, E., Ferri, R., Iranzo, A., Arnulf, I., Dauvilliers, Y., Bhatia, K.P., Liguori, R., Schenck, C.H., Plazzi, G., 2016. From state dissociation to status dissociatus. Sleep Med. Rev. 28, 1–13. https://doi.org/10.1016/j.smrv.2015.07.003

Ashburner, J., 2007. A fast diffeomorphic image registration algorithm. Neuroimage 38, 95–113. https://doi.org/10.1016/j.neuroimage.2007.07.007

Avants, B.B., Tustison, N.J., Song, G., Cook, P.A., Klein, A., Gee, J.C., 2011. A reproducible evaluation of ANTs similarity metric performance in brain image registration. Neuroimage 54, 2033–2044. https://doi.org/10.1016/j.neuroimage.2010.09.025

Babiloni, C., Del Percio, C., Bordet, R., Bourriez, J.L., Bentivoglio, M., Payoux, P., Derambure, P., Dix, S., Infarinato, F., Lizio, R., Triggiani, A.I., Richardson, J.C., Rossini, P.M., 2013. Effects of acetylcholinesterase inhibitors and memantine on resting-state electroencephalographic rhythms in Alzheimer's disease patients. Clin. Neurophysiol. 124, 837–850. https://doi.org/10.1016/j.clinph.2012.09.017

Babiloni, C., Del Percio, C., Lizio, R., Noce, G., Cordone, S., Lopez, S., Soricelli, A., Ferri, R., Pascarelli, M.T., Nobili, F., Arnaldi, D., Aarsland, D., Orzi, F., Buttinelli, C., Giubilei, F., Onofrj, M., Stocchi, F., Stirpe, P., Fuhr, P., Gschwandtner, U., Ransmayr, G., Caravias, G., Garn, H., Sorpresi, F., Pievani, M., Frisoni, G.B., D'Antonio, F., De Lena, C., Güntekin, B., Hanoğlu, L., Başar, E., Yener, G., Emek-Savaş, D.D., Triggiani, A.I., Franciotti, R., De Pandis, M.F., Bonanni, L., 2017. Abnormalities of cortical neural synchronization mechanisms in patients with dementia due to Alzheimer's and Lewy body diseases: an EEG study. Neurobiol. Aging 55, 143–158. https://doi.org/10.1016/j.neurobiolaging.2017.03.030

Baggio, H.-C., Segura, B., Sala-Llonch, R., Marti, M.-J., Valldeoriola, F., Compta, Y., Tolosa, E., Junqué, C., 2015. Cognitive impairment and resting-state network connectivity in Parkinson's disease. Hum. Brain Mapp. 36, 199–212.

https://doi.org/10.1002/hbm.22622

Ballard, C.G., Aarsland, D., Francis, P., Corbett, A., 2013. Neuropsychiatric symptoms in patients with dementias associated with cortical lewy bodies: Pathophysiology, clinical features, and pharmacological management. Drugs and Aging 30, 603–611. https://doi.org/10.1007/s40266-013-0092-x

Ballard, C.G., Aarsland, D., McKeith, I.G., O'Brien, J.T., Gray, A., Cormack, F., Burn, D., Cassidy, T., Starfeldt, R., Larsen, J.-P., Brown, R., Tovee, M., 2002a. Fluctuations in attention: PD dementia vs DLB with parkinsonism. Neurology 59, 1714–1720. https://doi.org/10.1212/01.WNL.0000036908.39696.FD

Ballard, C.G., Court, J.A., Piggott, M., Johnson, M., O'Brien, J.T., McKeith, I.G., Holmes, C., Lantos, P., Jaros, E., Perry, R., Perry, E., 2002b. Disturbances of consciousness in dementia with Lewy bodies associated with alteration in nicotinic receptor binding in the temporal cortex. Conscious. Cogn. 11, 461–474. https://doi.org/10.1016/S1053-8100(02)00013-2

Ballard, C.G., Jacoby, R., Del Ser, T., Khan, M.N., Munoz, D.G., Holmes, C., Nagy, Z., Perry, E.K., Joachim, C., Jaros, E., O'Brien, J.T., Perry, R.H., McKeith, I.G., 2004. Neuropathological Substrates of Psychiatric Symptoms in Prospectively Studied Patients With Autopsy-Confirmed Dementia With Lewy Bodies. Am. J. Psychiatry 161, 843–849. https://doi.org/10.1176/appi.ajp.161.5.843

Ballard, C.G., O'Brien, J.T., Gray, A., Cormack, F., Ayre, G., Rowan, E., Thompson, P., Bucks, R., McKeith, I.G., Walker, M., Tovee, M., 2001a. Attention and Fluctuating Attention in Patients With Dementia With Lewy Bodies and Alzheimer Disease. Arch. Neurol. 58, 977. https://doi.org/10.1001/archneur.58.6.977

Ballard, C.G., Piggott, M., Johnson, M., Cairns, N., Perry, R., McKeith, I.G., Jaros, E., O'Brien, J.T., Holmes, C., Perry, E., 2000. Delusions associated with elevated muscarinic binding in dementia with Lewy bodies. Ann. Neurol. 48, 868–876. https://doi.org/10.1002/1531-8249(200012)48:6<868::AID-ANA7>3.0.CO;2-0

Ballard, C.G., Walker, M., O'Brien, J.T., Rowan, E., McKeith, I.G., 2001b. The characterisation and impact of "fluctuating" cognition in dementia with Lewy bodies and Alzheimer's disease. Int. J. Geriatr. Psychiatry 16, 494–498. https://doi.org/10.1002/gps.368

Balota, D.A., Tse, C.S., Hutchison, K.A., Spieler, D.H., Duchek, J.M., Morris, J.C., 2010.

Predicting conversion to dementia of the Alzheimer's type in a healthy control sample: the power of errors in Stroop color naming. Psychol. Aging 25, 208–218. https://doi.org/10.1037/a0017474

Balota, D.A., Yap, M.J., 2011. Moving Beyond the Mean in Studies of Mental Chronometry: The Power of Response Time Distributional Analyses. Curr. Dir. Psychol. Sci. 20, 160–166. https://doi.org/10.1177/0963721411408885

Barber, R., Ballard, C.G., McKeith, I.G., Gholkar, A., O'Brien, J.T., 2000. MRI volumetric study of dementia with Lewy bodies: A comparison with AD and vascular dementia. Neurology 54, 1304–1309. https://doi.org/10.1212/WNL.54.6.1304

Beach, T.G., Adler, C.H., Lue, L.F., Sue, L.I., Bachalakuri, J., Henry-Watson, J., Sasse, J., Boyer, S., Shirohi, S., Brooks, R., Eschbacher, J., White, C.L., Akiyama, H., Caviness, J., Shill, H.A., Connor, D.J., Sabbagh, M.N., Walker, D.G., 2009. Unified staging system for Lewy body disorders: Correlation with nigrostriatal degeneration, cognitive impairment and motor dysfunction. Acta Neuropathol. 117, 613–634. https://doi.org/10.1007/s00401-009-0538-8

Beckmann, C.F., DeLuca, M., Devlin, J.T., Smith, S.M., 2005. Investigations into resting-state connectivity using independent component analysis. Philos. Trans. R. Soc. Lond. B. Biol. Sci. 360, 1001–13. https://doi.org/10.1098/rstb.2005.1634

Bell, P.T., Shine, J.M., 2016. Subcortical contributions to large-scale network communication. Neurosci. Biobehav. Rev. 71, 313–322. https://doi.org/10.1016/j.neubiorev.2016.08.036

Beyer, M.K., Larsen, J.P., Aarsland, D., 2007. Gray matter atrophy in Parkinson disease with dementia and dementia with Lewy bodies. Neurology 69, 747–754. https://doi.org/10.1212/01.wnl.0000269666.62598.1c

Binder, J.R., Frost, J.A., Hammeke, T.A., Bellgowan, P.S.F., Rao, S.M., Cox, R.W., 1999. Conceptual Processing during the Conscious Resting State: A Functional MRI Study. J. Cogn. Neurosci. 11, 80–93. https://doi.org/10.1162/089892999563265

Binnewijzend, M.A.A., Schoonheim, M.M., Sanz-Arigita, E., Wink, A.M., van der Flier, W.M., Tolboom, N., Adriaanse, S.M., Damoiseaux, J.S., Scheltens, P., van Berckel, B.N.M., Barkhof, F., 2012. Resting-state fMRI changes in Alzheimer's disease and mild cognitive impairment. Neurobiol. Aging 33, 2018–2028. https://doi.org/10.1016/j.neurobiolaging.2011.07.003

Biswal, B.B., Mennes, M., Zuo, X.-N., Gohel, S., Kelly, C., Smith, S.M., Beckmann, C.F., Adelstein, J.S., Buckner, R.L., Colcombe, S., Dogonowski, A.-M., Ernst, M., Fair, D., Hampson, M., Hoptman, M.J., Hyde, J.S., Kiviniemi, V.J., Kotter, R., Li, S.-J., Lin, C.-P., Lowe, M.J., Mackay, C., Madden, D.J., Madsen, K.H., Margulies, D.S., Mayberg, H.S., McMahon, K., Monk, C.S., Mostofsky, S.H., Nagel, B.J., Pekar, J.J., Peltier, S.J., Petersen, S.E., Riedl, V., Rombouts, S.A.R.B., Rypma, B., Schlaggar, B.L., Schmidt, S., Seidler, R.D., Siegle, G.J., Sorg, C., Teng, G.-J., Veijola, J., Villringer, A., Walter, M., Wang, L., Weng, X.-C., Whitfield-Gabrieli, S., Williamson, P., Windischberger, C., Zang, Y.-F., Zhang, H.-Y., Castellanos, F.X., Milham, M.P., 2010. Toward discovery science of human brain function. Proc. Natl. Acad. Sci. 107, 4734–4739. https://doi.org/10.1073/pnas.0911855107

Biswal, B.B., Zerrin Yetkin, F., Haughton, V.M., Hyde, J.S., 1995. Functional connectivity in the motor cortex of resting human brain using echo-planar mri. Magn. Reson. Med. 34, 537–541. https://doi.org/10.1002/mrm.1910340409

Blanc, F., Colloby, S.J., Cretin, B., de Sousa, P.L., Demuynck, C., O'Brien, J.T., Martin-Hunyadi, C., McKeith, I.G., Philippi, N., Taylor, J.-P., 2016. Grey matter atrophy in prodromal stage of dementia with Lewy bodies and Alzheimer's disease. Alzheimers. Res. Ther. 8, 31. https://doi.org/10.1186/s13195-016-0198-6

Blanc, F., Mahmoudi, R., Jonveaux, T., Galmiche, J., Chopard, G., Cretin, B., Demuynck, C., Martin-Hunyadi, C., Philippi, N., Sellal, F., Michel, J.-M., Tio, G., Stackfleth, M., Vandel, P., Magnin, E., Novella, J.-L., Kaltenbach, G., Benetos, A., Sauleau, E.A., 2017. Long-term cognitive outcome of Alzheimer's disease and dementia with Lewy bodies: dual disease is worse. Alzheimers. Res. Ther. 9, 47. https://doi.org/10.1186/s13195-017-0272-8

Bliwise, D.L., Scullin, M.K., Trotti, L.M., 2014. Fluctuations in cognition and alertness vary independently in dementia with Lewy bodies. Mov. Disord. 29, 83–89. https://doi.org/10.1002/mds.25707

Boddy, F., Rowan, E.N., Lett, D., O'Brien, J.T., McKeith, I.G., Burn, D.J., 2007. Subjectively reported sleep quality and excessive daytime somnolence in Parkinson's disease with and without dementia, dementia with Lewy bodies and Alzheimer's disease. Int. J. Geriatr. Psychiatry 22, 529–535. https://doi.org/10.1002/gps.1709

Bonanni, L., Franciotti, R., Nobili, F., Kramberger, M.G., Taylor, J.P., Garcia-Ptacek, S.,

Falasca, N.W., Famá, F., Cromarty, R.A., Onofrj, M., Aarsland, D., 2016. EEG Markers of Dementia with Lewy Bodies: A Multicenter Cohort Study. J. Alzheimer's Dis. 54, 1649–1657. https://doi.org/10.3233/JAD-160435

Bonanni, L., Franciotti, R., Onofrj, V., Anzellotti, F., Mancino, E., Monaco, D., Gambi, F., Manzoli, L., Thomas, A., Onofrj, M., 2010. Revisiting P300 cognitive studies for dementia diagnosis: Early dementia with Lewy bodies (DLB) and Alzheimer disease (AD). Neurophysiol. Clin. Neurophysiol. 40, 255–265. https://doi.org/10.1016/j.neucli.2010.08.001

Bonanni, L., Perfetti, B., Bifolchetti, S., Taylor, J.-P., Franciotti, R., Parnetti, L., Thomas, A., Onofrj, M., 2015. Quantitative electroencephalogram utility in predicting conversion of mild cognitive impairment to dementia with Lewy bodies. Neurobiol. Aging 36, 434–445. https://doi.org/10.1016/j.neurobiolaging.2014.07.009

Bonanni, L., Thomas, A., Tiraboschi, P., Perfetti, B., Varanese, S., Onofrj, M., 2008. EEG comparisons in early Alzheimer's disease, dementia with Lewy bodies and Parkinson's disease with dementia patients with a 2-year follow-up. Brain 131, 690–705. https://doi.org/10.1093/brain/awm322

Bonelli, S.B., Ransmayr, G., Steffelbauer, M., Lukas, T., Lampl, C., Deibl, M., 2004. L-Dopa responsiveness in dementia with Lewy bodies, Parkinson disease with and without dementia. Neurology 63, 376–378. https://doi.org/10.1212/01.WNL.0000130194.84594.96

Borsa, V.M., Della Rosa, P.A., Catricalà, E., Canini, M., Iadanza, A., Falini, A., Abutalebi, J., Iannaccone, S., 2016. Interference and conflict monitoring in individuals with amnestic mild cognitive impairment: A structural study of the anterior cingulate cortex. J. Neuropsychol. 1–18. https://doi.org/10.1111/jnp.12105

Bozzali, M., Falini, A., Cercignani, M., Baglio, F., Farina, E., Alberoni, M., Vezzulli, P., Olivotto, F., Mantovani, F., Shallice, T., Scotti, G., Canal, N., Nemni, R., 2005. Brain tissue damage in dementia with Lewy bodies: an in vivo diffusion tensor MRI study. Brain 128, 1595–1604. https://doi.org/10.1093/brain/awh493

Braak, H., Ghebremedhin, E., Rüb, U., Bratzke, H., Del Tredici, K., 2004. Stages in the development of Parkinson's disease-related pathology. Cell Tissue Res. 318, 121–134. https://doi.org/10.1007/s00441-004-0956-9

Braak, H., Tredici, K. Del, Rüb, U., de Vos, R.A.., Jansen Steur, E.N.., Braak, E., 2003.

Staging of brain pathology related to sporadic Parkinson's disease. Neurobiol. Aging 24, 197–211. https://doi.org/10.1016/S0197-4580(02)00065-9

Bradshaw, J., Saling, M., Hopwood, M., Anderson, V., Brodtmann, A., 2004. Fluctuating cognition in dementia with Lewy bodies and Alzheimer's disease is qualitatively distinct. J. Neurol. Neurosurg. Psychiatry 75, 382–7. https://doi.org/10.1136/jnnp.2002.002576

Bradshaw, J.M., Saling, M., Anderson, V., Hopwood, M., Brodtmann, a, 2006. Higher cortical deficits influence attentional processing in dementia with Lewy bodies, relative to patients with dementia of the Alzheimer's type and controls. J. Neurol. Neurosurg. Psychiatry 77, 1129–1135. https://doi.org/10.1136/jnnp.2006.090183

Briel, R.C.G., McKeith, I.G., Barker, W.A., Hewitt, Y., Perry, R.H., Ince, P.G., Fairbairn, A.F., 1999. EEG findings in dementia with Lewy bodies and Alzheimer's disease. J. Neurol. Neurosurg. Psychiatry 66, 401–403. https://doi.org/10.1136/jnnp.66.3.401

Britz, J., Van De Ville, D., Michel, C.M., 2010. BOLD correlates of EEG topography reveal rapid resting-state network dynamics. Neuroimage 52, 1162–1170. https://doi.org/10.1016/j.neuroimage.2010.02.052

Brønnick, K., Ehrt, U., Emre, M., De Deyn, P.P., Wesnes, K.A., Tekin, S., Aarsland, D., 2006. Attentional deficits affect activities of daily living in dementia-associated with Parkinson's disease. J. Neurol. Neurosurg. Psychiatry 77, 1136–42. https://doi.org/10.1136/jnnp.2006.093146

Brønnick, K.S., 2015. Cognitive profile in Parkinson's disease dementia, in: Emre, M. (Ed.), Cognitive Impairment and Dementia in Parkinson's Disease. Oxford University Press, pp. 27–45.

Brunet, D., Murray, M.M., Michel, C.M., 2011. Spatiotemporal analysis of multichannel EEG: CARTOOL. Comput. Intell. Neurosci. 2011. https://doi.org/10.1155/2011/813870

Buckner, R.L., 2005. Molecular, Structural, and Functional Characterization of Alzheimer's Disease: Evidence for a Relationship between Default Activity, Amyloid, and Memory. J. Neurosci. 25, 7709–7717. https://doi.org/10.1523/JNEUROSCI.2177-05.2005

Burchett, W.W., Ellis, A.R., Harrar, S.W., Bathke, A.C., 2017. Nonparametric Inference for Multivariate Data: The R Package npmv. J. Stat. Softw. 76. https://doi.org/10.18637/jss.v076.i04

Burn, D.J., Rowan, E.N., Minett, T., Sanders, J., Myint, P., Richardson, J., Thomas, A.,

Newby, J., Reid, J., O'Brien, J.T., McKeith, I.G., 2003. Extrapyramidal features in Parkinson's disease with and without dementia and dementia with lewy bodies: A cross-sectional comparative study. Mov. Disord. 18, 884–889. https://doi.org/10.1002/mds.10455

Burton, E.J., Barber, R., Mukaetova-Ladinska, E.B., Robson, J., Perry, R.H., Jaros, E., Kalaria, R.N., O'Brien, J.T., 2009. Medial temporal lobe atrophy on MRI differentiates Alzheimer's disease from dementia with Lewy bodies and vascular cognitive impairment: a prospective study with pathological verification of diagnosis. Brain 132, 195–203. https://doi.org/10.1093/brain/awn298

Burton, E.J., Karas, G., Paling, S.M., Barber, R., Williams, E.D., Ballard, C.G., McKeith, I.G., Scheltens, P., Barkhof, F., O'Brien, J.T., 2002. Patterns of Cerebral Atrophy in Dementia with Lewy Bodies Using Voxel-Based Morphometry. Neuroimage 17, 618–630. https://doi.org/10.1006/nimg.2002.1197

Burton, E.J., McKeith, I.G., Burn, D.J., Firbank, M.J., O'Brien, J.T., 2006. Progression of White Matter Hyperintensities in Alzheimer Disease, Dementia With Lewy Bodies, and Parkinson Disease Dementia: A Comparison With Normal Aging. Am. J. Geriatr. Psychiatry 14, 842–849. https://doi.org/10.1097/01.JGP.0000236596.56982.1c

Burton, E.J., McKeith, I.G., Burn, D.J., Williams, E.D., O'Brien, J.T., 2004. Cerebral atrophy in Parkinson's disease with and without dementia: A comparison with Alzheimer's disease, dementia with Lewy bodies and controls. Brain 127, 791–800. https://doi.org/10.1093/brain/awh088

Buschman, T.J., Miller, E.K., 2007. Top-Down Versus Bottom-Up Control of Attention in the Prefrontal and Posterior Parietal Cortices. Science (80-.). 315, 1860–1862. https://doi.org/10.1126/science.1138071

Bush, G., Luu, P., Posner, M.I., 2000. Cognitive and emotional influences in anterior cingulate cortex. Trends.Cogn Sci. 4, 215–222. https://doi.org/10.1016/S1364-6613(00)01483-2

Byrne, E.J., Lennox, G., Lowe, J., Godwin-Austen, R.B., 1989. Diffuse Lewy body disease: clinical features in 15 cases. J. Neurol. Neurosurg. Psychiatry 52, 709–717.

Cabral, J., Vidaurre, D., Marques, P., Magalhães, R., Silva Moreira, P., Miguel Soares, J., Deco, G., Sousa, N., Kringelbach, M.L., 2017. Cognitive performance in healthy older adults relates to spontaneous switching between states of functional connectivity during

rest. Sci. Rep. 7, 5135. https://doi.org/10.1038/s41598-017-05425-7

Cagnin, A., Bussè, C., Gardini, S., Jelcic, N., Guzzo, C., Gnoato, F., Mitolo, M., Ermani, M., Caffarra, P., 2015. Clinical and Cognitive Phenotype of Mild Cognitive Impairment Evolving to Dementia with Lewy Bodies. Dement. Geriatr. Cogn. Dis. Extra 5, 442–449. https://doi.org/10.1159/000441184

Cagnin, A., Fragiacomo, F., Camporese, G., Turco, M., Bussè, C., Ermani, M., Montagnese, S., 2016. Sleep-Wake Profile in Dementia with Lewy Bodies, Alzheimer's Disease, and Normal Aging. J. Alzheimer's Dis. 55, 1529–1536. https://doi.org/10.3233/JAD-160385

Calderon, J., 2001. Perception, attention, and working memory are disproportionately impaired in dementia with Lewy bodies compared with Alzheimer's disease. J. Neurol. Neurosurg. Psychiatry 70, 157–164. https://doi.org/10.1136/jnnp.70.2.157

Calhoun, V.D., Miller, R.L., Pearlson, G.D., Adali, T., 2014. The Chronnectome: Time-Varying Connectivity Networks as the Next Frontier in fMRI Data Discovery. Neuron 84, 262–274. https://doi.org/10.1016/j.neuron.2014.10.015

Cerliani, L., Mennes, M., Thomas, R.M., Di Martino, A., Thioux, M., Keysers, C., 2015. Increased Functional Connectivity Between Subcortical and Cortical Resting-State Networks in Autism Spectrum Disorder. JAMA Psychiatry 72, 767. https://doi.org/10.1001/jamapsychiatry.2015.0101

Chabran, E., Roquet, D., Gounot, D., Sourty, M., Armspach, J.-P., Blanc, F., 2018. Functional Disconnectivity during Inter-Task Resting State in Dementia with Lewy Bodies. Dement. Geriatr. Cogn. Disord. 45, 105–120. https://doi.org/10.1159/000486780

Chang, C., Glover, G.H., 2010. Time–frequency dynamics of resting-state brain connectivity measured with fMRI. Neuroimage 50, 81–98. https://doi.org/10.1016/j.neuroimage.2009.12.011

Chang, C., Liu, Z., Chen, M.C., Liu, X., Duyn, J.H., 2013. EEG correlates of time-varying BOLD functional connectivity. Neuroimage 72, 227–236. https://doi.org/10.1016/j.neuroimage.2013.01.049

Ciric, R., Wolf, D.H., Power, J.D., Roalf, D.R., Baum, G.L., Ruparel, K., Shinohara, R.T., Elliott, M.A., Eickhoff, S.B., Davatzikos, C., Gur, R.C., Gur, R.E., Bassett, D.S., Satterthwaite, T.D., 2017. Benchmarking of participant-level confound regression strategies for the control of motion artifact in studies of functional connectivity.

Neuroimage 154, 174–187. https://doi.org/10.1016/j.neuroimage.2017.03.020

Clerici, F., Ratti, P.L., Pomati, S., Maggiore, L., Elia, A., Mariani, C., 2007. Cholinergic balance in dementia with Lewy bodies: Reversible worsening of Parkinsonism at rivastigmine dosage modulation. Neurol. Sci. 28, 282–284. https://doi.org/10.1007/s10072-007-0837-6

Colloby, S.J., Elder, G.J., Rabee, R., O'Brien, J.T., Taylor, J.-P., 2017. Structural grey matter changes in the substantia innominata in Alzheimer's disease and dementia with Lewy bodies: a DARTEL-VBM study. Int. J. Geriatr. Psychiatry 32, 615–623. https://doi.org/10.1002/gps.4500

Colloby, S.J., Fenwick, J.D., Williams, D.E., Paling, S.M., Lobotesis, K., Ballard, C.G., McKeith, I.G., O'Brien, J.T., 2002. A comparison of 99mTc-HMPAO SPET changes in dementia with Lewy bodies and Alzheimer's disease using statistical parametric mapping. Eur. J. Nucl. Med. Mol. Imaging 29, 615–622. https://doi.org/10.1007/s00259-002-0778-5

Colloby, S.J., O'Brien, J.T., Fenwick, J.D., Firbank, M.J., Burn, D.J., McKeith, I.G., Williams, E.D., 2004. The application of statistical parametric mapping to 123I-FP-CIT SPECT in dementia with Lewy bodies, Alzheimer's disease and Parkinson's disease. Neuroimage 23, 956–966. https://doi.org/10.1016/j.neuroimage.2004.06.045

Colloby, S.J., O'Brien, J.T., Taylor, J.P., 2014. Patterns of cerebellar volume loss in dementia with Lewy bodies and Alzheimer's disease: A VBM-DARTEL study. Psychiatry Res. - Neuroimaging 223, 187–191. https://doi.org/10.1016/j.pscychresns.2014.06.006

Colosimo, C., 2003. Lewy body cortical involvement may not always predict dementia in Parkinson's disease. J. Neurol. Neurosurg. Psychiatry 74, 852–856. https://doi.org/10.1136/jnnp.74.7.852

Coull, J.T., Nobre, A.C., Frith, C.D., 2001. The Noradrenergic 2 Agonist Clonidine Modulates Behavioural and Neuroanatomical Correlates of Human Attentional Orienting and Alerting. Cereb. Cortex 11, 73–84. https://doi.org/10.1093/cercor/11.1.73

Cribben, I., Wager, T.D., Lindquist, M. a, 2013. Detecting functional connectivity change points for single-subject fMRI data. Front. Comput. Neurosci. 7, 143. https://doi.org/10.3389/fncom.2013.00143

Cromarty, R.A., 2016. Investigating attentional function and cognitive fluctuations in Lewy

body dementia.

Cromarty, R.A., Elder, G.J., Graziadio, S., Baker, M., Bonanni, L., Onofrj, M., O'Brien, J.T., Taylor, J.-P., 2015. Neurophysiological biomarkers for Lewy body dementias. Clin. Neurophysiol. https://doi.org/10.1016/j.clinph.2015.06.020

Cummings, J.L., 2004. Fluctuations in cognitive function in dementia with Lewy bodies. Lancet Neurol. 3, 266. https://doi.org/10.1016/S1474-4422(04)00728-8

Cummings, J.L., Mega, M., Gray, K., Rosenberg-Thompson, S., Carusi, D.A., Gornbein, J., 1994. The Neuropsychiatric Inventory: Comprehensive assessment of psychopathology in dementia. Neurology 44, 2308–2308. https://doi.org/10.1212/WNL.44.12.2308

Custo, A., Van De Ville, D., Wells, W.M., Tomescu, M.I., Brunet, D., Michel, C.M., 2017. Electroencephalographic Resting-State Networks: Source Localization of Microstates. Brain Connect. 7, 671–682. https://doi.org/10.1089/brain.2016.0476

Cyr, M., Parent, M.J., Mechawar, N., Rosa-Neto, P., Soucy, J.P., Clark, S.D., Aghourian, M., Bedard, M.A., 2015. Deficit in sustained attention following selective cholinergic lesion of the pedunculopontine tegmental nucleus in rat, as measured with both post-mortem immunocytochemistry and in vivo PET imaging with [18F]fluoroethoxybenzovesamicol. Behav. Brain Res. 278, 107–114. https://doi.org/10.1016/j.bbr.2014.09.021

Damaraju, E., Allen, E.A., Belger, A., Ford, J.M., McEwen, S., Mathalon, D.H., Mueller, B.A., Pearlson, G.D., Potkin, S.G., Preda, A., Turner, J.A., Vaidya, J.G., van Erp, T.G., Calhoun, V.D., 2014. Dynamic functional connectivity analysis reveals transient states of dysconnectivity in schizophrenia. NeuroImage Clin. 5, 298–308. https://doi.org/10.1016/j.nicl.2014.07.003

Damoiseaux, J.S., Beckmann, C.F., Arigita, E.J.S., Barkhof, F., Scheltens, P., Stam, C.J., Smith, S.M., Rombouts, S.A.R.B., 2008. Reduced resting-state brain activity in the "default network" in normal aging. Cereb. Cortex 18, 1856–1864. https://doi.org/10.1093/cercor/bhm207

Damoiseaux, J.S., Prater, K.E., Miller, B.L., Greicius, M.D., 2012. Functional connectivity tracks clinical deterioration in Alzheimer's disease. Neurobiol. Aging 33, 828.e19-828.e30. https://doi.org/10.1016/j.neurobiolaging.2011.06.024

Damoiseaux, J.S., Rombouts, S.A.R., Barkhof, F., Scheltens, P., Stam, C.J., Smith, S.M., Beckmann, C.F., 2006. Consistent resting-state networks across healthy subjects. Proc.

Natl. Acad. Sci. U. S. A. 103, 13848–13853. https://doi.org/10.1073/pnas.0601417103

Deco, G., Jirsa, V.K., 2012. Ongoing Cortical Activity at Rest: Criticality, Multistability, and Ghost Attractors. J. Neurosci. 32, 3366–3375. https://doi.org/10.1523/JNEUROSCI.2523-11.2012

Deco, G., Jirsa, V.K., McIntosh, A.R., 2011. Emerging concepts for the dynamical organization of resting-state activity in the brain. Nat. Rev. Neurosci. 12, 43–56. https://doi.org/10.1038/nrn2961

Del Tredici, K., Braak, H., 2013. Dysfunction of the locus coeruleus-norepinephrine system and related circuitry in Parkinson's disease-related dementia. J. Neurol. Neurosurg. Psychiatry 84, 774–783. https://doi.org/10.1136/jnnp-2011-301817

Delli Pizzi, S., Franciotti, R., Taylor, J.-P., Esposito, R., Tartaro, A., Thomas, A., Onofrj, M., Bonanni, L., 2015a. Structural Connectivity is Differently Altered in Dementia with Lewy Body and Alzheimer's Disease. Front. Aging Neurosci. 7. https://doi.org/10.3389/fnagi.2015.00208

Delli Pizzi, S., Franciotti, R., Taylor, J.-P., Thomas, A., Tartaro, A., Onofrj, M., Bonanni, L., 2015b. Thalamic Involvement in Fluctuating Cognition in Dementia with Lewy Bodies: Magnetic Resonance Evidences. Cereb. Cortex 25, 3682–3689. https://doi.org/10.1093/cercor/bhu220

Dickson, D.W., 2002. Dementia with Lewy Bodies: Neuropathology. J. Geriatr. Psychiatry Neurol. 15, 210–216. https://doi.org/10.1177/089198870201500406

Díez-Cirarda, M., Strafella, A.P., Kim, J., Peña, J., Ojeda, N., Cabrera-Zubizarreta, A., Ibarretxe-Bilbao, N., 2017. Dynamic functional connectivity in Parkinson's disease patients with mild cognitive impairment and normal cognition. NeuroImage Clin. https://doi.org/10.1016/j.nicl.2017.12.013

Dipasquale, O., Griffanti, L., Clerici, M., Nemni, R., Baselli, G., Baglio, F., 2015. High-Dimensional ICA Analysis Detects Within-Network Functional Connectivity Damage of Default-Mode and Sensory-Motor Networks in Alzheimer's Disease. Front. Hum. Neurosci. 9, 43. https://doi.org/10.3389/fnhum.2015.00043

Donaghy, P., Thomas, A.J., O'Brien, J.T., 2015. Amyloid PET Imaging in Lewy Body Disorders. Am. J. Geriatr. Psychiatry 23, 23–37. https://doi.org/10.1016/j.jagp.2013.03.001

Donaghy, P.C., Barnett, N., Olsen, K., Taylor, J.-P., McKeith, I.G., O'Brien, J.T., Thomas, A.J., 2017. Symptoms associated with Lewy body disease in mild cognitive impairment. Int. J. Geriatr. Psychiatry 32, 1163–1171. https://doi.org/10.1002/gps.4742

Donaghy, P.C., Firbank, M.J., Thomas, A.J., Lloyd, J., Petrides, G., Barnett, N., Olsen, K., O'Brien, J.T., 2018. Clinical and imaging correlates of amyloid deposition in dementia with Lewy bodies. Mov. Disord. 00, 1–9. https://doi.org/10.1002/mds.27403

Dugger, B.N., Adler, C.H., Shill, H.A., Caviness, J., Jacobson, S., Driver-Dunckley, E., Beach, T.G., 2014. Concomitant pathologies among a spectrum of parkinsonian disorders. Parkinsonism Relat. Disord. 20, 525–529. https://doi.org/10.1016/j.parkreldis.2014.02.012

Economou, A., Routsis, C., Papageorgiou, S.G., 2016. Episodic Memory in Alzheimer Disease, Frontotemporal Dementia, and Dementia With Lewy Bodies/Parkinson Disease Dementia. Alzheimer Dis. Assoc. Disord. 30, 47–52. https://doi.org/10.1097/WAD.0000000000000089

Edison, P., Rowe, C.C., Rinne, J.O., Ng, S., Ahmed, I., Kemppainen, N., Villemagne, V.L., O'Keefe, G., Nagren, K., Chaudhury, K.R., Masters, C.L., Brooks, D.J., 2008. Amyloid load in Parkinson's disease dementia and Lewy body dementia measured with [11C]PIB positron emission tomography. J. Neurol. Neurosurg. Psychiatry 79, 1331–1338. https://doi.org/10.1136/jnnp.2007.127878

Edwards, K., Royall, D., Hershey, L., Lichter, D., Hake, A., Farlow, M., Pasquier, F., Johnson, S., 2007. Efficacy and Safety of Galantamine in Patients with Dementia with Lewy Bodies: A 24-Week Open-Label Study. Dement. Geriatr. Cogn. Disord. 23, 401–405. https://doi.org/10.1159/000101512

Elder, G.J., Mactier, K., Colloby, S.J., Watson, R., Blamire, A.M., O'Brien, J.T., Taylor, J.-P., 2017. The influence of hippocampal atrophy on the cognitive phenotype of dementia with Lewy bodies. Int. J. Geriatr. Psychiatry 32, 1182–1189. https://doi.org/10.1002/gps.4719

Emre, M., Aarsland, D., Brown, R., Burn, D.J., Duyckaerts, C., Mizuno, Y., Broe, G.A., Cummings, J.L., Dickson, D.W., Gauthier, S., Goldman, J., Goetz, C., Korczyn, A., Lees, A., Levy, R., Litvan, I., McKeith, I.G., Olanow, W., Poewe, W., Quinn, N., Sampaio, C., Tolosa, E., Dubois, B., 2007. Clinical diagnostic criteria for dementia associated with Parkinson's disease. Mov. Disord. 22, 1689–1707.

https://doi.org/10.1002/mds.21507

Emre, M., Tsolaki, M., Bonuccelli, U., Destée, A., Tolosa, E., Kutzelnigg, A., Ceballos-Baumann, A., Zdravkovic, S., Bladström, A., Jones, R., 2010. Memantine for patients with Parkinson's disease dementia or dementia with Lewy bodies: a randomised, double-blind, placebo-controlled trial. Lancet Neurol. 9, 969–977. https://doi.org/10.1016/S1474-4422(10)70194-0

Eriksen, B.A., Eriksen, C.W., 1974. Effects of noise letters upon the identification of a target letter in a nonsearch task. Percept. Psychophys. 16, 143–149. https://doi.org/10.3758/BF03203267

Erskine, D., Taylor, J.P., Firbank, M.J., Patterson, L., Onofrj, M., O'Brien, J.T., McKeith, I.G., Attems, J., Thomas, A.J., Morris, C.M., Khundakar, A.A., 2015. Changes to the lateral geniculate nucleus in Alzheimer's disease but not dementia with Lewy bodies. Neuropathol. Appl. Neurobiol. 44, n/a-n/a. https://doi.org/10.1111/nan.12249

Escandon, A., Al-Hammadi, N., Galvin, J.E., 2010. Effect of cognitive fluctuation on neuropsychological performance in aging and dementia. Neurology 74, 210–217. https://doi.org/10.1212/WNL.0b013e3181ca017d

Esposito, R., Cieri, F., Chiacchiaretta, P., Cera, N., Lauriola, M., Di Giannantonio, M., Tartaro, A., Ferretti, A., 2017. Modifications in resting state functional anticorrelation between default mode network and dorsal attention network: comparison among young adults, healthy elders and mild cognitive impairment patients. Brain Imaging Behav. 1–15. https://doi.org/10.1007/s11682-017-9686-y

Fahn, S., Elton, R., 1987. Members of the UPDRS development committee. Recent Dev. Park. Dis. 2, 153.

Faisal, A.A., Selen, L.P.J., Wolpert, D.M., 2008. Noise in the nervous system. Nat. Rev. Neurosci. 9, 292–303. https://doi.org/10.1038/nrn2258

Fan, J., Byrne, J., Worden, M.S., Guise, K.G., McCandliss, B.D., Fossella, J., Posner, M.I., 2007. The Relation of Brain Oscillations to Attentional Networks. J. Neurosci. 27, 6197–6206. https://doi.org/10.1523/jneurosci.1833-07.2007

Fan, J., McCandliss, B.D., Fossella, J., Flombaum, J.I., Posner, M.I., 2005. The activation of attentional networks. Neuroimage 26, 471–479. https://doi.org/10.1016/j.neuroimage.2005.02.004

Fan, J., McCandliss, B.D., Sommer, T., Raz, A., Posner, M.I., 2002. Testing the efficiency and independence of attentional networks. J. Cogn. Neurosci. 14, 340–347. https://doi.org/10.1162/089892902317361886

Faust, M.E., Balota, D.A., 1997. Inhibition of return and visuospatial attention in healthy older adults and individuals with dementia of the Alzheimer type. Neuropsychology 11, 13–29. https://doi.org/10.1037/0894-4105.11.1.13

Ferman, T.J., Arvanitakis, Z., Fujishiro, H., Duara, R., Parfitt, F., Purdy, M., Waters, C., Barker, W., Graff-Radford, N.R., Dickson, D.W., 2013a. Pathology and temporal onset of visual hallucinations, misperceptions and family misidentification distinguishes dementia with Lewy bodies from Alzheimer's disease. Parkinsonism Relat. Disord. 19, 227–231. https://doi.org/10.1016/j.parkreldis.2012.10.013

Ferman, T.J., Boeve, B.F., Smith, G.E., Lin, S.-C., Silber, M.H., Pedraza, O., Wszolek, Z., Graff-Radford, N.R., Uitti, R., Van Gerpen, J., Pao, W., Knopman, D., Pankratz, V.S., Kantarci, K., Boot, B., Parisi, J.E., Dugger, B.N., Fujishiro, H., Petersen, R.C., Dickson, D.W., 2011. Inclusion of RBD improves the diagnostic classification of dementia with Lewy bodies. Neurology 77, 875–882. https://doi.org/10.1212/WNL.0b013e31822c9148

Ferman, T.J., Smith, G.E., Boeve, B.F., Graff-Radford, N.R., Lucas, J.A., Knopman, D.S., Petersen, R.C., Ivnik, R.J., Wszolek, Z., Uitti, R., Dickson, D.W., 2006. Neuropsychological Differentiation of Dementia with Lewy Bodies from Normal Aging and Alzheimer's Disease. Clin. Neuropsychol. 20, 623–636. https://doi.org/10.1080/13854040500376831

Ferman, T.J., Smith, G.E., Boeve, B.F., Ivnik, R.J., Petersen, R.C., Knopman, D., Graff-Radford, N., Parisi, J., Dickson, D.W., 2004. DLB fluctuations: Specific features that reliably differentiate DLB from AD and normal aging. Neurology 62, 181–187. https://doi.org/10.1212/WNL.62.2.181

Ferman, T.J., Smith, G.E., Dickson, D.W., Graff-Radford, N.R., Lin, S., Wszolek, Z., Van Gerpen, J.A., Uitti, R., Knopman, D.S., Petersen, R.C., Parisi, J.E., Silber, M.H., Boeve, B.F., 2014. Abnormal daytime sleepiness in dementia with Lewy bodies compared to Alzheimer's disease using the Multiple Sleep Latency Test. Alzheimers. Res. Ther. 6, 76. https://doi.org/10.1186/s13195-014-0076-z

Ferman, T.J., Smith, G.E., Kantarci, K., Boeve, B.F., Pankratz, V.S., Dickson, D.W., Graff-Radford, N.R., Wszolek, Z., Gerpen, J. Van, Uitti, R., Pedraza, O., Murray, M.E., Aakre,

J., Parisi, J., Knopman, D.S., Petersen, R.C., 2013b. Nonamnestic mild cognitive impairment progresses to dementia with Lewy bodies. Neurology 81, 2032–2038. https://doi.org/10.1212/01.wnl.0000436942.55281.47

Fernandez-Duque, D., Black, S.E., 2006. Attentional networks in normal aging and Alzheimer's disease. Neuropsychology 20, 133–143. https://doi.org/10.1037/0894-4105.20.2.133

Fields, J.A., 2017. Cognitive and Neuropsychiatric Features in Parkinson's and Lewy Body Dementias. Arch. Clin. Neuropsychol. 32, 786–801. https://doi.org/10.1093/arclin/acx085

Filoteo, J.V., Salmon, D.P., Schiehser, D.M., Kane, A.E., Hamilton, J.M., Rilling, L.M., Lucas, J.A., Zizak, V., Galasko, D.R., 2009. Verbal learning and memory in patients with dementia with Lewy bodies or Parkinson's disease with dementia. J. Clin. Exp. Neuropsychol. 31, 823–834. https://doi.org/10.1080/13803390802572401

Firbank, M.J., Colloby, S.J., Burn, D.J., McKeith, I.G., O'Brien, J.T., 2003. Regional cerebral blood flow in Parkinson's disease with and without dementia. Neuroimage 20, 1309–1319. https://doi.org/10.1016/S1053-8119(03)00364-1

Firbank, M.J., Kobeleva, X., Cherry, G., Killen, A., Gallagher, P., Burn, D.J., Thomas, A.J., O'Brien, J.T., Taylor, J.-P., 2016. Neural correlates of attention-executive dysfunction in lewy body dementia and Alzheimer's disease. Hum. Brain Mapp. 37, 1254–1270. https://doi.org/10.1002/hbm.23100

Firbank, M.J., O'Brien, J.T., Taylor, J.P., 2018. Long reaction times are associated with delayed brain activity in lewy body dementia. Hum. Brain Mapp. 39, 633–643. https://doi.org/10.1002/hbm.23866

Folstein, M.F., Folstein, S.E., McHugh, P.R., 1975. "Mini-mental state". A practical method for grading the cognitive state of patients for the clinician. J. Psychiatr. Res. 12, 189–198. https://doi.org/10.1016/0022-3956(75)90026-6

Forno, L.S., Barbour, P.J., Norville, R.L., 1978. Presenile Dementia with Lewy Bodies and Neurofibrillary Tangles. Arch. Neurol. 35, 818–822. https://doi.org/10.1001/archneur.1978.00500360042008

Foster, E.R., Campbell, M.C., Burack, M.A., Hartlein, J., Flores, H.P., Cairns, N.J., Hershey, T., Perlmutter, J.S., 2010. Amyloid imaging of Lewy body-associated disorders. Mov.

Disord. 25, 2516–2523. https://doi.org/10.1002/mds.23393

Fox, M.D., Raichle, M.E., 2007. Spontaneous fluctuations in brain activity observed with functional magnetic resonance imaging. Nat. Rev. Neurosci. 8, 700–711. https://doi.org/10.1038/nrn2201

Fox, M.D., Snyder, A.Z., Vincent, J.L., Corbetta, M., Van Essen, D.C., Raichle, M.E., 2005. The human brain is intrinsically organized into dynamic, anticorrelated functional networks. Proc. Natl. Acad. Sci. 102, 9673–9678. https://doi.org/10.1073/pnas.0504136102

Fox, M.D., Zhang, D., Snyder, A.Z., Raichle, M.E., 2009. The Global Signal and Observed Anticorrelated Resting State Brain Networks. J. Neurophysiol. 101, 3270–3283. https://doi.org/10.1152/jn.90777.2008

Franciotti, R., Falasca, N.W., Bonanni, L., Anzellotti, F., Maruotti, V., Comani, S., Thomas, A., Tartaro, A., Taylor, J.-P., Onofrj, M., 2013. Default network is not hypoactive in dementia with fluctuating cognition: an Alzheimer disease/dementia with Lewy bodies comparison. Neurobiol. Aging 34, 1148–1158. https://doi.org/10.1016/j.neurobiolaging.2012.09.015

Freund, H.-J., Kuhn, J., Lenartz, D., Mai, J., Schnell, T., Klosterkoetter, J., Sturm, V., 2009. Cognitive functions in a patient with parkinson-dementia syndrome undergoing deep-brain stimulation. Arch.Neurol. 66, 781–785.

Friedman, J.H., 2018. Dementia with Lewy Bodies and Parkinson Disease Dementia: It is the Same Disease! Park. Relat. Disord. 46, S6–S9. https://doi.org/10.1016/j.parkreldis.2017.07.013

Frigerio, R., Fujishiro, H., Ahn, T.-B., Josephs, K.A., Maraganore, D.M., DelleDonne, A., Parisi, J.E., Klos, K.J., Boeve, B.F., Dickson, D.W., Ahlskog, J.E., 2011. Incidental Lewy body disease: Do some cases represent a preclinical stage of dementia with Lewy bodies? Neurobiol. Aging 32, 857–863. https://doi.org/10.1016/j.neurobiolaging.2009.05.019

Fuentes, L.J., Fernández, P.J., Campoy, G., Antequera, M.M., García-Sevilla, J., Antúnez, C., 2010. Attention network functioning in patients with dementia with lewy bodies and Alzheimer's disease. Dement. Geriatr. Cogn. Disord. 29, 139–145. https://doi.org/10.1159/000275672

Fujishiro, H., Ferman, T.J., Boeve, B.F., Smith, G.E., Graff-Radford, N.R., Uitti, R.J., Wszolek, Z.K., Knopman, D.S., Petersen, R.C., Parisi, J.E., Dickson, D.W., 2008. Validation of the Neuropathologic Criteria of the Third Consortium for Dementia With Lewy Bodies for Prospectively Diagnosed Cases. J. Neuropathol. Exp. Neurol. 67, 649–656. https://doi.org/10.1097/NEN.0b013e31817d7a1d

Fujishiro, H., Iseki, E., Kasanuki, K., Chiba, Y., Ota, K., Murayama, N., Sato, K., 2013. A follow up study of non-demented patients with primary visual cortical hypometabolism: Prodromal dementia with Lewy bodies. J. Neurol. Sci. 334, 48–54. https://doi.org/10.1016/j.jns.2013.07.013

Galvin, J.E., Price, J.L., Yan, Z., Morris, J.C., Sheline, Y.I., 2011. Resting bold fMRI differentiates dementia with Lewy bodies vs Alzheimer disease. Neurology 76, 1797–1803. https://doi.org/10.1212/WNL.0b013e31821ccc83

Garrett, D.D., Epp, S.M., Perry, A., Lindenberger, U., 2018. Local temporal variability reflects functional integration in the human brain. Neuroimage 184739. https://doi.org/10.1016/j.neuroimage.2018.08.019

Garrett, D.D., Kovacevic, N., McIntosh, A.R., Grady, C.L., 2013a. The Modulation of BOLD Variability between Cognitive States Varies by Age and Processing Speed. Cereb. Cortex 23, 684–693. https://doi.org/10.1093/cercor/bhs055

Garrett, D.D., Kovacevic, N., McIntosh, A.R., Grady, C.L., 2011. The Importance of Being Variable. J. Neurosci. 31, 4496–4503. https://doi.org/10.1523/JNEUROSCI.5641-10.2011

Garrett, D.D., Samanez-Larkin, G.R., MacDonald, S.W.S., Lindenberger, U., McIntosh, A.R., Grady, C.L., 2013b. Moment-to-moment brain signal variability: A next frontier in human brain mapping? Neurosci. Biobehav. Rev. 37, 610–624. https://doi.org/10.1016/j.neubiorev.2013.02.015

Ghosh, A., Rho, Y., McIntosh, A.R., Kötter, R., Jirsa, V.K., 2008. Noise during Rest Enables the Exploration of the Brain's Dynamic Repertoire. PLoS Comput. Biol. 4, e1000196. https://doi.org/10.1371/journal.pcbi.1000196

Gibb, W.R.G., Esiri, M.M., Lees, A.J., 1987. Clinical and pathological features of diffuse cortical Lewy body disease (Lewy body dementia). Brain 110, 1131–1153. https://doi.org/10.1093/brain/110.5.1131

Goldberger, A.L., Amaral, L.A.N., Hausdorff, J.M., Ivanov, P.C., Peng, C.-K., Stanley, H.E., 2002. Fractal dynamics in physiology: Alterations with disease and aging. Proc. Natl. Acad. Sci. 99, 2466–2472. https://doi.org/10.1073/pnas.012579499

Gomperts, S.N., Rentz, D.M., Moran, E., Becker, J.A., Locascio, J.J., Klunk, W.E., Mathis, C.A., Elmaleh, D.R., Shoup, T., Fischman, A.J., Hyman, B.T., Growdon, J.H., Johnson, K.A., 2008. Imaging amyloid deposition in Lewy body diseases. Neurology 71, 903–910. https://doi.org/10.1212/01.wnl.0000326146.60732.d6

Grady, C.L., Garrett, D.D., 2018. Brain signal variability is modulated as a function of internal and external demand in younger and older adults. Neuroimage 169, 510–523. https://doi.org/10.1016/j.neuroimage.2017.12.031

Graff-Radford, J., Boeve, B.F., Murray, M.E., Ferman, T.J., Tosakulwong, N., Lesnick, T.G., Maroney-Smith, M., Senjem, M.L., Gunter, J., Smith, G.E., Knopman, D.S., Jack, C.R., Dickson, D.W., Petersen, R.C., Kantarci, K., 2014a. Regional proton magnetic resonance spectroscopy patterns in dementia with Lewy bodies. Neurobiol. Aging 35, 1483–1490. https://doi.org/10.1016/j.neurobiolaging.2014.01.001

Graff-Radford, J., Lesnick, T.G., Boeve, B.F., Przybelski, S.A., Jones, D.T., Senjem, M.L., Gunter, J.L., Ferman, T.J., Knopman, D.S., Murray, M.E., Dickson, D.W., Sarro, L., Jack, C.R., Petersen, R.C., Kantarci, K., 2016. Predicting Survival in Dementia With Lewy Bodies With Hippocampal Volumetry. Mov. Disord. 31, 989–994. https://doi.org/10.1002/mds.26666

Graff-Radford, J., Murray, M.E., Lowe, V.J., Boeve, B.F., Ferman, T.J., Przybelski, S.A., Lesnick, T.G., Senjem, M.L., Gunter, J.L., Smith, G.E., Knopman, D.S., Jack, C.R., Dickson, D.W., Petersen, R.C., Kantarci, K., 2014b. Dementia with Lewy bodies: Basis of cingulate island sign. Neurology 83, 801–809. https://doi.org/10.1212/WNL.0000000000000734

Gratwicke, J., Jahanshahi, M., Foltynie, T., 2015. Parkinson's disease dementia: a neural networks perspective. Brain 138, 1454–1476. https://doi.org/10.1093/brain/awv104

Gratwicke, J., Zrinzo, L., Kahan, J., Peters, A., Beigi, M., Akram, H., Hyam, J., Oswal, A., Day, B., Mancini, L., Thornton, J., Yousry, T., Limousin, P., Hariz, M., Jahanshahi, M., Foltynie, T., 2018. Bilateral deep brain stimulation of the nucleus basalis of meynert for Parkinson disease dementia a randomized clinical trial. JAMA Neurol. 75, 169–178. https://doi.org/10.1001/jamaneurol.2017.3762

Greicius, M.D., Krasnow, B., Reiss, A.L., Menon, V., 2003. Functional connectivity in the resting brain: A network analysis of the default mode hypothesis. Proc. Natl. Acad. Sci. 100, 253–258. https://doi.org/10.1073/pnas.0135058100

Greicius, M.D., Srivastava, G., Reiss, A.L., Menon, V., 2004. Default-mode network activity distinguishes Alzheimer's disease from healthy aging: evidence from functional MRI. Proc. Natl. Acad. Sci. U. S. A. 101, 4637–42. https://doi.org/10.1073/pnas.0308627101

Greicius, M.D., Supekar, K., Menon, V., Dougherty, R.F., 2009. Resting-State Functional Connectivity Reflects Structural Connectivity in the Default Mode Network. Cereb. Cortex 19, 72–78. https://doi.org/10.1093/cercor/bhn059

Grieder, M., Koenig, T., Kinoshita, T., Utsunomiya, K., Wahlund, L.O., Dierks, T., Nishida, K., 2016. Discovering EEG resting state alterations of semantic dementia. Clin. Neurophysiol. 127, 2175–2181. https://doi.org/10.1016/j.clinph.2016.01.025

Griffanti, L., Rolinski, M., Szewczyk-Krolikowski, K., Menke, R.A., Filippini, N., Zamboni, G., Jenkinson, M., Hu, M.T.M., Mackay, C.E., 2016. Challenges in the reproducibility of clinical studies with resting state fMRI: An example in early Parkinson's disease. Neuroimage 124, 704–713. https://doi.org/10.1016/j.neuroimage.2015.09.021

Grothe, M.J., Schuster, C., Bauer, F., Heinsen, H., Prudlo, J., Teipel, S.J., 2014. Atrophy of the cholinergic basal forebrain in dementia with Lewy bodies and Alzheimer's disease dementia. J. Neurol. 1939–1948. https://doi.org/10.1007/s00415-014-7439-z

Guitart-Masip, M., Salami, A., Garrett, D., Rieckmann, A., Lindenberger, U., Bäckman, L., 2016. BOLD Variability is Related to Dopaminergic Neurotransmission and Cognitive Aging. Cereb. Cortex 26, 2074–2083. https://doi.org/10.1093/cercor/bhv029

Gusnard, D.A., Raichle, M.E., 2001. Searching for a baseline: Functional imaging and the resting human brain. Nat. Rev. Neurosci. 2, 685–694. https://doi.org/10.1038/35094500

Halliday, G.M., McCann, H., 2010. The progression of pathology in Parkinson's disease. Ann. N. Y. Acad. Sci. 1184, 188–195. https://doi.org/10.1111/j.1749-6632.2009.05118.x

Hanyu, H., Shimizu, S., Tanaka, Y., Hirao, K., Iwamoto, T., Abe, K., 2007. MR features of the substantia innominata and therapeutic implications in dementias. Neurobiol. Aging 28, 548–554. https://doi.org/10.1016/j.neurobiolaging.2006.02.009

Hanyu, H., Tanaka, Y., Shimizu, S., Sakurai, H., Iwamoto, T., Abe, K., 2005. Differences in MR features of the substantia innominata between dementia with Lewy bodies and

Alzheimer's disease. J. Neurol. 252, 482–484. https://doi.org/10.1007/s00415-005-0611-8

Hao, L., Sang, N., Du, X., Qiu, J., Wei, D., Chen, X., 2015. Examining brain structures associated with attention networks in a large sample of young adults: a voxel-based morphometry study. Sci. Bull. 60, 1824–1832. https://doi.org/10.1007/s11434-015-0910-0

Harding, A.J., Broe, G.A., Halliday, G.M., 2002. Visual hallucinations in Lewy body disease relate to Lewy bodies in the temporal lobe. Brain 125, 391–403. https://doi.org/10.1093/brain/awf033

Harding, A.J., Halliday, G.M., 2001. Cortical Lewy body pathology in the diagnosis of dementia. Acta Neuropathol. 102, 355–63. https://doi.org/10.1007/s004010100390

Hattori, T., Orimo, S., Aoki, S., Ito, K., Abe, O., Amano, A., Sato, R., Sakai, K., Mizusawa, H., 2012. Cognitive status correlates with white matter alteration in Parkinson's disease. Hum. Brain Mapp. 33, 727–739. https://doi.org/10.1002/hbm.21245

He, B.J., 2011. Scale-Free Properties of the Functional Magnetic Resonance Imaging Signal during Rest and Task. J. Neurosci. 31, 13786–13795. https://doi.org/10.1523/JNEUROSCI.2111-11.2011

Henderson, J.M., Carpenter, K., Cartwright, H., Halliday, G.M., 2000. Degeneration of the centré median-parafascicular complex in Parkinson's disease. Ann. Neurol. 47, 345–352. https://doi.org/10.1002/1531-8249(200003)47:3<345::AID-ANA10>3.0.CO;2-V

Hervey, A.S., Epstein, J.N., Curry, J.F., Tonev, S., Eugene Arnold, L., Keith Conners, C., Hinshaw, S.P., Swanson, J.M., Hechtman, L., 2006. Reaction Time Distribution Analysis of Neuropsychological Performance in an ADHD Sample. Child Neuropsychol. 12, 125–140. https://doi.org/10.1080/09297040500499081

Hesse, J., Gross, T., 2014. Self-organized criticality as a fundamental property of neural systems. Front. Syst. Neurosci. 8, 1–14. https://doi.org/10.3389/fnsys.2014.00166

Hindriks, R., Adhikari, M.H., Murayama, Y., Ganzetti, M., Mantini, D., Logothetis, N.K., Deco, G., 2016. Can sliding-window correlations reveal dynamic functional connectivity in resting-state fMRI? Neuroimage 127, 242–256. https://doi.org/10.1016/j.neuroimage.2015.11.055

Honey, C.J., Sporns, O., Cammoun, L., Gigandet, X., Thiran, J.P., Meuli, R., Hagmann, P.,

2009. Predicting human resting-state functional connectivity from structural connectivity. Proc. Natl. Acad. Sci. 106, 2035–2040. https://doi.org/10.1073/pnas.0811168106

Howlett, D.R., Whitfield, D., Johnson, M., Attems, J., O'Brien, J.T., Aarsland, D., Lai, M.K.P., Lee, J.H., Chen, C., Ballard, C.G., Hortobágyi, T., Francis, P.T., 2015. Regional Multiple Pathology Scores Are Associated with Cognitive Decline in Lewy Body Dementias. Brain Pathol. 25, 401–408. https://doi.org/10.1111/bpa.12182

Hurtig, H.I., Trojanowski, J.Q., Galvin, J., Ewbank, D., Schmidt, M.L., Lee, V.M.Y., Clark, C.M., Glosser, G., Stern, M.B., Gollomp, S.M., Arnold, S.E., 2000. α-synuclein cortical Lewy bodies correlate with dementia in Parkinson's disease. Neurology 54, 1916–1921.

Hutchison, R.M., Morton, J.B., 2015. Tracking the Brain's Functional Coupling Dynamics over Development. J. Neurosci. 35, 6849–6859. https://doi.org/10.1523/JNEUROSCI.4638-14.2015

Hutchison, R.M., Womelsdorf, T., Allen, E.A., Bandettini, P.A., Calhoun, V.D., Corbetta, M., Della Penna, S., Duyn, J.H., Glover, G.H., Gonzalez-Castillo, J., Handwerker, D.A., Keilholz, S.D., Kiviniemi, V., Leopold, D.A., de Pasquale, F., Sporns, O., Walter, M., Chang, C., 2013a. Dynamic functional connectivity: Promise, issues, and interpretations. Neuroimage 80, 360–378. https://doi.org/10.1016/j.neuroimage.2013.05.079

Hutchison, R.M., Womelsdorf, T., Gati, J.S., Everling, S., Menon, R.S., 2013b. Resting-state networks show dynamic functional connectivity in awake humans and anesthetized macaques. Hum. Brain Mapp. 34, 2154–2177. https://doi.org/10.1002/hbm.22058

Iizuka, T., Kameyama, M., 2016. Cingulate island sign on FDG-PET is associated with medial temporal lobe atrophy in dementia with Lewy bodies. Ann. Nucl. Med. 30, 421–429. https://doi.org/10.1007/s12149-016-1076-9

Imamura, T., Ishii, K., Hirono, N., Hashimoto, M., Tanimukai, S., Kazuai, H., Hanihara, T., Sasaki, M., Mori, E., 1999. Visual hallucinations and regional cerebral metabolism in dementia with Lewy bodies (DLB). Neuroreport 10, 1903–7.

Irwin, D.J., Grossman, M., Weintraub, D., Hurtig, H.I., Duda, J.E., Xie, S.X., Lee, E.B., Van Deerlin, V.M., Lopez, O.L., Kofler, J.K., Nelson, P.T., Jicha, G.A., Woltjer, R., Quinn, J.F., Kaye, J., Leverenz, J.B., Tsuang, D., Longfellow, K., Yearout, D., Kukull, W., Keene, C.D., Montine, T.J., Zabetian, C.P., Trojanowski, J.Q., 2017. Neuropathological and genetic correlates of survival and dementia onset in synucleinopathies: a

retrospective analysis. Lancet Neurol. 16, 55–65. https://doi.org/10.1016/S1474-4422(16)30291-5

Ishii, K., Imamura, T., Sasaki, M., Yamaji, S., Sakamoto, S., Kitagaki, H., Hashimoto, M., Hirono, N., Shimomura, T., Mori, E., 1998. Regional cerebral glucose metabolism in dementia with Lewy bodies and Alzheimer's disease. Neurology 51, 125–130. https://doi.org/10.1212/WNL.51.1.125

Jackson, J.D., Balota, D.A., Duchek, J.M., Head, D., 2012. White matter integrity and reaction time intraindividual variability in healthy aging and early-stage Alzheimer disease. Neuropsychologia 50, 357–366. https://doi.org/10.1016/j.neuropsychologia.2011.11.024

Janzen, J., van 't Ent, D., Lemstra, A.W., Berendse, H.W., Barkhof, F., Foncke, E.M.J., 2012. The pedunculopontine nucleus is related to visual hallucinations in Parkinson's disease: preliminary results of a voxel-based morphometry study. J. Neurol. 259, 147–154. https://doi.org/10.1007/s00415-011-6149-z

Jellinger, K.A., 2003. Neuropathological spectrum of synucleinopathies. Mov. Disord. 18, 2–12. https://doi.org/10.1002/mds.10557

Jellinger, K.A., Attems, J., 2006. Does striatal pathology distinguish Parkinson disease with dementia and dementia with Lewy bodies? Acta Neuropathol. 112, 253–260. https://doi.org/10.1007/s00401-006-0088-2

Jellinger, K.A., Korczyn, A.D., 2018. Are dementia with Lewy bodies and Parkinson's disease dementia the same disease? BMC Med. 16, 34. https://doi.org/10.1186/s12916-018-1016-8

Jeong, J., 2004. EEG dynamics in patients with Alzheimer's disease. Clin. Neurophysiol. 115, 1490–1505. https://doi.org/10.1016/j.clinph.2004.01.001

Jia, H., Hu, X., Deshpande, G., 2014. Behavioral Relevance of the Dynamics of the Functional Brain Connectome. Brain Connect. 4, 741–759. https://doi.org/10.1089/brain.2014.0300

Jicha, G.A., Schmitt, F.A., Abner, E., Nelson, P.T., Cooper, G.E., Smith, C.D., Markesbery, W.R., 2010. Prodromal clinical manifestations of neuropathologically confirmed Lewy body disease. Neurobiol. Aging 31, 1805–1813. https://doi.org/10.1016/j.neurobiolaging.2008.09.017

Johannsson, M., Snaedal, J., Johannesson, G.H., Gudmundsson, T.E., Johnsen, K., 2015. The Acetylcholine Index: An Electroencephalographic Marker of Cholinergic Activity in the Living Human Brain Applied to Alzheimer's Disease and Other Dementias. Dement. Geriatr. Cogn. Disord. 39, 132–142. https://doi.org/10.1159/000367889

Joki, H., Higashiyama, Y., Nakae, Y., Kugimoto, C., Doi, H., Kimura, K., Kishida, H., Ueda, N., Nakano, T., Takahashi, T., Koyano, S., Takeuchi, H., Tanaka, F., 2018. White matter hyperintensities on MRI in dementia with Lewy bodies, Parkinson's disease with dementia, and Alzheimer's disease. J. Neurol. Sci. 385, 99–104. https://doi.org/10.1016/j.jns.2017.12.018

Jones, D.T., Vemuri, P., Murphy, M.C., Gunter, J.L., Senjem, M.L., Machulda, M.M., Przybelski, S.A., Gregg, B.E., Kantarci, K., Knopman, D.S., Boeve, B.F., Petersen, R.C., Jr, C.R.J., 2012. Non-Stationarity in the '"Resting Brain's"' Modular Architecture. PLoS Biol. 7, e39731. https://doi.org/10.1371/journal.pone.0039731

Kaiser, R.H., Whitfield-Gabrieli, S., Dillon, D.G., Goer, F., Beltzer, M., Minkel, J., Smoski, M., Dichter, G., Pizzagalli, D.A., 2015. Dynamic Resting-State Functional Connectivity in Major Depression. Neuropsychopharmacology 41, 1–9. https://doi.org/10.1038/npp.2015.352

Kantarci, K., Avula, R., Senjem, M.L., Samikoglu, A.R., Zhang, B., Weigand, S.D., Przybelski, S.A., Edmonson, H.A., Vemuri, P., Knopman, D.S., Ferman, T.J., Boeve, B.F., Petersen, R.C., Jack, C.R., 2010. Dementia with Lewy bodies and Alzheimer disease: Neurodegenerative patterns characterized by DTI. Neurology 74, 1814–1821. https://doi.org/10.1212/WNL.0b013e3181e0f7cf

Kantarci, K., Graff-Radford, J., 2013. Magnetic resonance spectroscopy in Alzheimer's disease. Neuropsychiatr. Dis. Treat. 9, 687. https://doi.org/10.2147/NDT.S35440

Kantarci, K., Lowe, V.J., Boeve, B.F., Weigand, S.D., Senjem, M.L., Przybelski, S.A., Dickson, D.W., Parisi, J.E., Knopman, D.S., Smith, G.E., Ferman, T.J., Petersen, R.C., Jack, C.R., 2012. Multimodality imaging characteristics of dementia with Lewy bodies. Neurobiol. Aging 33, 2091–2105. https://doi.org/10.1016/j.neurobiolaging.2011.09.024

Kehagia, A.A., Barker, R.A., Robbins, T.W., 2012. Cognitive impairment in Parkinson's disease: The dual syndrome hypothesis. Neurodegener. Dis. 11, 79–92. https://doi.org/10.1159/000341998

Kehagia, A.A., Housden, C.R., Regenthal, R., Barker, R.A., Müller, U., Rowe, J., Sahakian,

B.J., Robbins, T.W., 2014. Targeting impulsivity in Parkinson's disease using atomoxetine. Brain 137, 1986–1997. https://doi.org/10.1093/brain/awu117

Kelly, R.E., Alexopoulos, G.S., Wang, Z., Gunning, F.M., Murphy, C.F., Morimoto, S.S., Kanellopoulos, D., Jia, Z., Lim, K.O., Hoptman, M.J., 2010. Visual inspection of independent components: Defining a procedure for artifact removal from fMRI data. J. Neurosci. Methods 189, 233–245. https://doi.org/10.1016/j.jneumeth.2010.03.028

Kemp, P.M., Hoffmann, S.A., Holmes, C., Bolt, L., Ward, T., Holmes, R.B., Fleming, J.S., 2005. The contribution of statistical parametric mapping in the assessment of precuneal and medial temporal lobe perfusion by 99mTc-HMPAO SPECT in mild Alzheimer's and Lewy body dementia. Nucl. Med. Commun. 26, 1099–1106. https://doi.org/10.1097/00006231-200512000-00009

Kenny, E.R., Blamire, A.M., Firbank, M.J., O'Brien, J.T., 2012. Functional connectivity in cortical regions in dementia with Lewy bodies and Alzheimer's disease. Brain 135, 569–581. https://doi.org/10.1093/brain/awr327

Kenny, E.R., Burton, E.J., O'Brien, J.T., 2008. A Volumetric Magnetic Resonance Imaging Study of Entorhinal Cortex Volume in Dementia with Lewy Bodies. Dement. Geriatr. Cogn. Disord. 26, 218–225. https://doi.org/10.1159/000153432

Kenny, E.R., O'Brien, J.T., Firbank, M.J., Blamire, A.M., 2013. Subcortical connectivity in dementia with Lewy bodies and Alzheimer's disease. Br. J. Psychiatry 203, 209–214. https://doi.org/10.1192/bjp.bp.112.108464

Khanna, A., Pascual-Leone, A., Farzan, F., 2014. Reliability of resting-state microstate features in electroencephalography. PLoS One 9, 1–21. https://doi.org/10.1371/journal.pone.0114163

Khanna, A., Pascual-Leone, A., Michel, C.M., Farzan, F., 2015. Microstates in resting-state EEG: current status and future directions. Neurosci. Biobehav. Rev. 49, 105–13. https://doi.org/10.1016/j.neubiorev.2014.12.010

Kikuchi, M., Koenig, T., Munesue, T., Hanaoka, A., Strik, W.K., Dierks, T., Koshino, Y., Minabe, Y., 2011. EEG Microstate Analysis in Drug-Naive Patients with Panic Disorder. PLoS One 6, e22912. https://doi.org/10.1371/journal.pone.0022912

Kim, J., Criaud, M., Cho, S.S., Díez-Cirarda, M., Mihaescu, A., Coakeley, S., Ghadery, C., Valli, M., Jacobs, M.F., Houle, S., Strafella, A.P., 2017. Abnormal intrinsic brain

functional network dynamics in Parkinson's disease. Brain 140, 2955–2967. https://doi.org/10.1093/brain/awx233

Klein, A., Andersson, J., Ardekani, B.A., Ashburner, J., Avants, B., Chiang, M.C., Christensen, G.E., Collins, D.L., Gee, J., Hellier, P., Song, J.H., Jenkinson, M., Lepage, C., Rueckert, D., Thompson, P., Vercauteren, T., Woods, R.P., Mann, J.J., Parsey, R. V., 2009. Evaluation of 14 nonlinear deformation algorithms applied to human brain MRI registration. Neuroimage 46, 786–802. https://doi.org/10.1016/j.neuroimage.2008.12.037

Klein, J.C., Eggers, C., Kalbe, E., Weisenbach, S., Hohmann, C., Vollmar, S., Baudrexel, S., Diederich, N.J., Heiss, W.D., Hilker, R., 2010. Neurotransmitter changes in dementia with Lewy bodies and Parkinson disease dementia in vivo. Neurology 74, 885–892. https://doi.org/10.1212/WNL.0b013e3181d55f61

Kobeleva, X., Firbank, M., Peraza, L.R., Gallagher, P., Thomas, A., Burn, D.J., O'Brien, J.T., Taylor, J.-P., 2017. Divergent functional connectivity during attentional processing in Lewy body dementia and Alzheimer's disease. Cortex 92, 8–18. https://doi.org/10.1016/j.cortex.2017.02.016

Koenig, T., Kottlow, M., Stein, M., Melie-García, L., 2011. Ragu: A free tool for the analysis of EEG and MEG event-related scalp field data using global randomization statistics. Comput. Intell. Neurosci. 2011, 1–14. https://doi.org/10.1155/2011/938925

Koenig, T., Lehmann, D., Merlo, M.C.G., Kochi, K., Hell, D., Koukkou, M., 1999. A deviant EEG brain microstate in acute, neuroleptic-naive schizophrenics at rest. Eur. Arch. Psychiatry Clin. Neurosci. 249, 205–211. https://doi.org/10.1007/s004060050088

Kotagal, V., Müller, M.L.T.M., Kaufer, D.I., Koeppe, R.A., Bohnen, N.I., 2012. Thalamic cholinergic innervation is spared in Alzheimer disease compared to parkinsonian disorders. Neurosci. Lett. 514, 169–172. https://doi.org/10.1016/j.neulet.2012.02.083

Kövari, E., Gold, G., Herrmann, F.R., Canuto, A., Hof, P.R., Bouras, C., Giannakopoulos, P., 2003. Lewy body densities in the entorhinal and anterior cingulate cortex predict cognitive deficits in Parkinson's disease. Acta Neuropathol. 106, 83–88. https://doi.org/10.1007/s00401-003-0705-2

Kövari, E., Horvath, J., Bouras, C., 2009. Neuropathology of Lewy body disorders. Brain Res. Bull. 80, 203–210. https://doi.org/10.1016/j.brainresbull.2009.06.018

Kramer, M.L., Schulz-Schaeffer, W.J., 2007. Presynaptic -Synuclein Aggregates, Not Lewy

Bodies, Cause Neurodegeneration in Dementia with Lewy Bodies. J. Neurosci. 27, 1405–1410. https://doi.org/10.1523/JNEUROSCI.4564-06.2007

Kraybill, M.L., Larson, E.B., Tsuang, D.W., Teri, L., McCormick, W.C., Bowen, J.D., Kukull, W.A., Leverenz, J.B., Cherrier, M.M., 2005. Cognitive differences in dementia patients with autopsy-verified AD, Lewy body pathology, or both. Neurology 64, 2069–2073. https://doi.org/10.1212/01.WNL.0000165987.89198.65

Kucyi, A., Hove, M.J., Esterman, M., Hutchison, R.M., Valera, E.M., 2017. Dynamic Brain Network Correlates of Spontaneous Fluctuations in Attention. Cereb. Cortex 27, 1831–1840. https://doi.org/10.1093/cercor/bhw029

Kulisevsky, J., Avila, A., Barbanoj, M., Antonijoan, R., Berthier, M.L., Gironell, A., 1996. Acute effects of levodopa on neuropsychological performance in stable and fluctuating Parkinson ' s disease patients at different levodopa plasma levels. Brain 119, 2121–2132.

Lacouture, Y., Cousineau, D., 2008. How to use MATLAB to fit the ex-Gaussian and other probability functions to a distribution of response times. Tutor. Quant. Methods Psychol. 4, 35–45.

Latora, V., Marchiori, M., 2001. Efficient Behavior of Small-World Networks. Phys. Rev. Lett. 87, 198701. https://doi.org/10.1103/PhysRevLett.87.198701

Laumann, T.O., Snyder, A.Z., Mitra, A., Gordon, E.M., Gratton, C., Adeyemo, B., Gilmore, A.W., Nelson, S.M., Berg, J.J., Greene, D.J., McCarthy, J.E., Tagliazucchi, E., Laufs, H., Schlaggar, B.L., Dosenbach, N.U.F., Petersen, S.E., 2016. On the Stability of BOLD fMRI Correlations. Cereb. Cortex 27, 4719–4732. https://doi.org/10.1093/cercor/bhw265

Lee, D.R., McKeith, I.G., Mosimann, U., Ghosh-Nodial, A., Grayson, L., Wilson, B., Thomas, A.J., 2014. The Dementia Cognitive Fluctuation Scale, a New Psychometric Test for Clinicians to Identify Cognitive Fluctuations in People with Dementia. Am. J. Geriatr. Psychiatry 22, 926–935. https://doi.org/10.1016/j.jagp.2013.01.072

Lee, D.R., McKeith, I.G., Mosimann, U., Ghosh-Nodyal, A., Thomas, A.J., 2013. Examining carer stress in dementia: The role of subtype diagnosis and neuropsychiatric symptoms. Int. J. Geriatr. Psychiatry 28, 135–141. https://doi.org/10.1002/gps.3799

Lee, D.R., Taylor, J.-P., Thomas, A.J., 2012. Assessment of cognitive fluctuation in dementia: a systematic review of the literature. Int. J. Geriatr. Psychiatry 27, 989–998. https://doi.org/10.1002/gps.2823

Lee, J.E., Park, B., Song, S.K., Sohn, Y.H., Park, H.-J., Lee, P.H., 2010. A comparison of gray and white matter density in patients with Parkinson's disease dementia and dementia with Lewy bodies using voxel-based morphometry. Mov. Disord. 25, 28–34. https://doi.org/10.1002/mds.22858

Lehmann, B.C.L., White, S.R., Henson, R.N., Cam-CAN, Geerligs, L., 2017. Assessing dynamic functional connectivity in heterogeneous samples. Neuroimage 157, 635–647. https://doi.org/10.1016/j.neuroimage.2017.05.065

Lehmann, D., 1990. Brain Electric Microstates and Cognition: The Atoms of Thought. Mach. Mind 209–224. https://doi.org/10.1007/978-1-4757-1083-0_10

Lehmann, D., Faber, P.L., Galderisi, S., Herrmann, W.M., Kinoshita, T., Koukkou, M., Mucci, A., Pascual-Marqui, R.D., Saito, N., Wackermann, J., Winterer, G., Koenig, T., 2005. EEG microstate duration and syntax in acute, medication-naïve, first-episode schizophrenia: a multi-center study. Psychiatry Res. Neuroimaging 138, 141–156. https://doi.org/10.1016/j.pscychresns.2004.05.007

Lehmann, D., Ozaki, H., Pal, I., 1987. EEG alpha map series: brain micro-states by space-oriented adaptive segmentation. Electroencephalogr. Clin. Neurophysiol. 67, 271–288. https://doi.org/10.1016/0013-4694(87)90025-3

Lehmann, D., Skrandies, W., 1980. Reference-free identification of components of checkerboard-evoked multichannel potential fields. Electroencephalogr. Clin. Neurophysiol. 48, 609–621. https://doi.org/10.1016/0013-4694(80)90419-8

Lemstra, A.W., de Beer, M.H., Teunissen, C.E., Schreuder, C., Scheltens, P., van der Flier, W.M., Sikkes, S.A.M., 2017. Concomitant AD pathology affects clinical manifestation and survival in dementia with Lewy bodies. J. Neurol. Neurosurg. Psychiatry 88, 113–118. https://doi.org/10.1136/jnnp-2016-313775

Li, R., Wu, X., Fleisher, A.S., Reiman, E.M., Chen, K., Yao, L., 2012. Attention-related networks in Alzheimer's disease: A resting functional MRI study. Hum. Brain Mapp. 33, 1076–1088. https://doi.org/10.1002/hbm.21269

Liégeois, R., Laumann, T.O., Snyder, A.Z., Zhou, J., Yeo, B.T.T., 2017. Interpreting temporal fluctuations in resting-state functional connectivity MRI. Neuroimage 1–19. https://doi.org/10.1016/j.neuroimage.2017.09.012

Lim, S.M., Katsifis, A., Villemagne, V.L., Best, R., Jones, G., Saling, M., Bradshaw, J.,

Merory, J., Woodward, M., Hopwood, M., Rowe, C.C., 2009. The 18F-FDG PET Cingulate Island Sign and Comparison to 123I- -CIT SPECT for Diagnosis of Dementia with Lewy Bodies. J. Nucl. Med. 50, 1638–1645. https://doi.org/10.2967/jnumed.109.065870

Lippa, C.F., Smith, T.W., Perry, E., 1999. Dementia with Lewy bodies: choline acetyltransferase parallels nucleus basalis pathology. J. Neural Transm. 106, 525–535. https://doi.org/10.1007/s007020050176

Lippa, S.M., Lippa, C.F., Mori, H., 2005. α-Synuclein aggregation in pathological aging and Alzheimer's disease: The impact of ß-amyloid plaque level. Am. J. Alzheimer's Dis. Other Dementiasr 20, 315–318. https://doi.org/10.1177/153331750502000506

Litvan, I., Bhatia, K.P., Burn, D.J., Goetz, C.G., Lang, A.E., McKeith, I.G., Quinn, N., Sethi, K.D., Shults, C., Wenning, G.K., 2003. SIC Task Force appraisal of clinical diagnostic criteria for parkinsonian disorders. Mov. Disord. 18, 467–486. https://doi.org/10.1002/mds.10459

Litvan, I., MacIntyre, A., Goetz, C.G., Wenning, G.K., Jellinger, K., Verny, M., Bartko, J.J., Jankovic, J., McKee, A., Brandel, J.P., Chaudhuri, K.R., Lai, E.C., D'Olhaberriague, L., Pearce, R.K.B., Agid, Y., 1998. Accuracy of the Clinical Diagnoses of Lewy Body Disease, Parkinson Disease, and Dementia With Lewy Bodies. Arch. Neurol. 55, 969. https://doi.org/10.1001/archneur.55.7.969

Liu, A.K.L., Chang, R.C.-C., Pearce, R.K.B., Gentleman, S.M., 2015. Nucleus basalis of Meynert revisited: anatomy, history and differential involvement in Alzheimer's and Parkinson's disease. Acta Neuropathol. 129, 527–540. https://doi.org/10.1007/s00401-015-1392-5

Lobotesis, K., Fenwick, J.D., Phipps, A., Ryman, A., Swann, A., Ballard, C.G., McKeith, I.G., O'Brien, J.T., 2001. Occipital hypoperfusion on SPECT in dementia with Lewy bodies but not AD. Neurology 56, 643–649. https://doi.org/10.1212/WNL.56.5.643

Lopes da Silva, F., 1991. Neural mechanisms underlying brain waves: from neural membranes to networks. Electroencephalogr. Clin. Neurophysiol. 79, 81–93. https://doi.org/10.1016/0013-4694(91)90044-5

Lopez, O.L., Becker, J.T., Kaufer, D.I., Hamilton, R.L., Sweet, R.A., Klunk, W., DeKosky, S.T., 2002. Research Evaluation and Prospective Diagnosis of Dementia With Lewy Bodies. Arch. Neurol. 59, 43. https://doi.org/10.1001/archneur.59.1.43

Lowe, M.J., Mock, B.J., Sorenson, J.A., 1998. Functional Connectivity in Single and Multislice Echoplanar Imaging Using Resting-State Fluctuations. Neuroimage 7, 119–132. https://doi.org/10.1006/nimg.1997.0315

Lowther, E.R., O'Brien, J.T., Firbank, M.J., Blamire, A.M., 2014. Lewy body compared with Alzheimer dementia is associated with decreased functional connectivity in resting state networks. Psychiatry Res. Neuroimaging 223, 192–201. https://doi.org/10.1016/j.pscychresns.2014.06.004

Mak, E., Su, L., Williams, G.B., O'Brien, J.T., 2014. Neuroimaging characteristics of dementia with Lewy bodies. Alzheimers. Res. Ther. 6, 18. https://doi.org/10.1186/alzrt248

Mak, E., Su, L., Williams, G.B., Watson, R., Firbank, M.J., Blamire, A.M., O'Brien, J.T., 2015a. Progressive cortical thinning and subcortical atrophy in dementia with Lewy bodies and Alzheimer's disease. Neurobiol. Aging 36, 1743–1750. https://doi.org/10.1016/j.neurobiolaging.2014.12.038

Mak, E., Su, L., Williams, G.B., Watson, R., Firbank, M.J., Blamire, A.M., O'Brien, J.T., 2015b. Longitudinal assessment of global and regional atrophy rates in Alzheimer's disease and dementia with Lewy bodies. NeuroImage Clin. 7, 456–462. https://doi.org/10.1016/j.nicl.2015.01.017

Marquand, A.F., Rezek, I., Buitelaar, J., Beckmann, C.F., 2016. Understanding Heterogeneity in Clinical Cohorts Using Normative Models: Beyond Case-Control Studies. Biol. Psychiatry 80, 552–561. https://doi.org/10.1016/j.biopsych.2015.12.023

Marquie, M., Locascio, J.J., Rentz, D.M., Becker, J.A., Hedden, T., Johnson, K.A., Growdon, J.H., Gomperts, S.N., 2014. Striatal and extrastriatal dopamine transporter levels relate to cognition in Lewy body diseases: an 11C altropane positron emission tomography study. Alzheimers. Res. Ther. 6, 52. https://doi.org/10.1186/s13195-014-0052-7

Marusak, H.A., Calhoun, V.D., Brown, S., Crespo, L.M., Sala-Hamrick, K., Gotlib, I.H., Thomason, M.E., 2016. Dynamic functional connectivity of neurocognitive networks in children. Hum. Brain Mapp. 00, 1–12. https://doi.org/10.1002/hbm.23346

McDonnell, M.D., Ward, L.M., 2011. The benefits of noise in neural systems: bridging theory and experiment. Nat. Rev. Neurosci. 12, 415–426. https://doi.org/10.1038/nrn3061

McIntosh, A.R., Kovacevic, N., Itier, R.J., 2008. Increased brain signal variability

accompanies lower behavioral variability in development. PLoS Comput. Biol. 4. https://doi.org/10.1371/journal.pcbi.1000106

McKeith, I.G., 2002. Dementia with Lewy bodies. Br. J. Psychiatry 180, 144–147. https://doi.org/10.1192/bjp.180.2.144

McKeith, I.G., Ballard, C.G., Perry, R.H., Ince, P.G., O'Brien, J.T., Neill, D., Lowery, K., Jaros, E., Barber, R., Thompson, P., Swann, A., Fairbairn, a F., Perry, E.K., 2000a. Prospective validation of Consensus criteria for the diagnosis of dementia with Lewy bodies. Neurology 54, 1050–1058. https://doi.org/10.1212/WNL.54.5.1050

McKeith, I.G., Boeve, B.F., Dickson, D.W., Halliday, G., Aarsland, D., Attems, J., Ballard, C.G., Bayston, A., Beach, T.G., Chen-plotkin, A., Singleton, A., Taylor, A., 2017. Diagnosis and management of dementia with Lewy bodies Fourth consensus report of the DLB Consortium. Neurology 0, 1–13.

McKeith, I.G., Del Ser, T., Spano, P., Emre, M., Wesnes, K.A., Anand, R., Cicin-Sain, A., Ferrara, R., Spiegel, R., 2000b. Efficacy of rivastigmine in dementia with Lewy bodies: a randomised, double-blind, placebo-controlled international study. Lancet 356, 2031–2036. https://doi.org/10.1016/S0140-6736(00)03399-7

McKeith, I.G., Dickson, D.W., Lowe, J., Emre, M., O'Brien, J.T., Feldman, H., Cummings, J., Duda, J.E., Lippa, C., Perry, E.K., Aarsland, D., Arai, H., Ballard, C.G., Boeve, B., Burn, D.J., Costa, D., Del Ser, T., Dubois, B., Galasko, D., Gauthier, S., Goetz, C.G., Gomez-Tortosa, E., Halliday, G., Hansen, L.A., Hardy, J., Iwatsubo, T., Kalaria, R.N., Kaufer, D., Kenny, R.A., Korczyn, A., Kosaka, K., Lee, V.M.Y., Lees, A., Litvan, I., Londos, E., Lopez, O.L., Minoshima, S., Mizuno, Y., Molina, J.A., Mukaetova-Ladinska, E.B., Pasquier, F., Perry, R.H., Schulz, J.B., Trojanowski, J.Q., Yamada, M., 2005. Diagnosis and management of dementia with Lewy bodies: Third report of the DLB consortium. Neurology 65, 1863–1872. https://doi.org/10.1212/01.wnl.0000187889.17253.b1

McKeith, I.G., Fairbairn, A., Perry, R., Thompson, P., Perry, E., 1992a. Neuroleptic sensitivity in patients with senile dementia of Lewy body type. BMJ 305, 673–678. https://doi.org/10.1136/bmj.305.6855.673

McKeith, I.G., Galasko, D., Kosaka, K., Perry, E.K., Dickson, D.W., Hansen, L.A., Salmon, D.P., Lowe, J., Mirra, S.S., Byrne, E.J., Lennox, G., Quinn, N.P., Edwardson, J.A., Ince, P.G., Bergeron, C., Burns, A., Miller, B.L., Lovestone, S., Collerton, D., Jansen, E.N.H.,

Ballard, C.G., de Vos, R.A.I., Wilcock, G.K., Jellinger, K.A., Perry, R.H., 1996. Consensus guidelines for the clinical and pathologic diagnosis of dementia with Lewy bodies (DLB): Report of the consortium on DLB international workshop. Neurology 47, 1113–1124. https://doi.org/10.1212/WNL.47.5.1113

McKeith, I.G., O'Brien, J.T., Walker, Z., Tatsch, K., Booij, J., Darcourt, J., Padovani, A., Giubbini, R., Bonuccelli, U., Volterrani, D., Holmes, C., Kemp, P.M., Tabet, N., Meyer, I., Reininger, C., 2007. Sensitivity and specificity of dopamine transporter imaging with 123I-FP-CIT SPECT in dementia with Lewy bodies: a phase III, multicentre study. Lancet Neurol. 6, 305–313. https://doi.org/10.1016/S1474-4422(07)70057-1

McKeith, I.G., Perry, R.H., Fairbairn, A.F., Jabeen, S., Perry, E.K., 1992b. Operational criteria for senile dementia of Lewy body type (SDLT). Psychol. Med. 22, 911. https://doi.org/10.1017/S0033291700038484

McKhann, G., Drachman, D., Folstein, M., Katzman, R., 1984. Clinical diagnosis of Alzheimer's disease: report of the NINCDS- ADRDA Work Group under the auspices of Department of Health and Human Services Task Force on Alzheimer's Disease. Neurology 34, 939–44. https://doi.org/10.3233/JAD-122299

McKhann, G.M., Knopman, D.S., Chertkow, H., Hyman, B.T., Jack, C.R., Kawas, C.H., Klunk, W.E., Koroshetz, W.J., Manly, J.J., Mayeux, R., Mohs, R.C., Morris, J.C., Rossor, M.N., Scheltens, P., Carrillo, M.C., Thies, B., Weintraub, S., Phelps, C.H., 2011. The diagnosis of dementia due to Alzheimer's disease: Recommendations from the National Institute on Aging-Alzheimer's Association workgroups on diagnostic guidelines for Alzheimer's disease. Alzheimer's Dement. 7, 263–269. https://doi.org/10.1016/j.jalz.2011.03.005

Mega, M.S., Masterman, D.L., Benson, D.F., Vinters, H. V, Tomiyasu, U., Craig, a H., Foti, D.J., Kaufer, D., Scharre, D.W., Fairbanks, L., Cummings, J.L., 1996. Dementia with Lewy bodies: Reliability and validity of clinical and pathologic criteria. Neurology 47, 1403–1409. https://doi.org/10.1212/WNL.47.6.1403

Mevel, K., Chételat, G., Eustache, F., Desgranges, B., 2011. The Default Mode Network in Healthy Aging and Alzheimer's Disease. Int. J. Alzheimers. Dis. 2011, 1–9. https://doi.org/10.4061/2011/535816

Michel, C.M., Koenig, T., 2017. EEG microstates as a tool for studying the temporal dynamics of whole-brain neuronal networks: A review. Neuroimage 1–17.

https://doi.org/10.1016/j.neuroimage.2017.11.062

Minoshima, S., Foster, N.L., Sima, A.A.F., Frey, K.A., Albin, R.L., Kuhl, D.E., 2001. Alzheimer's disease versus dementia with Lewy bodies: Cerebral metabolic distinction with autopsy confirmation. Ann. Neurol. 50, 358–365. https://doi.org/10.1002/ana.1133

Mišić, B., Mills, T., Taylor, M.J., McIntosh, A.R., 2010. Brain Noise Is Task Dependent and Region Specific. J. Neurophysiol. 104, 2667–2676. https://doi.org/10.1152/jn.00648.2010

Mišić, B., Vakorin, V.A., Kovačević, N., Paus, T., McIntosh, A.R., 2011. Extracting Message Inter-Departure Time Distributions from the Human Electroencephalogram. PLoS Comput. Biol. 7, e1002065. https://doi.org/10.1371/journal.pcbi.1002065

Mito, Y., Yoshida, K., Yabe, I., Makino, K., Hirotani, M., Tashiro, K., Kikuchi, S., Sasaki, H., 2005. Brain 3D-SSP SPECT analysis in dementia with Lewy bodies, Parkinson's disease with and without dementia, and Alzheimer's disease. Clin. Neurol. Neurosurg. 107, 396–403. https://doi.org/10.1016/j.clineuro.2004.12.005

Molano, J., Boeve, B., Ferman, T.J., Smith, G., Parisi, J., Dickson, D., Knopman, D., Graff-Radford, N., Geda, Y., Lucas, J., Kantarci, K., Shiung, M., Jack, C., Silber, M., Pankratz, V.S., Petersen, R., 2010. Mild cognitive impairment associated with limbic and neocortical lewy body disease: a clinicopathological study. Brain 133, 540–556. https://doi.org/10.1093/brain/awp280

Molloy, S.A., McKeith, I.G., O'Brien, J.T., Burn, D.J., 2005. The role of levodopa in the management of dementia with Lewy bodies. J. Neurol. Neurosurg. Psychiatry 76, 1200–1203. https://doi.org/10.1136/jnnp.2004.052332

Molloy, S.A., Rowan, E.N., O'Brien, J.T., McKeith, I.G., Wesnes, K.A., Burn, D.J., 2006. Effect of levodopa on cognitive function in Parkinson's disease with and without dementia and dementia with Lewy bodies. J. Neurol. Neurosurg. Psychiatry 77, 1323–1328. https://doi.org/10.1136/jnnp.2006.098079

Mondon, K., Gochard, A., Marqué, A., Armand, A., Beauchamp, D., Prunier, C., Jacobi, D., De Toffol, B., Autret, A., Camus, V., Hommet, C., 2007. Visual recognition memory differentiates dementia with Lewy bodies and Parkinson's disease dementia. J Neurol Neurosurg Psychiatry 78, 738–741. https://doi.org/10.1136/jnnp.2006.104257

Mosimann, U.P., Mather, G., Wesnes, K.A., O'Brien, J.T., Burn, D.J., McKeith, I.G., 2004.

Visual perception in Parkinson disease dementia and dementia with Lewy bodies. Neurology 63, 2091–2096. https://doi.org/10.1212/01.WNL.0000145764.70698.4E

Mosimann, U.P., Rowan, E.N., Partington, C.E., Collerton, D., Littlewood, E., O'Brien, J.T., Burn, D.J., McKeith, I.G., 2006. Characteristics of Visual Hallucinations in Parkinson Disease Dementia and Dementia With Lewy Bodies. Am. J. Geriatr. Psychiatry 14, 153–160. https://doi.org/10.1097/01.JGP.0000192480.89813.80

Murray, M.M., Brunet, D., Michel, C.M., 2008. Topographic ERP analyses: A step-by-step tutorial review. Brain Topogr. 20, 249–264. https://doi.org/10.1007/s10548-008-0054-5

Musso, F., Brinkmeyer, J., Mobascher, A., Warbrick, T., Winterer, G., 2010. Spontaneous brain activity and EEG microstates. A novel EEG/fMRI analysis approach to explore resting-state networks. Neuroimage 52, 1149–1161. https://doi.org/10.1016/j.neuroimage.2010.01.093

Nedelska, Z., Ferman, T.J., Boeve, B.F., Przybelski, S. a., Lesnick, T.G., Murray, M.E., Gunter, J.L., Senjem, M.L., Vemuri, P., Smith, G.E., Geda, Y.E., Graff-Radford, J., Knopman, D.S., Petersen, R.C., Parisi, J.E., Dickson, D.W., Jack, C.R., Kantarci, K., 2015. Pattern of brain atrophy rates in autopsy-confirmed dementia with Lewy bodies. Neurobiol. Aging 36, 452–461. https://doi.org/10.1016/j.neurobiolaging.2014.07.005

Nishida, K., Morishima, Y., Yoshimura, M., Isotani, T., Irisawa, S., Jann, K., Dierks, T., Strik, W.K., Kinoshita, T., Koenig, T., 2013. EEG microstates associated with salience and frontoparietal networks in frontotemporal dementia, schizophrenia and Alzheimer's disease. Clin. Neurophysiol. 124, 1106–1114. https://doi.org/10.1016/j.clinph.2013.01.005

Noe, E., Marder, K., Bell, K.L., Jacobs, D.M., Manly, J.J., Stern, Y., 2004. Comparison of dementia with Lewy bodies to Alzheimer's disease and Parkinson's disease with dementia. Mov. Disord. 19, 60–67. https://doi.org/10.1002/mds.10633

Noudoost, B., Moore, T., 2011. Control of visual cortical signals by prefrontal dopamine. Nature 474, 372–375. https://doi.org/10.1038/nature09995

O'Brien, J.T., Colloby, S.J., Fenwick, J., Williams, E.D., Firbank, M.J., Burn, D.J., Aarsland, D., McKeith, I.G., 2004. Dopamine Transporter Loss Visualized With FP-CIT SPECT in the Differential Diagnosis of Dementia With Lewy Bodies. Arch. Neurol. 61, 919. https://doi.org/10.1001/archneur.61.6.919

O'Brien, J.T., Firbank, M.J., Davison, C., Barnett, N., Bamford, C., Donaldson, C., Olsen, K., Herholz, K., Williams, D., Lloyd, J., 2014. 18F-FDG PET and Perfusion SPECT in the Diagnosis of Alzheimer and Lewy Body Dementias. J. Nucl. Med. 55, 1959–1965. https://doi.org/10.2967/jnumed.114.143347

O'Brien, J.T., Firbank, M.J., Mosimann, U.P., Burn, D.J., McKeith, I.G., 2005. Change in perfusion, hallucinations and fluctuations in consciousness in dementia with Lewy bodies. Psychiatry Res. Neuroimaging 139, 79–88. https://doi.org/10.1016/j.pscychresns.2005.04.002

Onofrj, M., Thomas, A., Iacono, D., Luciano, A.L., Di Iorio, A., 2003. The Effects of a Cholinesterase Inhibitor Are Prominent in Patients With Fluctuating Cognition: A Part 3 Study of the Main Mechanism of Cholinesterase Inhibitors in Dementia. Clin. Neuropharmacol. 26, 239–251. https://doi.org/10.1097/00002826-200309000-00008

Osaki, Y., Morita, Y., Fukumoto, M., Akagi, N., Yoshida, S., Doi, Y., 2005. Three-dimensional stereotactic surface projection SPECT analysis in Parkinson's disease with and without dementia. Mov. Disord. 20, 999–1005. https://doi.org/10.1002/mds.20463

Ossenkoppele, R., Cohn-Sheehy, B.I., La Joie, R., Vogel, J.W., Möller, C., Lehmann, M., Van Berckel, B.N.M., Seeley, W.W., Pijnenburg, Y.A., Gorno-Tempini, M.L., Kramer, J.H., Barkhof, F., Rosen, H.J., Van der Flier, W.M., Jagust, W.J., Miller, B.L., Scheltens, P., Rabinovici, G.D., 2015. Atrophy patterns in early clinical stages across distinct phenotypes of Alzheimer's disease. Hum. Brain Mapp. 36, 4421–4437. https://doi.org/10.1002/hbm.22927

Pao, W.C., Boeve, B.F., Ferman, T.J., Lin, S.-C., Smith, G.E., Knopman, D.S., Graff-Radford, N.R., Petersen, R.C., Parisi, J.E., Dickson, D.W., Silber, M.H., 2013. Polysomnographic Findings in Dementia With Lewy Bodies NIH Public Access. Neurologist 19, 1–6. https://doi.org/10.1097/NRL.0b013e31827c6bdd

Park, K.W., Kim, H.S., Cheon, S.-M., Cha, J.-K., Kim, S.-H., Kim, J.W., 2011. Dementia with Lewy Bodies versus Alzheimer's Disease and Parkinson's Disease Dementia: A Comparison of Cognitive Profiles. J. Clin. Neurol. 7, 19. https://doi.org/10.3988/jcn.2011.7.1.19

Parkes, L., Fulcher, B., Yücel, M., Fornito, A., 2018. An evaluation of the efficacy, reliability, and sensitivity of motion correction strategies for resting-state functional MRI. Neuroimage 171, 415–436. https://doi.org/10.1016/j.neuroimage.2017.12.073

Parkkinen, L., Kauppinen, T., Pirttilä, T., Autere, J.M., Alafuzoff, I., 2005. α-Synuclein pathology does not predict extrapyramidal symptoms or dementia. Ann. Neurol. 57, 82–91. https://doi.org/10.1002/ana.20321

Parkkinen, L., Pirttilä, T., Alafuzoff, I., 2008. Applicability of current staging/categorization of α-synuclein pathology and their clinical relevance. Acta Neuropathol. 115, 399–407. https://doi.org/10.1007/s00401-008-0346-6

Pedersen, M., Omidvarnia, A., Zalesky, A., Jackson, G.D., 2018. On the relationship between instantaneous phase synchrony and correlation-based sliding windows for time-resolved fMRI connectivity analysis. Neuroimage 181, 85–94. https://doi.org/10.1016/j.neuroimage.2018.06.020

Peraza, L.R., Colloby, S.J., Deboys, L., O'Brien, J.T., Kaiser, M., Taylor, J.-P., 2016. Regional functional synchronizations in dementia with Lewy bodies and Alzheimer's disease. Int. Psychogeriatrics 28, 1143–1151. https://doi.org/10.1017/S1041610216000429

Peraza, L.R., Colloby, S.J., Firbank, M.J., Greasy, G.S., McKeith, I.G., Kaiser, M., O'Brien, J.T., Taylor, J.-P., 2015a. Resting state in Parkinson's disease dementia and dementia with Lewy bodies: commonalities and differences. Int. J. Geriatr. Psychiatry 30, 1135–1146. https://doi.org/10.1002/gps.4342

Peraza, L.R., Cromarty, R.A., Kobeleva, X., Firbank, M.J., Killen, A., Graziadio, S., Thomas, A.J., O'Brien, J.T., Taylor, J.-P., 2018. Electroencephalographic derived network differences in Lewy body dementia compared to Alzheimer's disease patients. Sci. Rep. 8, 4637. https://doi.org/10.1038/s41598-018-22984-5

Peraza, L.R., Kaiser, M., Firbank, M., Graziadio, S., Bonanni, L., Onofrj, M., Colloby, S.J., Blamire, A., O'Brien, J., Taylor, J.P., 2014. FMRI resting state networks and their association with cognitive fluctuations in dementia with Lewy bodies. NeuroImage Clin. 4, 558–565. https://doi.org/10.1016/j.nicl.2014.03.013

Peraza, L.R., Taylor, J.-P., Kaiser, M., 2015b. Divergent brain functional network alterations in dementia with Lewy bodies and Alzheimer's disease. Neurobiol. Aging 36, 2458–2467. https://doi.org/10.1016/j.neurobiolaging.2015.05.015

Perneczky, R., Drzezga, A., Boecker, H., Förstl, H., Kurz, A., Häussermann, P., 2008. Cerebral Metabolic Dysfunction in Patients with Dementia with Lewy Bodies and Visual Hallucinations. Dement. Geriatr. Cogn. Disord. 25, 531–538.

https://doi.org/10.1159/000132084

Perry, E., Walker, M., Grace, J., Perry, R., 1999. Acetylcholine in mind: a neurotransmitter correlate of consciousness? Trends Neurosci. 22, 273–280. https://doi.org/10.1016/S0166-2236(98)01361-7

Petersen, R.C., 2004. Mild cognitive impairment as a diagnostic entity. J. Intern. Med. 256, 183–194. https://doi.org/10.1111/j.1365-2796.2004.01388.x

Pimlott, S.L., Piggott, M., Ballard, C.G., McKeith, I.G., Perry, R., Kometa, S., Owens, J., Wyper, D., Perry, E., 2006. Thalamic nicotinic receptors implicated in disturbed consciousness in dementia with Lewy bodies. Neurobiol. Dis. 21, 50–56. https://doi.org/10.1016/j.nbd.2005.06.008

Popescu, A., Lippa, C.F., Lee, V.M.-Y., Trojanowski, J.Q., 2004. Lewy Bodies in the Amygdala. Arch. Neurol. 61. https://doi.org/10.1001/archneur.61.12.1915

Poppe, A.B., Wisner, K., Atluri, G., Lim, K.O., Kumar, V., MacDonald, A.W., 2013. Toward a neurometric foundation for probabilistic independent component analysis of fMRI data. Cogn. Affect. Behav. Neurosci. 13, 641–659. https://doi.org/10.3758/s13415-013-0180-8

Posner, M.I., Petersen, S.E., 1990. The Attention System of the Human Brain. Annu. Rev. Neurosci. 13, 25–42. https://doi.org/10.1146/annurev.ne.13.030190.000325

Power, J.D., Barnes, K.A., Snyder, A.Z., Schlaggar, B.L., Petersen, S.E., 2012. Spurious but systematic correlations in functional connectivity MRI networks arise from subject motion. Neuroimage 59, 2142–2154. https://doi.org/10.1016/j.neuroimage.2011.10.018

Power, J.D., Schlaggar, B.L., Petersen, S.E., 2015. Recent progress and outstanding issues in motion correction in resting state fMRI. Neuroimage 105, 536–551. https://doi.org/10.1016/j.neuroimage.2014.10.044

Pruim, R.H.R., Mennes, M., Buitelaar, J.K., Beckmann, C.F., 2015a. Evaluation of ICA-AROMA and alternative strategies for motion artifact removal in resting state fMRI. Neuroimage 112, 278–287. https://doi.org/10.1016/j.neuroimage.2015.02.063

Pruim, R.H.R., Mennes, M., van Rooij, D., Llera, A., Buitelaar, J.K., Beckmann, C.F., 2015b. ICA-AROMA: A robust ICA-based strategy for removing motion artifacts from fMRI data. Neuroimage 112, 267–277. https://doi.org/10.1016/j.neuroimage.2015.02.064

Rae, C.L., Nombela, C., Rodríguez, P.V., Ye, Z., Hughes, L.E., Jones, P.S., Ham, T., Rittman,

T., Coyle-Gilchrist, I., Regenthal, R., Sahakian, B.J., Barker, R.A., Robbins, T.W., Rowe, J.B., 2016. Atomoxetine restores the response inhibition network in Parkinson's disease. Brain 139, 2235–2248. https://doi.org/10.1093/brain/aww138

Raichle, M.E., 2015. The restless brain: how intrinsic activity organizes brain function. Philos. Trans. R. Soc. B Biol. Sci. 370, 20140172–20140172. https://doi.org/10.1098/rstb.2014.0172

Raichle, M.E., 2010. Two views of brain function. Trends Cogn. Sci. 14, 180–190. https://doi.org/10.1016/j.tics.2010.01.008

Raichle, M.E., 2009. A brief history of human brain mapping. Trends Neurosci. 32, 118–126. https://doi.org/10.1016/j.tins.2008.11.001

Raichle, M.E., MacLeod, A.M., Snyder, A.Z., Powers, W.J., Gusnard, D.A., Shulman, G.L., 2001. A default mode of brain function. Proc. Natl. Acad. Sci. 98, 676–682. https://doi.org/10.1073/pnas.98.2.676

Raichle, M.E., Mintun, M.A., 2006. BRAIN WORK AND BRAIN IMAGING. Annu. Rev. Neurosci. 29, 449–476. https://doi.org/10.1146/annurev.neuro.29.051605.112819

Rashid, B., Arbabshirani, M.R., Damaraju, E., Cetin, M.S., Miller, R., Pearlson, G.D., Calhoun, V.D., 2016. Classification of schizophrenia and bipolar patients using static and dynamic resting-state fMRI brain connectivity. Neuroimage 134, 645–657. https://doi.org/10.1016/j.neuroimage.2016.04.051

Rashid, B., Damaraju, E., Pearlson, G.D., Calhoun, V.D., 2014. Dynamic connectivity states estimated from resting fMRI Identify differences among Schizophrenia, bipolar disorder, and healthy control subjects. Front. Hum. Neurosci. 8, 897. https://doi.org/10.3389/fnhum.2014.00897

Ratcliff, R., 1979. Group reaction time distributions and an analysis of distribution statistics. Psychol. Bull. 86, 446–461. https://doi.org/10.1037/0033-2909.86.3.446

Raz, A., 2004. Anatomy of attentional networks. Anat. Rec. - Part B New Anat. 281, 21–36. https://doi.org/10.1002/ar.b.20035

Ridgway, G.R., Omar, R., Ourselin, S., Hill, D.L.G., Warren, J.D., Fox, N.C., 2009. Issues with threshold masking in voxel-based morphometry of atrophied brains. Neuroimage 44, 99–111. https://doi.org/10.1016/j.neuroimage.2008.08.045

Rizzo, G., Arcuti, S., Copetti, M., Alessandria, M., Savica, R., Fontana, A., Liguori, R., Logroscino, G., 2017. Accuracy of clinical diagnosis of dementia with Lewy bodies: a systematic review and meta-analysis. J. Neurol. Neurosurg. Psychiatry jnnp-2017-316844. https://doi.org/10.1136/jnnp-2017-316844

Rolinski, M., Griffanti, L., Szewczyk-Krolikowski, K., Menke, R.A.L., Wilcock, G.K., Filippini, N., Zamboni, G., Hu, M.T.M., Mackay, C.E., 2015. Aberrant functional connectivity within the basal ganglia of patients with Parkinson's disease. NeuroImage Clin. 8, 126–132. https://doi.org/10.1016/j.nicl.2015.04.003

Rosazza, C., Minati, L., Ghielmetti, F., Mandelli, M.L., Bruzzone, M.G., 2012. Functional Connectivity during Resting-State Functional MR Imaging: Study of the Correspondence between Independent Component Analysis and Region-of-Interest−Based Methods. Am. J. Neuroradiol. 33, 180–187. https://doi.org/10.3174/ajnr.A2733

Roth, M., Tym, E., Mountjoy, C.Q., Huppert, F.A., Hendrie, H., Verma, S., Goddard, R., 1986. CAMDEX. A standardised instrument for the diagnosis of mental disorder in the elderly with special reference to the early detection of dementia. Br. J. Psychiatry 149, 698–709. https://doi.org/10.1192/bjp.149.6.698

Rüb, U., Del Tredici, K., Schultz, C., Ghebremedhin, E., de Vos, R.A.., Jansen Steur, E., Braak, H., 2002. Parkinson's disease: the thalamic components of the limbic loop are severely impaired by α-synuclein immunopositive inclusion body pathology. Neurobiol. Aging 23, 245–254. https://doi.org/10.1016/S0197-4580(01)00269-X

Rubinov, M., Sporns, O., 2010. Complex network measures of brain connectivity: Uses and interpretations. Neuroimage 52, 1059–1069. https://doi.org/10.1016/j.neuroimage.2009.10.003

Sadiq, D., Whitfield, T., Lee, L., Stevens, T., Costafreda, S., Walker, Z., 2017. Prodromal Dementia with Lewy Bodies and Prodromal Alzheimer's Disease: A Comparison of the Cognitive and Clinical Profiles. J. Alzheimer's Dis. 58, 463–470. https://doi.org/10.3233/JAD-161089

Sanchez-Castaneda, C., Rene, R., Ramirez-Ruiz, B., Campdelacreu, J., Gascon, J., Falcon, C., Calopa, M., Jauma, S., Juncadella, M., Junque, C., 2009. Correlations between gray matter reductions and cognitive deficits in dementia with Lewy Bodies and Parkinson's disease with dementia. Mov. Disord. 24, 1740–1746. https://doi.org/10.1002/mds.22488

Sarro, L., Senjem, M.L., Lundt, E.S., Przybelski, S.A., Lesnick, T.G., Graff-Radford, J.,

Boeve, B.F., Lowe, V.J., Ferman, T.J., Knopman, D.S., Comi, G., Filippi, M., Petersen, R.C., Jack, C.R., Kantarci, K., 2016. Amyloid-β deposition and regional grey matter atrophy rates in dementia with Lewy bodies. Brain 139, 2740–2750. https://doi.org/10.1093/brain/aww193

Sarro, L., Tosakulwong, N., Schwarz, C.G., Graff-Radford, J., Przybelski, S.A., Lesnick, T.G., Zuk, S.M., Reid, R.I., Raman, M.R., Boeve, B.F., Ferman, T.J., Knopman, D.S., Comi, G., Filippi, M., Murray, M.E., Parisi, J.E., Dickson, D.W., Petersen, R.C., Jack, C.R., Kantarci, K., 2017. An investigation of cerebrovascular lesions in dementia with Lewy bodies compared to Alzheimer's disease. Alzheimer's Dement. 13, 257–266. https://doi.org/10.1016/j.jalz.2016.07.003

Sato, T., Hanyu, H., Hirao, K., Shimizu, S., Kanetaka, H., Iwamoto, T., 2007. Deep gray matter hyperperfusion with occipital hypoperfusion in dementia with Lewy bodies. Eur. J. Neurol. 14, 1299–1301. https://doi.org/10.1111/j.1468-1331.2007.01951.x

Sauer, J., Ffytche, D.H., Ballard, C.G., Brown, R.G., Howard, R., 2006. Differences between Alzheimer's disease and dementia with Lewy bodies: An fMRI study of task-related brain activity. Brain 129, 1780–1788. https://doi.org/10.1093/brain/awl102

Savica, R., Grossardt, B.R., Bower, J.H., Boeve, B.F., Ahlskog, J.E., Rocca, W.A., 2013. Incidence of Dementia With Lewy Bodies and Parkinson Disease Dementia. JAMA Neurol. 70, 1396. https://doi.org/10.1001/jamaneurol.2013.3579

Schmiedek, F., Oberauer, K., Wilhelm, O., Süß, H.-M., Wittmann, W.W., 2007. Individual differences in components of reaction time distributions and their relations to working memory and intelligence. J. Exp. Psychol. Gen. 136, 414–429. https://doi.org/10.1037/0096-3445.136.3.414

Schneider, J.A., Arvanitakis, Z., Yu, L., Boyle, P.A., Leurgans, S.E., Bennett, D.A., 2012. Cognitive impairment, decline and fluctuations in older community-dwelling subjects with Lewy bodies. Brain 135, 3005–3014. https://doi.org/10.1093/brain/aws234

Schneider, J.S., Pioli, E.Y., Jianzhong, Y., Li, Q., Bezard, E., 2013. Levodopa improves motor deficits but can further disrupt cognition in a macaque parkinson model. Mov. Disord. 28, 663–667. https://doi.org/10.1002/mds.25258

Schwab, S., Koenig, T., Morishima, Y., Dierks, T., Federspiel, A., Jann, K., 2015. Discovering frequency sensitive thalamic nuclei from EEG microstate informed resting state fMRI. Neuroimage 118, 368–375.

https://doi.org/10.1016/j.neuroimage.2015.06.001

Shimada, H., Shinotoh, H., Hirano, S., Miyoshi, M., Sato, K., Tanaka, N., Ota, T., Fukushi, K., Irie, T., Ito, H., Higuchi, M., Kuwabara, S., Suhara, T., 2013. β-amyloid in lewy body disease is related to Alzheimer's disease-like atrophy. Mov. Disord. 28, 169–175. https://doi.org/10.1002/mds.25286

Shimizu, S., Hanyu, H., Kanetaka, H., Iwamoto, T., Koizumi, K., Abe, K., 2005. Differentiation of Dementia with Lewy Bodies from Alzheimer's Disease Using Brain SPECT. Dement. Geriatr. Cogn. Disord. 20, 25–30. https://doi.org/10.1159/000085070

Shimizu, S., Hirose, D., Namioka, N., Kanetaka, H., Hirao, K., Hatanaka, H., Takenoshita, N., Kaneko, Y., Ogawa, Y., Umahara, T., Sakurai, H., Hanyu, H., 2017. Correlation between clinical symptoms and striatal DAT uptake in patients with DLB. Ann. Nucl. Med. 31, 390–398. https://doi.org/10.1007/s12149-017-1166-3

Shulman, G.L., Fiez, J.A., Corbetta, M., Buckner, R.L., Miezin, F.M., Raichle, M.E., Petersen, S.E., 1997. Common Blood Flow Changes across Visual Tasks: II. Decreases in Cerebral Cortex. J. Cogn. Neurosci. 9, 648–663. https://doi.org/10.1162/jocn.1997.9.5.648

Shulman, K.I., Hull, I.M., Dekoven, S., Amodeo, S., Mainland, B.J., Herrmann, N., 2015. Cognitive Fluctuations and the Lucid Interval in Dementia: Implications for Testamentary Capacity. J Am Acad Psychiatry Law 43, 287–292.

Smith, S.M., Fox, P.T., Miller, K.L., Glahn, D.C., Fox, P.M., Mackay, C.E., Filippini, N., Watkins, K.E., Toro, R., Laird, A.R., Beckmann, C.F., 2009. Correspondence of the brain's functional architecture during activation and rest. Proc. Natl. Acad. Sci. 106, 13040–13045. https://doi.org/10.1073/pnas.0905267106

Smith, S.M., Miller, K.L., Salimi-Khorshidi, G., Webster, M., Beckmann, C.F., Nichols, T.E., Ramsey, J.D., Woolrich, M.W., 2011. Network modelling methods for FMRI. Neuroimage 54, 875–891. https://doi.org/10.1016/j.neuroimage.2010.08.063

Solé-Padullés, C., Bartrés-Faz, D., Lladó, A., Bosch, B., Peña-Gómez, C., Castellví, M., Rami, L., Bargalló, N., Sánchez-Valle, R., Molinuevo, J.L., 2013. Donepezil Treatment Stabilizes Functional Connectivity During Resting State and Brain Activity During Memory Encoding in Alzheimer's Disease. J. Clin. Psychopharmacol. 33, 199–205. https://doi.org/10.1097/JCP.0b013e3182825bfd

Sonuga-Barke, E.J.S., Castellanos, F.X., 2007. Spontaneous attentional fluctuations in impaired states and pathological conditions: A neurobiological hypothesis. Neurosci. Biobehav. Rev. 31, 977–986. https://doi.org/10.1016/j.neubiorev.2007.02.005

Sorg, C., Riedl, V., Mühlau, M., Calhoun, V.D., Eichele, T., Läer, L., Drzezga, A., Förstl, H., Kurz, A., Zimmer, C., Wohlschläger, A.M., 2007. Selective changes of resting-state networks in individuals at risk for Alzheimer's disease. Proc. Natl. Acad. Sci. U. S. A. 104, 18760–18765. https://doi.org/10.1073/pnas.0708803104

Sourty, M., Thoraval, L., Roquet, D., Armspach, J.-P., Foucher, J., Blanc, F., 2016. Identifying Dynamic Functional Connectivity Changes in Dementia with Lewy Bodies Based on Product Hidden Markov Models. Front. Comput. Neurosci. 10, 60. https://doi.org/10.3389/fncom.2016.00060

Stinton, C., McKeith, I.G., Taylor, J.-P., Lafortune, L., Mioshi, E., Mak, E., Cambridge, V., Mason, J., Thomas, A., O'Brien, J.T., 2015. Pharmacological Management of Lewy Body Dementia: A Systematic Review and Meta-Analysis. Am. J. Psychiatry 172, 731–742. https://doi.org/10.1176/appi.ajp.2015.14121582

Stoffers, D., Bosboom, J.L.W., Deijen, J.B., Wolters, E.C., Berendse, H.W., Stam, C.J., 2007. Slowing of oscillatory brain activity is a stable characteristic of Parkinson's disease without dementia. Brain 130, 1847–1860. https://doi.org/10.1093/brain/awm034

Strik, W.K., Dierks, T., Becker, T., Lehmann, D., 1995. Larger topographical variance and decreased duration of brain electric microstates in depression. J. Neural Transm. 99, 213–222. https://doi.org/10.1007/BF01271480

Stylianou, M., Murphy, N., Peraza, L.R., Graziadio, S., Cromarty, R.A., Killen, A., O'Brien, J.T., Thomas, A.J., LeBeau, F.E.N., Taylor, J.-P., 2018. Quantitative electroencephalography as a marker of cognitive fluctuations in dementia with Lewy bodies and an aid to differential diagnosis. Clin. Neurophysiol. 129, 1209–1220. https://doi.org/10.1016/j.clinph.2018.03.013

Su, L., Blamire, A.M., Watson, R., He, J., Hayes, L., O'Brien, J.T., 2016. Whole-brain patterns of 1H-magnetic resonance spectroscopy imaging in Alzheimer's disease and dementia with Lewy bodies. Transl. Psychiatry 6, e877–e877. https://doi.org/10.1038/tp.2016.140

Sun, M., Mainland, B.J., Ornstein, T.J., Mallya, S., Fiocco, A.J., Sin, G.L., Shulman, K.I., Herrmann, N., 2018. The association between cognitive fluctuations and activities of

daily living and quality of life among institutionalized patients with dementia. Int. J. Geriatr. Psychiatry 33, e280–e285. https://doi.org/10.1002/gps.4788

Szewczyk-Krolikowski, K., Menke, R.A.L., Rolinski, M., Duff, E., Salimi-Khorshidi, G., Filippini, N., Zamboni, G., Hu, M.T.M., Mackay, C.E., 2014. Functional connectivity in the basal ganglia network differentiates PD patients from controls. Neurology 83, 208–214. https://doi.org/10.1212/WNL.0000000000000592

Szot, P., 2006. Compensatory Changes in the Noradrenergic Nervous System in the Locus Ceruleus and Hippocampus of Postmortem Subjects with Alzheimer's Disease and Dementia with Lewy Bodies. J. Neurosci. 26, 467–478. https://doi.org/10.1523/JNEUROSCI.4265-05.2006

Tagliazucchi, E., Balenzuela, P., Fraiman, D., Chialvo, D.R., 2012a. Criticality in large-scale brain fmri dynamics unveiled by a novel point process analysis. Front. Physiol. 3 FEB, 1–12. https://doi.org/10.3389/fphys.2012.00015

Tagliazucchi, E., Wegner, F. Von, Morzelewski, A., Brodbeck, V., Laufs, H., von Wegner, F., Morzelewski, A., Brodbeck, V., Laufs, H., 2012b. Dynamic BOLD functional connectivity in humans and its electrophysiological correlates. Front. Hum. Neurosci. 6, 339. https://doi.org/10.3389/fnhum.2012.00339

Tahmasian, M., Bettray, L.M., van Eimeren, T., Drzezga, A., Timmermann, L., Eickhoff, C.R., Eickhoff, S.B., Eggers, C., 2015. A systematic review on the applications of resting-state fMRI in Parkinson's disease: Does dopamine replacement therapy play a role? Cortex 73, 80–105. https://doi.org/10.1016/j.cortex.2015.08.005

Takahashi, R., Ishii, K., Miyamoto, N., Yoshikawa, T., Shimada, K., Ohkawa, S., Kakigi, T., Yokoyama, K., 2010. Measurement of Gray and White Matter Atrophy in Dementia with Lewy Bodies Using Diffeomorphic Anatomic Registration through Exponentiated Lie Algebra: A Comparison with Conventional Voxel-Based Morphometry. Am. J. Neuroradiol. 31, 1873–1878. https://doi.org/10.3174/ajnr.A2200

Takahashi, T., Cho, R.Y., Murata, T., Mizuno, T., Kikuchi, M., Mizukami, K., Kosaka, H., Takahashi, K., Wada, Y., 2009. Age-related variation in EEG complexity to photic stimulation: A multiscale entropy analysis. Clin. Neurophysiol. 120, 476–483. https://doi.org/10.1016/j.clinph.2008.12.043

Tam, C.W.C., Burton, E.J., McKeith, I.G., Burn, D.J., O'Brien, J.T., 2005. Temporal lobe atrophy on MRI in Parkinson disease with dementia. Neurology 64, 861–865.

https://doi.org/10.1212/01.WNL.0000153070.82309.D4

Taylor, J.-P., Colloby, S.J., McKeith, I.G., O'Brien, J.T., 2013. Covariant perfusion patterns provide clues to the origin of cognitive fluctuations and attentional dysfunction in dementia with Lewy bodies. Int. Psychogeriatr. 25, 1917–28. https://doi.org/10.1017/S1041610213001488

Taylor, J.-P., Firbank, M.J., He, J., Barnett, N., Pearce, S., Livingstone, A., Vuong, Q., McKeith, I.G., O'Brien, J.T., 2012. Visual cortex in dementia with Lewy bodies: magnetic resonance imaging study. Br. J. Psychiatry 200, 491–8. https://doi.org/10.1192/bjp.bp.111.099432

Teaktong, T., Piggott, M. a, Mckeith, I.G., Perry, R.H., Ballard, C.G., Perry, E.K., 2005. Muscarinic M2 and M4 receptors in anterior cingulate cortex: relation to neuropsychiatric symptoms in dementia with Lewy bodies. Behav. Brain Res. 161, 299–305. https://doi.org/10.1016/j.bbr.2005.02.019

Terzaghi, M., Arnaldi, D., Rizzetti, M.C., Minafra, B., Cremascoli, R., Rustioni, V., Zangaglia, R., Pasotti, C., Sinforiani, E., Pacchetti, C., Manni, R., 2013. Analysis of video-polysomnographic sleep findings in dementia with Lewy bodies. Mov. Disord. 28, 1416–1423. https://doi.org/10.1002/mds.25523

Tessitore, A., Giordano, A., de Micco, R., Russo, A., Tedeschi, G., 2014. Sensorimotor connectivity in Parkinson's disease: The role of functional neuroimaging. Front. Neurol. 5, 1–5. https://doi.org/10.3389/fneur.2014.00180

Thomas, A.J., Mahin-Babaei, F., Saidi, M., Lett, D., Taylor, J.P., Walker, L., Attems, J., 2018. Improving the identification of dementia with Lewy bodies in the context of an Alzheimer's-type dementia. Alzheimers. Res. Ther. 10, 27. https://doi.org/10.1186/s13195-018-0356-0

Thompson, G.J., Magnuson, M.E., Merritt, M.D., Schwarb, H., Pan, W.J., Mckinley, A., Tripp, L.D., Schumacher, E.H., Keilholz, S.D., 2013. Short-time windows of correlation between large-scale functional brain networks predict vigilance intraindividually and interindividually. Hum. Brain Mapp. 34, 3280–3298. https://doi.org/10.1002/hbm.22140

Tomlinson, C.L., Stowe, R., Patel, S., Rick, C., Gray, R., Clarke, C.E., 2010. Systematic review of levodopa dose equivalency reporting in Parkinson's disease. Mov. Disord. 25, 2649–2653. https://doi.org/10.1002/mds.23429

Trachsel, M., Hermann, H., Biller-Andorno, N., 2015. Cognitive Fluctuations as a Challenge for the Assessment of Decision-Making Capacity in Patients With Dementia. Am. J. Alzheimers. Dis. Other Demen. 30, 360–363. https://doi.org/10.1177/1533317514539377

Tse, C.S., Balota, D.A., Yap, M.J., Duchek, J.M., Mccabe, D.P., 2010. Effects of healthy aging and early-stage dementia of the Alzheimer's type on components of reponse time distributions in three attention tasks. Neuropsychology 24, 300–315. https://doi.org/10.1037/a0018274.Effects

Tsuboi, Y., Dickson, D.W., 2005. Dementia with Lewy bodies and Parkinson's disease with dementia: Are they different? Parkinsonism Relat. Disord. 11, S47–S51. https://doi.org/10.1016/j.parkreldis.2004.10.014

Ungerleider, L., Haxby, J. V., 1994. "What" and "where" in the human brain. Curr. Opin. Neurobiol. 4, 157–165. https://doi.org/10.1016/0959-4388(94)90066-3

Van De Ville, D., Britz, J., Michel, C.M., 2010. EEG microstate sequences in healthy humans at rest reveal scale-free dynamics. Proc. Natl. Acad. Sci. 107, 18179–18184. https://doi.org/10.1073/pnas.1007841107

van der Zande, J.J., Steenwijk, M.D., ten Kate, M., Wattjes, M.P., Scheltens, P., Lemstra, A.W., 2018. Gray matter atrophy in dementia with Lewy bodies with and without concomitant Alzheimer pathology. Neurobiol. Aging. https://doi.org/10.1016/j.neurobiolaging.2018.07.005

van Dijk, K.R.A., Sabuncu, M.R., Buckner, R.L., 2012. The influence of head motion on intrinsic functional connectivity MRI. Neuroimage 59, 431–438. https://doi.org/10.1016/j.neuroimage.2011.07.044

Van Dyk, K., Towns, S., Tatarina, O., Yeung, P., Dorrejo, J., Zahodne, L.B., Stern, Y., 2016. Assessing Fluctuating Cognition in Dementia Diagnosis: Interrater Reliability of the Clinician Assessment of Fluctuation. Am. J. Alzheimer's Dis. Other Dementiasr 31, 137–143. https://doi.org/10.1177/1533317515603359

van Steenoven, I., Aarsland, D., Weintraub, D., Londos, E., Blanc, F., van der Flier, W.M., Teunissen, C.E., Mollenhauer, B., Fladby, T., Kramberger, M.G., Bonanni, L., Lemstra, A.W., 2016. Cerebrospinal Fluid Alzheimer's Disease Biomarkers Across the Spectrum of Lewy Body Diseases: Results from a Large Multicenter Cohort. J. Alzheimer's Dis. 54, 287–295. https://doi.org/10.3233/JAD-160322

van Wijk, B.C.M., Stam, C.J., Daffertshofer, A., 2010. Comparing brain networks of different size and connectivity density using graph theory. PLoS One 5. https://doi.org/10.1371/journal.pone.0013701

Vann Jones, S.A., O'Brien, J.T., 2014. The prevalence and incidence of dementia with Lewy bodies: a systematic review of population and clinical studies. Psychol. Med. 44, 673–83. https://doi.org/10.1017/S0033291713000494

Varanese, S., Perfetti, B., Gilbert-Wolf, R., Thomas, A., Onofrj, M., Di Rocco, A., 2013. Modafinil and armodafinil improve attention and global mental status in Lewy bodies disorders: preliminary evidence. Int. J. Geriatr. Psychiatry 28, 1095–1097. https://doi.org/10.1002/gps.3952

Varanese, S., Perfetti, B., Monaco, D., Thomas, A., Bonanni, L., Tiraboschi, P., Onofrj, M., 2010. Fluctuating cognition and different cognitive and behavioural profiles in Parkinson's disease with dementia: comparison of dementia with Lewy bodies and Alzheimer's disease. J. Neurol. 257, 1004–1011. https://doi.org/10.1007/s00415-010-5453-3

Verghese, J., Crystal, H.A., Dickson, D.W., Lipton, R.B., 1999. Validity of clinical criteria for the diagnosis of dementia with Lewy bodies. Neurology 53.

Vidaurre, D., Smith, S.M., Woolrich, M.W., 2017. Brain network dynamics are hierarchically organized in time. Proc. Natl. Acad. Sci. 114, 12827–12832. https://doi.org/10.1073/pnas.1705120114

Viviano, R.P., Raz, N., Yuan, P., Damoiseaux, J.S., 2017. Associations between dynamic functional connectivity and age, metabolic risk, and cognitive performance. Neurobiol. Aging 59, 135–143. https://doi.org/10.1016/j.neurobiolaging.2017.08.003

Vlagsma, T.T., Koerts, J., Tucha, O., Dijkstra, H.T., Duits, A.A., van Laar, T., Spikman, J.M., 2016. Mental slowness in patients with Parkinson's disease: Associations with cognitive functions? J. Clin. Exp. Neuropsychol. 38, 844–852. https://doi.org/10.1080/13803395.2016.1167840

Voytko, M., Olton, D., Richardson, R., Gorman, L., Tobin, J., Price, D., 1994. Basal forebrain lesions in monkeys disrupt attention but not learning and memory. J. Neurosci. 14, 167–186. https://doi.org/10.1523/JNEUROSCI.14-01-00167.1994

Walker, M.P., Ayre, G.A., Cummings, J.L., Wesnes, K.A., McKeith, I.G., O'Brien, J.T.,

Ballard, C.G., 2000a. Quantifying fluctuation in dementia with Lewy bodies, Alzheimer's disease, and vascular dementia. Neurology 54, 1616–1625. https://doi.org/10.1212/WNL.54.8.1616

Walker, M.P., Ayre, G.A., Cummings, J.L., Wesnes, K.A., McKeith, I.G., O'Brien, J.T., Ballard, C.G., 2000b. The Clinician Assessment of Fluctuation and the One Day Fluctuation Assessment Scale. Br. J. Psychiatry 177, 252–256. https://doi.org/10.1192/bjp.177.3.252

Walker, M.P., Ayre, G.A., Perry, E.K., Wesnes, K.A., McKeith, I.G., Tovee, M., Edwardson, J.A., Ballard, C.G., 2000c. Quantification and Characterisation of Fluctuating Cognition in Dementia with Lewy Bodies and Alzheimer's Disease. Dement. Geriatr. Cogn. Disord. 11, 327–335. https://doi.org/10.1159/000017262

Walker, Z., Costa, D.C., Walker, R.W.H., Shaw, K., Gacinovic, S., Stevens, T., Livingston, G., Ince, P.G., McKeith, I.G., Katona, C.L.E., 2002. Differentiation of dementia with Lewy bodies from Alzheimer's disease using a dopaminergic presynaptic ligand. J. Neurol. Neurosurg. Psychiatry 73, 134–140. https://doi.org/10.1136/jnnp.73.2.134

Walker, Z., Possin, K.L., Boeve, B.F., Aarsland, D., 2015. Lewy body dementias. Lancet 386, 1683–1697. https://doi.org/10.1016/S0140-6736(15)00462-6

Wang, H.-F., Yu, J.-T., Tang, S.-W., Jiang, T., Tan, C.-C., Meng, X.-F., Wang, C., Tan, M.-S., Tan, L., 2015. Efficacy and safety of cholinesterase inhibitors and memantine in cognitive impairment in Parkinson's disease, Parkinson's disease dementia, and dementia with Lewy bodies: systematic review with meta-analysis and trial sequential analysis. J. Neurol. Neurosurg. Psychiatry 86, 135–143. https://doi.org/10.1136/jnnp-2014-307659

Watson, R., Colloby, S.J., Blamire, A.M., Wesnes, K.A., Wood, J., O'Brien, J.T., 2017. Does attentional dysfunction and thalamic atrophy predict decline in dementia with Lewy bodies? Parkinsonism Relat. Disord. 45, 69–74. https://doi.org/10.1016/j.parkreldis.2017.10.006

Watson, R., O'Brien, J.T., Barber, R., Blamire, A.M., 2012. Patterns of gray matter atrophy in dementia with Lewy bodies: a voxel-based morphometry study. Int. Psychogeriatrics 24, 532–540. https://doi.org/10.1017/S1041610211002171

Weissman, D.H., Roberts, K.C., Visscher, K.M., Woldorff, M.G., 2006. The neural bases of momentary lapses in attention. Nat. Neurosci. 9, 971–978.

https://doi.org/10.1038/nn1727

Wesnes, K.A., Aarsland, D., Ballard, C.G., Londos, E., 2015. Memantine improves attention and episodic memory in Parkinson's disease dementia and dementia with Lewy bodies. Int. J. Geriatr. Psychiatry 30, 46–54. https://doi.org/10.1002/gps.4109

Wesnes, K.A., McKeith, I.G., Ferrara, R., Emre, M., Del Ser, T., Spano, P.F., Cicin-Sain, A., Anand, R., Spiegel, R., 2002. Effects of Rivastigmine on Cognitive Function in Dementia with Lewy Bodies: A Randomised Placebo-Controlled International Study Using the Cognitive Drug Research Computerised Assessment System. Dement. Geriatr. Cogn. Disord. 13, 183–192. https://doi.org/10.1159/000048651

Westlye, L.T., Grydeland, H., Walhovd, K.B., Fjell, A.M., 2011. Associations between regional cortical thickness and attentional networks as measured by the attention network test. Cereb. Cortex 21, 345–356. https://doi.org/10.1093/cercor/bhq101

Whitwell, J.L., Weigand, S.D., Shiung, M.M., Boeve, B.F., Ferman, T.J., Smith, G.E., Knopman, D.S., Petersen, R.C., Benarroch, E.E., Josephs, K.A., Jack, C.R., 2007. Focal atrophy in dementia with Lewy bodies on MRI: A distinct pattern from Alzheimer's disease. Brain 130, 708–719. https://doi.org/10.1093/brain/awl388

Woodard, J.S., 1962. Concentric Hyaline Inclusion Body Formation in Mental Disease Analysis of Twenty-Seven Cases. J. Neuropathol. Exp. Neurol. 21, 442–449.

Wu, T., Long, X., Wang, L., Hallett, M., Zang, Y., Li, K., Chan, P., 2011. Functional connectivity of cortical motor areas in the resting state in Parkinson's disease. Hum. Brain Mapp. 32, 1443–1457. https://doi.org/10.1002/hbm.21118

Yong, S.W., Yoon, J.K., An, Y.S., Lee, P.H., 2007. A comparison of cerebral glucose metabolism in Parkinson's disease, Parkinson's disease dementia and dementia with Lewy bodies. Eur. J. Neurol. 14, 1357–1362. https://doi.org/10.1111/j.1468-1331.2007.01977.x

Yoshida, T., Mori, T., Yamazaki, K., Sonobe, N., Shimizu, H., Matsumoto, T., Kikuchi, K., Miyagawa, M., Mochizuki, T., Ueno, S., 2015. Relationship between regional cerebral blood flow and neuropsychiatric symptoms in dementia with Lewy bodies. Int. J. Geriatr. Psychiatry 30, 1068–1075. https://doi.org/10.1002/gps.4263

Yu, R., Liu, B., Wang, L., Chen, J., Liu, X., 2013. Enhanced Functional Connectivity between Putamen and Supplementary Motor Area in Parkinson's Disease Patients. PLoS One 8.

https://doi.org/10.1371/journal.pone.0059717

Yuste, R., MacLean, J.N., Smith, J., Lansner, A., 2005. The cortex as a central pattern generator. Nat. Rev. Neurosci. 6, 477–483. https://doi.org/10.1038/nrn1686

Zaccai, J., Brayne, C., McKeith, I.G., Matthews, F., Ince, P.G., 2008. Patterns and stages of -synucleinopathy: Relevance in a population-based cohort. Neurology 70, 1042–1048. https://doi.org/10.1212/01.wnl.0000306697.48738.b6

Zalesky, A., Fornito, A., Cocchi, L., Gollo, L.L., Breakspear, M., 2014. Time-resolved resting-state brain networks. Proc. Natl. Acad. Sci. 111, 10341–10346. https://doi.org/10.1073/pnas.1400181111

Zappasodi, F., Olejarczyk, E., Marzetti, L., Assenza, G., Pizzella, V., Tecchio, F., 2014. Fractal dimension of EEG activity senses neuronal impairment in acute stroke. PLoS One 9, 1–8. https://doi.org/10.1371/journal.pone.0100199

Zhang, D., Raichle, M.E., 2010. Disease and the brain's dark energy. Nat. Rev. Neurol. 6, 15–28. https://doi.org/10.1038/nrneurol.2009.198

Zhong, J., Pan, P., Dai, Z., Shi, H., 2014. Voxelwise meta-analysis of gray matter abnormalities in dementia with Lewy bodies. Eur. J. Radiol. 83, 1870–1874. https://doi.org/10.1016/j.ejrad.2014.06.014

Ziebell, M., Andersen, B.B., Pinborg, L.H., Knudsen, G.M., Stokholm, J., Thomsen, G., Karlsborg, M., Hogh, P., Mork, M.L., Hasselbalch, S.G., 2013. Striatal Dopamine Transporter Binding Does Not Correlate with Clinical Severity in Dementia with Lewy Bodies. J. Nucl. Med. 54, 1072–1076. https://doi.org/10.2967/jnumed.112.114025